

# **Novel approaches for impurity and isotopic profiling of synthetic cannabinoids**

**Kumulative Dissertation**

zur

Erlangung des akademischen Grades

doctor rerum naturalium (Dr. rer. nat.)

der Mathematisch-Naturwissenschaftlichen Fakultät

der Universität Rostock

vorgelegt von

Sascha Münster-Müller, geb. am 23 Juni 1989 in Frankfurt Höchst  
aus Wiesbaden

Rostock, Oktober 2019

**Gutachter:**

Prof. Dr. Ralf Zimmermann, Universität Rostock, Institut für Chemie

Prof. Dr. Heiko Hayen, Universität Münster, Institut für Anorganische und Analytische Chemie

**Jahr der Einreichung:** 2019

**Jahr der Verteidigung:** 2020

## Scientific publications

### First-authorships

The listed manuscripts were prepared by Sascha Münster-Müller as first- or equally contributing author and published in peer-reviewed journals. The contributions to each manuscript are described individually.

*A Novel Impurity-Profiling Workflow with the Combination of Flash-Chromatography, UHPLC-MS, and Multivariate Data Analysis for Highly Pure Drugs: A Study on the Synthetic Cannabinoid MDMB-CHMICA*

Sascha Münster-Müller, Ralf Zimmermann, Michael Pütz

Analytical Chemistry 2018, 90(17): 10559-10567

Sascha Münster-Müller developed and validated the flash-chromatography method, prepared the samples and carried out all UHPLC-MS measurements. Additionally, he evaluated and interpreted the results. The manuscript was written and submitted by Sascha Münster-Müller.

Overall contribution: 90 %

*Chemical profiling of the synthetic cannabinoid MDMB-CHMICA: identification, assessment and stability study of synthesis-related impurities in seized and synthesized samples*

Sascha Münster-Müller, Steven Hansen, Till Opatz, Ralf Zimmermann, Michael Pütz

Drug Testing and Analysis 2019, 11(8): 1192-1206

Controlled synthesis were conducted by Steven Hansen with the aid of Sascha Münster-Müller. Sascha Münster-Müller then further processed all samples, carried out the UHPLC-MS measurements and was responsible for the HR-MS<sup>n</sup> and NMR spectra interpretations. Additionally, he assessed and evaluated all impurity signatures of seized samples and controlled syntheses. The manuscript was written and submitted by Sascha Münster-Müller.

Overall contribution: 80 %

*Profiling of synthesis-related impurities of the synthetic cannabinoid Cumyl-5F-PINACA in seized samples of e-liquids via multivariate analysis of UHPLC-MS<sup>n</sup> data*

Sascha Münster-Müller, Isabelle Matzenbach, Thomas Knepper,

Ralf Zimmermann, Michael Pütz

Drug Testing and Analysis 2019, in press, DOI: 10.1002/dta.2673

The experimental work was conducted by Isabelle Matzenbach as a part of her Bachelor studies. Sascha Münster-Müller was responsible for the scientific and experimental supervision and the final interpretation of the data. The original manuscript of Isabelle Matzenbach was majorly revised and submitted by Sascha Münster-Müller.

Overall contribution: 50 %

*Profiling of new psychoactive substances (NPS) by using stable isotope ratio mass spectrometry (IRMS): study on the synthetic cannabinoid 5F-PB-22*

Sascha Münster-Müller, Nicole Scheid, Thomas Holdermann, Sabine Schneiders, Michael Pütz

Drug Testing and Analysis 2018, 10(8): 1323-1327

The IRMS measurements were conducted by Nicole Scheid and Thomas Holdermann. Sascha Münster-Müller prepared all samples and evaluated the results. The manuscript was written and submitted by Sascha Münster-Müller.

Overall contribution: 75 %

*Combination of stable isotope ratio data and chromatographic impurity signatures as a comprehensive concept for the profiling of highly prevalent synthetic cannabinoids and their precursors*

Sascha Münster-Müller, Nicole Scheid, Ralf Zimmermann, Michael Pütz

Submitted to: Analytica Chimica Acta

The IRMS measurements were conducted by Nicole Scheid. Sascha Münster-Müller prepared all samples and evaluated the results. The manuscript was written and submitted by Sascha Münster-Müller. The manuscript is listed in the appendix without the final journal format.

Overall contribution: 75 %



## Co-authorships

The listed manuscripts were co-authored by Sascha Münster-Müller and published in peer-reviewed journals. The contributions to each manuscript are described individually.

*Absolute configuration of the synthetic cannabinoid MDMB-CHMICA with its chemical characteristics in illegal products*

Lars Andernach, Stefan Pusch, Carina Weber, Dieter Schollmeyer, Sascha Münster-Müller, Michael Pütz, Till Opatz

Forensic Toxicology 2016, 34: 344-352

Sascha Münster-Müller provided the samples and wrote a corresponding experimental part.

Overall contribution: 5 %

*Characterization of the synthetic cannabinoid MDMB-CHMCZCA*

Carina Weber, Stefan Pusch, Dieter Schollmeyer,

Sascha Münster-Müller, Michael Pütz, Till Opatz

Beilstein Journal of Organic Chemistry 2016, 12: 2808–2815

Sascha Münster-Müller provided the samples and wrote a corresponding experimental part.

Overall contribution: 5 %

This dissertation was prepared at the chair of Analytical Chemistry of the University Rostock. The practical work was carried out between October 2014 to Mai 2019 at the Federal Criminal Police Office in Wiesbaden in the toxicology department (KT-45), in close cooperation to the central analytics II department (KT43).

Most of the presented data was generated within the project “SPICE-profiling”, funded within the EU’s ISEC 2013 programme (Directorate-General JUST/2013/ISEC/DRUGS/AG/ISEC/4000006421). However, the content of this thesis is the sole responsibility of the author and do not necessarily reflect the opinion of the European Commission.

## **Acknowledgements**

This work is dedicated to all the people who have supported me so well during my work, both scientifically and on a personal level. Although my practical work was based in Wiesbaden, I had the chance to travel around Germany and different parts of the world, where I met and worked with a lot of wonderful people. I am convinced, the unique combination of experiences acquired in my doctoral time let me mature both as person and scientist.

My special gratitude goes to...

... Prof. Ralf Zimmermann for his scientific supervision and for providing me with the chance to write my thesis at the University of Rostock as external doctoral student,

... Michael Pütz, without whom the preparation of this work would not have been possible. In the five years of my time at the BKA we connected both on an intellectual and personal level. He supervised me for the entire period as a scientist and at the same time gave me the freedom to pursue my own independent research. In addition, he enabled my numerous visits to scientific conferences around the world, which remain in my memory as a personal highlight,

... the whole Toxicology Department, in particular Diana Weigel, for their support in my time at the BKA and for providing me with the necessary conditions to carry out my research,

... the General Analytics II Department, in particular Nicole Scheid, Dieter Kirsch and Vincent Guillou, for the IRMS measurements, and the possibility to conduct HR-MS/MS experiments and NMR measurements, which were a key part of this thesis,

... Prof. Volker Auwärter, Verena Angerer and the remaining doctoral students from the Freiburg working group for their support in all questions around NPS and the provision of numerous samples for my experimental work,

... Prof. Till Opatz and Steven Hansen from the Organic Chemistry Department of the University of Mainz for the fruitful cooperation,

... all partners involved in “Spice-Profiling” which lead this project to its major success,

... my family and friends who made my time while studying the best time of my life,

... and finally, Carina Zumnick who now accompanies my way for nearly eight years throughout my ups and downs and is a constant source for warmth, care and good advice.

# Index

Abstract .....	I
Zusammenfassung .....	II
<b>1. Introduction .....</b>	<b>1</b>
1.1 Illicit drugs .....	1
1.1.1 Classical drugs .....	1
1.2 New psychoactive substances (NPS) .....	4
1.2.1 Arising legal challenges from a German perspective .....	5
1.2.2 Marketing and distribution .....	6
1.2.4 Risks .....	6
1.3 Synthetic cannabinoid receptor agonists .....	7
1.3.1 History .....	7
1.3.2 Receptor activity .....	8
1.3.3 Systematic naming .....	9
1.3.4 Structural diversity and appearance on the drug market .....	9
1.3.5 Administration forms .....	10
1.1 Forensic drug profiling .....	11
1.2.2 Impurity profiling .....	13
1.2.3 Isotopic profiling .....	14
1.2.4 Project “Spice Profiling” .....	14
1.3 Aims of this thesis .....	15
1.3.1 Research area 1: Development and validation of an impurity profiling .....	16
1.3.2 Research area 2: Isotopic profiling .....	18
1.3.2 Research area 3: Linking seizures and online-test-purchases .....	19
<b>2. Methodology .....</b>	<b>20</b>
2.1 Sample pool and preparation .....	20
2.2 Flash chromatography .....	21
2.3 Assessment and evaluation of impurity signatures .....	23
2.3.1 Ultra high-performance liquid chromatography mass spectrometry .....	23
2.3.2 Data structure and treatment .....	24
2.3.3 Multivariate data analysis .....	25
2.4 Characterization of impurities .....	28
2.4.1 High-resolution mass spectrometry .....	28
2.4.2 Nuclear magnetic resonance spectroscopy .....	29
2.5 Synthesis of MDMB-CHMICA .....	29

2.5.1 Controlled synthesis of the amino acid coupling step using different reaction conditions..	29
2.6 Isotope ratio mass spectrometry .....	30
<b>3. Results and discussion.....</b>	<b>32</b>
3.1 Development and validation of an impurity profiling workflow for highly pure samples of synthetic cannabinoids <sup>Publication 1 and 2</sup> .....	32
3.2 Adaptability of the central workflow to different formulations of synthetic cannabinoids <sup>Publication 1, 3, 4 and 5</sup> .....	36
3.3 Comprehensive profiling using impurity and isotopic signatures <sup>Publication 4 and 5</sup> .....	38
<b>4. Summary and outlook.....</b>	<b>40</b>
<b>5. References .....</b>	<b>41</b>
<b>6. Scientific publications (published).....</b>	<b>48</b>
6.1 Publication 1 .....	49
6.2 Publication 2.....	59
6.3 Publication 3.....	75
6.4 Publication 4.....	84
<b>7. Appendix .....</b>	<b>90</b>
7.1 List of Abbreviations.....	90
7.2 List of Figures .....	92
7.3 List of Tables.....	93
7.4 Oral/poster presentations and conferences .....	93
7.5 Scientific curriculum vitae .....	95
7.6 Scientific publications (submitted).....	96
7.5.1 Publication 5 .....	97

## Abstract

The novel phenomenon of new psychoactive substances (NPS) is challenging the forensic science institutions and legislative authorities with an ongoing flood of new individual substances and substance classes of recreational drugs delivered to the European drug market. In comparison to the classical drugs like amphetamine, heroin or cocaine, the information base on the origin, manufacturing and distribution of NPS is relatively narrow and also difficult to expand, as no original manufacturing sites could be seized by European police forces so far (compared to the large number of clandestine laboratories producing methamphetamine for example). This is why this thesis discovers the potential of different analytical techniques to extract as much strategic information as possible solely from police seizures and online-test-purchases of NPS products about the underlying manufacturing and distribution networks. Synthetic cannabinoids are the most prevalent sub-class of NPS in Germany and thus were chosen as target in the here presented studies.

The main focus of this thesis was the development, validation and application of a profiling methodology for synthetic cannabinoids targeting (1) the chromatographic impurity signatures, providing deeper insights into the manufacturing methods including the synthesis pathway, educts, reagents or batch sizes and (2) the analysis of the stable isotopes of the main components to reveal links between samples that were synthesized using educts with a specific isotopic composition.

Although this work targets several different synthetic cannabinoids at some point of the workflow development, like 5F-PB-22, MDMB-CHMZCZA, Cumyl-PeGaClone or Cumyl-5F-PINACA, the main focus was put on the MDMB-CHMICA as most prevalent synthetic cannabinoid in Germany from 2014 to 2016. On a large seizure from Luxembourg customs of 40 individually packed 1 kg samples and twenty-one other seized and online-test-purchased samples of pure material, the general impurity profiling methodology was developed, centred around the isolation of impurities from the main component via flash-chromatography. The pooled impurity fractions were measured via high-pressure liquid chromatography coupled to mass spectrometry and evaluated via multivariate data analysis to discriminate between individual synthesis batches. The comparative analysis was based on fifteen key-impurities, previously assessed and characterized via high resolution mass spectrometry and nuclear magnetic resonance spectroscopy. Controlled syntheses of MDMB-CHMICA were carried out to better understand variations in impurity signatures and to assess the significance of variations in the impurity patterns of seized samples. The workflow was adapted and validated for the two most common forms of consumption for synthetic cannabinoids: E-liquids and herbal blends (also called “Spice-Products”). Lastly, 118 Spice-product samples of MDMB-CHMICA were analyzed for their chromatographic impurity composition and isotope ratios of the main component, and combined in a comprehensive evaluation model. From the obtained results it could be concluded, that the European market is supplied by consecutive shipments of bulk material of synthetic cannabinoid (collection of several individual synthesis batches) in periods of several month. This material is then divided amongst the European intermediaries for further distribution. For each individual synthetic cannabinoid, a single manufacturer is expected, producing pure material in batch sizes between 5-10 kg.

## Zusammenfassung

Das relative junge Phänomen der neuen psychoaktiven Substanzen (NPS) stellt sowohl die europäischen kriminaltechnischen Institute als auch die Gesetzgeber vor eine Herausforderung. Im Vergleich zu den klassischen Drogen wie Amphetamin, Heroin oder Kokain ist die Informationsbasis über Herkunft, Herstellung und Vertrieb von NPS relativ gering und auch schwer zu erweitern, da bisher nur wenige Synthese/Produktionsstätten von NPS sichergestellt werden konnten. Aus diesem Grund wird in dieser Arbeit das Potenzial verschiedener Analysetechniken erforscht, um alleinig aus Sicherstellungen und Online-Testkäufen von NPS-Produkten so viele strategische Informationen wie möglich über die zugrunde liegenden Produktions- und Vertriebsnetze zu gewinnen. Synthetische Cannabinoide sind die in Deutschland am häufigsten vorkommende NPS Unterklasse und wurden daher in den hier vorgestellten Arbeiten als Zielsubstanzen ausgewählt.

Der methodische Schwerpunkt dieser Arbeit lag in der Entwicklung, Validierung und Anwendung eines Profiling-Verfahrens für synthetische Cannabinoide. Ziel waren (1) die Erfassung der chromatographischen Verunreinigungssignaturen (Einblicke in die Herstellungsmethoden einschließlich Syntheseweg, Edukte, Reagenzien oder Chargengrößen) und (2) die Messung der Stabilisotopen-Verhältnisse der Hauptkomponente (Links zwischen Proben die aus einem Syntheseansatz kommen oder mit denselben Vorläufersubstanzen hergestellt wurden).

Obwohl verschiedene synthetische Cannabinoide in dieser Arbeit erwähnt werden (z.B. Cumyl-PeGaClone, Cumyl-5F-PINACA oder 5F-PB-22), lag der methodische Schwerpunkt auf dem in 2015/2016 in Deutschland am weitesten verbreitete synthetisch Cannabinoid MDMB-CHMICA. Anhand von einer Großsicherstellung des luxemburgischen Zolls von vierzig einzeln verpackter 1 kg Proben und einundzwanzig weiteren beschlagnahmten und testgekauften Proben von reinem MDMB-CHMICA wurde die allgemeine Methodik für das Verunreinigungs-Profiling entwickelt. Als zentrales Element diente eine Flash-Chromatographie, mit der die Verunreinigungen von der Hauptkomponente getrennt werden konnte. Die wieder zusammengeführten Verunreinigungsfractionen wurden dann mittels Hochdruck-Flüssigkeits-Chromatographie gekoppelt an Massenspektrometrie gemessen und per multivariater Datenanalyse ausgewertet, um zwischen einzelnen Syntheseansätzen zu unterscheiden. Die vergleichende Analyse basierte auf den semi-quantitativen Signalen von fünfzehn Schlüsselverunreinigungen, die zuvor mittels hochauflösender Massenspektrometrie und Kernspinresonanzspektroskopie charakterisiert wurden. Zusätzlich wurden kontrollierte Synthese von MDMB-CHMICA durchgeführt, um die allgemeinen Schwankungen der Verunreinigungssignaturen zwischen mehreren Synthesen besser zu verstehen. Die Probenvorbereitung wurde für die zwei häufigsten Konsumformen für synthetische Cannabinoide angepasst und oberflächlich validiert: E-Liquids und Kräutermischungen (auch als "Spice-Produkte" bekannt). Zuletzt wurde der gesamte verfügbare Satz an 118 Spice-Produkten von MDMB-CHMICA untersucht und die Verunreinigungssignaturen zusammen mit den Isotopenverhältnissen in einem kombinierten Modell ausgewertet. Die zentralen Rückschlüsse dieser Studien waren, dass der europäische Markt durch aufeinanderfolgende Lieferungen von reinem synthetischen Cannabinoid in Zeiträumen von mehreren Monaten beliefert wird. Dieses Material wird dann zur weiteren Verteilung auf die einzelnen europäischen Zwischenhändler aufgeteilt, die es zur Produktion der Spice-Produkte verwenden. Für jedes einzelne synthetische Cannabinoid wird ein einziger Hersteller erwartet, der reines Material in Ansatzgrößen zwischen 5 und 10 kg produziert.

# 1. Introduction

## 1.1 Illicit drugs

A variety of different substances can be used to create a state of intoxication without the intention of any therapeutic benefit, of which the most are described in our legislation system as illicit drugs. They can be divided into four larger groups: opioid-type, cocaine, cannabis-type and synthetic drugs like amphetamine-type stimulants (ATS) or new psychoactive substances (NPS).

According to the recent World Drug Report of 2018 by the United Nations Office on Drugs and Crime (UNODC), approximately 5.6 per cent of the global population between the ages of 15-64 years are estimated to have used drugs at least once in 2016. Eleven percent of these people suffer from a drug use disorder, where regular consumption poses a threat to their health. In 2016, roughly 452,000 people died as a result of drug consumption, accounting for 0.83 % of death from all causes<sup>1</sup>. Only 31.8 % of those deaths were associated with the direct drug use (e.g. overdoses, marked green in Figure 1). The rest can be attributed to the transmission of diseases with fatal outcome such as HIV or hepatitis C through unsterile injection practices.

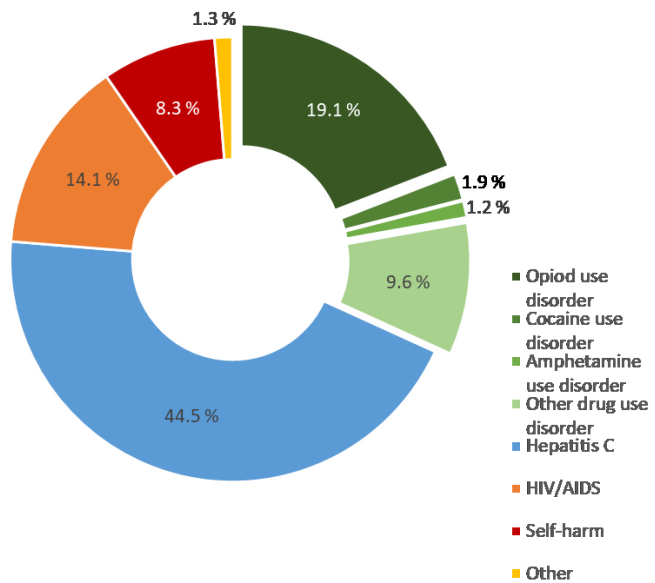


Figure 1: Leading causes of death attributable to drug use, 2016<sup>1</sup>. Data taken from the World Drug Report 2018<sup>2</sup>

The consumption behaviour of drugs is highly dependent on their corresponding geographical availability. In Columbia, for example, approximately 0.7 % of the population between the ages of 15-64 years are estimated to have used cocaine in 2013, whereas the annual prevalence of ATS was below 0.1 %<sup>2</sup>. This data is not surprising as Colombia has the highest density of coca plantations and an estimated annual cocaine production of 866 tons in 2016 (solely based on the estimated coca leaf production). Similarly, opiates had the highest prevalence in the region around the near and middle east/southwest Asia, as 86% of the globally seized opiate volume in 2016 came from this region, especially Afghanistan, Iran and Pakistan.

### 1.1.1 Classical drugs

The classification of drugs as “classical” is derived from their long-term persistence (at least since the 20<sup>th</sup> century) and high prevalence on the worldwide drug market. Furthermore, they are listed in the “1961 Single Convention on Narcotic Drugs”<sup>3</sup> or the “Convention on

Psychotropic Substances” from 1971<sup>4</sup>. Some of the most prevalent examples for classical drugs are shown in Figure 2 and will be described in detail.

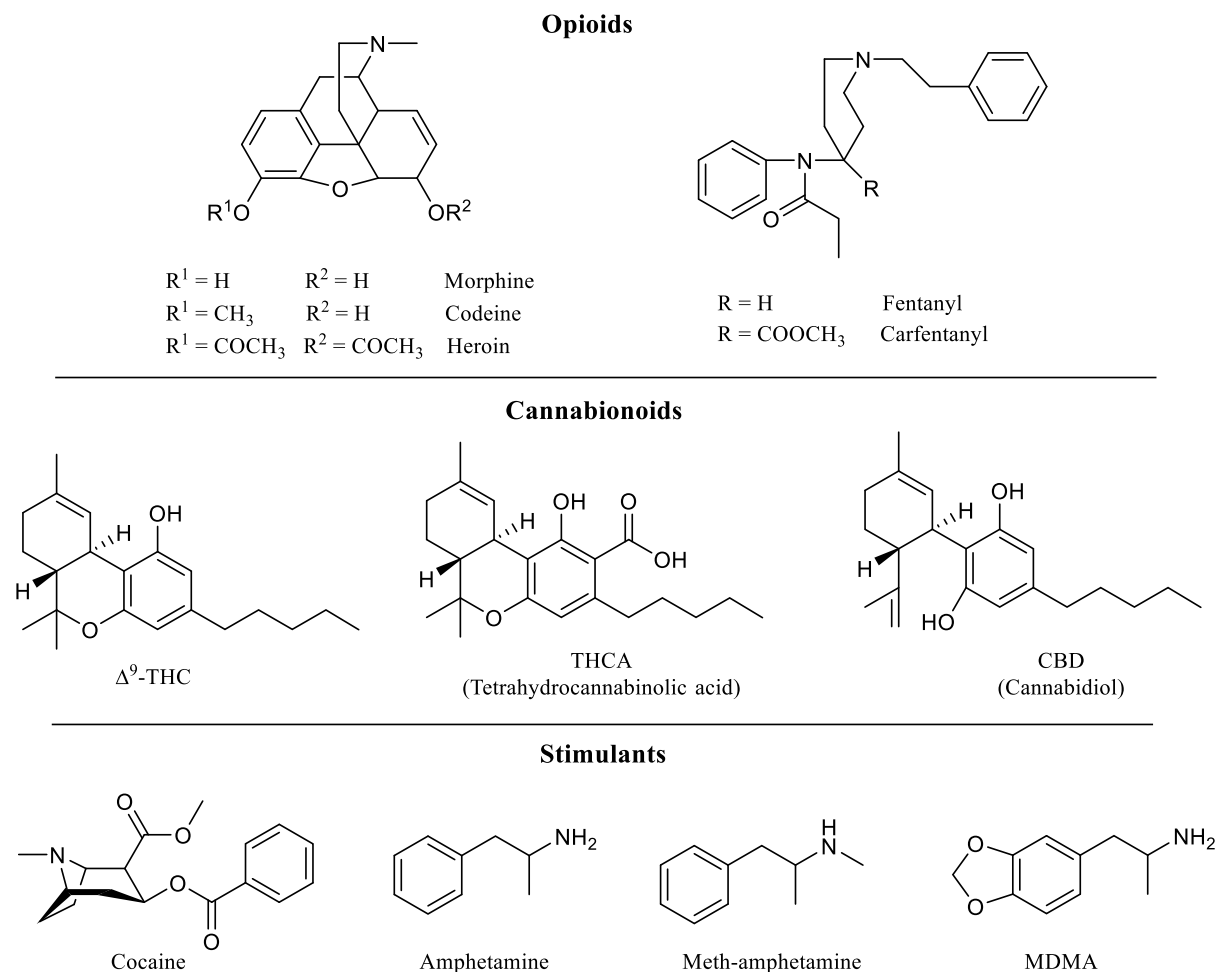


Figure 2 Structural formulas of selected opiates, cannabinoids and stimulants

**Opioids** is a term for a variety of chemically diverse substances, which bind to the opioid receptors in the human gastrointestinal tract and central and peripheral nervous system. The three major opioid receptor types are:  $\mu$  (MOP),  $\kappa$  (KOP) and  $\delta$  (DOP). The pharmacological effects of opioids range from respiratory depression, constipation, a strong sense of euphoria to analgetic effects including sedation, accompanied by a severe physical and psychological dependence with regular consumption<sup>5</sup>. Endogenous opioid receptor agonists are endorphins<sup>6</sup> or enkephalins<sup>7</sup>, first identified in 1975. However, the use of opium, derived from the dried latex of the opium poppy (*Papaver somniferum*), dates back a few hundred years BC<sup>8</sup>. The black, resinous mass is a mixture of various natural opium alkaloids such as morphine, codeine or narcotine<sup>9</sup>. By simple chemical manipulation of these alkaloids, semi-synthetic opioids can be manufactured such as diacetylmorphine (heroin), naloxone or oxycodone, which were and still are used for medicinal purposes<sup>10</sup>. In the 20<sup>th</sup> century, the first synthetic opioids were synthesized, with fentanyl and its analogues being the most frequently used in clinical practice but also the most sociologically problematic due to their high analgesic properties (100-10000 times more potent than morphine<sup>11</sup>, Table 1). Around 2015, drug dealers in the US started to “cut” their powder drugs such as heroin with fentanyl and its analogues, without any notice for



the consumer, which lead to an increased rate of fatal overdoses, especially recognizable in the increase of drug related deaths by 21 %, as recorded in the US between 2015 and 2016<sup>2</sup>.

Table 1 Analgesic potency of a selection of opioids, referenced to morphine = 1

Opioid	Rel. analgesic potency <sup>12</sup>
Carfentanyl	10000
Sufentanyl	1000
Fentanyl	100-300
Diacetylmorphin (Heroin)	1-5
Oxycodon	1.5-1.8
Methadon	1.5
Morphine	1
Codeine	0.2
Tramadol	0.05-0.07

**Cocaine** (benzoylecgonine) is a strong stimulating drug, extracted from leaves of the coca plant (*Ethroxylum coca*). With 1,129 tons seized in 2016, it takes the second place in terms of globally trafficked volume<sup>2</sup>. Generally, it is sold as white powder in form of a water-soluble hydrochloric salt and consumed by snorting or injection into a vein. After consumption, it inhibits the reuptake of dopamine, noradrenaline and serotonin into the presynaptic membrane, which leads to an exaggerated euphoria, increased activity and a feeling of invincibility<sup>13</sup>. As for the opioids, already a short-termed regular consumption of cocaine can lead to psychological and later to physical dependency<sup>14</sup>.

**Cannabis** includes a variety of different products and preparations that can be won from the Cannabis plant (*Cannabis sativa*). The most popular forms of consumption are the dried flower and subtending leaves of the female plant, also called marijuana, and concentrated cannabis resin, called Hashish. It is by far the most used drug amongst the general population with approximately 3.9 % annual prevalence in 2016, trend increasing due to the continuing legalization in various countries<sup>2</sup>. It comprises for the largest seized volume with 6,313 tons in 2016 (herb and resin)<sup>2</sup>. Common forms of consumption are smoking, vaporizing or oral intake via baked pastries. Until 2002, 483 different natural components including 66 cannabinoids were identified in *Cannabis sativa*<sup>15</sup>, of which tetrahydrocannabinol (THC) was isolated and identified in 1964 as the principle psychoactive ingredient<sup>16,17</sup>. Cannabinoids, including several endocannabinoids, act as agonist to the cannabinoid receptors 1 and 2 (CB1, CB2), which are located in the human central nervous and immune system and various intestines<sup>18</sup>.

**Amphetamine-type stimulants** are defined as a group of synthetic stimulant substances with a phenethylamine core. Phenethylamine itself is a naturally occurring substance with endogenous analogues like dopamine, the amino acid tyrosine or the hormone adrenaline. The three most prevalent synthetic ATS analogues are amphetamine (**alpha-methyl-phenethylamine**), methamphetamine (**N-methyl-alpha-methyl-phenethylamine**) and ecstasy (3,4-methyl

enedioxymethamphetamine, MDMA) with an overall globally seized volume of 242 tons in 2016<sup>2</sup>. Their psychological and physiological effects mimic those of the endogenous substances to a certain level and range from euphoria, increased activity and energy to organ damages, anxiety and depression, coherent with a quickly developing dependency<sup>19</sup>. Table 2 lists the receptor binding affinities of amphetamine, methamphetamine and MDMA to dopamine (DA), nor-adrenaline (NE) and serotonin (5-HT) receptors for neurotransmitter release and transporter proteins for the corresponding re-uptake<sup>20</sup>. The data shows, that amphetamine and methamphetamine are both more potent releaser and uptake inhibitors of DA and NE, whilst MDMA binds more selectively to 5-HT receptors (low molarities indicate a high binding affinity).

Table 2 Affinity of the three most prevalent ATS to synaptic receptors and transporter proteins. Dopamine (DA), nor-adrenaline (NE), and serotonin (5-HT)

Drug	Release IC <sub>50</sub> (nM ± SD) <sup>20</sup>			Uptake inhibition K <sub>i</sub> (nM ± SD) <sup>20</sup>		
	DA	NE	5-HT	DA	NE	5-HT
(+)-Amphetamine	24.8 ± 3.5	7.07 ± 0.95	1765 ± 94	34 ± 6	38.9 ± 1.8	3830 ± 170
(+)-Methamphetamine	24.5 ± 2.1	13.3 ± 0.7	736 ± 45	114 ± 11	48.0 ± 5.1	2137 ± 98
(±)-MDMA	376 ± 16	77.4 ± 3.4	56.6 ± 2.1	1572 ± 59	462 ± 18	238 ± 13

## 1.2 New psychoactive substances (NPS)

The term “new psychoactive substances”, formerly entitled as “designer drugs”, is relatively young and was defined by the council of the EU<sup>21</sup> to create a terminology for new, recreational synthetic drugs. NPS are substances that have no or only a limited therapeutic value but pose a comparatively serious threat to public health. They are not listed in the “1961 Single Convention on Narcotic Drugs”<sup>3</sup> or the “Convention on Psychotropic Substances” from 1971<sup>4</sup>. However, the majority of NPS and early designer drugs were specifically designed to mimic the effects of the established classical drugs and at the same time circumvent existing legislative regulations. Summarizing by effect group, synthetic cannabinoids, or more precisely synthetic cannabinoid receptor agonists, are the most prevalent group of NPS and the main topic of this thesis. They are sold either in pure form (mostly powder) as so-called “research chemical” (RC), dissolved into a liquid matrix of glycerine and propylene glycol as E-liquids (EL) or laced onto an otherwise inherent herbal matrix, called “Spice-Product” (SP)<sup>22</sup>. After consumption, they produce similar effects as Cannabis-type drugs. The second largest group are stimulants, often sold as crystalline “bath salts” or in tablet form, including derivatives of phenethylamines, cathinones, aminoindanes and piperazines, mimicking the effects of classical drugs such as MDMA or amphetamine. Further less prevalent sub-groups are hallucinogens (psychedelics), dissociatives, sedatives and synthetic opioids. Several NPS yet remain unclassified, as their effects on the human body are highly diverse and do not fit in any of the existing groups.

Although the NPS phenomenon is more a concern of the 21<sup>st</sup> century, the appearance of novel substances on the drug market is not new. Two prime examples were the distribution of the synthetic opioid “China White” (α-methylfentanyl)<sup>23</sup> in 1979 or MDMA<sup>24</sup> in the mid-1980s. These substances were originally developed by Janssen Pharmaceutical and Merck, respectively, in search for new therapeutic medication years before their appearance as

recreational drugs<sup>25,26</sup>. In the 1990s, Alexander and Ann Shulgin published their books *PiHKAL*<sup>27</sup> and *TiHKAL*<sup>28</sup>, describing the detailed synthesis routes, bioassays and dosage recommendations of overall 234 phenethylamine and tryptamine derivatives, most of which they discovered themselves. The origin of several NPS can be found in the literature (like these two books), old patents or publications of the pharmaceutical industry, listing and claiming the broadband synthesis of potential medication. NPS manufacturers are expected to browse the corresponding literature for the most promising candidates and synthesize them, in original form or with slight structural modifications. Until 2008, primarily new representatives of phenethylamines and tryptamines were reported for the first time to the Early Warning System (EWS) of the EU. However, the continuing globalisation and availability of cheap precursor components and chemical synthesis opened the European market for manufacturers in emerging industrial countries, like China or India. Starting in 2007/2008, one or more of these manufacturers seemed to have discovered the potential of the NPS market and started to produce a variety of substances, previously never observed on the drug market, e.g. synthetic cannabinoids or cathinone derivatives. The appearance of new substances and even completely new substance-classes continued to increase consecutively in number each year, to more than 670 new substances until 2017, as monitored by the European Monitoring Centre for Drugs and Drug Addiction (EMCDDA) (Figure 3)<sup>29</sup>.

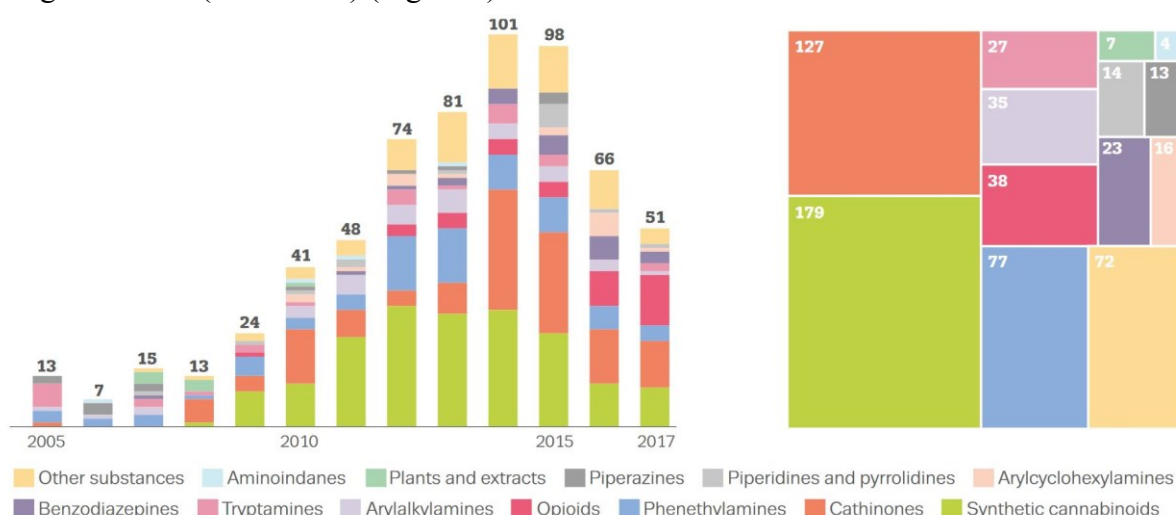


Figure 3: NPS reported to the EWS for the first time 2005-2017: per year (left) and per category (right). The graphic is taken from the EMCDDA<sup>29</sup>.

### 1.2.1 Arising legal challenges from a German perspective

In Germany, the two most important laws for the regulation of pharmaceutically active substances are the Medicinal Products Act (*Arzneimittelgesetz*, AMG)<sup>30</sup> and Narcotic Drugs Act (*Betäubungsmittelgesetz*, BtMG)<sup>31</sup>. The AMG regulates the production and distribution of non-precarious and precarious pharmaceuticals. The latter are defined in §5 of the AMG as substances, “which are reasonably suspected to cause harm beyond a scientifically accepted level, even when they are applied as intended”. “It is prohibited to put precarious pharmaceuticals into circulation”. The BtMG defines substances as narcotics, which are listed in one of the three annexes with their corresponding IUPAC nomenclatures. Compared to the AMG, with its generic definitions, the BtMG is less flexible and requires active changes of the

law (Betäubungsmittelrechts-Änderungsverordnung, BtMÄndV) to include new substances in the list of narcotics.

In the early stages of the phenomenon, highly prevalent and harmful NPS were submitted to the BtMG and further treated as narcotics. Since such a change in legislation was made public in good time before it came into force, it was easy for NPS sellers to convert their product portfolio to other substances with slight chemical modifications, e.g. an additional methyl group, and thus circumvented possible future prosecution through the BtMG. However, the trade of NPS could be charged according to the sentences stated in the AMG, as they were defined as precarious pharmaceuticals. This was no longer possible after a ruling of the European Court of Justice in July of 2014, creating a criminal liability gap for all those NPS not yet included in the BtMG. In the following two years, even multiple changes of the BtMG could not adequately respond to the situation. In November 2016, the generic New Psychoactive Substance Law (Neue-psychoaktive-Stoffe-Gesetz, NpSG) came into force in Germany, regulating entire substance groups instead of single substances. This concerns synthetic cannabinoids and 2-phenethylamine derived compounds, including cathinones. Thenceforward, the trade, marketing, manufacture, transfer (import, export or transit) and acquisition of these substances was prohibited. However, even this generic approach is subject to certain limits and can be circumvented. Two prime examples are the synthetic cannabinoid MDMB-CHMCA and CUMYL-PeGaClone (Figure 5), with a carbazole and gamma-carboline-1-on as core structure, respectively, which were not yet covered by the NpSG at that time but are now implemented via a recent amendment.

### 1.2.2 Marketing and distribution

Possibly, under the cover of large chemical companies in even larger industrial areas, NPS can be produced in high chemical purities with sophisticated instrumentation. The bulk material is then shipped by air or sea to European vendors, who further process the pure material into their final formulations, e.g. as Tablets or SP. In the mid-2000s at the beginning of the phenomenon, the finished products were mainly assessable through so-called head shops, which were primarily visited by customers who had a general idea of what they want to buy. However, a face-to-face confrontation could be a threshold for some potential but inexperienced new customers, as a personal drug purchase is usually associated with shady individuals and places. The use of online-shops as alternative eliminates this "danger factor" through a higher degree of anonymity and opened the market to a broader crowd that can safely shop from their home-PC<sup>32</sup>. Additionally, online advertisement via social networks, video channels or simple pop-ups is more effective in reaching a larger crowd than mouth-to-mouth propaganda<sup>33</sup> between individuals. It is no surprise that in the peak of the NPS phenomenon in the mid-2010s the number of openly available online shops grew drastically<sup>34</sup>. Certainly, for NPS the use of the internet as advertising and distribution medium was one of the secrets to success.

### 1.2.4 Risks

Several health risks are associated with the consumption of NPS<sup>35</sup>. The consumer never knows which or how many substances are actually contained in his purchased product. Although the same product was purchased at one month's distance in the same internet-shop, it is quite possible that a completely different synthetic cannabinoid with potentially 10 to 100 times

increased effectiveness is included. This was the case for the SP “Lava Red” in 2012<sup>36</sup>, which lead to a wave of overdoses. Similarly, an SP purchased multiple times may contain varying amounts of cannabinoid due to poorly controlled production by the manufacturer. Additionally, a product can contain more than one NPS, which might interact in unpredictable manner, especially in combination with additional consumption of alcohol or over the counter medication. As the inexperienced consumer expects a product of consistent quality and psychotropic effectiveness, already one of these variations can easily lead to an overdose after consumption of his regular unit. Various report of hospitalized intoxications and death related to NPS can be found in the literature<sup>37-40</sup>.

## 1.3 Synthetic cannabinoid receptor agonists

### 1.3.1 History

The effects of cannabis consumption on the human body and mind are well known for at least a few thousand years, although rather by consumption reports than scientific data. The discovery of the cannabinoid receptor 1 (CB1) in the mammalian brain by Devane et al.<sup>41</sup> in 1988 was a major breakthrough in cannabinoid research. Through mapping experiments via the radio-labelled highly potent synthetic cannabinoid CP-47,497<sup>42</sup> (named after Charles Pfizer, Figure 5) it was found that the highest concentration of CB1 receptors were located in regions responsible for mental and physiological processes. CB2 was discovered by Munro et al.<sup>43</sup> in 1992, which is prevalent throughout the immune and peripheral nervous system, several intestines and the reproductive organs. Identification of the corresponding gene sequences<sup>43,44</sup> enabled scientists to clone the receptors for in-vitro binding studies or to knock out this specific gene sequence in rats for in-vivo studies<sup>45</sup>. Apart from the obvious distribution diversity in the body, it was found that CB1 mediates psychoactivity and CB2 regulates immune responses. Nearly at the same time, Devane et al.<sup>46</sup> and Mechoulam et al.<sup>47</sup> firstly discovered the two endocannabinoids anandamide and 2-arachidonoylglycerol, which function as neurotransmitters in the endocannabinoid system. All these new advances in neurochemistry and the recently won insights in the endocannabinoid system raised the interest of the pharmaceutical industries and led to an increased funding for research projects in this specific field. Their main aim was to provide clinical medication that primarily induces the positive aspects associated with THC consumption, like pain relief or reduced nausea while receiving chemotherapy. First attempts of modifying the structure of THC dates back to the early 1940s<sup>48</sup> and continued through the years with progressively enhanced receptor binding potencies, e.g. CP-47,497 or HU-210<sup>49</sup> (named after the Hebrew University, Figure 5). A completely new class of cannabinoids was invited by Bell and D'Ambra in 1991 during their research for new non-steroidal anti-inflammatory drugs. They synthesized a range of aminoalkylindoles such as WIN-55212<sup>50</sup> (named after Sterling-Winthrop, Figure 5), which is a 20-times more potent CB1 receptor agonist than THC<sup>51</sup>. This research was later picked up by John William Huffman<sup>52</sup> (JWH) and Alexander Makriyannis<sup>53,54</sup> (AM), who specifically designed and optimized a large number of aminoalkylindole synthetic cannabinoid receptor agonists, recognizable through their name shortcuts followed by a number like JWH-018 or AM-2201 (Figure 5). In the following years, multiple publications and patents were published, extending the range of structurally diverse synthetic cannabinoids<sup>55-58</sup>.

### 1.3.2 Receptor activity

The CB1 and CB2 receptor binding affinity of synthetic cannabinoids is measured via a competitive binding assay reported by Rinaldi-Carmona et al.<sup>59</sup> and Campton et al.<sup>60</sup>. Radiolabelled [<sup>3</sup>H]SR141716A or [<sup>3</sup>H]CP 55,490 is incubated with CB1 or CB2 receptors. The cannabinoid to be tested is added in increasing concentration until 50% of the radiolabelled agonist is displaced. This so-called specific inhibitory concentration (IC<sub>50</sub>) can be used to calculate the ligand receptor activity K<sub>i</sub> (in nM) via the Chen-Prusoff equation<sup>61</sup>:

$$K_i = \frac{IC_{50}}{1 + \frac{[L]}{K_d}}$$

[L] Concentration of radiolabelled ligand

K<sub>d</sub> Equilibrium dissociation constant for radiolabelled ligand

Low K<sub>i</sub> values indicate a high binding affinity of the cannabinoid to a receptor and vice versa. Most of the synthetic cannabinoids were measured for their CB1 and CB2 binding affinities, either by the inventors themselves, to test their potential use as a pharmaceutical, or by forensic scientists to estimate how effective a substance is as recreational drug. Table 3 shows a selection of K<sub>i</sub> values for THC and prevalent synthetic cannabinoids.

Table 3: List of K<sub>i</sub> values for CB1 and CB2 receptors of a selection of cannabinoids

Substance	K <sub>i</sub> CB1 (nM)	K <sub>i</sub> CB2 (nM)
Δ <sup>9</sup> -THC	41 ± 2 <sup>60</sup>	36 ± 10 <sup>60</sup>
WIN-55,212	1.9 ± 0.1 <sup>62</sup>	0.28 ± 0.16 <sup>62</sup>
JHW-018	9.00 ± 5.00 <sup>63</sup>	2.94 ± 2.65 <sup>63</sup>
AM-2201	1.0 <sup>53</sup>	2.6 <sup>53</sup>
Cumyl-5F-PINACA	8.53 ± 0.04 <sup>64</sup>	9.12 ± 0.12 <sup>64</sup>
MDMB-CHMICA	0.410 ± 0.141 <sup>65</sup>	0.354 ± 0.050 <sup>65</sup>
MDMB-CHMCZCA	5.75 ± 1.65 <sup>65</sup>	6.67 ± 1.40 <sup>65</sup>
Cumyl-PeGaClone	1.37 ± 0.24 <sup>66</sup>	2.09 ± 0.33 <sup>66</sup>

### 1.3.3 Systematic naming

In general, chemical structures of modern synthetic cannabinoids show a recurrent pattern that can be categorized into four major components: core, tail, linker and linked residue. For several species, the initial names were given by the drug distributors for marketing purposes. Prime examples are AKB-48 (Figure 5) or 2NE1, which are both popular Asian girl bands, or XLR-11, which is a rocket fuel developed in the US. To cope with the growing number and diversity of substructures, the EMCDDA introduced a systematic naming approach using abbreviations of the corresponding IUPAC name in the following order:

Linked residue - TailCoreLinker

This nomenclature enables the experienced reader to derive a chemical structure, or at least characteristic substructures, from the name of a compound although the substance is new to him. Figure 4 provides an example for the formerly mislabelled 5F-ADB.

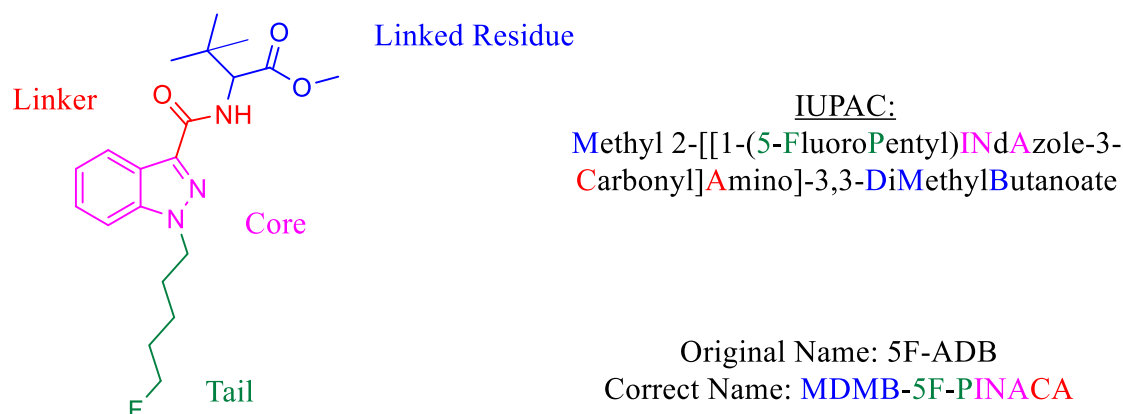


Figure 4: Example for the systematic naming of synthetic cannabinoids according to its structure

### 1.3.4 Structural diversity and appearance on the drug market

Figure 5 shows the original chemical structure of  $\Delta^9$ -THC and a selection of classical and modern synthetic cannabinoids. Only a small portion of the overall published synthetic cannabinoids were found on the drug market. JWH-018 and the C8-analogue of CP-47,497 were the first to be identified in herbal smoking mixtures in 2008<sup>22,67</sup>. These were followed by multiple other aminoalkylindoles from JWH and AM with a methanone linker group and aliphatic linker residues. In the early 2010s, esters (5F-PB-22<sup>68</sup>) and carboxamides (APICA<sup>69</sup>) were implemented as linkers. Also the first indazole core structures were observed (APINACA<sup>69</sup>). The following generation of synthetic cannabinoids were mainly aminoalkylindoles and indazoles with amino acids as linker residues as stated in the patents from Buchler et al.<sup>56</sup> (e.g. ADB-FUBINACA<sup>68</sup> or AB-PINACA<sup>70</sup>). Less prevalent were structures with 4-fluorophenyl-1H-pyrazole (AB-CHMFUPPYCA<sup>71</sup>) or azaindole core (Cumyl-5F-P7AICA<sup>72</sup>). Most recently, two cannabinoids with carbazole (MDMB-CHMCZCA<sup>73</sup>) and gamma-carboline-1-on core (Cumyl-PeGaClone<sup>66</sup>) were identified. In the coming years, other structures might emerge on the market that were not yet in focus, but for which the scientific basis already exists in patents and publications like azaindazoles<sup>74</sup>, imidazopyridines<sup>75</sup>, pyridine derivatives<sup>76</sup> or other bicyclic and spirocyclic compounds<sup>77</sup>.

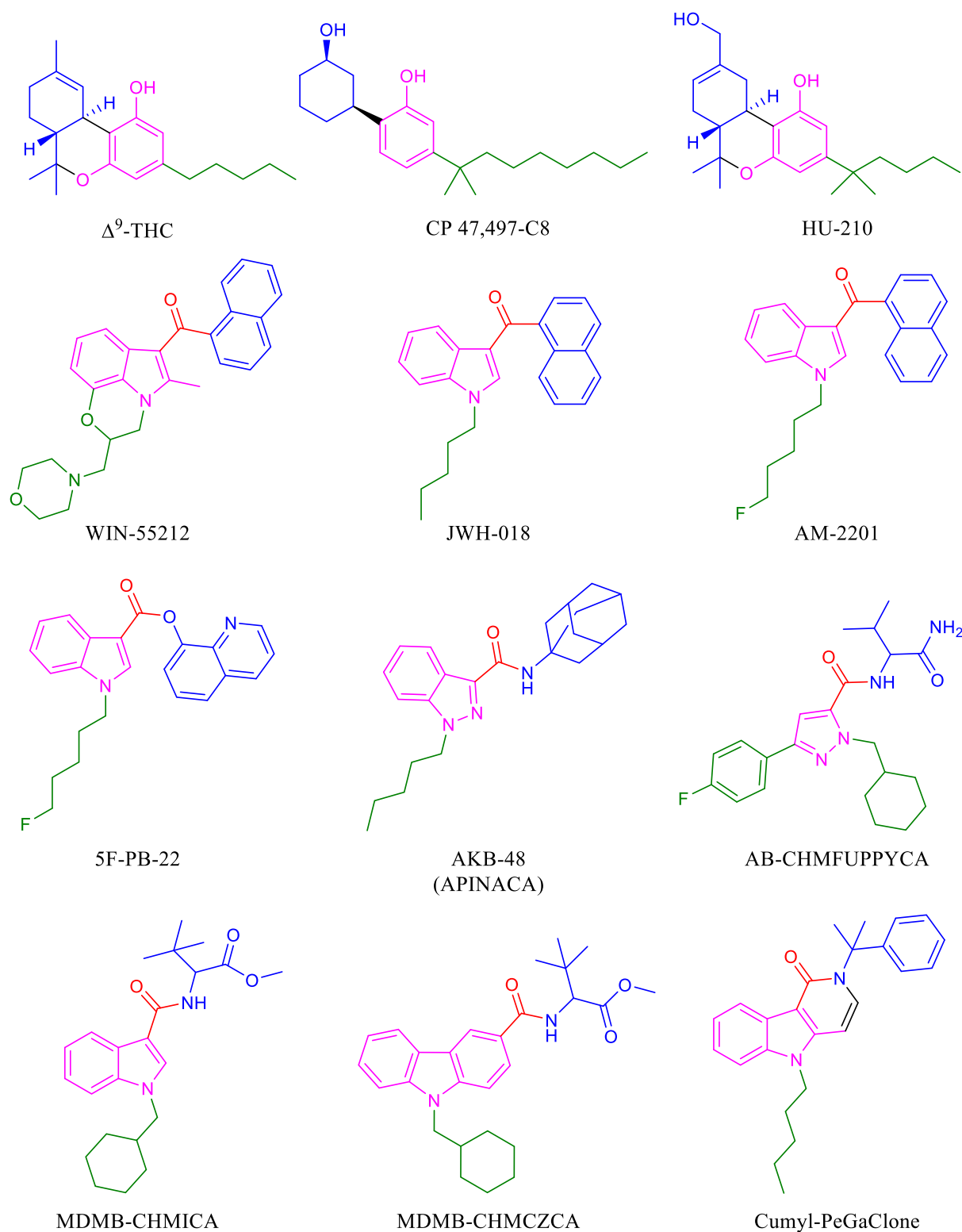


Figure 5: Structural formulas of THC and a selection of classical and modern synthetic cannabinoids. Colouring of the individual molecule structure was done according to the same code as Figure 4 (Linked residue - TailCoreLinker) to highlight the structural similarities between the different types of cannabinoids.

### 1.3.5 Administration forms

In their pure form, synthetic cannabinoids are either solids or resins. Although it might be possible to consume the pure material via snorting or insertion into a vein, the most common mode of admission is by inhalation (smoking). The first products on the market were herbal



mixtures, so called “Spice-Products” (Figure 6) named after one of the first broadly available brands “Spice”<sup>22</sup>. The distribution of synthetic cannabinoids as herbal formulation is only logical, providing the customers with a familiar form of consumption with comparable effects to cannabis. One or more synthetic cannabinoids are dissolved and laced onto inherently inactive plant material such as dried Damiana (*Turnera diffusa* Willd. Ex Schults) or strawberry leaves in concrete mixers. Aliquots of the bulk material are then packed into aluminized plastic sachets with approximately 3 g of herbal material. The sachets are printed with various logos and brands, with the intention to attract particularly young consumers and ensure recognition. In some cases, the list of alleged ingredients (mostly herbal material, more rarely a synthetic cannabinoid) is stated on the labels with warnings like “not for human consumption”. As the production process of SPs, including contained cannabinoids and their dosage, are not retraceable by the consumer, it is impossible to deduce the ingredients solely based on the branding or label of the SP.

The growing popularity of e-cigarettes led to an increased demand for ELs. Therefore, it was a matter of time before the first e-liquids with synthetic cannabinoids came onto the market. As advantage over herb-based forms of consumption, they can be consumed at public places without shedding suspicious odours. In most cases, the e-liquid matrix consists of a mixture of propylene glycol (PG), vegetable glycerin (VG) and ethanol with additional aroma compounds and an active substance (e.g. nicotine or synthetic cannabinoids). Cumyl-5F-PINACA<sup>78</sup> was one of the most commonly found synthetic cannabinoid in E-liquids, as it is resinous at room temperature.

Less popular are “fake-hash” products containing synthetic cannabinoids, mimicking the physical form of cannabis hashish.

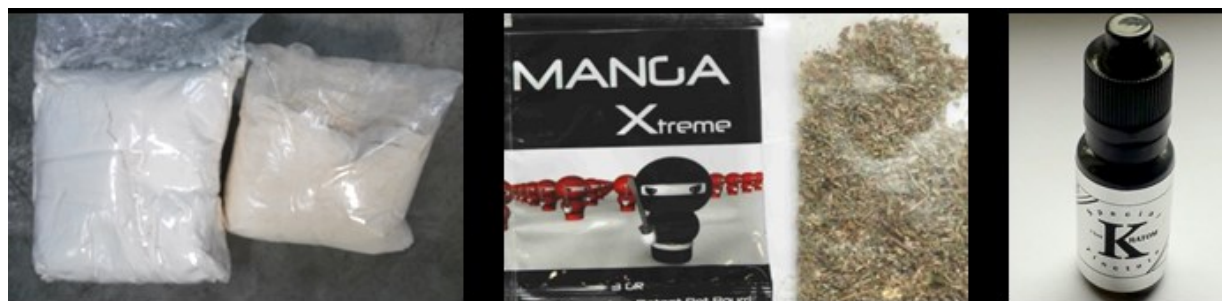


Figure 6: Synthetic cannabinoids can be obtained in three different formulations: as pure “research chemical” in powder form (left), as “Spice-Product”, laced on a herbal matrix (middle), or as e-liquid, dissolved in a matrix of propylene-glycol and glycerine (right)

## 1.1 Forensic drug profiling

Forensic drug profiling describes the comparative characterization and interpretation of the physical and chemical properties of a sample<sup>79</sup>. It is used to complement law enforcement investigative work in specific cases and can increase the overall police intelligence on a global scale<sup>80</sup>. Depending on the target issue, drug profiling aids in questions like links between seizures, dealer-user relationships, trafficking routes, geographic origin, manufacturing methods or precursor use<sup>81</sup>.

Drugs with distinct external properties, e.g. ecstasy tablets, can be characterized based on physical parameters as colour, shape, logo or weight. In the case of visually indistinguishable powders, a sample must be characterized chemically according to its qualitative and

quantitative composition of active ingredients, cutting agents, residual solvents, organic synthesis impurities, trace metals or isotopic composition. Various examples can be found for characterization of illicit drugs using different analytical techniques. For organic profiling: headspace (HS)<sup>82</sup> and normal gas chromatography coupled to different detectors (GC)<sup>83-85</sup>, (ultra) high pressure liquid chromatography coupled to mass spectrometry ((U)HPLC-MS)<sup>86</sup>, capillary electrophoresis (CE) coupled to MS<sup>87</sup> or ultraviolet-(UV)-detectors<sup>88</sup>, infrared spectroscopy (IR)<sup>89</sup> or Raman spectroscopy<sup>90</sup>. Profiling of elements was conducted via inductive coupled plasma mass spectrometry (ICP-MS)<sup>91</sup> and atomic emission spectroscopy (ICP-AES)<sup>92</sup>. Information about precursor material or geographic origin could be won by isotopic analysis via site-specific isotope fractionation nuclear magnetic resonance spectroscopy (SNIF-NMR)<sup>93,94</sup> or isotope ratio mass spectrometry (IRMS)<sup>95-97</sup>.

Although characterization is the basic step for comparative analysis as it generates “hard data”, it is directly interrelated with the subsequent interpretation in a self-evaluating and evolving process to determine which data is useful, and which is not. For example, two seizures of ecstasy tablets are compared according to several chemical parameters, isotopic ratios and their colour and shape, of which the latter two are important physical descriptive factors. Analytical measurements then show tight accordance for all chemical and isotopic parameters but not for the colour and shape. In this case, it is likely that the producer used the same powder material but different colorants and punches in his tableting process, which is a valuable information itself. However, interpretation of the data suggests that these two parameters lose their discrimination potential to identify a common source for both seizures. Whether to include or exclude a parameter is always the decision of the forensic scientist and different for each case. The general strategic interpretation of chemical profiling data was categorized by H. Huizer<sup>79</sup> into three levels:

- I        sample A and B, measured on the same day, same instrument
- II       sample A and B compared to other samples
- III      multiple samples compared to each other

At level I, three possibilities are considered:

1. Both samples show very similar signatures, indicating a link. This might be the case when analysing samples that originate from a single batch.
2. They show very different signatures, making a link unlikely. For example, when investigating two samples of different batches or even different synthesis from a single or multiple manufacturer.
3. A situation between 1 and 2, with multiple similarities but also a few clear differences. Many factors can be responsible for this, which the forensic scientist must identify or at least consider. Examples might be a highly consistent working chemist, producing multiple batches with only small inter-batch variations. The post-production handling, e.g. cutting with adulterants, inhomogeneous formulation or storage under stressful environmental conditions (chemical degradation) might have a negative impact and alter the impurity signatures. In addition, the natural variation in the analytical methods have to be considered, especially when analysing low concentrated trace components. The correct interpretation of case 3 necessitates an increase to a level II comparison.

Level II is useful for a level I case 1 scenario, but necessary for case 3. A and B are compared to a set of other samples to better understand the observed variations in impurity signatures and assess their level of uniqueness (to see the bigger picture). When comparing A or B to a set of other unrelated samples, it might be found that differences between A and B are only minor, indicating a link between these two samples, despite their differences. Level II is generally used to aid law enforcement investigative work in specific cases with a limited set of samples, like a seized clandestine laboratory.

Level III aims to identify groups of related samples on a global scale, e.g. a common producer or trafficking networks. An optimal scenario would be that limited amounts of producers manufacture their drugs with individual pathways, making it easy to group samples according to similarities in their chemical signatures. However, in reality multiple producers with varying raw materials in inconsistent synthesis processes can manufacture a single drug. In the worst case, differences between individual batches may be the same magnitude as differences between the individual producers; or different manufacturers produce material with similar chemical signatures by chance. Additionally, in multiple stages of the production or distribution, batches might be mixed for transportation, leading to further blurring of batch specific signatures. This level of comparison is the most complicated and requires great expertise to identify and classify samples. Three cases have to be considered<sup>81</sup>: (1) samples are linked by a common history (the same producer and distribution channels); (2) they are linked by a common source, but have different distribution channels; (3) the same distribution channels but different sources. To grasp the whole complexity of the drug market and its channels by profiling of the final product will hardly be possible as it is too much of a “black box” system. However, by international cooperation between police and forensic institutes, a general intelligence about major drug dealers and centres of drug supply can be gathered.

### 1.2.2 Impurity profiling

Independent of the source of an illicit drug sample, it does not only contain the main component but a mixture of various organic side components. The composition of these components is called impurity signature and dependant on multiple factors like synthesis route, precursor material, synthesis conditions (environmental and experimental), packaging or storing of a samples<sup>81</sup>. The qualitative and quantitative analysis of these side components is called impurity profiling. Of primary interest are those minor and trace components that are directly related to the manufacturing method (synthetic drugs like ATS) or the plant material and its processing (plant-based drugs like cocaine). By comparative analysis of the impurity signatures of multiple samples, links can be established based on the degree of similarity between the individual signatures. For that purpose, GC or LC-MS are the most common analytical tools to separate and analyse complex mixture of organic components<sup>98-101</sup>. For a relatively small sample pool, visual comparison of the peak-pattern in the corresponding chromatograms might provide a sufficient evidential base to identify links between samples. Difficult cases, e.g. drug formulations in complex matrices, require a pre-defined list of target components (key-impurities) that are known to stand in relation with the main component and its manufacturing process. Based on peak integrals for these components, samples can be compared, while ignoring all signals with no discrimination potential, like matrix components or degradation products.

Multiple impurity profiling procedures are established for classical drugs, some even on international basis<sup>102</sup>. Their general procedure consists of a fast liquid-liquid (LLE) or solid phase extraction (SPE) to deplete the main component and matrix components and thus enrich present impurities. These are measured via analytical tools like GC or LC-MS and evaluated via multivariate chemometric models<sup>101,103</sup> and matching of target compound signals against databases of previously measured samples<sup>102,104</sup>. The scientific basis for the validity of these pre-selected “key-impurities” is gathered in experimental procedures. In respect to the court-proofness of links generated through impurity signatures, the relationship of individual impurities to the main component and their stability had to be proven. Additionally, it was necessary to know, at which point differences between sample profiles are significant and what magnitudes of influence can be responsible for these differences. Exemplary studies on classical drugs can be taken from the literature: impurity characterization via MS-fragmentation, high resolution MS (HR-MS) or nuclear magnetic resonance spectroscopy<sup>105-107</sup>; identification of synthesis route specific markers and the overall reproducibility of the chemical profile thorough controlled synthesis<sup>108-111</sup>; impacts of storing conditions, e.g. heat or moisture, on the chemical profile and identification of potential degradation products<sup>112</sup>.

### 1.2.3 Isotopic profiling

Most elements have more than one stable nuclide that do not undergo spontaneous radioactive decay. Speaking of specific elements, these nuclides are called stable isotopes and each element has a specific natural abundance, e.g.  $^{12}\text{C}$ : $^{13}\text{C}$  in a ratio of 98.90:1.10. Measurement of these ratios via mass spectrometry is called isotope-ratio mass spectrometry (IRMS). Through natural isotopic fractionation, the isotope ratios can shift depending on the geographic location or biological ecosystem. For example, through equilibrium fractionation in the water cycle (Rayleigh fractionation<sup>113</sup>), slightly more light water (with  $^1\text{H}$  and  $^{16}\text{O}$ ) evaporates from the ocean than heavy water (with  $^2\text{H}$  and  $^{18}\text{O}$ ), and rains down in the inland and mountainsides. Plants prefer the use of  $^{12}\text{C}$  to  $^{13}\text{C}$  in different ratios, dependant on their corresponding photosynthesis pathways (e.g. C3<sup>114</sup>, C4<sup>115</sup> or CAM<sup>115</sup>). These ratios are then distributed to other living forms through the food chain. Thus, by measuring the isotopic ratios of natural organic material, it is possible to narrow down its geographical origin (with the knowledge of geographic distribution patterns for the specific elements). The same applies for the majority of fine chemicals, as their source was, at some point, a natural product. Although the information about the geographic origin is lost, in some cases it is possible to link synthetic material to a manufacturer, who synthesizes material with a specific isotopic composition in larger scale.

In forensics, this technique has found several applications. The origin of cocaine leaves could be traced back to certain areas of the Andean Ridge<sup>116</sup>. Grouping of diacetylmorphine samples and information on the acetylation agent was won by analysis via GC-IRMS<sup>117</sup>. Several studies are published on the origin of precursor material for amphetamine<sup>97</sup> and methamphetamine<sup>95,96</sup>, including isotopic changes during the synthesis<sup>118</sup>. Collins et al. published the first isotopic analysis of NPS (in particular synthetic cathinones) to link seizures<sup>119</sup>.

### 1.2.4 Project “Spice Profiling”

The main objective of the project SPICE-profiling (JUST/2013/ISEC/DRUGS/AG/ISEC/4000006421) was to increase the knowledge base on the origin, production and supply chain

of NPS. For that purpose, NPS samples from test purchases in internet shops, authentic samples from chemical manufacturers and NPS samples from customs and police seizures were used as an information pool that was extracted by a wide range of analytical methods. The experimental work was carried out by the project coordinator, the Federal Criminal Police Office of Germany and the beneficiaries, the University Medical Center Freiburg and the Institut National de Police Scientifique (INPS) in France, with the aid of several international associated partners.

The systematic test purchases of new products in the whole time-frame of the project allowed precise observation and interpretation of the development of the NPS market, especially in dependence on changes in the legal treatment of single substances or substance classes in the narcotics or medicine acts of European member states. A total of 1120 NPS-containing products (802 SPs, 22 synthetic hashish samples, 45 e-liquids, 89 bath salt samples with synthetic stimulants and 162 RCs) were bought in 108 different internet shops and analytically characterized over 2 years project time. The monitoring activities clearly indicated that products selling evolved with legislation, e.g. a quick replacement cycle after an NPS has been scheduled as a narcotic.

Problems in the detectability of NPS in human bio samples, important for the proof of consumption of NPS related to driving or the surveillance of imprisoned persons or persons in drug control programmes was addressed by metabolism studies of important NPS. After analysis of approximately 13500 urine and 2942 serum samples, a positive response for the presence of NPS metabolites was found in 19 % and 21 % of the cases, respectively. The same trends of legislation dependency and replacement cycles for NPS as observed in the online-shop survey could also be observed via the monitoring of human bio-samples

One of the core activities, also found in the name of the project, was organic impurity profiling including controlled syntheses with focus on synthetic cannabinoids and “Spice-Products” with LC-MS and isotopic profiling by IRMS. The corresponding motivation and output are the main topic of this thesis.

### 1.3 Aims of this thesis

The knowledge about the production and the supply chain of NPS (Figure 7) is very limited and quite different from classic synthetic drugs (amphetamine-type-stimulants) which are typically clandestinely produced in European countries. Most of the NPS are presumably produced by specialized chemical companies in Asia, typically in China. The syntheses of amino alkyl indoles are not very complicated and can be achieved with comparatively inexpensive equipment and chemicals, producing highly pure substances (> 97 % purity). Details of the production, the synthesis routes including the nature of the precursor chemicals and reagents are not known. As most of the published synthesis are only for small-scale production, it is likely that the actual manufacturers evaluated and modified these syntheses to improve the economic aspects and enable up-scaling from laboratory to pilot-plant. The emergence of substances like 5F-PB-22 or MDMB-CHMCZCA, at that date never described in the literature, is another indication for the independence of these producers and proves their willingness to invest resources to develop own products.

The pure material synthesized in Asia is shipped in bulk to Europe and further sold as RCs, SPs or EL (after formulation and repackaging). So far, it has only been possible to draw conclusions about the distribution channels based on police seizures from larger batches (in the kg range)

of pure material (delivered from China to European distributors) and individual seizures and test purchases of RCs, SPs and ELs (from European distributors to single customers). Online-test purchases that had similar sachet designs of SPs or included the same advertising flyers in the delivered packages allowed for initial conclusions about the distribution channels by specific SP producers. However, with increasing popularity of these products, the number of designs increased drastically and different producers started to copy popular brandings like “Jamaican Gold Extreme”, which complicates conclusions about common sources based on these external parameters.

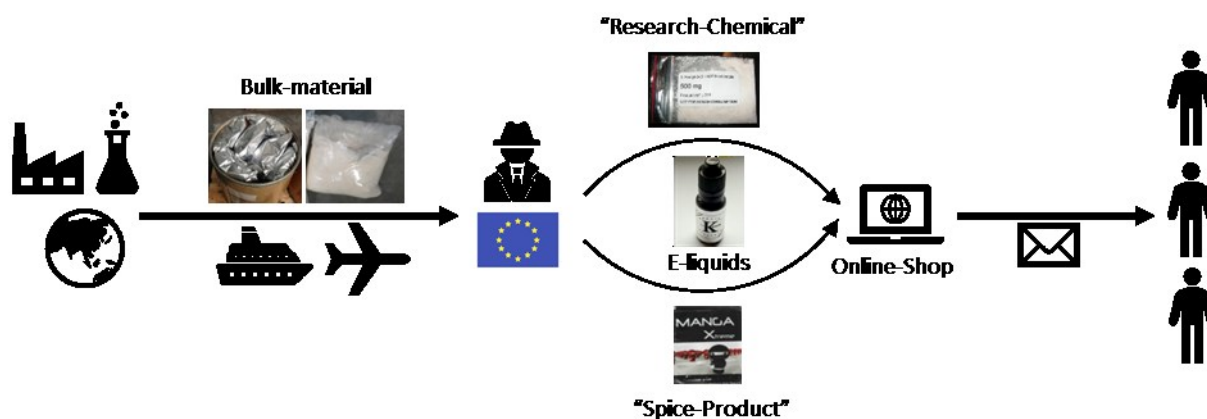


Figure 7: Scheme of the distribution channels of synthetic cannabinoids, starting from the production in China, over the shipment of pure material via air or ship to European distributors, which either sell the pure material as research-chemical, dissolved in an E-liquid matrix or sprayed onto a herbal matrix via online shops. These products can then be ordered in online-shops and are sent to the individual customers by mail.

The aim of this thesis was to obtain as much information as possible about the manufacturing of synthetic cannabinoids and each of the distribution steps (as displayed in Figure 7), based on the forensic analysis of police seizures and test purchases. Analysis of the corresponding products by means of stable isotope analysis and impurity profiling allows linking of seizures based on similarities in their isotopic composition and impurity signatures, and thus revealing potential co-operations between internet shops and might help to understand underlying distribution channels and mechanisms (shops might have the same provider of pure synthetic cannabinoids or they are run by the same person/company). Basic information about the manufacturing, in particular the synthesis pathway, can be obtained by structural identification of marker impurity, as they might be specific for the use of certain educts or coupling reagents. The retro synthesis of potentially identified synthesis pathways under controlled conditions then aid to better understand the overall variations in impurity signatures found in seized material and might provide deeper insights in the procedure of the original manufacturer.

The evaluation of all analytical data is based on the assumption, that a single batch of synthetic cannabinoids carries a specific impurity signature and isotopic composition. It was necessary to prove, that these parameters are maintained even after the synthetic cannabinoids are sprayed onto an herbal matrix or are dissolved in an e-liquid matrix.

### 1.3.1 Research area 1: Development and validation of an impurity profiling

Primary target for the impurity profiling was the synthetic cannabinoid MDMB-CHMICA (methyl (S)-2-(1-(cyclohexylmethyl)-1H-indole-3-carboxamido)-3,3-dimethylbutanoate), which was highly prevalent in Europe in 2015/2016. Although the fast-paced replacement cycle

of synthetic cannabinoids on the NPS market, it was intended to develop an in-depth impurity profiling study for a single, representative synthetic cannabinoid to, more generally, extend the knowledge base on the structure, modi operandi and development of the international NPS and designer drug market and increase the overall police intelligence about this phenomenon.

One major seizure by Luxembourg customs of 40 kg pure cannabinoid, packed individually into 1 kg bags, was available at that time. This material was a perfect sample pool for an impurity profiling study, as the complete material presumably came from a single source and several important aspects about the manufacturing conditions could be worked out:

- Does the material come from one or multiple synthesis batches?
- In the latter case, how many batches are there in total?
- How much material can be produced in a single batch?
- How many different synthesis pathways were used?
- Are there synthesis pathway specific impurities?

As no impurity profiling methodology was published for synthetic cannabinoids so far to answer these questions, the first major aim was to develop and validate a completely new workflow. Several tasks were to be tackled in the process:

#### Sample preparation

Preliminary measurements of pure synthetic cannabinoids showed, that only very few impurities could be detected without any sample preparation. It was necessary to include a preceding extraction step to isolate related impurities from the main component. The commonly used SPE was not specific enough and LLE could not be used, as the majority of synthetic cannabinoids are insoluble in water. Hence, flash chromatography (F-LC), an automated type of preparative column chromatography, was a fitting alternative to selectively cut out the main component from chromatographic run and thus enrich present impurities. This semi-automatic system brings further advantages, like a high reproducibility and precision. It is highly adaptable to a wide range of substances (e.g. via change of columns or eluents) and the separated main component can be further qualified as reference standard or measured via IRMS to generate orthogonal analytical information. Thus, a suitable F-LC method had to be developed and validated to reproducibly isolate related synthesis impurities from the main component.

#### Assessment and characterization of discriminating key-impurities

The next step was to assess suitable impurities, which can be used in a batch-to-batch discrimination. Requirements for these so-called “key-impurities” are that they must originate from the synthesis process of the main active ingredient, are characteristic for each synthesis batch and are stable over time and must not decompose or are a result of decomposition. Multiple semi-quantitative chromatographic impurity signatures of pure seized samples of MDMD-CHMICA were compared and the signals (representing individual substances) with the most discriminating potential (responsible for differences between the samples) were worked out. Measurements were done on an UHPLC-MS rather than GC-MS, as some synthetic cannabinoids are known to dissociate at higher temperatures (e.g. in the GC injector)<sup>120</sup>. The soft ionization via electro-spray ionization (ESI) produces intact molecular ions with a defined mass to charge ratio ( $m/z$ ), which, in addition to the retention time, provides another variable

for data evaluation. Comparison of the LC-MS runs were done by an automated integration algorithm (bucketing) and subsequent evaluation by multivariate data analysis (MDA, see chapter 2.3.3).

To prove, that the assessed key-impurities are related to the main component, they were structurally characterized by HR-MS<sup>3</sup>. Through precise fractionation of the F-LC run, it was possible to isolate and enrich single impurities for unambiguous structural elucidation via NMR.

#### Adaptability to different matrices

A requirement for the sample preparation by means of F-LC was, that it is also possible to work up samples that were previously extracted from a matrix like SP or EL. For both matrices, a reproducible procedure had to be developed and validated to extract the main component and all related synthesis impurities, while separating the majority of matrix. Links between the impurity signatures of synthetic cannabinoids in SP or EL, in combination with corresponding meta-data (e.g. the name of online shop or the date of purchase), can be a powerful tool to obtain information about the underlying production and distribution network.

#### Controlled synthesis

By interpretation of structural elements of the previously identified and structurally characterized key-impurities of MDMB-CHMICA, hints about the synthesis pathway and reagents used by the original manufacturer could be obtained. Replicate synthesis were carried out for the synthetic cannabinoid MDMB-CHMICA, some following the general instructions from Buchler et al.<sup>56</sup> for the corresponding indazole analogue and other with multiple modifications of the reaction parameters (different coupling reagents, temperature, time) according to the conclusions drawn from the previously characterized synthesis impurities in the seized samples. The major intentions behind this approach were to reproduce some of the impurities found in the seized samples to draw conclusions about the synthesis of the original manufacturer, to better understand the significance of variations in impurity patterns and the overall reproducibility of the synthesis. For all controlled synthesis, the chromatographic signatures were recorded on UHPLC-MS and subsequently compared to work out pathway-specific impurities.

### **1.3.2 Research area 2: Isotopic profiling**

#### Isotope ratios of synthetic cannabinoid precursors

Nearly all modern synthetic cannabinoids appearing on the drug market can be synthesized using a modular system, exchanging single parts of the molecule like the core, linker, aliphatic residue or the linked residue (similar to the four parts in the naming of synthetic cannabinoids in Figure 4). Although the exact synthesis procedures for synthetic cannabinoids of the original manufacturers is yet unknown, it is expected that at least three synthesis steps are taken: the coupling of the aliphatic residue to the core and the coupling of the bridge residue to the linker (and thus the core), necessitating at least three individual precursor substances.

One of the aims in this work was to use IRMS to assess the diversity of isotopic data in precursor material purchased from different global vendors, to better judge the isotopic variations in the final products. In the case, that all globally available material of a single precursor such as tert-



leucine methyl ester (TLME) is produced by a single manufacturer with no isotopic diversity between batches, IRMS loses approximately 1/3 of its discrimination power for all synthetic cannabinoids with a TLME residue. However, if precursor substances from different vendors show a highly diverse isotopic composition, the degree of certainty increases for assigning two synthetic cannabinoids with similar isotopic composition to a common source, solely based on the low probability of two unrelated manufacturers producing material with similar isotopic composition using educts from different sources.

#### Isotope ratios of synthetic cannabinoids

The isotope ratios for a variety of synthetic cannabinoids in pure form and extracted from SPs were measured via IRMS to generate links between seizures and online-test-purchases. Each batch of synthetic cannabinoids synthesized with a specific combination of precursor substances should also carry a specific isotopic composition, provided no excessive isotopic fractionation is induced in the synthesis. After delivery to the European market and formulation in the forms of consumption (RC, SP or EL), by IMRS analysis it might be possible to trace back and group seized and online-test purchased samples to their original manufacturer and possibly even synthesis batch. By implementing metadata such as date of seizure or the source in the data evaluation, first insights in the distribution pathways or underlying networks between the original manufacturers and/or the European online-shops might be revealed.

As for the impurity profiling study, it was necessary to validate that the sample preparation like extraction and clean-up via F-LC had no influence on the isotopic composition of the main component.

#### **1.3.2 Research area 3: Linking seizures and online-test-purchases**

After development and validation of the sample preparation and assessment and characterization of suitable key-impurities, the impurity signatures and isotopic composition for all available seized and test-purchased samples of MDMB-CHMICA were recorded and evaluated in a comprehensive model. Again, the intention was to identify links between samples for which the same batch of MDMB-CHMICA was used, this time combining the orthogonal information generated by both analytical techniques, generating information about the used combination of precursor substances and the applied synthesis pathway, including batch discrimination.

Again, this might provide unique insight into the manufacturing procedures of the original drug manufacturers and in potential co-operation or shared underlying distribution channels for the European NPS distributors.

## 2. Methodology

### 2.1 Sample pool and preparation

Although a large variety of different NPS products were acquired by police seizures and online-test purchases in the course of the project “Spice-Profiling” (e.g. cathinones, synthetic cannabinoids, benzodiazepines), we focused on pure samples of the synthetic cannabinoid MDMB-CHMICA as “flag-ship” compound to develop the impurity profiling. The adaptability of the impurity profiling workflow to other matrices was conducted for the cannabinoid Cumyl-5F-PINACA. The IRMS profiling was done for all samples of MDMB-CHMICA and Cumyl-PeGaClone and a few samples of 5F-PB-22.

In detail, the following samples were used (with source):

*Table 4: Listing and additional information for the synthetic cannabinoid seizures and online-test purchases used in this work*

Synthetic cannabinoid	Formulation	Obtained from	Number	Source	Date
MDMB-CHMICA	pure	seizure	40 x 1kg	Luxembourg Customs (Figure 8)	Dec 2014
			17	Finish customs	2015 - 2016
			1	Slovenia	2015
	SP	Online-test purchase	3	FR <sup>a</sup>	2015
		seizure	44	RLP <sup>b</sup>	Jan - Jun 2015
		Online-test purchase	74	FR	Nov 2014 - Dec 2015
Cumyl-5F-PINACA	pure	seizure	1	Laboratory in Slovenia	Aug 2015
	EL	seizure	4	Laboratory in Slovenia	Aug 2015
		Online-test purchase	10	FR	2016
Cumyl-PeGaClone	pure	seizure	1	BKA <sup>c</sup>	2016
	SP	Online-test purchase	30	FR	Dec 2016 - Jul 2017
5F-PB-22	pure	seizure	2	BKA	2014, 2017
	SP	seizure	14	BKA	2014

<sup>a</sup> FR = University Medical Center Freiburg

<sup>b</sup> RLP = Land Office of Criminal Investigation of Rhineland Palatine

<sup>c</sup> BKA = Federal Criminal Police Office Germany



Figure 8: Seizure of 40 kg pure MDMB-CHMICA by Luxembourg customs in December 2014 going from Shanghai to Madrid.

All pure samples could be directly dissolved for injection into the flash-chromatography. For the SPs and ELs, an additional extraction step had to be included, to remove the synthetic cannabinoid and related compounds from the corresponding matrix.

A short extraction with acetonitrile was developed and validated for SPs. The herbal material is rinsed multiple times with acetonitrile, while the contact time between solvent and plant material was kept short, to avoid excessive extraction of plant-based substances (it was inevitable to extract some minor plant components, already visible though a slight green colouring of the extract). However, it should be ensured that the desired cannabinoids and related impurities are completely dissolved in this short time. After extraction, the acetonitrile is evaporated and the dry residual is dissolved again in the F-LC eluents. To validate the extraction procedure and investigate the potential extraction of matrix substances, native herbal material was impregnated with synthetic cannabinoids of known impurity composition. The self-made SP was extracted again and the chromatographic impurity signatures compared to those of the corresponding pure material.

The extraction of synthetic cannabinoids from ELs was more complex than for the SPs, due to the nature of the matrix. Before the samples can be injected into the F-LC, it was necessary to remove the polar matrix, as it would disrupt the normal phase chromatography. A short LLE with water and chloroform was developed. The majority of polar matrix remained in the water phase, while the target compounds remain in the chloroform phase. The chloroform is evaporated and the dry residual is dissolved again in the F-LC eluents. Similar to the procedure of the SPs, self-made e-liquids with a pure sample with known impurity composition were prepared to validate the extraction procedure. By comparing both the original signature and the one after extraction, additional matrix substances and potential loss of impurity signatures could be identified.

## 2.2 Flash chromatography

Preparative column chromatography is a widely used method to separate or clean-up larger quantities (milligrams to grams) of compounds<sup>121-123</sup>. It was optimized and formally introduced in 1978 by Still et al.<sup>124</sup>, using a glass column topped with a gas flow inlet to regulate (mostly increase) the flow rate of the mobile phase and thus speed up the separation in contrast to non-pressurized preparative chromatography, thus the name “flash”-chromatography. In recent days, the pressure of the mobile phase flow is generated by solvent pumps instead of air pressure. Figure 9 shows the instrumental setup used for the here presented work, a Sepacore X50 by Büchi (Switzerland). The modular setup consists of two pumps to generate a flow rate of up to 250 mL/min and a pressure of up to 50 bar, an online-UV/VIS detector (parallel detection on 4 wavelengths, 200-840 nm) and an automated fraction control unit. With two

individually operating pumps, it was possible to run both an isocratic and a gradient eluent system. Samples can either be loaded as solid via a special adapter or by injection as solution on a sample loop. A selection of prepacked columns is commercially available, eliminating possible inaccuracies in the density or homogeneity of the column material through manual handling and thus increasing the reproducibility of the separation. The automated fraction controller with numbered vials in combination with the online UV-VIS detector and the corresponding software enables reproducible and retraceable fractionation of eluting peaks. Sample injection was done via commercially available disposable syringes.

Separation of impurities from the main component was done using only the smallest types of columns (4g) for several reasons. Most importantly the economic aspects, as these columns could be operated with comparatively low flow rates of 15-20 mL/min. Per run, approximately 200 mL of organic solvents were used and every five runs the column was changed. The separation capacity of the small columns was sufficient for the amount of sample (10-100 mg) to be separated, as only small quantities of impurities (few  $\mu\text{g}$ ) were necessary for subsequent analysis. For structural characterization via NMR, the automatic fractionation was adjusted to selectively cut out single impurities. Multiple replicate runs were carried out to accumulate these impurities, which were further purified by individual F-LC runs after enough substance was collected.

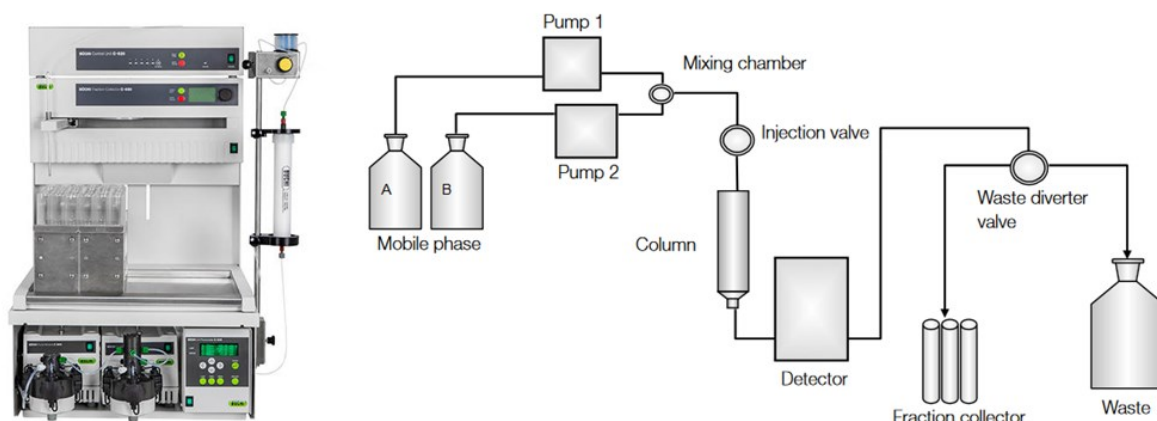


Figure 9: Sepacore® X50 Flash-Chromatography system by Büchi, consisting of two pumps, a UV-VIS spectrometer, an automated fraction collector and a control unit. The pictures belong to and is used with the allowance of Büchi.

Several pitfalls have been detected while operating the system, which are to be avoided for an accurate operation using small injection volumes and small columns. This was of special interest for the developed methodology for impurity profiling. It was of utmost importance, that the separation and fractionation is reproducible in the course of multiple hundred runs:

- It is recommended to dissolve the sample material in the same solvents as the eluent system to maintain a homogenous flow. Different viscous liquids could lead to an irregular flow on the column and disrupt the separation.
- If small columns are used (e.g. 4 g of packaging material), the composition and volume of the injected solvent, even though it consists of the eluents, significantly influence the separation. With a high injection volume and concentration of the solvent with strong elution power (in the case of normal phase chromatography, the more polar eluent), the dissolved sample migrates far onto the column even though the separation has not even started. This migration stops only when the eluent flow with low separation power

flushes the injected volume away. In the worst case, substances with low affinity to the column material might elute with the injection peak. In any case, this migration leads to peak-broadening and far less resolution of eluting peaks. However, in some cases it is inevitable to use larger concentration of the stronger eluents, as the sample might only dissolve in this more polar solvent.

- The nature of the injection system is not very well suited for low injection volumes (1-2 mL), as multiple hundred  $\mu\text{L}$  of sample might go into the waste. The normal procedure is to put the syringe into the injection nozzle, then turn the 6-way-valve to load the sample onto the sample loop. The syringe is emptied and the 6-way-valve is turned again to inject the sample onto the column. However, the volume of the tube from the injection nozzle (where the syringe is put on) to the 6-way-valve already can take several hundred  $\mu\text{L}$  of injected sample. This sample is lost in the normal injection process, as the second turn of the 6-way-valve connects this short transfer-tube with the waste. To load the complete amount of sample onto the sample loop, the empty syringe has to be taken off the injection nozzle before turning the 6-way-valve a second time, so that the volume in the transfer tube can flow onto the sample loop by hydraulic force (natural suction of the flow through gravitation, as the end of the sample loop is connected with the waste bottle, which itself is lower on the laboratory bench than the injection valve). Shortly before air reaches the 6-way-valve, it is turned the second time and the loading of the sample is complete.

## **2.3 Assessment and evaluation of impurity signatures**

### **2.3.1 Ultra high-performance liquid chromatography mass spectrometry**

The hyphenation of UHPLC and MS is a well-established method in analytical chemistry. The combination of high throughput and strong separation power of the chromatography with the high discrimination power of the MS finds many applications ranging from environmental studies, metabolomics, proteomics and forensics (doping, toxicology) to clinical medicine. The basic principle of LC and MS and their corresponding applications can be taken from the literature<sup>125,126</sup>.

For the assessment of the chromatographic impurity signatures, we used a combination of reverse phase (RP) LC coupled to an ion trap MS with ESI. This combination is well suited for the development of an impurity profiling methodology for synthetic cannabinoids, although other profiling routines utilize GC-MS. However, some synthetic cannabinoids are known to dissociate at higher temperatures, which would disrupt the impurity signatures with additional peaks and injector artefacts.

RP is the most common type of LC with a non-polar stationary phase (e.g. polymer granulate with covalently bound alkyl chains) and a polar (water based) eluent system to separate mixtures according to their polarity. Its robustness, cheap eluents and high separation power are only a few of the positive aspects. For the impurity profiling, an established method, developed by the Federal Criminal Police Office, was used, as it was well suited for the separation of synthetic cannabinoids and related synthesis impurities. After separation, eluting substances were ionized by ESI and analysed via mass spectrometry. We preferred ESI as

ionization source to other common atmospheric pressure methods, such as chemical or photo ionisation. We are aware, that some substances might not be ionized at all by ESI, however, first measurements showed good ionisation of > 100 synthesis impurities of synthetic cannabinoids, sufficient for a semi quantitative profiling. Another major reason for soft ionisation is related to the evaluation algorithm via  $m/z$  specific integration (see following chapter). Increased in-source decay (ICD) by hard ionisation techniques could reduce the signal of the original molecular peak and thus leads to a falsified integration (the integral of the product ion is not accounted for in the data evaluation). Finally, an ion trap MS (AmaZon Speed, Bruker) was used as mass analyser, with a fast scan rate (32500  $m/z/s$ ), an  $m/z$  peak width of < 0.5 u and automated (smart) fragmentation up to  $MS^3$ . The fragmentation was of special use in the process of method development to characterize eluting substances and assess their relation to the main component. However, as the MS takes a certain time to fragment up to  $MS^3$ , no scan signal is recorded in this period. As the data evaluation only targets the  $m/z$  intensities of the scan spectra, comparing two LC-MS runs might lead to different accumulated intensities due to the different sum of recorded scan spectra in a specific chromatographic runtime. Thus, all LC-MS runs intended for the semi-quantitative impurity profiling were recorded without automated fragmentation.

### 2.3.2 Data structure and treatment

The data generated by an LC-MS run can be divided into three dimensions, the retention time (RT),  $m/z$  value and intensity. Given the case that a chromatogram shows only a few, baseline-separated signals, the evaluation/integration of the base peak chromatogram (BPC) or total ion chromatogram (TIC) is sufficient to extract semi-quantitative information about these signals. However, in the case of complex mixtures with multiple overlapping or non-baseline separated peaks, this integration method can lack in accuracy and deconvolution of peaks is necessary. As the data structure of LC-MS provides a third discriminating variable ( $m/z$  value) in addition to the RT and intensity, an alternative for precise integration can be applied. For Bruker instrumentation, the software Profile Analysis can be used for automated integration, subdividing the retention time and mass range of a LC-MS run into distinct pairs (so-called buckets) and summing up all intensities falling into each of these ranges. The software allows the use of different bucketing algorithms (e.g. automating peak detection), however, the one used for this work was rectangular bucketing, the most static but also reproducible approach. As example: A bucket size of  $\Delta t = 0.5$  min and  $\Delta m/z = 1$  between 1 min and 9.5 min of the chromatogram for the  $m/z$  range of 150 to 500 was set. The LC-MS data is then converted into a table of 5967 buckets with their corresponding accumulated intensities. A major advantage of the algorithm is the automatic peak detection. If a peak is located across a border of two adjacent buckets, the intensity of this peak will not be split, but rated to the bucket containing the peak maximum. This way, a single bucket contains the complete integral of an eluting substance. Even though this feature helps to avoid a “blurring” of the LC-MS data, the settings for bucketing should be chosen carefully. Going back to the given example: if multiple substances with identical  $m/z$  values (e.g. positional isomers) elute with approximately 0.5 min difference, two or even three peaks of otherwise individual substances might be rated into a single bucket. With the set time interval of  $\Delta t = 0.5$ , a part of the original information is “deleted”. However, by setting the time interval not wide enough, small shifts in the retention time (e.g. when

comparing two runs of a sample measured several months apart) are not compensated for and an eluting peak might be rated into different buckets for each of these runs, although both peaks describe the same substance. Depending on the given sample and the complexity of mixture of substances, appropriate settings have to be found by trial and error until a satisfactory bucket table is generated.

Profile Analysis provides a direct evaluation of the bucket table via principle component analysis (PCA), a type of MDA. Although multivariate evaluation was in our interest, this software-feature was not used for this work. Instead, the bucket table was exported into an Excel sheet to reduce the number of buckets (data point) before evaluation. Most of the buckets do not carry any relevant information as they describe measurement background noise or signals with no relevant information. Even though the MDA (in our case PCA) is able to cope with unnecessary noise data, we chose to “clean” our dataset. The overall amount of data points was reduced by applying an intensity threshold for all measurements. Buckets that did not exceed this specific threshold were deleted by an Excel macro, reducing the number of relevant RT/m/z pairs by more than 98% (target number of remaining buckets were less than 100). As final normalization/baseline correction step, the whole dataset was divided by  $10^8$ . Figure 10 is a graphical interpretation of this process.

As mentioned before, this work was a proof of concept study for the impurity profiling of synthetic cannabinoids, in particular targeting MDMB-CHMICA. The impurity signatures of the available 61 samples were measured, the LC-MS data converted into a bucket table and the noise buckets deleted. The cleaned bucket table with the remaining most intense signals was analyzed via MDA, in particular via PCA to assess those buckets (and the underlying signals/substances), which are responsible for differences between these samples.

### **2.3.3 Multivariate data analysis**

For small data sets with two or three variables it is easy to see patterns in the distribution of data points by plotting them against each other. However, trying to analyse complex systems with hundreds or even millions of variables, a visual approach without any data treatment is either very time consuming or even impossible. To extract the most amount of information and to find hidden underlying structures in large datasets, multivariate mathematical models can be used. Ideally, after MDA the number of observed dimensions is reduced to a level, at which a visual interpretation is possible again, while the maximum amount of the original information is maintained. In this work, hierarchical cluster analysis (HCA) and PCA were used. A review of the corresponding mathematical background<sup>127</sup> and the applications in analytical science<sup>103,128,129</sup> can be taken from the literature. In summary, PCA is a model to analyse the overall variability in a given dataset and to understand the relationship between samples and variables. It is an unsupervised exploratory model, where no prior information is implemented and the samples are solely analysed based on their variables. The data is separated into a few principal components (PCs), each contributing to explain a percentage of the total variability. PC1 always explains the highest percentage of information, followed by the other PCs in decreasing order.

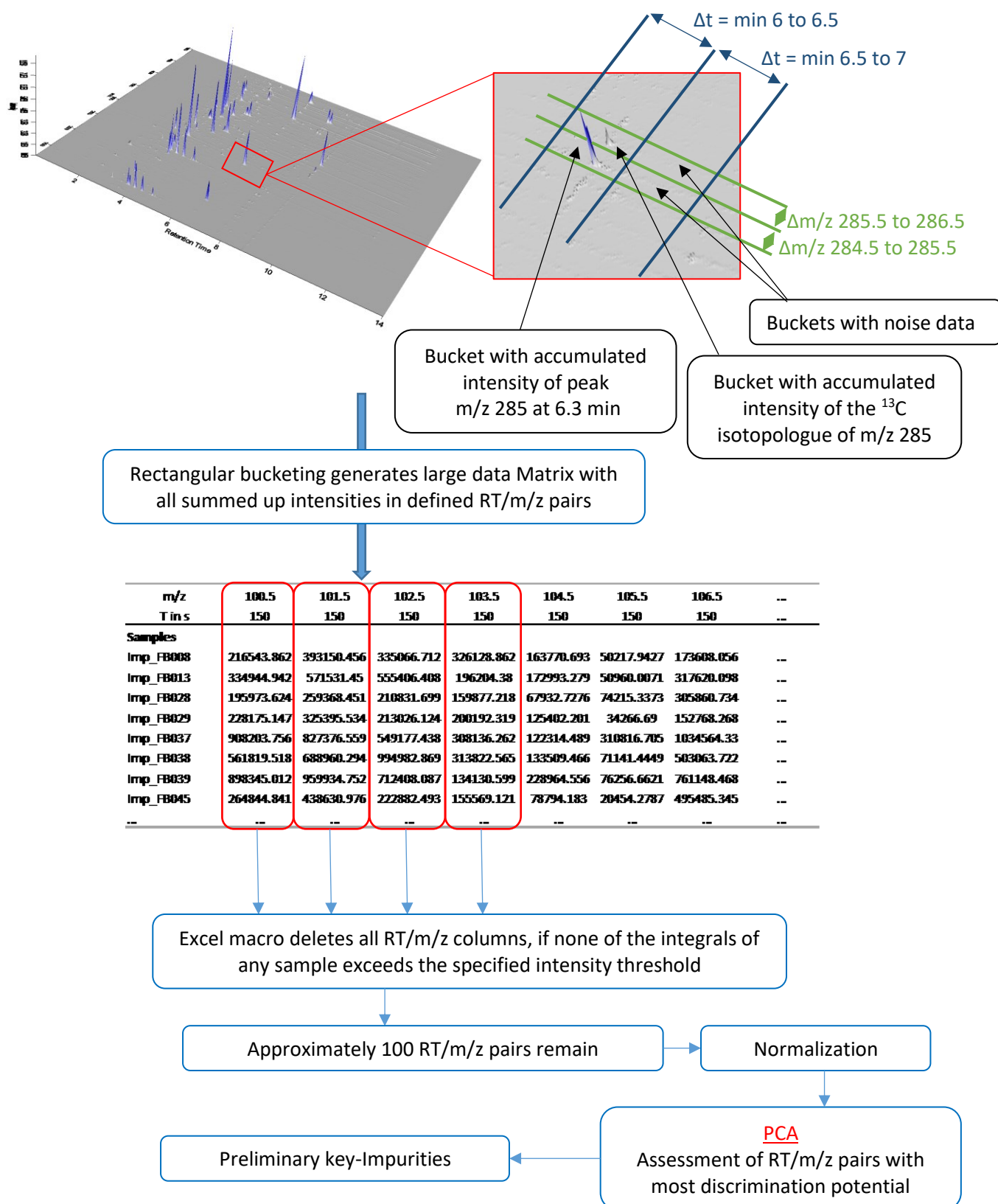


Figure 10: Schematic of rectangular bucketing via Profile Analysis with subsequent data treatment for assessment of discriminating key-impurities. The 3D-graphic was modelled using MZmine 2.38<sup>130</sup>

In a good PCA model, the number of individual PCs should be as low as possible, while the accumulated percentage of all PCs should be near to 100% to describe the dataset as complete as possible. PCA is a highly graphic type of MDA, thus interpretation of the data is done by



plotting the PCs against each other to see patterns in the data. The two most important graphs are the Scores and Loadings plot. The Loadings plot provides a map of the variables and shows, which variables contribute most to the overall variability, in other words show the most variance between the given set of samples. Furthermore, the relationship between variables is described and variables with no information can be identified. The Scores plot provides a map of the samples, being directly related to corresponding Loadings plot. Samples with a high score on a specific PC generally consist of a variable or multiple variable with a high loading on the same PC. Samples with a similar composition of variables tend to cluster in the Scores plot.

Referring to this work, each variable represents an impurity. The Scores plot is the most important feature of the PCA to group samples with similar impurity composition. By interpretation of the Loadings plot, key-impurities with high discrimination potential can be identified. Figure 11 provides an example how a Scores and Loadings plot might look like and what type of information can be extracted of each individual plot.

In practical terms, the PCA was used for both method development and final data evaluation. The process of choosing key impurities was iterative, meaning that the bucket table (LC-MS data of pure MDMB-CHMICA samples) with approximately 100 variables was analysed via PCA and the resulting loadings plot was carefully investigated for the corresponding  $m/z$  value with high inter-sample variability. Each of these  $m/z$  values was then crosschecked in the LC-MS spectrum for its relationship to MDMB-CHMICA. Version 1.1 of Profile Analysis was used in this work for bucketing, which was not yet programmed to automatically detect isotopologues, splitting both the nominal mass and corresponding isotopes (e.g.  $^{13}\text{C}$  or  $^{37}\text{Cl}$ ) into individual buckets. Thus, bucketing of high concentrated substances produces multiple data points with high intensities of which the isotope signals do not provide any additional information. Thus, after the “key-impurities” were assessed, their corresponding isotopologue RT/ $m/z$  pairs were deleted by hand as they were still present in the bucket table after applying the intensity threshold to remove noise buckets.

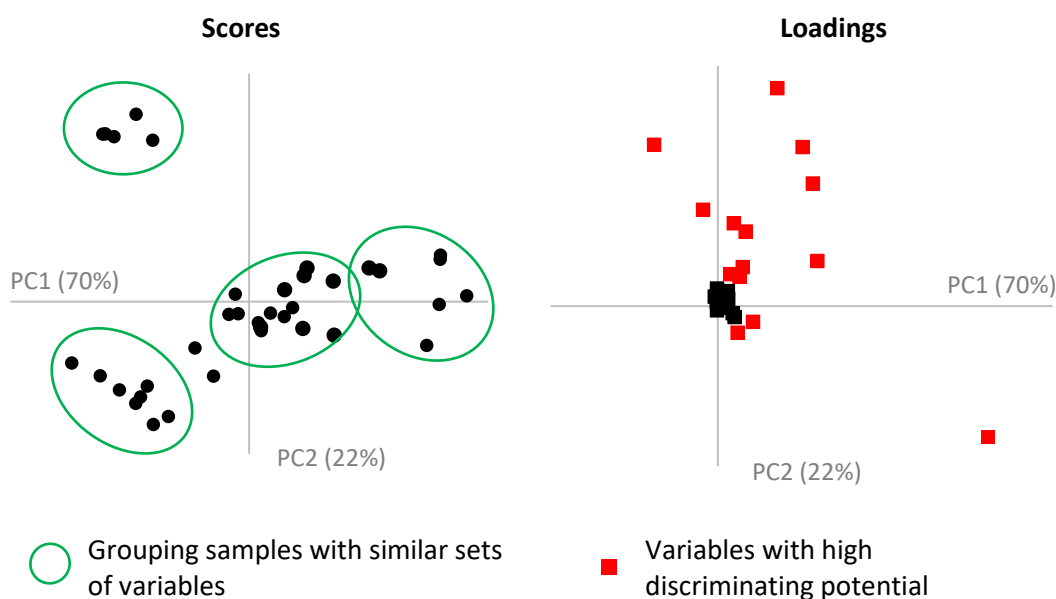


Figure 11: Examples for the different types of information that can be extracted from a PCA Scores (left) and Loadings plot (right).

HCA is a classification model (sometimes also rated to the exploratory methods), sorting a group of objects based on distinct features in this object. In general, agglomerative algorithms are used for grouping, starting from single samples and searching for the most similar. In the second step, the next most similar sample is grouped to this cluster and so on until one cluster remains. The distance of the groups or samples to each other are expressed as relative distance and visualized in form of a dendrogram (see Figure 12). The investigator then has to choose the appropriate relative distance for assigning samples into distinct groups. Depending on the previous knowledge of the objects to be classified, supervised or unsupervised classification can be used. Unsupervised classification groups samples solely based on similarities/dissimilarities in their corresponding variables (also the case for PCA). In supervised classification, classes with a specific set of parameters are known and new samples are tested if they are a member of any of these classes or not.

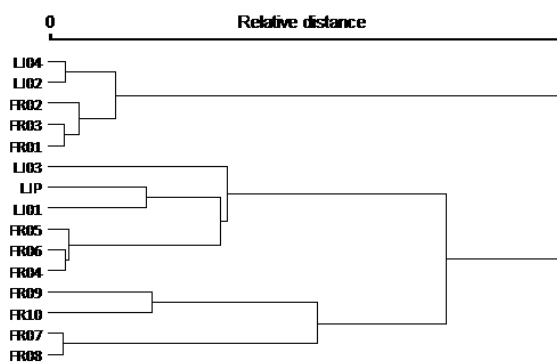


Figure 12: Exemplary dendrogram of an HCA

In this work, only unsupervised classification was used to visualize links between impurity signatures of seized samples. The data was pre-treated with PCA reducing the large number of variables to a few PCs, where each sample has a distinct score in the Scores plot. While each PCs describes only a certain percentage of the complete dataset, a combination of the first four or five PCs (depending on the model) nearly describe 100% of the information. Although visual interpretation of the data is much simpler than before, still all PCs need to be plotted against each other to reveal all connections between samples. By applying HCA to the scores of these first PCs, the number of variables can be further reduced to give a summarized picture of the complete dataset in just two dimensions.

## 2.4 Characterization of impurities

### 2.4.1 High-resolution mass spectrometry

Resolution in MS is defined as the accuracy with which an  $m/z$  ratio can be measured. A common method for calculation is by dividing a given  $m/z$  ratio by the measured peak width at 50% (full width at half-maximum FWHM)<sup>131</sup>. HR-MS is a technique to measure the  $m/z$  value of a peak with high accuracy. Mass analysers with high resolving power are time of flight (TOF)<sup>132</sup>, Orbitrap®<sup>133</sup>, or Fourier transform ion cyclotron resonance spectroscopy (FT-ICR)<sup>134</sup>. Reviews on these techniques and their applications can be taken from the literature<sup>135,136</sup>.

One of the major advantages of HR-MS is the generation of sum-formulas based on the accurate determination of the  $m/z$  value, possible through the so-called mass-defect in atoms. The monoisotopic mass of all elements (except hydrogen) is not a simple accumulation of the weight of their corresponding number of sub-atomic particles (neutrons, protons, electrons). The energy, necessary for binding these constituents to intact atoms is subtracted from the accumulated mass following Einstein's equation for mass-energy equivalence. The mass defect

increases with higher number of sub-atomic particles. Thus, an accurately determined  $m/z$  value can only consist of a specific combination of elements, which can be calculated by modern software. This feature is of special interest for characterization of unknown substances, as the sum-formula already provides valuable information of the underlying chemical structure. The discrimination strength of this technique can even be increased, by combining the sum-formula generation with preceding fragmentation experiments. In this work, we used an HPLC-Iontrap-Orbitrap system to fragment and elucidate the structure of synthesis impurities.

#### 2.4.2 Nuclear magnetic resonance spectroscopy

NMR was first described in 1938<sup>137</sup> and has become one of the most powerful tools for structural elucidation of organic compounds. Samples are submitted to a strong magnetic field and the sample nuclei are excited by radio waves. The emitted relaxation frequencies of the nuclei are then recorded and transformed via Fourier-Transformation into signals. Depending on the intramolecular magnetic interactions of the nuclei and their corresponding electrons, the emitted frequency can be different for each nucleus in the molecule. By interpreting these differences and interactions visualized in the NMR-spectrum, information about the structure of a molecule can be won. Although the 1-dimensional NMR of single nuclei like  $^1\text{H}$  or  $^{13}\text{C}$  are the most common type of NMR analysis, it is possible to measure the direct interaction of nuclei in close proximity by different two-dimensional experiments ( $^1\text{H}$ - $^1\text{H}$  correlation spectroscopy, COSY or  $^1\text{H}$ - $^{13}\text{C}$  heteronuclear single quantum coherence, HSQC) or through the room (nuclear overhauser enhancement and exchange spectroscopy, NOESY). These 2-D experiments might be necessary for molecules, where 1-D techniques fail to provide all necessary information for unambiguous structural identification. Harald Günther published a good review about the principles and applications of NMR<sup>138</sup>.

Impurities of MDMB-CHMICA, which could be isolated in larger quantities and sufficient purity, were measured by NMR. In combination with the HR-MS data, a nearly univocal structural characterization of impurities was possible.

### 2.5 Synthesis of MDMB-CHMICA

#### 2.5.1 Controlled synthesis of the amino acid coupling step using different reaction conditions

To this date, the precise synthesis of NPS conducted by the original manufacturers is unknown, although it is expected that they derive their general procedures from patents and publications. Thus, with the characterization of impurities in seized samples of MDMB-CHMICA, conclusions about the synthesis pathway and respective used chemicals and reagents could be drawn. In the majority of published synthesis for synthetic cannabinoids, the residue on 3-position of the indole is coupled after the N-alkyl residue. Thus, it is expected that the manufacturers in Asia also follow this order and for MDMB-CHMICA the coupling of the amino acid TLME to the respective 3-indole-carboxylic acid is the last reaction step. The majority of impurities identified in seized samples of MDMB-CHMICA consisted of derivatives of the indole with the cyclohexyl methyl already attached to the indole core, validating the postulated reaction order. Thus, we decided to focus our efforts of controlled synthesis to the last coupling step of the amino acid to reduce the number of variables which might have an impact on the finished impurity composition. The main aim was to better

understand variations in the impurity signatures, including the identification of route specific markers, resulting from different reaction conditions or coupling agents and to assess the overall reproducibility of the impurity signatures by replicate synthesis using the exact same reaction conditions.

In a patent of Buchler et al.<sup>56</sup> the synthesis of multiple hundred structurally different synthetic cannabinoids are started, including the indazole analogue of MDMB-CHMICA, which also appeared on the drug market as MDMB-CHMINACA. The respective coupling of the amide bond was achieved by N-N-dicyclohexylcarbodiimide (DCC) or 1-ethyl-3-(3-dimethylaminopropyl) carbodiimide hydrochloride (EDC) in combination with hydroxybenzotriazole (HOBt) or uronium reagents such as O-(7-azabenzotriazol-1-yl)-1,1,3,3-tetramethyluronium hexafluorophosphate (HATU). Banister et al.<sup>139</sup>, who first published the complete synthesis of MDMB-CHMICA, also used the same combination of EDC and HOBt for amide bond formation. However, one of the most abundant impurities found in seized samples of MDMB-CHMICA was identified as a respective 2-chloro indole derivative, indicating the use of a chlorination agent for coupling, most certainly the activation of the carboxylic acid via an acyl halide with subsequent nucleophilic substitution of the amino acid. Thus, several amino acid couplings were conducted (always in triplicate) by Steven Hansen of the University Mainz in cooperation with the Federal Criminal Police Office, summarized in Figure 13, once with HATU according to Buchler et al., once using the chlorination agent thionyl chloride, and three-fold using the chlorination agent oxalyl chloride. One of the oxalyl chloride synthesis was conducted according to the usual coupling conditions, another with an extended reaction time of 23 hours, which was monitored after 1 hour, 2 hours, 3 hours and 23 hours and the last with a reduced reaction temperature to 0 °C (instead of room temperature). As educt for all couplings, a purified batch of 1-(cyclohexylmethyl)-1*H*-indole-3-carboxylic acid, synthesized by an optimized method in a classified master thesis from Steven Hansen.

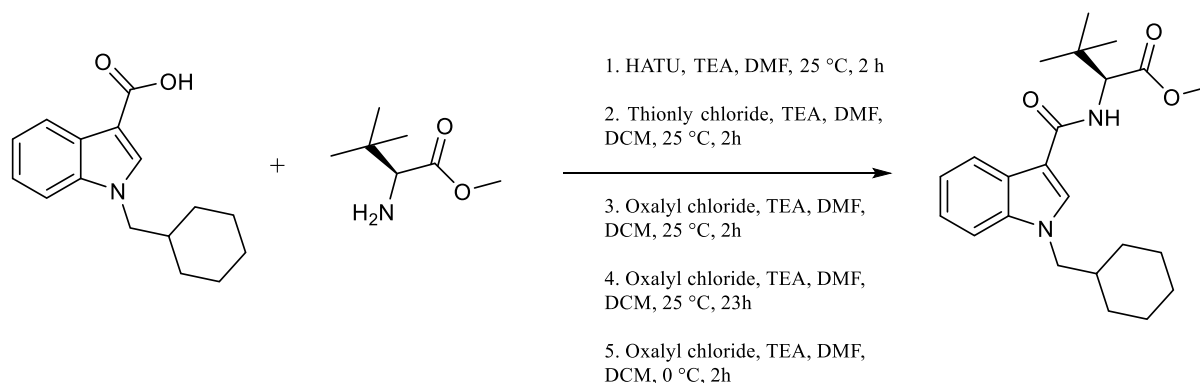


Figure 13: Last step of the amino acid coupling in the synthesis of MDMB-CHMICA using five different reaction conditions

The finished reaction mixtures were cleaned up by standard procedures like liquid-liquid extraction and washing with water. The impurity profiles of each synthesis were assessed and compared according to the procedures stated in 2.3.

## 2.6 Isotope ratio mass spectrometry

Via IRMS, the relative abundance of isotopes (e.g.  $^2\text{H}/^1\text{H}$ ,  $^{13}\text{C}/^{12}\text{C}$  or  $^{15}\text{N}/^{14}\text{N}$ ) are measured in a sample. In principle, samples are combusted at high temperatures and converted into gases like  $\text{CO}_2$  or  $\text{N}_2$  (after reduction), which are ionized by an electron impact ion source (EI). The

ions are measured via a combination of a single magnetic sector analyser for separation by  $m/z$  ratio (e.g.  $m/z$  44, 45 and 46 for ions of  $\text{CO}_2$  with various combinations of  $^{12}\text{C}$ ,  $^{13}\text{C}$ ,  $^{16}\text{O}$ ,  $^{17}\text{O}$  and  $^{18}\text{O}$ ) and subsequent detection via an array of so-called Faraday cups.

For each element, samples are measured against an international primary standard selected by the International Atomic Energy Agency in Vienna (IAEA). The primary standard for C was a fossil Belemnite found in the Pee Dee-formation in South Carolina (referred to as Vienna Pee Dee Belemnite, V-PDB) and is now exhausted. For N, atmospheric nitrogen is used, as it does not vary measurably around the world. The so-called mean ocean water (which never physically existed) is used for H and O (referred to as Vienna Standard Mean Ocean Water, V-SMOW). The measured isotope ratios are expressed in ‰ and relative to the international standards using the delta definition equation<sup>140</sup> (exemplarily shown for C):

$$\delta^{13}\text{C}_{\text{unknown}} = \left( \frac{R(^{13}\text{C}/^{12}\text{C})_{\text{unknown}} - R(^{13}\text{C}/^{12}\text{C})_{\text{standard}}}{R(^{13}\text{C}/^{12}\text{C})_{\text{standard}}} \right)$$

Guidelines for good practice in IRMS for forensic purposes can be taken from the Forensic IRMS network<sup>141</sup>. A review on the natural distribution of stable isotopes can be taken from the U.S. department of the interior<sup>142</sup>.

### 3. Results and discussion

The results obtained in the practical work of this thesis can be condensed in a few superordinate topics. In the following chapters, each topic is outlined in short, primarily summarising the results already published in the peer reviewed scientific literature. The corresponding original publications can be taken from the appendix. Figure 15 sketches the developed workflow with the different topics marked by individual colours: Green is the central workflow, blue the method development with structural identification of single impurities and controlled synthesis, orange the adaption of the workflow to samples in e-liquid matrices, red the adaption to samples on herbal matrices including the comprehensive profiling of the main active ingredient via IMRS and purple controlled synthesis and binding studies of specific synthetic cannabinoids.

#### 3.1 Development and validation of an impurity profiling workflow for highly pure samples of synthetic cannabinoids <sup>Publication 1 and 2</sup>

The major topic of this thesis was the development of an impurity profiling for synthetic cannabinoids, which at that time did not exist. As several of the results and developed processes serve as basis for all following publications, they are already outlined in the experimental section.

Although impurity profiling of classical drugs is well described in the literature, these methodologies mainly target samples of low purities and utilize unspecific enrichment techniques like LLE or SPE to separate the impurities from the main component. Since synthetic cannabinoids are both highly pure and the common enrichment methods fail for this substance (they are insoluble in water and impurities are structurally very similar to the main active ingredient), we found F-LC as fast paced preparative chromatography as feasible alternative to selectively cut out the main component of a chromatographic run and yield a combined impurity fraction. The adaptability of the F-LC was demonstrated by development of different gradient systems to isolate the individual related impurities of the four structurally diverse synthetic cannabinoids MDMB-CHMICA, MDMB-CHMZCA, AB-CHMINACA, Cumyl-PeGaClone and Cumyl-5F-PINACA, depleting more than 99 % of the main component from the pooled impurity fractions. Two overlaid BPCs of a native sample of MDMB-CHMICA (red) and the corresponding pooled impurity fractions (blue) are shown in Figure 14. Small peaks which were nearly below the detection limit in the native sample are more intense in the combined impurity sample and even additional, previously superimposed peaks appear.

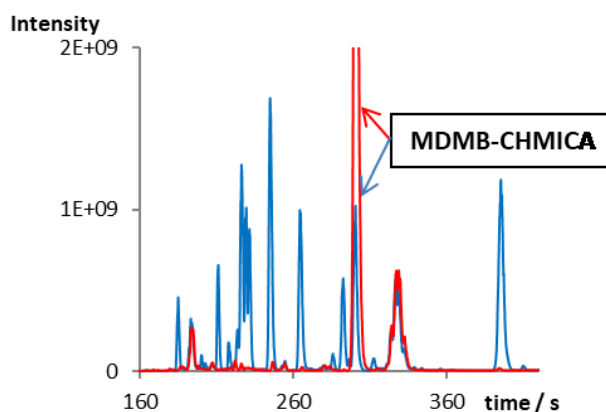


Figure 14: Excerpts of overlaid UHPLC-MS base peak chromatograms. red: native sample of MDMB-CHMICA, blue: isolated impurities of the corresponding red labeled sample injected with a lower dilution factor.

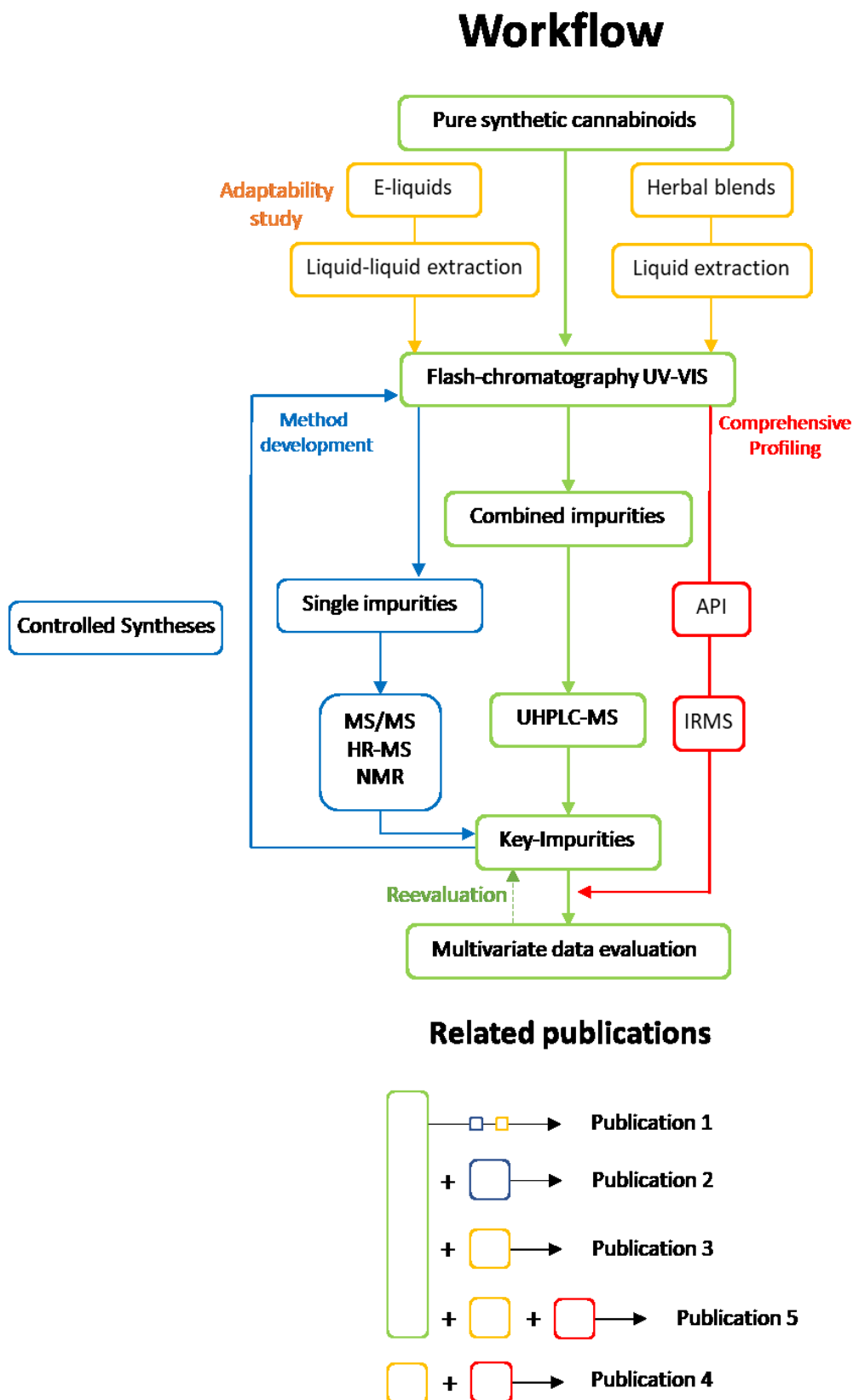


Figure 15: Sketched summary of the final workflow for impurity profiling of synthetic cannabinoids with the assignment of individual parts to their respective publications. Green is the general workflow, blue the method development with structural identification of single impurities and controlled synthesis, orange the adaption of the workflow to samples in e-liquid matrices, red the adaption to samples on herbal matrices including the comprehensive profiling of the main active ingredient via IMRS and purple the controlled synthesis and binding studies of specific synthetic cannabinoids. In general, the respective publications were mixtures of the individual parts of the workflow.

The complete workflow as stated in Figure 15 was not conducted for each of these cannabinoids, but only for MDMB-CHMICA (and Cumyl-5F-PINACA) as most prevalent synthetic cannabinoid in Germany in 2015 and 2016. Sixty-one pure samples of MDMB-CHMICA from different sources were available to exemplarily exercise each of the shown steps.

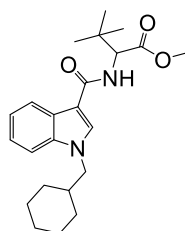
In the process of developing an impurity profiling for any substance, one of the most important steps is to assess suitable key-impurities, which are responsible for differences between the samples and are characteristic for a specific synthesis and its conditions. Thus, the integrated chromatographic impurity signature of the sixty-one samples of MDMB-CHMICA were evaluated by multivariate means via PCA and those impurities with high inter-sample variance were assessed by preliminary ion-trap MS/MS fragmentation experiments and all other signals of unrelated matrix components were excluded. Thus, the workflow is not fully linear but has an iterative self-optimization feature of key-impurity assessment and data-evaluation. Although it might be possible to profile a sample pool based on this preliminary set of key-impurities, the validity of the key-impurities can be further increased by more elaborate structural elucidation. Via precise fractionation of the F-LC run, single impurities can be isolated in larger quantity. For the given sample pool of MDMB-CHMICA, eleven impurities could be enriched in larger quantities and high purity for structural characterization via NMR. Four other impurities were only characterized by means of HR-MS/MS experiments, giving a set of fifteen key-impurities for MDMB-CHMICA (Figure 16) on which all following data evaluation is based on.

As mentioned before, overall sixty-one samples of pure material from different sources were available for analysis (see chapter 2.1). For each sample, the impurity signatures were recorded and compared by PCA and HCA on the basis of the fifteen key-impurities to possibly discriminate between individual synthesis pathways and group samples according to similarities in their impurity signatures. The forty samples from the large Luxembourg seizure could be grouped into six clusters between five and ten samples, representing a maximum possible batch size of 10 kg of pure MDMB-CHMICA. Three of the forty samples were identified as outliers, possibly synthesized by a different synthesis. The remaining twenty-one samples from unrelated seizures or online-test purchases could be grouped according to similarities in their impurity composition.

To validate the workflow and the key impurities, stability test and controlled synthesis were carried out. Two oxidation products of MDMB-CHMICA were found after storage for two months under direct sunlight and at room temperature. With the knowledge about specific structural elements of the impurities and the available literature sources, several retrosynthesis of MDMB-CHMICA were carried out with two intentions: to better understand variations in impurity signatures between multiple batches using the same and different reaction conditions, assessing the significance of variations in the impurity patterns of seized samples, and to reproduce the impurity patterns of seized samples to learn about the synthesis pathway used by the original manufacturers. Five different types of controlled synthesis of what is presumably the last coupling step (amino acid to indole-carboxylic acid) were performed (see chapter 2.5.1). Overall, eight new impurities were found in the controlled synthesis. Replicates of a synthesis conducted on the same day showed similar impurity signatures, on different days very dissimilar signatures. As expected, the use of different coupling reagents or conditions gave

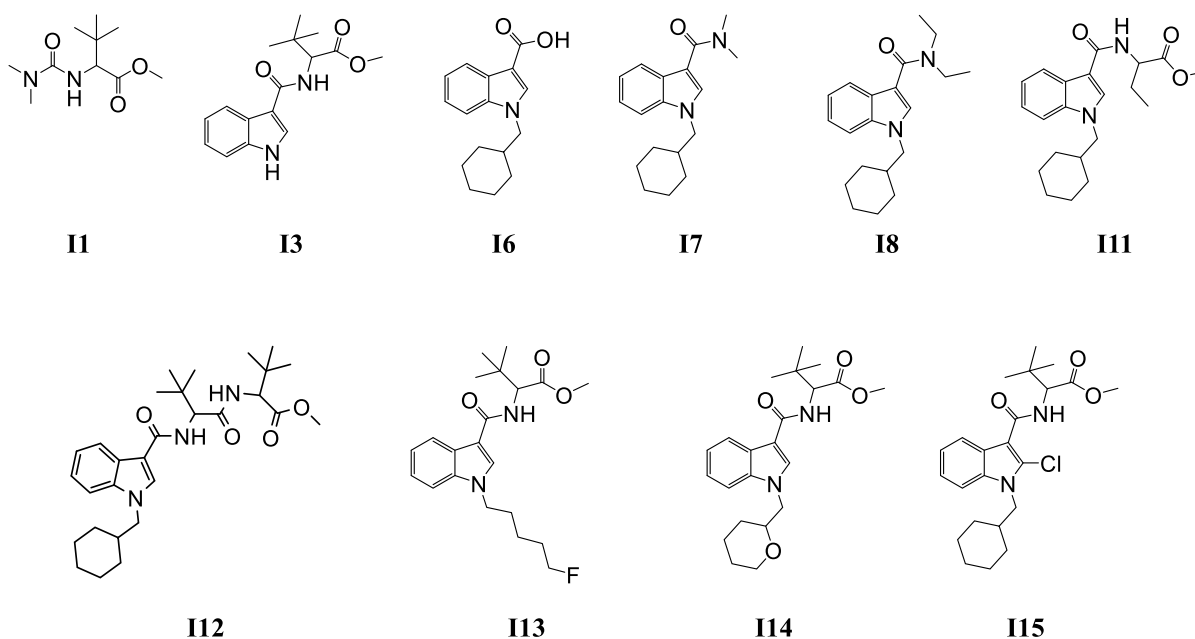


distinguishable impurity signatures. The controlled synthesis by amino acid coupling over an acyl halide were identified to be the most probable synthesis of choice of the original manufactures.



**MDMB-CHMICA**

**Impurities elucidated via NMR and HR-MS/MS experiments**



**Impurities elucidated via HR-MS/MS experiments**

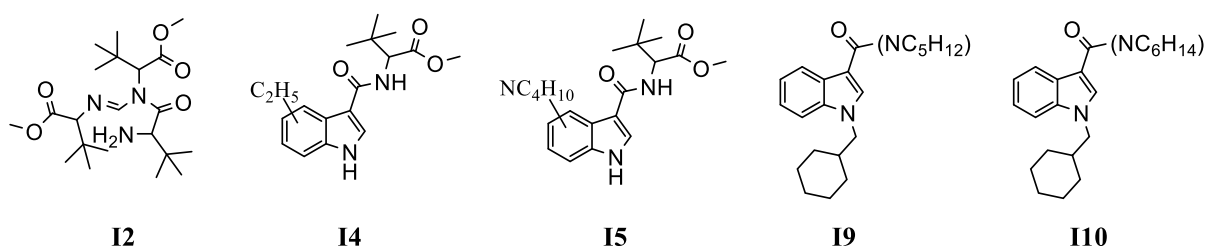


Figure 16: Structural formulas of the fifteen assessed key-impurities for MDMB-CHMICA. (top) elucidated via NMR and HR-MS/MS experiments. (bottom) elucidated only by HR-MS/MS experiments.

Although the here presented impurity profiling was only carried out on one synthetic cannabinoids, already large amounts of case specific and strategic information could already be extracted, providing first valuable insights into the manufacturing of synthetic cannabinoids. However, the range of possible application also include other chemicals of high purity for which an impurity profiling would be applicable, such as counterfeit pharmaceuticals or crystalline methamphetamine.

### 3.2 Adaptability of the central workflow to different formulations of synthetic cannabinoids Publication 1, 3, 4 and 5

The applicability of the workflow was demonstrated on pure samples of synthetic cannabinoids. The next step was to adapt and extend the sample preparation to the common formulations of synthetic cannabinoids: SP Publication 1, 4 and 5 and EL Publication 3.

Compared to the pure samples of synthetic cannabinoid, which can just be dissolved and injected into the F-LC, the active ingredient and related synthesis impurities on SP need to be extracted from the plant material first. As the impurity profiling targets trace components of the respective synthetic cannabinoids, it was necessary to prove, that even though the synthetic cannabinoid was sprayed onto and is extracted from an herbal matrix, the original impurity composition is not affected either by loss of substance or any type of degradation. Furthermore, it was necessary to keep the number of extracted plant components to a minimum, to not influence the subsequent F-LC measurements by column clogging through sugars or polymers and the UHPLC-MS measurements by ion-suppression, signal superimposition or interference. Thus, in first experiments, several self-made herbal blends were produced by dissolving pure MDMB-CHMICA with known impurity composition in acetone and impregnating two of the most common herbal matrices damiana and strawberry leaves. After the acetone was evaporated, the synthetic cannabinoid and related impurity components were extracted again from the plant surface by rinsing the herbal material twice with acetonitrile. These extracts generally had a greenish colour and a resin like consistency after the acetonitrile was evaporated. However, they could be submitted to the same F-LC gradient and fractionation system as the pure samples with no shifts in retention time or disruption of the chromatography. With each successive extract clean-up run, the F-LC column started to saturate with a green colour, which is why a run limit of five herbal extract samples was set until the column was changed to prevent potential retention time shifts or the elution of the green colourants.

Both the extracts of the damiana and strawberry leaves were submitted to the regular sample preparation procedure as the pure samples of MDMB-CHMICA. The corresponding chromatographic impurity signatures were compared to that of the pure material initially impregnated onto the herbal matrix. The BPCs of both extracts and the pure material are shown in Figure 17. The chromatographic impurity signatures of MDMB-CHMICA in the herbal were highly similar to that of the pure power sample. Only the damiana extract showed minor interferences of additional signals. However, the corresponding overlaid m/z signal intensities of related impurity components were not influenced by the matrix components. As the automated integration targets specific m/z values, co-eluting interferences without any ion-suppression effects can be disregarded and do not influence the final integral. The integrated peak areas of the impurities related to MDMB-CHMICA were highly similar for the pure sample and both self-produced SPs over the complete chromatographic range. In a preliminary test, ten herbal blend samples containing MDMB-CHMICA were available from a police seizure (2 x 4 and 1 x 2 products of the same brand) and were analyzed for their chromatographic impurity compositions following the general sample preparation and data evaluation procedure. All products from the same brand were found to form clusters in a PCA model. In conclusion, these products were expected to be produced using the same synthesis

batch of MDMB-CHMICA and its characteristic impurities, validating the applicability of the developed workflow for this consumption form.

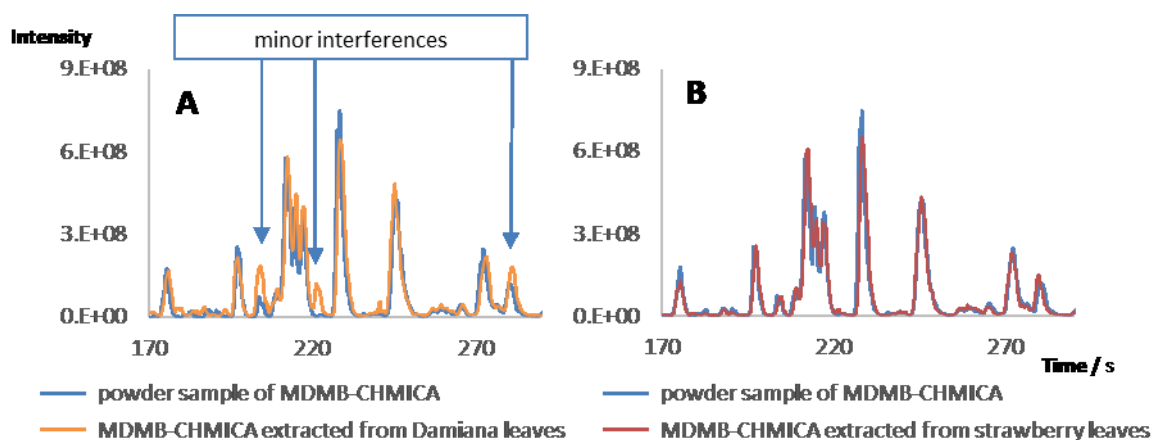


Figure 17: Excerpts of the most discriminating areas of the base peak chromatograms (BPC) for impurity profiles of MDMB-CHMICA after extraction from damiana (orange, A) and strawberry (red, B) leaves compared to the corresponding powder sample (blue, A and B).

As mentioned before, the purpose of the F-LC was to separate the main component from related synthesis impurities. The main component can then further be used for a comprehensive profiling via IRMS. However, similar to the impurity profile it was necessary to prove, that the extraction and clean-up had no influence on the isotopic composition of the main component through isotopic fractionation and no contaminant plant components falsify the measured isotope ratios. For this separate study, again several self-produced SPs were manufactured with the synthetic cannabinoids MDMB-CHMICA<sup>Publication 5</sup>, Cumyl-PeGaClone<sup>Publication 5</sup> and 5F-PB-22<sup>Publication 4</sup> of known isotopic composition in the same manner as it was done for the impurity profiling. After extraction and clean-up via preparative column chromatography (for 5F-PB-22) and F-LC, the isotopic composition of the extracts was compared to the corresponding original material. It was found, that the sample preparation had no influence on the isotopic composition of any synthetic cannabinoid. Furthermore, the purity (absence of by-products or matrix components from herbal material) of the main components were validated via UHPLC-MS and GC-MS prior to IRMS measurements.

The extraction of synthetic cannabinoids and related impurities from EL was more complex compared to the SPs, due to the liquid nature of the matrix. Although the EL samples could be injected directly in the F-LC system, the highly polar PG and VG would directly bind to the silica gel solid phase and clog the column. Hence, it was necessary to remove the majority of polar matrix components from the synthetic cannabinoid and related synthesis impurities. For this extraction the same validation parameters were set as for the extraction from herbal material. It was necessary to reproducibly extract all important substances without disruption of the F-LC or UHPLC-MS. For this study the synthetic cannabinoid Cumyl-5F-PINACA was chosen that belongs to the class of indazole carboxamides and is a liquid at room temperature, making it a prime candidate for mixing with a liquid matrix. One pure sample was available for the complete method development and assessment of suitable key-impurities for batch discrimination. Via HR-MS/MS experiments, twelve related impurities were tentatively identified. Several self-made EL were prepared with PG, VG and ethanol and varying

concentrations of Cumyl-5F-PINACA (0.1, 0.2, 0.5, 0.7 and 1.0 % (w/w)) with the known impurity composition. To remove the matrix, small quantities of EL were diluted with water and chloroform was added. After vortexing, the chloroform phase was removed and evaporated to dryness, yielding a resinlike residue of the synthetic cannabinoid and related components, which can be injected into the F-LC for further sample preparation. The pooled impurity fractions are then measured on UHPLC-MS to record the chromatographic impurity signatures. The complete sample preparation sequence (F-LC + UHPLC-MS) was validated by comparing the semi-quantitative signal integrals of the chromatographic impurity signatures of the five self-made e-liquids with the original material of Cumyl-5F-PINACA, giving an average signal relative standard deviation of 10.5 % between the measurements of the five preparations with different concentrations with no loss of any important signal or ion suppression through matrix components. On the basis of the previously assessed twelve key-impurities for Cumyl-5F-PINACA, fifteen seized and online test-purchased EL samples were analyzed for potential links. It was found that date of purchase, the identity of the online shop and brand name were the critical factors for differences in the by-product profiles of samples and the type flavor was insignificant. With the given data, a hypothetical *modus operandi* for the production of EL was deduced as follows: One large batch of e-liquid matrix is prepared and pure material of Cumyl-5F-PINACA is dissolved. This large batch is then split into smaller aliquots and mixed with various flavors. These aliquots are filled into small bottles with equal brand names but different flavor types and sold. This process is repeated whenever an e-liquid runs out of stock.

### 3.3 Comprehensive profiling using impurity and isotopic signatures <sup>Publication 4 and 5</sup>

In an early short communication <sup>Publication 4</sup>, the general applicability of IRMS to discriminate synthesis batches of pure and SP samples of synthetic cannabinoids, in particular 5F-PB-22, was investigated. As the active ingredient had to be extracted from the herbal material, a sample clean-up by preparative column chromatography (self-packed) was developed and validated to not influence the isotopic composition of the synthetic cannabinoid. The extracted 5F-PB-22 from fourteen SP samples obtained from police seizures were analysed for their  $\delta^{13}\text{C}$ ,  $\delta^{15}\text{N}$  and  $\delta^2\text{H}$  isotope ratios and could be discriminated into three clusters which presumably have been manufactured from individual batches.

With the applicability proven, a larger sample pool of overall 61 pure and 118 SP samples of MDMB-CHMICA and 1 pure and 30 SP samples of Cumyl-PeGaClone were measured on IRMS for their  $\delta^{13}\text{C}$  and  $\delta^{15}\text{N}$  isotope ratios. Furthermore, the three precursor substances TLME, indole and cumylamine were purchased from different global vendors and measured on IRMS to assess the overall diversity of their isotopic composition, helping to better understand variations in the corresponding synthetic cannabinoids.

Figure 19 shows the  $\delta^{13}\text{C}$  and  $\delta^{15}\text{N}$  ratios for MDMB-CHMICA, Cumyl-PeGaClone and 5F-PB-22. The synthetic cannabinoids were found to form individual clusters, independent from their source, formulation or date of acquisition. In respect to the high diversity of isotopic composition for the individual precursor substances, it was concluded that each of these cannabinoids were synthesized by one manufacturer, who repeatedly uses bulk material of precursor substances from a specific provenance. Slight variations in isotopic composition are most probably the result of a different synthesis procedure leading to slight isotopic fractionation or the manufacturer supplementing his precursor stock. By focusing on the IRMS data of MDMB-CHMICA and implementing the corresponding dates of purchase/seizure for each SP, a tendency for agglomeration was observed for samples from similar periods (Figure 18). Each of the agglomerates was expected to represent at least one synthesis batch of MDMB-CHMICA shipped from Asia to Europe, which then was distributed amongst the European SP producers, indicated by the unspecificity of agglomerates for individual product brands or online-shops. Although the IRMS data shown in Figure 18 suggest the presence of three individual shipments, the impurity profiling of the corresponding SP revealed the fine-structure of the dataset. It was found, that each IRMS agglomerate consisted of multiple synthesis

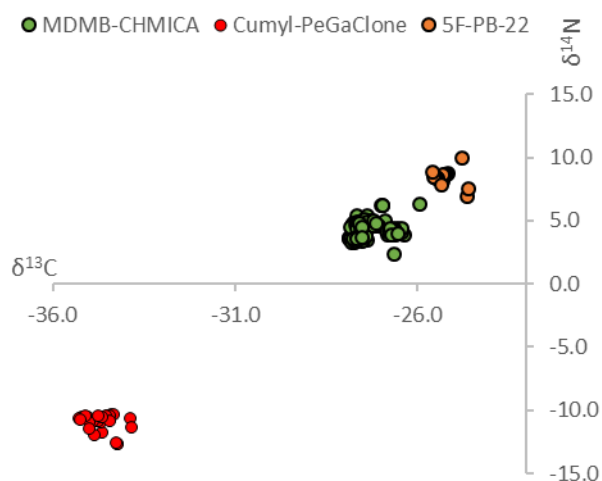


Figure 19:  $\delta^{13}\text{C}$  and  $\delta^{15}\text{N}$  values for all samples of MDMB-CHMICA (green), Cumyl-PeGaClone (red) and 5F-PB-22 (orange). Each synthetic cannabinoid clustered individually.

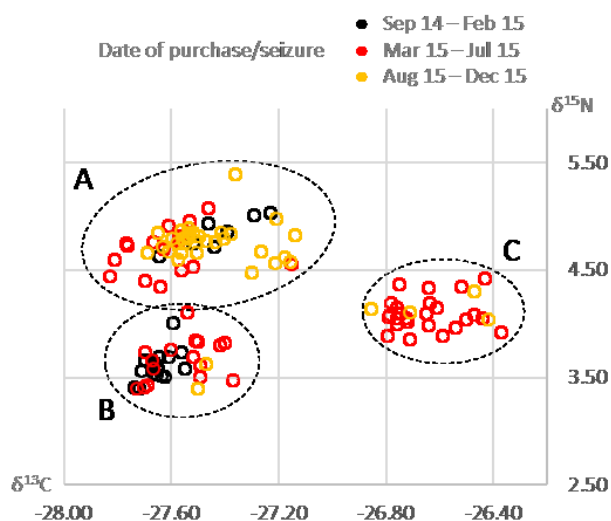


Figure 18:  $\delta^{13}\text{C}$  and  $\delta^{15}\text{N}$  values for all "Spice-Products" of MDMB-CHMICA, either measured via EA- or GC-IRMS. Colouring of samples is corresponding to the date of purchase or seizure of the "Spice-Products" in intervals of 5 month (● September 2014 to February 2015; ● March 2015 to July 2015; ● August 2015 to December 2015).

batches, distinguishable by differences in the chromatographic impurity signatures. The samples in Agglomerate B and C showed only minor differences between the individual identified batches, whereas the batches in agglomerate A could be separated into two larger groups through major differences for two of the fifteen key-impurities for MDMB-CHMICA. One of the groups comprised for all products of the period between September 2014 to February 2015 and the majority of products from March to July 2015. The second for the majority of products from August to December 2015. In conclusion, it is expected that four larger shipments of pure synthetic cannabinoids, similar to the seizure in

Luxembourg, were delivered by a single manufacturer to the European market in intervals of several month in the course of the years 2014 and 2015.

## 4. Summary and outlook

In the presented work, a novel profiling workflow for synthetic cannabinoids was developed, validated and exercised for powder, Spice-product (SP) and E-liquid (EL) samples of different synthetic cannabinoids. The final workflow consisted of a sample preparation step, either a liquid-liquid extraction for E-liquids or a solid extraction for SP. The powder samples and extracts of synthetic cannabinoids were then submitted to Flash-chromatography (F-LC), to isolate related synthesis impurities from the main component. The chromatographic impurity signatures were assessed via ultra-high-pressure liquid chromatography coupled to mass spectrometry (UHPLC-MS). In the first cycle of the self-optimizing workflow, the automatically integrated LC-MS data was submitted to multivariate data analysis, in particular principle component analysis (PCA), to assess a selection of key-impurities with high discrimination potential. These key-impurities were then selectively isolated in larger quantities for structural elucidation via high resolution MS (HR-MS) and nuclear magnetic resonance spectroscopy (NMR). In parallel, controlled synthesis were carried out to better understand variations in impurity signatures and to assess the significance of variations in the impurity patterns of seized samples. As comprehensive profiling approach, the previously isolated main component was measured via isotope ratio mass spectrometry (IRMS). The chromatographic impurity signatures and the corresponding isotopic composition of the main component can either be evaluated individually or can again be combined in a single evaluation model to deduce as much strategic information about the origin, number of different manufacturers, types of different synthesis, batch sizes and distribution networks of the finished products as possible from a given sample pool.

Although the initial development of the profiling workflow was the main topic of this thesis, by exemplarily exercising the workflow for the highly prevalent synthetic cannabinoid MDMB-CHMICA, a valuable portion of police intelligence could be acquired about synthetic cannabinoids and the new psychoactive substances (NPS) phenomenon as such. From the obtained results it could be concluded, that the European market is supplied by consecutive shipments of bulk material of synthetic cannabinoid (collection of several individual synthesis batches) in periods of several month. This material is then divided amongst the European intermediaries for further distribution. For each individual synthetic cannabinoid, a single manufacturer is expected, producing pure material in batch sizes between 5-10 kg.

One of the major requirements for the workflow was a high adaptability to various types of substances. Thus, in the future other highly pure drugs can be profiled by their synthesis impurities and isotopic composition such as counterfeit pharmaceuticals or crystalline methamphetamine with purities over 99 %. Although the framework for other applications is described in this work, every new substance that is to be profiled by means of the workflow requires a certain amount of work, e.g. assessment and characterization of key- impurities, controlled synthesis and adaptability to typical types of formulations.

## 5. References

1. Collaborators GBDRF. Global, regional, and national comparative risk assessment of 84 behavioural, environmental and occupational, and metabolic risks or clusters of risks, 1990-2016: a systematic analysis for the Global Burden of Disease Study 2016. *Lancet (London, England)*. 2017;390(10100):1345-1422.
2. UNODC. UNODC World drug report 2018. 2018.
3. UN. Single Convention on Narcotic Drugs. United Nations Conference on Narcotic Drugs; 1961; New York, USA.
4. UN. Convention on Psychotropic Substances; 1971; Vienna, Austria.
5. Ghelardini C, Di Cesare Mannelli L, Bianchi E. The pharmacological basis of opioids. *Clinical cases in mineral and bone metabolism : the official journal of the Italian Society of Osteoporosis, Mineral Metabolism, and Skeletal Diseases*. 2015;12(3):219-221.
6. Hughes J, Smith TW, Kosterlitz HW, Fothergill LA, Morgan BA, Morris HR. Identification of two related pentapeptides from the brain with potent opiate agonist activity. *Nature*. 1975;258:577.
7. Hughes J. Isolation of an endogenous compound from the brain with pharmacological properties similar to morphine. *Brain research*. 1975;88(2):295-308.
8. White PT, Raymer S. The Poppy. *National Geographic*. 1985;167:142-188.
9. Blakemore PR, White JD. Morphine, the Proteus of organic molecules. *Chemical Communications*. 2002(11):1159-1168.
10. Pathan H, Williams J. Basic opioid pharmacology: an update. *British Journal of Pain*. 2012;6(1):11-16.
11. Van Bever WF, Niemegeers CJ, Schellekens KH, Janssen PA. N-4-Substituted 1-(2-arylethyl)-4-piperidiny-N-phenylpropanamides, a novel series of extremely potent analgesics with unusually high safety margin. *Arzneimittel-Forschung*. 1976;26(8):1548-1551.
12. Freye E. Wirkungen und Nebenwirkungen der Opiode. In: Freye E, ed. *Opiode in der Medizin*. Berlin, Heidelberg: Springer Berlin Heidelberg; 2010:55-77.
13. Trifilieff P, Martinez D. Chapter Five - Cocaine: Mechanism and Effects in the Human Brain. In: *The Effects of Drug Abuse on the Human Nervous System*. Academic Press; 2014:103-133.
14. Gawin F. Cocaine addiction: psychology and neurophysiology. *Science*. 1991;251(5001):1580-1586.
15. Grotenhermen F, Russo E. *Cannabis and Cannabinoids: Pharmacology, Toxicology, and Therapeutic Potential*. The Hamworth Integrative Healing press; 2002.
16. Adams R, Hunt M, Clark JH. Structure of Cannabidiol, a Product Isolated from the Marijuana Extract of Minnesota Wild Hemp. I. *Journal of the American Chemical Society*. 1940;62(1):196-200.
17. Gaoni Y, Mechoulam R. Isolation, Structure, and Partial Synthesis of an Active Constituent of Hashish. *Journal of the American Chemical Society*. 1964;86(8):1646-1647.
18. Pertwee RG. The diverse CB1 and CB2 receptor pharmacology of three plant cannabinoids:  $\Delta^9$ -tetrahydrocannabinol, cannabidiol and  $\Delta^9$ -tetrahydrocannabivarin. *British Journal of Pharmacology*. 2008;153(2):199-215.
19. Courtney KE, Ray LA. Chapter 15 - Clinical neuroscience of amphetamine-type stimulants: From basic science to treatment development. In: Ekhtiari H, Paulus M, eds. *Prog. Brain Res*. Vol 223. Elsevier; 2016:295-310.
20. Rothman RB, Baumann MH, Dersch CM, et al. Amphetamine-type central nervous system stimulants release norepinephrine more potently than they release dopamine and serotonin. *Synapse*. 2001;39(1):32-41.
21. EU. COUNCIL DECISION 2005/387/JHA; On the information exchange, risk-assessment and control of new psychoactive substances. *Official Journal of the European Union*. 2005.
22. Auwärter V, Dresen S, Weinmann W, Müller M, Pütz M, Ferreirós N. 'Spice' and other herbal blends: harmless incense or cannabinoid designer drugs? *J. Mass Spectrom*. 2009;44(5):832-837.
23. Kram TC, Cooper DA, Allen AC. Behind the Identification of China White. *Analytical Chemistry*. 1981;53(12):1379A-1386A.

24. Climko R, Roehrich H, R. Sweeney D, Al-Razi J. *Ecstasy: a review of MDMA and MDA*. Vol 161986.
25. Freudenmann RW, Oxler F, Bernschneider-Reif S. The origin of MDMA (ecstasy) revisited: the true story reconstructed from the original documents. *Addiction (Abingdon, England)*. 2006;101(9):1241-1245.
26. Janssen P; Research Laboratorium C Janssen NV, 1-aralkyl-4-(n-aryl-carbonyl amino)-piperidines and related compounds US3164600A, 1961.
27. Shulgin A, Shulgin A. *PiHKAL: A Chemical Love Story*. Transform Press; 1991.
28. Shulgin A, Shulgin A. *TiHKAL: A Continuation*. Transform Press; 1997.
29. EMCDDA. 2018; Available at: <http://www.emcdda.europa.eu/system/files/publications/8870/2018-2489-td0118414enn.pdf>. Accessed August 2019
30. Deutsches Bundesministerium der Justiz und Verbraucherschutz. 2017; Available at: [http://www.gesetze-im-internet.de/englisch\\_amg/medicinal\\_products\\_act.pdf](http://www.gesetze-im-internet.de/englisch_amg/medicinal_products_act.pdf). Accessed December 2018
31. Deutsches Bundesministerium der Justiz und Verbraucherschutz. 2018; Available at: [http://www.gesetze-im-internet.de/bundesrecht/btmg\\_1981/gesamt.pdf](http://www.gesetze-im-internet.de/bundesrecht/btmg_1981/gesamt.pdf). Accessed December 2018
32. Sedefov R, Gallegos A, Mounteney J, Kenny P. Chapter 2 - Monitoring Novel Psychoactive Substances: A Global Perspective. In: Dargan PI, Wood DM, eds. *Novel Psychoactive Substances*. Boston: Academic Press; 2013:29-54.
33. Miliano C, Margiani G, Fattore L, De Luca MA. Sales and Advertising Channels of New Psychoactive Substances (NPS): Internet, Social Networks, and Smartphone Apps. *Brain sciences*. 2018;8(7):123.
34. EMCDDA. The internet and drug markets. 2016.
35. Zamengo L, Frison G, Bettin C, Sciarrone R. Understanding the risks associated with the use of new psychoactive substances (NPS): high variability of active ingredients concentration, mislabelled preparations, multiple psychoactive substances in single products. *Toxicology letters*. 2014;229(1):220-228.
36. Ernst L, Schiebel HM, Theuring C, Lindigkeit R, Beuerle T. Identification and characterization of JWH-122 used as new ingredient in "Spice-like" herbal incenses. *Forensic Sci. Int*. 2011;208(1-3):e31-35.
37. Bersani FS, Corazza O, Albano G, et al. 25C-NBOMe: Preliminary Data on Pharmacology, Psychoactive Effects, and Toxicity of a New Potent and Dangerous Hallucinogenic Drug. *BioMed Research International*. 2014;2014:6.
38. Kersten BP, McLaughlin ME. Toxicology and management of novel psychoactive drugs. *Journal of pharmacy practice*. 2015;28(1):50-65.
39. Loi B, Corkery JM, Claridge H, et al. Deaths of individuals aged 16–24 years in the UK after using mephedrone. *Human Psychopharmacology: Clinical and Experimental*. 2015;30(4):225-232.
40. Tait RJ, Caldicott D, Mountain D, Hill SL, Lenton S. A systematic review of adverse events arising from the use of synthetic cannabinoids and their associated treatment. *Clinical toxicology (Philadelphia, Pa.)*. 2016;54(1):1-13.
41. Devane WA, Dysarz FA, 3rd, Johnson MR, Melvin LS, Howlett AC. Determination and characterization of a cannabinoid receptor in rat brain. *Molecular pharmacology*. 1988;34(5):605-613.
42. Weissman A, Milne GM, Melvin LS, Jr. Cannabimimetic activity from CP-47,497, a derivative of 3-phenylcyclohexanol. *The Journal of pharmacology and experimental therapeutics*. 1982;223(2):516-523.
43. Munro S, Thomas KL, Abu-Shaar M. Molecular characterization of a peripheral receptor for cannabinoids. *Nature*. 1993;365(6441):61-65.
44. Matsuda LA, Lolait SJ, Brownstein MJ, Young AC, Bonner TI. Structure of a cannabinoid receptor and functional expression of the cloned cDNA. *Nature*. 1990;346(6284):561-564.
45. Ledent C, Valverde O, Cossu G, et al. Unresponsiveness to cannabinoids and reduced addictive effects of opiates in CB1 receptor knockout mice. *Science*. 1999;283(5400):401-404.
46. Devane WA, Hanus L, Breuer A, et al. Isolation and structure of a brain constituent that binds to the cannabinoid receptor. *Science*. 1992;258(5090):1946-1949.



47. Mechoulam R, Ben-Shabat S, Hanus L, et al. Identification of an endogenous 2-monoglyceride, present in canine gut, that binds to cannabinoid receptors. *Biochemical Pharmacology*. 1995;50(1):83-90.
48. Adams R, Loewe S, Jelinek C, Wolff H. Tetrahydrocannabinol Homologs with Marihuana Activity. IX1. *Journal of the American Chemical Society*. 1941;63(7):1971-1973.
49. Mechoulam R, Feigenbaum JJ, Lander N, et al. Enantiomeric cannabinoids: stereospecificity of psychotropic activity. *Experientia*. 1988;44(9):762-764.
50. Bell MR, D'Ambra TE, Kumar V, et al. Antinociceptive (aminoalkyl)indoles. *Journal of Medicinal Chemistry*. 1991;34(3):1099-1110.
51. Kuster JE, Stevenson JI, Ward SJ, D'Ambra TE, Haycock DA. Aminoalkylindole binding in rat cerebellum: selective displacement by natural and synthetic cannabinoids. *Journal of Pharmacology and Experimental Therapeutics*. 1993;264(3):1352-1363.
52. Huffman JW, Dai D, Martin BR, Compton DR. Design, Synthesis and Pharmacology of Cannabimimetic Indoles. *Bioorganic & Medicinal Chemistry Letters*. 1994;4(4):563-566.
53. Makriyannis A, Hongfeng D, Cannabimimetic indole derivatives. US6900236 B1, 2005.
54. Makriyannis A, Liu Q, Heteroindanes: A new class of potent cannabimimetic ligands. WO2003035005, 2003.
55. Bowden M, Williamson J, Cannabinoid compounds. WO2014167530, 2014.
56. Buchler P, Indazole derivatives. WO2009106980, 2009.
57. Huffman JW, Mabon R, Wu M-J, et al. 3-Indolyl-1-naphthylmethanes: new cannabimimetic indoles provide evidence for aromatic stacking interactions with the CB1 cannabinoid receptor. *Bioorganic & Medicinal Chemistry*. 2003;11(4):539-549.
58. Huffman JW, Szklennik PV, Almond A, et al. 1-Pentyl-3-phenylacetylindoles, a new class of cannabimimetic indoles. *Bioorganic & Medicinal Chemistry Letters*. 2005;15(18):4110-4113.
59. Rinaldi-Carmona M, Barth F, Héaulme M, et al. SR141716A, a potent and selective antagonist of the brain cannabinoid receptor. *FEBS Letters*. 1994;350(2):240-244.
60. Compton DR, Rice KC, De Costa BR, et al. Cannabinoid structure-activity relationships: correlation of receptor binding and in vivo activities. *The Journal of pharmacology and experimental therapeutics*. 1993;265(1):218-226.
61. Cheng Y, Prusoff WH. Relationship between the inhibition constant (K<sub>i</sub>) and the concentration of inhibitor which causes 50 per cent inhibition (I<sub>50</sub>) of an enzymatic reaction. *Biochem. Pharmacol.* 1973;22(23):3099-3108.
62. Showalter VM, Compton DR, Martin BR, Abood ME. Evaluation of binding in a transfected cell line expressing a peripheral cannabinoid receptor (CB2): identification of cannabinoid receptor subtype selective ligands. *The Journal of pharmacology and experimental therapeutics*. 1996;278(3):989-999.
63. Aung MM, Griffin G, Huffman JW, et al. Influence of the N-1 alkyl chain length of cannabimimetic indoles upon CB1 and CB2 receptor binding. *Drug and Alcohol Dependence*. 2000;60(2):133-140.
64. Banister SD, Adams A, Kevin RC, et al. Synthesis and pharmacology of new psychoactive substance 5F-CUMYL-P7AICA, a scaffold- hopping analog of synthetic cannabinoid receptor agonists 5F-CUMYL-PICA and 5F-CUMYL-PINACA. *Drug Testing and Analysis*. 2018;0(0).
65. Schoeder CT, Hess C, Madea B, Meiler J, Müller CE. Pharmacological evaluation of new constituents of "Spice": synthetic cannabinoids based on indole, indazole, benzimidazole and carbazole scaffolds. *Forensic Toxicology*. 2018;36(2):385-403.
66. Angerer V, Mogler L, Steitz JP, et al. Structural characterization and pharmacological evaluation of the new synthetic cannabinoid CUMYL-PEGACLONE. *Drug Test Anal.* 2018;10(3):597-603.
67. Uchiyama N, Kikura-Hanajiri R, Kawahara N, Haishima Y, Goda Y. Identification of a Cannabinoid Analog as a New Type of Designer Drug in a Herbal Product. *Chemical and Pharmaceutical Bulletin*. 2009;57(4):439-441.
68. Uchiyama N, Matsuda S, Kawamura M, Kikura-Hanajiri R, Goda Y. Two new-type cannabimimetic quinolinyl carboxylates, QUPIC and QUCHIC, two new cannabimimetic carboxamide derivatives, ADB-FUBINACA and ADBICA, and five synthetic cannabinoids detected with a thiophene derivative  $\alpha$ -PVT and an opioid receptor agonist AH-7921 identified in illegal products. *Forensic Toxicology*. 2013;31(2):223-240.

69. Uchiyama N, Kawamura M, Kikura-Hanajiri R, Goda Y. Identification of two new-type synthetic cannabinoids, N-(1-adamantyl)-1-pentyl-1H-indole-3-carboxamide (APICA) and N-(1-adamantyl)-1-pentyl-1H-indazole-3-carboxamide (APINACA), and detection of five synthetic cannabinoids, AM-1220, AM-2233, AM-1241, CB-13 (CRA-13), and AM-1248, as designer drugs in illegal products. *Forensic Toxicology*. 2012;30(2):114-125.
70. Uchiyama N, Matsuda S, Wakana D, Kikura-Hanajiri R, Goda Y. New cannabimimetic indazole derivatives, N-(1-amino-3-methyl-1-oxobutan-2-yl)-1-pentyl-1H-indazole-3-carboxamide (AB-PINACA) and N-(1-amino-3-methyl-1-oxobutan-2-yl)-1-(4-fluorobenzyl)-1H-indazole-3-carboxamide (AB-FUBINACA) identified as designer drugs in illegal products. *Forensic Toxicology*. 2013;31(1):93-100.
71. McLaughlin G, Morris N, Kavanagh PV, et al. The synthesis and characterization of the 'research chemical' N-(1-amino-3-methyl-1-oxobutan-2-yl)-1-(cyclohexylmethyl)-3-(4-fluorophenyl)-1H-pyrazole-5-carboxamide (3,5-AB-CHMFUPPYCA) and differentiation from its 5,3-regioisomer. *Drug Testing and Analysis*. 2016;8(9):920-929.
72. Ernst L, Brandhorst K, Papke U, et al. Identification and quantification of synthetic cannabinoids in 'spice-like' herbal mixtures: Update of the German situation in early 2017. *Forensic Science International*. 2017;277:51-58.
73. Weber C, Pusch S, Schollmeyer D, Münster-Müller S, Pütz M, Opatz T. Characterization of the synthetic cannabinoid MDMB-CHMCZCA. *Beilstein Journal of Organic Chemistry*. 2016;12:2808-2815.
74. Bernotas RC, Heterocycl-3-sulfonylazaindole or -azaindazole derivatives as 5-hydroxytryptamine-6 ligands US7576087B2, 2003.
75. Trotter BW, Nanda KK, Burgey CS, et al. Imidazopyridine CB2 agonists: Optimization of CB2/CB1 selectivity and implications for in vivo analgesic efficacy. *Bioorganic & Medicinal Chemistry Letters*. 2011;21(8):2354-2358.
76. Eatherton AJ, Pyridine derivatives as cb2 receptor modulators WO2004029026A1, 2002.
77. Chackalamannil S, Chelliah M, Clasby M, Eagen K, Cannabinoid receptor modulators. US7897601B2, 2007.
78. Angerer V, Franz F, Moosmann B, Bisel P, Auwärter V. 5F-Cumyl-PINACA in 'e-liquids' for electronic cigarettes: comprehensive characterization of a new type of synthetic cannabinoid in a trendy product including investigations on the in vitro and in vivo phase I metabolism of 5F-Cumyl-PINACA and its non-fluorinated analog Cumyl-PINACA. *Forensic Toxicol*. 2018.
79. Huizer H. A contribution to comparison. *Forensic Science International*. 1994;69(1):17-22.
80. Morelato M, Beavis A, Tahtouh M, Ribaux O, Kirkbride P, Roux C. The use of forensic case data in intelligence-led policing: The example of drug profiling. *Forensic Science International*. 2013;226(1):1-9.
81. UNODC. *Drug characterization/Impurity profiling*. Vienna: UNODC; 2001. Available from: <https://www.unodc.org/pdf/publications/st-nar-32-rev1.pdf>. Accessed 26. March 2019.
82. Dujourdy L, Besacier F. Headspace profiling of cocaine samples for intelligence purposes. *Forensic Sci. Int*. 2008;179(2-3):111-122.
83. Alm S, Granstam I, Jonson S, Strömberg L. Classification of illegal Leuckart amphetamine by gas chromatographic profiling. *Forensic Science Center, Linköping University, Report 25*. 1992.
84. Ensing J, Racamy C, De Zeeuw R. A rapid gas chromatographic method for the fingerprinting of illicit cocaine samples. *Journal of Forensic Science*. 1992;37(2):446-459.
85. Neumann H, Gloger M. Profiling of illicit heroin samples by high-resolution capillary gas chromatography for forensic application. *Chromatographia*. 1982;16(1):261-264.
86. Cheng WC, Poon NL, Chan MF. Chemical profiling of 3,4-methylenedioxymethamphetamine (MDMA) tablets seized in Hong Kong. *Journal of forensic sciences*. 2003;48(6):1249-1259.
87. Hommerson P, Khan AM, Bristow T, Harrison MW, de Jong GJ, Somsen GW. Drug impurity profiling by capillary electrophoresis/mass spectrometry using various ionization techniques. *Rapid communications in mass spectrometry : RCM*. 2009;23(18):2878-2884.
88. Huhn C, Pütz M, Dahlenburg R, Pyell U. Sassafras oils as precursors for the production of synthetic drugs: profiling via MEKC-UVD. Paper presented at: Beiträge zum XIV GTFCh-Symposium: Ausgewählte Aspekte der Forensischen Toxikologie 2005.

89. Marcelo MC, Mariotti KC, Ferrao MF, Ortiz RS. Profiling cocaine by ATR-FTIR. *Forensic Sci. Int.* 2015;246:65-71.
90. Bell SE, Burns DT, Dennis AC, Matchett LJ, Speers JS. Composition profiling of seized ecstasy tablets by Raman spectroscopy. *The Analyst.* 2000;125(10):1811-1815.
91. Watling RJ. Sourcing the provenance of cannabis crops using inter-element association patterns 'fingerprinting' and laser ablation inductively coupled plasma mass spectrometry. *Journal of Analytical Atomic Spectrometry.* 1998;13(9):917-926.
92. Koper C, van den Boom C, Wiarda W, et al. Elemental analysis of 3,4-methylenedioxymethamphetamine (MDMA): A tool to determine the synthesis method and trace links. *Forensic Sci. Int.* 2007;171(2-3):171-179.
93. Armellini S, Brenna E, Fronza G, Fuganti C, Pinciroli M, Serra S. Establishing the synthetic origin of amphetamines by <sup>2</sup>H NMR spectroscopy. *The Analyst.* 2004;129(2):130-133.
94. Beckett NM, Cresswell SL, Grice DI, Carter JF. Isotopic profiling of seized benzylpiperazine and trifluoromethylphenylpiperazine tablets using  $\delta^{13}\text{C}$  and  $\delta^{15}\text{N}$  stable isotopes. *Sci. Justice.* 2015;55(1):51-56.
95. Kurashima N, Makino Y, Sekita S, Urano Y, Nagano T. Determination of Origin of Ephedrine Used as Precursor for Illicit Methamphetamine by Carbon and Nitrogen Stable Isotope Ratio Analysis. *Analytical Chemistry.* 2004;76(14):4233-4236.
96. Salouros H, Sutton GJ, Howes J, Hibbert DB, Collins M. Measurement of Stable Isotope Ratios in Methylamphetamine: A Link to Its Precursor Source. *Analytical Chemistry.* 2013;85(19):9400-9408.
97. Schneiders S, Holdermann T, Dahlenburg R. Comparative analysis of 1-phenyl-2-propanone (P2P), an amphetamine-type stimulant precursor, using stable isotope ratio mass spectrometry. *Science and Justice.* 2009;49(2):94-101.
98. Chiarotti M, Marsili R, Moreda-Pineiro A. Gas chromatographic-mass spectrometric analysis of residual solvent trapped into illicit cocaine exhibits using head-space solid-phase microextraction. *J. Chromatogr. B Analyt. Technol. Biomed. Life Sci.* 2002;772(2):249-256.
99. Palhol F, Boyer S, Naulet N, Chabrilat M. Impurity profiling of seized MDMA tablets by capillary gas chromatography. *Analytical and Bioanalytical Chemistry.* 2002;374(2):274-281.
100. Zacca JJ, Grobério TS, Maldaner AO, Vieira ML, Braga JWB. Correlation of cocaine hydrochloride samples seized in Brazil based on determination of residual solvents: An innovative chemometric method for determination of linkage thresholds. *Anal. Chem.* 2013;85(4):2457-2464.
101. Zhang JX, Zhang DM, Han XG. Identification of impurities and statistical classification of methamphetamine hydrochloride drugs seized in the China. *Forensic Sci. Int.* 2008;182(1-3):13-19.
102. Ballany J, Caddy B, Cole M, et al. Development of a harmonised pan-European method for the profiling of amphetamines. *Sci. Justice.* 2001;41(3):193-196.
103. Esseiva P, Anglada F, Dujourdy L, et al. Chemical profiling and classification of illicit heroin by principal component analysis, calculation of inter sample correlation and artificial neural networks. *Talanta.* 2005;67(2):360-367.
104. Janzen KE, Fernando AR, Walter L. A database for comparison analysis of illicit cocaine samples. *Forensic Science International.* 1994;69(1):23-29.
105. Power JD, Kavanagh P, McLaughlin G, et al. Forensic analysis of P2P derived amphetamine synthesis impurities: identification and characterization of indene by-products. *Drug Testing and Analysis.* 2017;9(3):446-452.
106. Toske SG, McConnell JB, Brown JL, et al. Isolation and characterization of a newly identified impurity in methamphetamine synthesized via reductive amination of 1-phenyl-2-propanone (P2P) made from phenylacetic acid/lead (II) acetate. *Drug Testing and Analysis.* 2015;9(3):453-461.
107. Hauser F, Rößler T, Hulshof J, Weigel D, Zimmermann R, Pütz M. Identification of specific markers for amphetamine synthesised from the pre-precursor APAAN following the Leuckart route and retrospective search for APAAN markers in profiling databases from Germany and the Netherlands. *Drug. Test. Anal.* 2018;10(4):671-680.

108. Aalberg L, Andersson K, Bertler C, et al. Development of a harmonized method for the profiling of amphetamines. I. Synthesis of standards and compilation of analytical data. *Forensic Sci. Int.* 2005;149(2-3):219-229.
109. Doughty D, Painter B, Pigou P, Johnston MR. The synthesis and investigation of impurities found in clandestine laboratories: Baeyer-Villiger route part II; synthesis of phenyl-2-propanone (P2P) analogues from substituted benzaldehydes. *Forensic Chem.* 2018;9:1-11.
110. Kunalan V, Nic Daéid N, Kerr WJ, Buchanan HAS, McPherson AR. Characterization of Route Specific Impurities Found in Methamphetamine Synthesized by the Leuckart and Reductive Amination Methods. *Analytical Chemistry.* 2009;81(17):7342-7348.
111. Lambrechts M, Rasmussen KE. Leuckart-specific impurities in amphetamine and methamphetamine seized in Norway. *Bulletin on narcotics.* 1984;36(1):47-57.
112. Aalberg L, Andersson K, Bertler C, et al. Development of a harmonised method for the profiling of amphetamines: II. Stability of impurities in organic solvents. *Forensic Science International.* 2005;149(2):231-241.
113. Kendall C, Caldwell EA. Fundamentals of isotope geochemistry. In: *Isotope tracers in catchment hydrology.* Elsevier; 1998:51-86.
114. Kohn MJ. Carbon isotope compositions of terrestrial C3 plants as indicators of (paleo)ecology and (paleo)climate. *Proceedings of the National Academy of Sciences.* 2010;107(46):19691-19695.
115. O'Leary MH. Carbon Isotopes in Photosynthesis: Fractionation techniques may reveal new aspects of carbon dynamics in plants. *BioScience.* 1988;38(5):328-336.
116. Ehleringer JR, Casale JF, Lott MJ, Ford VL. Tracing the geographical origin of cocaine. *Nature.* 2000;408:311.
117. Zhang D, Sun W, Yuan Z, Ju H, Shi X, Wang C. Origin Differentiation of a Heroin Sample and its Acetylating Agent with  $^{13}\text{C}$  Isotope Ratio Mass Spectrometry. *European Journal of Mass Spectrometry.* 2005;11(3):277-285.
118. Carter JF, Titterton EL, Grant H, Sleeman R. Isotopic changes during the synthesis of amphetamines. *Chemical Communications.* 2002(21):2590-2591.
119. Collins M, Doddridge A, Salouros H. Cathinones: Isotopic profiling as an aid to linking seizures. *Drug Testing and Analysis.* 2016;8(9):903-909.
120. Tsujikawa K, Yamamuro T, Kuwayama K, Kanamori T, Iwata YT, Inoue H. Thermal degradation of a new synthetic cannabinoid QUPIC during analysis by gas chromatography-mass spectrometry. *Forensic Toxicology.* 2014;32(2):201-207.
121. Kramer JR, Deming TJ. General Method for Purification of  $\alpha$ -Amino acid-N-carboxyanhydrides Using Flash Chromatography. *Biomacromolecules.* 2010;11(12):3668-3672.
122. Patsavas MC, Byrne RH, Liu X. Purification of meta-cresol purple and cresol red by flash chromatography: Procedures for ensuring accurate spectrophotometric seawater pH measurements. *Marine Chemistry.* 2013;150:19-24.
123. Roge AB, Firke SN, Kawade RM, Sarje SK, Vadvalkar SM. Brief Review on Flash Chromatography. *International Journal of Pharmaceutical Sciences and Research.* 2011;2(8):1930-1937.
124. Still WC, Kahn M, Mitra A. Rapid chromatographic technique for preparative separations with moderate resolution. *The Journal of Organic Chemistry.* 1978;43(14):2923-2925.
125. Gross JH. *Mass Spectrometry.* Heidelberg: Springer Verlag; 2017.
126. Guilleme D, Veuthey JL, Chemistry RSo. *UHPLC in Life Sciences.* Royal Society of Chemistry; 2012.
127. Everitt BS, Dunn G. *Applied Multivariate Data Analysis.* Wiley; 2013.
128. Ullsten S, Danielsson R, Bäckström D, Sjöberg P, Bergquist J. Urine profiling using capillary electrophoresis-mass spectrometry and multivariate data analysis. *Journal of Chromatography A.* 2006;1117(1):87-93.
129. Chan ECY, Yap S-L, Lau A-J, Leow P-C, Toh D-F, Koh H-L. Ultra-performance liquid chromatography/time-of-flight mass spectrometry based metabolomics of raw and steamed *Panax notoginseng*. *Rapid Communications in Mass Spectrometry.* 2007;21(4):519-528.
130. Pluskal T, Castillo S, Villar-Briones A, Oresic M. MZmine 2: modular framework for processing, visualizing, and analyzing mass spectrometry-based molecular profile data. *BMC bioinformatics.* 2010;11:395.

131. IUPAC. 1997; Available at: <http://goldbook.iupac.org/html/R/R05318.html>. Accessed February 2019
132. Mamyrin B, Karataev V, Shmikk D, Zagulin V. The mass-reflectron. A new nonmagnetic time-of-flight high resolution mass-spectrometer. *Zhurnal Eksperimental'noj i Teoreticheskoy Fiziki*. 1973;64(1):82-89.
133. Makarov A. Electrostatic Axially Harmonic Orbital Trapping: A High-Performance Technique of Mass Analysis. *Analytical Chemistry*. 2000;72(6):1156-1162.
134. Comisarow MB, Marshall AG. Fourier transform ion cyclotron resonance spectroscopy. *Chemical Physics Letters*. 1974;25(2):282-283.
135. Xian F, Hendrickson CL, Marshall AG. High Resolution Mass Spectrometry. *Analytical Chemistry*. 2012;84(2):708-719.
136. Marshall AG, Hendrickson CL. High-Resolution Mass Spectrometers. *Annual Review of Analytical Chemistry*. 2008;1(1):579-599.
137. Rabi II, Zacharias JR, Millman S, Kusch P. A New Method of Measuring Nuclear Magnetic Moment. *Physical Review*. 1938;53(4):318-318.
138. Günther H. *NMR Spectroscopy: Basic Principles, Concepts and Applications in Chemistry, 3rd Edition*. Germany: Wiley VCH Verlag GmbH 2013.
139. Banister SD, Longworth M, Kevin R, et al. Pharmacology of Valinate and tert-Leucinate Synthetic Cannabinoids 5F-AMBICA, 5F-AMB, 5F-ADB, AMB-FUBINACA, MDMB-FUBINACA, MDMB-CHMICA, and Their Analogues. *ACS Chem. Neurosci*. 2016;7(9):1241-1254.
140. Brand WA. New reporting guidelines for stable isotopes – an announcement to isotope users. *Isotopes in Environmental and Health Studies*. 2011;47(4):535-536.
141. Forensic Isotope Ratio Mass Spectrometry Network. 2011; Available at: [http://www.forensic-isotopes.org/assets/IRMS%20Guide%20Finalv3.1\\_Web.pdf](http://www.forensic-isotopes.org/assets/IRMS%20Guide%20Finalv3.1_Web.pdf). Accessed February 2018
142. Coplen TB, Hopple J, Boehike J, Peiser H, Rieder S. Compilation of minimum and maximum isotope ratios of selected elements in naturally occurring terrestrial materials and reagents. *US Geology Survey*. 2002.

## 6. Scientific publications (published)

<b>Publication 1:</b>	Münster-Müller et al., Analytical Chemistry, 2018, 90(17): 10559-10567 DOI: 10.1021/acs.analchem.8b02679	Pages 49 - 58
<b>Publication 2:</b>	Münster-Müller et al., Drug Testing and Analysis, 2019, 11(8): 1192-1206 DOI: 10.1002/dta.2652	Pages 59 - 74
<b>Publication 3:</b>	Münster-Müller et al., Drug Testing and Analysis, 2019, in press DOI: 10.1002/dta.2673	Pages 75 - 83
<b>Publication 4:</b>	Münster-Müller et al., Drug Testing and Analysis, 2018, 10(8): 1323-1327 DOI: 10.1002/dta.2407	Pages 84 - 89

## 6.1 Publication 1

*A Novel Impurity-Profiling Workflow with the Combination of Flash-Chromatography, UHPLC-MS, and Multivariate Data Analysis for Highly Pure Drugs: A Study on the Synthetic Cannabinoid MDMB-CHMICA*

Sascha Münster-Müller, Ralf Zimmermann, Michael Pütz

Analytical Chemistry

2018


90(17): 10559-10567

# A Novel Impurity-Profiling Workflow with the Combination of Flash-Chromatography, UHPLC-MS, and Multivariate Data Analysis for Highly Pure Drugs: A Study on the Synthetic Cannabinoid MDMB-CHMICA

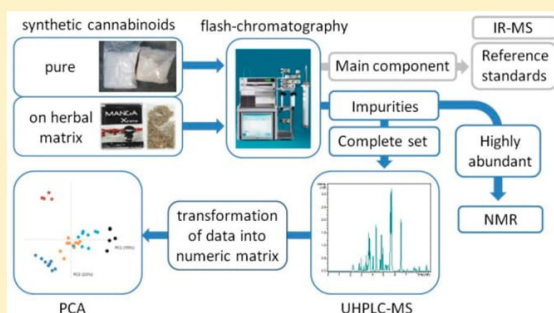
Sascha Münster-Müller,<sup>\*,†,‡</sup> Ralf Zimmermann,<sup>‡</sup> and Michael Pütz<sup>†</sup>

<sup>†</sup>Federal Criminal Police Office, Appelallee 45, 65203 Wiesbaden, Germany

<sup>‡</sup>University of Rostock, Dr.-Lorenz-Weg 2, 18059 Rostock, Germany

 Supporting Information

**ABSTRACT:** In this paper we present a new, versatile workflow for a synthesis impurity profiling concept, using the combination of flash chromatography (F-LC), liquid chromatography coupled to mass spectrometry (LC-MS), and multivariate data analysis. For three highly pure, structurally different synthetic cannabinoids, we demonstrate that via F-LC more than 99% of the main component (API) can be removed from a sample to enrich present impurities and yield combined fractions of targeted synthesis impurities with reproducible chromatographic signatures via LC-MS. The maximum overall relative standard deviation (RSD) of the complete experimental procedure for isolation and measurement of the impurity profiles (FL-C + LC-MS) was found to be 13.8% on average. The impurity signatures of 40 1 kg samples of MDMB-CHMICA (methyl (S)-2-(1-(cyclohexylmethyl)-1H-indole-3-carboxamido)-3,3-dimethylbutanoate) from one large seizure by Luxembourg customs were assessed via UHPLC-MS and compared via principle component analysis (PCA) to possibly discriminate between individual synthesis pathways or production batches and to deduce batch sizes. Three of these 40 samples could be identified as outliers, i. a., as a result of a highly abundant impurity with  $m/z$  498, isolated via F-LC and identified as methyl 2-(2-(1-(cyclohexylmethyl)-1H-indole-3-carboxamido)-3,3-dimethylbutanamido)-3,3-dimethylbutanoate, most probably manufactured with a varying synthesis pathway. The remaining 37 samples were subdivided via PCA and hierarchical cluster analysis into five clusters between five and ten samples, representing a maximum possible batch size of 10 kg of pure MDMB-CHMICA. Furthermore, the profiling concept was successfully applied to self-produced and seized “spice-products” to extract impurity profiles of MDMB-CHMICA without any ion suppression or chemical interference.



Drug profiling is a useful tool for the comparative characterization of the physical and chemical properties of illicit drugs, which is generally used by police authorities to establish links between samples of different seizures (“batch-to-batch comparison”), to obtain information on trafficking routes and to gather background information on the origin of samples. Some drugs can be profiled by assessing characteristic external parameters such as color, shape, and logo in combination with the chemical composition (API and excipients), e.g., Ecstasy tablets. However, when dealing with visually indistinguishable powders, a more extensive study of the chemical characteristics of possibly related drug samples is necessary. Apart from diluents or formulation agents, the impurities which are formed in the clandestine synthesis process are the most important discriminating chemical feature in a seized illicit drug sample. In the process of manufacturing, usually not only the desired main active ingredients but also a variety of inherent impurities arise which are characteristic for

the applied synthesis pathway and its conditions. For most of the illicit drugs, syntheses are carried out in clandestine laboratories by personnel with little chemical knowhow, producing a variety of impurities in rather high concentrations (e.g., the clandestine production of amphetamine via the Leuckart route or reductive amination<sup>1,2</sup>). A set of targeted synthesis impurities with high discrimination potential, so-called “key-impurities”, can be used to differentiate between individual sample collectives. These are selected by characterizing samples from varying sources (samples from seizures and from controlled syntheses) and conducting stability tests to minimize the influence of varying environmental and storage conditions on the targeted impurity profile. Several profiling studies have been already published for illicit drugs such as

Received: June 13, 2018

Accepted: August 6, 2018

Published: August 6, 2018





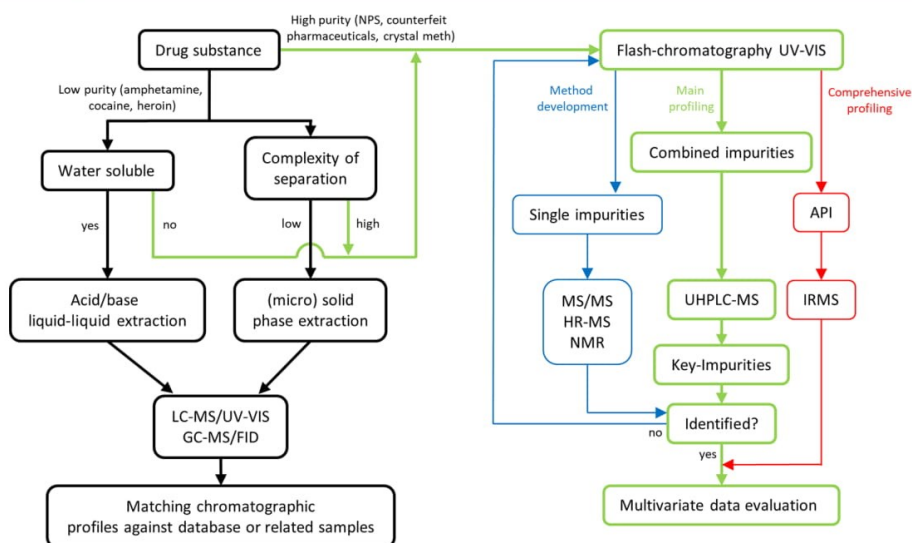


**Figure 1.** (Left) In black, examples of classical impurity profiling workflows for low purity illicit drugs. (Right) In color, the newly developed workflow with flash chromatography as the central element for enrichment and extraction of related synthesis impurities from highly pure drug substances, e.g., NPS or counterfeit pharmaceuticals. After isolation, chromatographic signatures of previously identified key impurities can be recorded by UHPLC-MS and evaluated in a multivariate model to link seizures or perform a batch discrimination. If necessary, unknown and newly appearing components with high discrimination potential can be selectively isolated via F-LC to characterize them via MS/MS, sum formula generation (HR-MS), or NMR experiments. Lastly, the cleaned API can be subjected to IRMS to assess isotopic composition. These data can be combined with the chromatographic impurity signatures to provide a comprehensive profiling concept with two orthogonal analytical techniques evaluated in one multivariate model.

heroin,<sup>3–5</sup> cocaine,<sup>6–8</sup> methamphetamine,<sup>9–12</sup> and amphetamine.<sup>13–15</sup> Their general analytical methodology, as sketched in Figure 1, consists of a straightforward sample preparation via a fast acid–base liquid–liquid extraction step or solid-phase extraction (SPE) to separate and enrich present impurities from the main component, cutting agents, and other adulterants, followed by analysis via gas chromatography (GC) or high performance liquid chromatography (HPLC) coupled to a mass spectrometer (MS), UV–vis spectrometer, or flame ionization detector (FID). The impurity profiles are then matched via chemometric models to databases of previously seized samples to link seizures.<sup>16–18</sup> More difficult is the impurity profiling of counterfeit pharmaceuticals, as these products are typically manufactured at professional industrial sites and exhibit chemical purities similar to that of genuine pharmaceutical preparations of >99.9% purity (0.05–0.1% permissible impurities, depending on the allowed maximum daily intake<sup>19</sup>). A few publications concerning the identification of counterfeit and genuine PDE-5 inhibitor drugs are available, using LC-MS<sup>20,21</sup> or a combination of LC-MS and LC-photodiode array (LC-PDA).<sup>22</sup> Dumarey et al. used trace-enriched HPLC-UV to identify different synthesis pathways for paracetamol,<sup>23</sup> Schneider et al. compared the impurity profiles of original and generic preparations of orlistat via tandem MS,<sup>24</sup> and Carrier et al. published a workflow of impurity enrichment via SPE followed by LC-MS and multivariate data analysis to identify impurities specific for a certain synthesis pathway of a drug substance.<sup>25</sup> In recent years, a new group of psychotropic compounds, formerly developed by the pharma industry as new drug candidates that were rejected from further development, appear on the European market as designer drugs, predicated as “new psychoactive substances” (NPS), mainly represented by

synthetic cannabinoids, cathinones, and opioids. In Germany, the subclass of synthetic cannabinoids exhibited the highest prevalence since 2008 when two of them, JWH-018 and CP 47,497-C8, were first detected in herbal smoking products<sup>26,27</sup> (so-called Spice products). Thenceforth, this class of NPS showed the highest degree of structural diversification and increased consecutively in numbers each year as reported by the European Monitoring Centre for Drugs and Drug Addiction (EMCDDA).<sup>28</sup> As the source for these substances, large-scale production in China is suspected, with trained chemists and sophisticated equipment in industrial sites, manufacturing reasonably pure designer drug substances. Apart from isotope ratio mass spectrometry (IRMS) profiling<sup>29,30</sup> and characterization of the plant matrix of seized herbal blend samples containing synthetic cannabinoids using two-dimensional gas chromatography,<sup>31</sup> no comprehensive profiling studies, in particular based on impurity profiling contributing to expand the knowledge base on their marketing structures, synthesis routes, and precursor chemicals, have been reported for NPS as of yet.

A direct measurement of high-purity pharmaceutical samples with modern instruments generally allows the detection of some abundant chemical impurities.<sup>20,21</sup> However, the implementation of an additional impurity enrichment procedure would lead to a better signal-to-noise ratio and reproducible integration of impurity peaks. As shown in Figure 1, liquid–liquid extraction (LLE) or solid-phase extraction (SPE) cannot be used for products that are insoluble in water or consist of a complex mixture of substances with similar chemical or physical properties. In this case, flash chromatography (F-LC) would be a promising alternative to isolate impurities from the main component. F-LC was first introduced in 1978 by Still et al.<sup>32</sup> and is a cost-effective and

convenient preparative separation method that has been used for many years in chemical synthesis, pharmacokinetics, and combinatorial chemistry.<sup>33–35</sup> The use of F-LC offers several advantages, for example its robustness against matrix effects and the high degree of adaptability and reproducibility with automatically operated pumps and prepacked columns. If necessary, highly abundant synthesis impurities can be isolated by targeted fractionation for identification via high-resolution mass spectrometry (HR-MS) and/or nuclear magnetic resonance spectroscopy (NMR), and the purified main components can be measured with IRMS to gather orthogonal information to the impurity profiling in a comprehensive profiling concept. Chromatographic signatures of the isolated impurities were recorded via UHPLC-MS with electrospray ionization (ESI), producing intact molecular ions. Instead of integrated peak areas from the base peak or total ion chromatogram, the intensities of  $m/z$  values at defined retention times can be integrated, while maintaining the information about the molecular mass as additional variable for data analysis via hierarchical cluster analysis and principle component analysis (PCA). PCA of impurity profiling data sets produces a scores plot, providing information about clustering of samples with similar impurity profiles and a loadings plot helping to select the most discriminating “key impurities” for a targeted impurity profiling procedure. Both statistical models are established tools for complex data analysis in various analytical profiling applications.<sup>3,36–38</sup>

In this paper we present a comprehensive study on a flexible, fast, and universal impurity profiling concept for highly pure NPS based on the combination of F-LC, UHPLC-MS, and data evaluation via multivariate data analysis, conducted on the synthetic cannabinoid MDMB-CHMICA **1** (Figure 2).

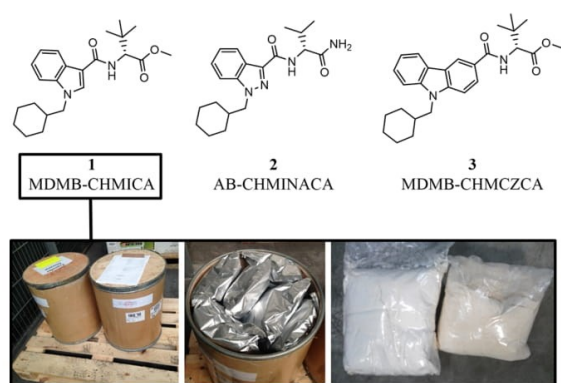


**Figure 2.** (Top) Structural formula of MDMB-CHMICA (**1**), AB-CHMINACA (**2**), and MDMB-CHMCZCA (**3**). (Bottom) Photographs of the original seizure of 40 kg of MDMB-CHMICA at Luxembourg customs, mislabeled as “polyethylene-co-vinyl acetate”.

MDMB-CHMICA was selected as main target drug for this study because it was one of the most prevalent synthetic cannabinoids in Europe in 2015/2016 and found in large quantities on herbal blends from test purchases in online shops and police seizures.<sup>39</sup> One of the largest seizures was in December 2014, where 40 1 kg packages of pure MDMB-CHMICA were seized by customs at Luxembourg airport. Since the first appearance of this cannabinoid, numerous fatal intoxications have been reported to the authorities,<sup>40–42</sup> the most severe being related to the consumption of the herbal

blend “Mocarz” (strongman) in Poland,<sup>43</sup> resulting in the first formal risk assessment for a synthetic cannabinoid conducted by the EMCDDA due to the eminent danger from this substance.<sup>44</sup> Because of the very fast replacement cycle for the NPS on the Internet market (due to the rapid reaction of NPS product manufacturers to NPS-related legislative measures of state governments), it is not intended or proposed to establish a long-term database-assisted profiling program for single substances as it is in force for established classic drugs such as amphetamine or heroin. The strategic aim of this study is to work out a set of suitable impurities for a relevant and representative synthetic cannabinoid that can be used for batch-to-batch profiling of seized material and, this way, find out about links between different seized products or links between a seized product sample and similar products from Internet test purchases and thus, more generally, to extend the knowledge base on the structure, modi operandi, and development of the international NPS and designer drug market.

To demonstrate the applicability of the presented profiling workflow also to other substance classes, a less comprehensive adaptability study of the sample preparation was carried out for the two structurally different cannabinoids AB-CHMINACA<sup>45</sup> **2** (Figure 2 *N*-[(1*S*)-1-(aminocarbonyl)-2-methylpropyl]-1-(cyclohexylmethyl)-1*H*-indazole-3-carboxamide), and MDMB-CHMCZCA<sup>46</sup> **3** (Figure 2 methyl (*S*)-2-(9-(cyclohexylmethyl)-9*H*-carbazole-3-carboxamido)-3,3-dimethylbutanoate), with indazole and carbazole core structures, which, in combination with the indole core of MDMB-CHMICA, represent the three most common classes of synthetic cannabinoids on the NPS market.

Typically, synthetic cannabinoids are not consumed as pure substances but smoked as herbal blends containing a single digit concentration of them. We included this most prevalently used form in the presented study to demonstrate the applicability of the profiling workflow to an already formulated product as it can be found on the market. For that purpose, 10 seized herbal blends containing **1** of different brands were chosen to prove that even after a cannabinoid has been applied to the herbal matrix, the individual impurity profiles can be distinguished.

## MATERIALS AND METHODS

**Chemicals.** Deionized water was tapped by a Milli-Q Synthesis A10 device (Millipore, Schwalbach, Germany), hypergrade acetonitrile (ACN) for LC-MS was purchased from Merck (Darmstadt, Germany), and formic acid (~98%), ammonium formate (>99%), *n*-hexane (>99.99%), and ethyl acetate (≥99.0%) were from Fluka (Buchs, Germany).

**Synthetic Cannabinoid Samples. Pure Material.** Samples of **1**, **2**, and **3** were available from police seizures. Forty samples of pure **1** were obtained by sampling 40 1 kg packages of a large seizure by Luxembourg customs individually (photos of the seizure are shown in Figure 2).

**Herbal Blends.** Two herbal blends were prepared in two separate evaporating dishes with 500 mg of chopped, dried damiana (*Turnera diffusa* Willd. ex Schult.) and strawberry leaves, respectively. A solution of 50 mg of **1** in 50 mL of acetone was added to each of the herbs and allowed to dry for 4 h with occasional mixing with a glass rod until all acetone was evaporated. Additionally, 10 herbal blends containing **1** with three different product brands from a single BKA seizure were selected for analysis.



**1** was extracted from the plant matrix by rinsing 500 mg of herbal material twice, once with 5 mL ACN, and again with 2 mL ACN. The extracts were combined and evaporated to dryness.

**Flash Chromatography. MDMB-CHMICA.** Separation of **1** from related impurities was achieved by normal phase preparative chromatography with a Sepacore flash system X50 from Büchi Labortechnik (Flawil, Switzerland) consisting of two pump modules (max. 50 bar pressure), a UV–vis spectrometer (set to 285 nm), an automated fraction collector, and a control unit. A prepacked 4 g silica gel HP column from Büchi (particle size 15–40  $\mu\text{m}$ ) was used. The loaded sample amount was 40 mg of pure **1**, dissolved in 1.5 mL 2:1 ethyl acetate:hexane. Separation was achieved with a gradient program of eluent A (hexane) and B (ethyl acetate) with a flow rate of 20 mL  $\text{min}^{-1}$ , starting with 0% B, increasing over 90 s to 30% B. After 60 s, eluent B is further increased within 20 s to 100%, which is held for 180 s, giving an overall chromatographic runtime of 350 s. The applied gradient takes approximately 1 min to pass the complete column from pump to detector. This time shift has to be taken into account for the development of the gradient program. The main component finishes eluting 30 s before the last major increase of eluent B. After that, the maintenance of a slowly increasing gradient is unnecessary and would only prolong the chromatographic run. By running on 100% B, all remaining compounds should elute from the column.

Over the complete runtime, fractions were collected, whereas the fraction containing **1** was collected from second 189 for 63 s, evaporated to dryness, and weighed. All other fractions containing the impurities were combined, evaporated to dryness, and dissolved again in 1 mL of acetonitrile.

**AB-CHMINACA.** The instrument setup, column, sample amount, and preparation is the same as for **1**. Separation of **2** from its impurities was achieved with a gradient program of eluent A (hexane) and B (ethyl acetate) with a flow rate of 20 mL  $\text{min}^{-1}$ , starting with 0% B, increasing over 120 s to 30% B. After 50 s hold, eluent B is further increased within 1 s to 60%, which is held for 60 s. Lastly, eluent B is increased to 100% within 1 s and held for 248 s, giving an overall chromatographic runtime of 480 s. **2** is collected after 306 s for 60 s. All other fractions are combined, evaporated to dryness, and dissolved again in 1 mL acetonitrile.

**MDMB-CHMCZCA.** The instrument setup, column, sample amount, and preparation is the same as for **1**. Separation of **3** from its impurities was achieved with a gradient program of eluent A (hexane) and B (ethyl acetate) with a flow rate of 20 mL  $\text{min}^{-1}$ , starting with 0% B, increasing over 30 s to 10% B. After 60 s hold, eluent B is further increased within 40 s to 30%, which is held for 30 s. Lastly, eluent B is increased to 100% within 1 s and held for 24 s, giving an overall chromatographic runtime of 401 s. **3** is collected after 190 s for 50 s. All other fractions are combined, evaporated to dryness, and dissolved again in 1 mL of acetonitrile.

**UHPLC-ESI-MS<sup>n</sup>.** When injecting small volumes into the F-LC system, loss of sample is nearly inevitable. Therefore, the weight of the sample not before but after the flash chromatography should be determined to actually know how much substance was cleaned up. This weight is also used to normalize the pooled impurity fractions before UHPLC measurement. All impurity fractions are diluted in such fashion, that the impurities of 2 mg of their corresponding sample of **1** is injected into the UHPLC.

UHPLC measurements were conducted on the tertiary system UltiMate 3000 by Dionex (Thermo Scientific, Waltham, MA), consisting of a pump module, auto sampler, and column compartment. Separation was achieved on a Kinetex C18 (2.6  $\mu\text{m}$ , 100 Å, 100  $\times$  2  $\times$  10 mm) column including a KrudKatcher precolumn by Phenomenex (Aschaffenburg, Germany) at 40 °C. Each analysis was carried out with a binary mobile phase consisting of solvent A (98.9% water, 1% acetonitrile, 0.1% formic acid, 2 mM ammonium formate) and solvent B (1% water, 98.9% acetonitrile, 0.1% formic acid, 2 mM ammonium formate). The elution program was 80% A/20% B (1 min hold), followed by 40% A/60% B (1–2.5 min) to 35% A/65% B (2.5–4 min, 1.5 min hold) and up to 1% A/99% B (5.5–8 min, 2 min hold). In the end, an equilibration step was introduced with 80% A/20% B (10–10.2 min, 1.8 min hold), giving an overall runtime of 12 min at a flow rate of 0.5 mL/min. The injection volume was set to 5  $\mu\text{L}$ . The ESI was operated in positive mode at 4.5 kV with 29 psi of nitrogen as nebulizer gas. For mass spectrometry, a Bruker amaZon Speed ion trap MS (Billerica, MA) was operated in ultrascan mode from 70 to 600  $m/z$  with 32500  $m/z$ /s. Dry gas flow rate was set to 10 L/min at a temperature of 320 °C.

**Transferability.** As for the established impurity profiling workflows for classic drugs, to produce comparable results for samples analyzed in different laboratories with our novel F-LC/UHPLC-ESI-MS<sup>n</sup> profiling workflow a strictly defined instrumentation and method setup has to be implemented with regular analysis of control samples and/or participation in proficiency tests. Data generated by a different type of MS or ion source (e.g., atmospheric pressure chemical ionization APCI) are generally not comparable, as these factors have a major impact on signal intensities and ionization potential. However, if shifts occur in data generated by the same instrument due to exchange of wear parts (e.g., ESI sprayer), it is still possible to correct these deviations via postprocessing (e.g., weighting) of the impurity signatures with the software Unscrambler X.

Although the bucketing algorithm (see [Data-Processing](#)) is able to compensate for minor deviations in retention time, the UHPLC-column should not exceed a certain usage period to maintain its separation strength.

**Data-Processing.** Each data point in an LC-MS run is described by its retention time (RT),  $m/z$  value, and intensity. To transform the enormous amounts of data points from each LC-MS run into a numeric matrix, rectangular bucketing of the LC-MS data with the software Profile Analysis 1.1 (Bruker, Billerica, MA) was carried out. Bucketing subdivides the retention time (RT) and mass range of a LC-MS run into distinct pairs of RT- $m/z$  ranges, called buckets. Within each of these ranges (buckets) the intensity of all data points of the LC-MS run are summed up. This way, information loss can be avoided, which might result from integration of overlapping or nonbaseline separated peaks in the base peak (BPC) or total ion chromatogram (TIC). One major advantage of the bucketing algorithm used by Profile Analysis is the automatic peak detection. Peaks located at or across the border of a bucket will not be split, but the intensity of the peak will be rated for that bucket containing the peak maximum. In this way, a “blurring” of the spectral and chromatographic data can be avoided and each bucket carries the entire information on an eluting substance with a defined  $m/z$  range at a given time. The time intervals for integration should be set wide enough to

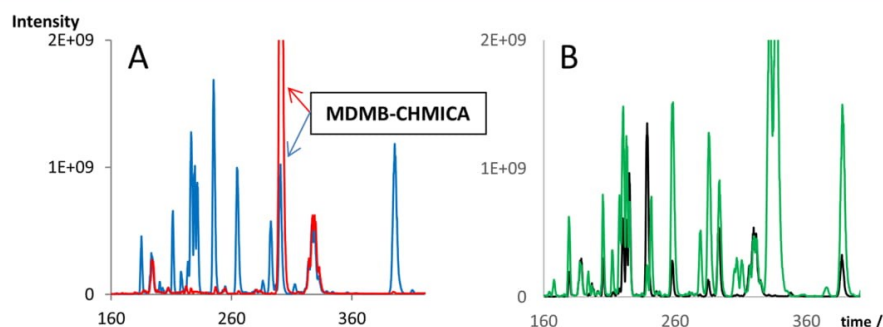


**Figure 3.** Excerpts of overlaid UHPLC-MS base peak chromatograms. (A) Red: native sample of MDMB-CHMICA, blue: isolated impurities of the corresponding red labeled sample injected with a lower dilution factor. (B) Isolated impurities of two different MDMB-CHMICA samples.

compensate small retention time shifts in-between measurements to maintain a reproducible bucketing but not too wide because neighboring peaks of substances with equal  $m/z$  values (e.g., positional isomers) might be rated into one bucket.

Rectangular bucketing with a bucket size of  $\Delta t = 0.2$  min and  $\Delta m/z = 1$  between 1 and 9.5 min of the chromatogram for the  $m/z$  range of 150 to 500 was chosen. Each sample is further described by 15050 buckets of which most are “noise buckets” carrying no relevant information. Therefore, all buckets that did not exceed a specific intensity threshold for any samples were deleted. This threshold is highly dependent on the used chromatography, mass spectrometer, and its setting and should be adjusted individually for each instrumental setup and investigated analytes. In our case, the most intense 57 buckets remained, which were further evaluated for their relevance and association with **1** by MS<sup>n</sup> experiments, representing the impurity set for **1** to be evaluated.

Profiling of herbal blends containing **1** was performed by using only these predefined buckets representing the most discriminating impurities of **1** to avoid the inclusion of matrix components or nonrelated cannabinoids present on the herbal material. The PCA and hierarchical cluster analysis (HCA) was computed with the software Unscrambler X (Camo, Oslo, Norway).

## RESULTS AND DISCUSSION

**Extraction Efficiency and Precision of the Flash Chromatography.** Only very few impurity-related peaks were detected in LC-MS runs of pure samples of synthetic cannabinoids that were not sufficient in intensity and number to perform a reliable profiling. Without any sample preparation, these signals might only be enhanced by increasing the sample concentration or the injection volume into the UHPLC. This approach, however, has its limits due to overloading of the column or pollution of the MS with the excess of MC. An enrichment of impurities via removal of the main component to inject the sample with lower dilution factors was the most promising strategy. As stated before, the majority of modern synthetic cannabinoids and their synthesis-related impurities are different from the classical drugs in regard to abundance, solubility in water, and structural diversity so that commonly used extraction or enrichment methods such as liquid–liquid or solid phase extraction do not fulfill the requirements set for extraction efficiency and selectivity. We found automated F-LC with the possibility to apply a gradient program of a large selection of mobile phases

and the availability of prepacked columns with different solid phases in various dimensions to be the perfect tool for this application. With this highly adaptable setup, a wide range of substances with different polarities or functional groups can be chromatographically separated.

To demonstrate this adaptability we developed multiple F-LC methods to isolate the impurities from the main component for the three synthetic cannabinoids with different core structures **1**, **2**, and **3**. In each case, it was not possible to eliminate the MC completely from its impurities. However, by comparing the LC-MS peak intensities of the MC and the most intense impurity before and after the F-LC in each cannabinoid sample, the percentage of depleted MC could be estimated. For all three structurally different cannabinoids, more than 99% of the main component could be removed from its impurities via F-LC (see SI for more information). Comparing both chromatograms of the native cannabinoid samples and their corresponding impurity fractions (exemplarily shown for **1** in Figure 3(A)), small peaks which were nearly below the detection limit in the native sample are more intense in the combined impurity sample and even additional, previously superimposed peaks appear. Furthermore, the F-LC did not disrupt the impurity profile of the original sample, validated by the consistent intensity ratios of impurities already found in the native sample (those which were above the limit of detection) and after their isolation via F-LC.

**Reproducibility and Robustness of the F-LC and UHPLC-MS Procedures.** After successful isolation of impurities, multiple samples of MDMB-CHMICA were processed and their impurity signatures measured by UHPLC-MS. By comparing their chromatographic profiles, variations in impurity distribution and abundance were recognized, exemplarily shown for two samples in Figure 3(B). To prove that these differences originate from a varying chemical composition and are not a result of a poorly conducted sample preparation, a reproducibility study was carried out. While handling the samples and instruments, attempts were made to allow as little variation as possible in the experimental procedure. However, the performance of the used instruments may be subject to certain inevitable fluctuations.

A sample of **1** was flashed in a 5-fold replicate and measured via UHPLC-MS. Relative standard deviations (RSDs) were calculated for all impurities individually between the replicates and averaged, to give an overall RSD between the five replicates of 12.5%. This was repeated for two other samples of **1**, giving overall RSDs of 12.8% and 13.8%. To assess the



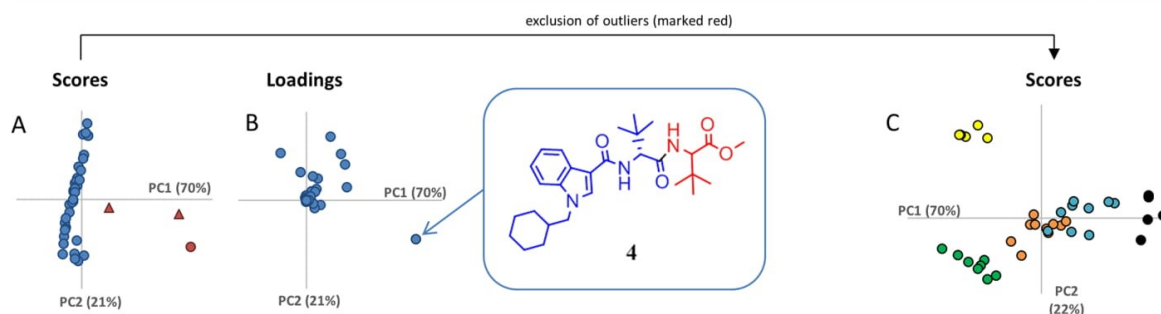


**Figure 4.** Scores (A) and loadings (B) plot of the impurities fractions from the 40 Luxembourg samples of MDMB-CHMICA. Three major outliers in the scores plot are marked red, showing an increased concentration of **4**. For better visualization, in the structural formula of **4** the original parts of **1** are marked blue, the additional amino acid red. (C) Scores plots of the impurity fractions of all remaining 37 after exclusion of outliers. Grouping of samples into clusters (marked with different colors) was achieved by HCA of the first four PCs.

impact of the UHPLC-MS alone, one of the previously flashed replicates was measured in a 10-fold sequence, giving an overall RSD of 4.7%. As expected the UHPLC-MS shows a good reproducibility, accounted for by the high degree of automatization of the instrument. In combination with F-LC, the RSDs were slightly increased, most probably because of the rather manual handling of the sample injection and fractionation. However, for all replicates the deviation was in acceptable limits, proving that differences between the recorded impurity signatures are not a result of the sample preparation.

**Assessment of Sample Cluster in a Large Seizure of MDMB-CHMICA.** Given the initial assumption that a synthesis procedure with precisely defined conditions produces characteristic impurity profiles, the aim of our study was to determine whether and how well samples of **1** can be grouped or discriminated on the basis of their chromatographic impurity profiles and which information about the source and production can be extracted from these data, for example varying synthesis pathways, reaction batches, and batch sizes. All 40 samples of the Luxembourg seizure of **1** were flash chromatographed and the isolated impurities measured via UHPLC-MS. Via PCA their chromatographic impurity profiles were compared on the basis of the 57 most intense impurities related to **1**. The T-shape of the scores plot (Figure 4(A)) is the result of a single impurity with  $m/z$  498 **4** (Figure 4 methyl 2-(2-(1-(cyclohexylmethyl)-1H-indole-3-carboxamido)-3,3-dimethylbutanamido)-3,3-dimethylbutanoate), showing a high influence on the first principle component (PC1) evidenced by the corresponding loadings plot (Figure 4(B)). Isolation of **4** was performed via precise fractionation of the F-LC run and structural elucidation via high-resolution MS and NMR. The structure of **4** is similar to **1**, where another *tert*-leucine methyl ester moiety is substituted with the initial methyl ester group of **1**, forming another amide bond. The analytical data necessary for structural identification can be taken from SI. The high positive loadings in the scores plot of the three red marked samples in Figure 4(A) for PC1 suggest a high concentration of **4** in these samples. It is noteworthy that the three samples point in an imaginary line toward the remaining set of samples, indicating a consecutive concentration decrease of **4** starting from the sample with the highest PC1 loading. Several other impurities in all three red marked samples exhibited a similar “dilution pattern”, suggesting a proportional relationship. In other words, the two intermediate red marked samples

(triangles in Scores plot Figure 4(B)) seem to be blends in varying compositions of the red marked sample (circle) with the highest PC1 score with material from one or more of the remaining 37 blue marked samples distributed alongside PC2. While handling the 40 samples of the Luxembourg seizure, three samples already had a different odor and a minor yellowness separating it from the remaining collective. All 40 samples from the Luxembourg seizure were packed and delivered mutually, indicating a common source. However, it is possible that more than one manufacturer contributed small portions of **1** to the bulk material, with equal or different synthesis pathways, carried out at different times and places with varying equipment or operators. Another explanation for the appearance of **4** would be two differently conducted syntheses, one producing a smaller batch with an increased concentration of **4** as reaction byproduct, probably due to excess use of the amino acid, and one or more larger batches, where the formation of this impurity was suppressed. A more thorough structural elucidation of the remaining important impurities for **1** and their origin does not fit the scope of this article and will be published in another publication.

After exclusion of the three outlier samples, another PCA model was generated for the remaining 37 samples of **1** from Luxembourg to further divide this collective into subgroups based on their impurity signatures. Final grouping of the samples was achieved via HCA of the first four PCs, covering 98% of the complete variance for this data set (Scores plot Figure 4 (C)).

Deviations in impurity composition between these batches are mainly a result of varying concentrations rather than particular presence or absence of single impurities. Still, each of the clusters might represent an individual synthesis batch due to the accumulation of these differences to a significant level. In some cases small inhomogeneities in sample distribution within the larger clusters can be observed, for example the two samples in-between the orange and green cluster, presumably resulting from the mixing of individual synthesis batches as for the three outliers discussed previously. In this display of PC1 against PC2 the orange and teal cluster seem to overlap; on PC3 however these two clusters are easily distinguishable. Because each sample represents 1 kg of pure **1**, it can be estimated that the producers are able to synthesize single batches of pure cannabinoid of up to 10 kg.

**Adaptability to Herbal Blends.** The impurity profiling of synthetic cannabinoids in herbal blends is much more complex

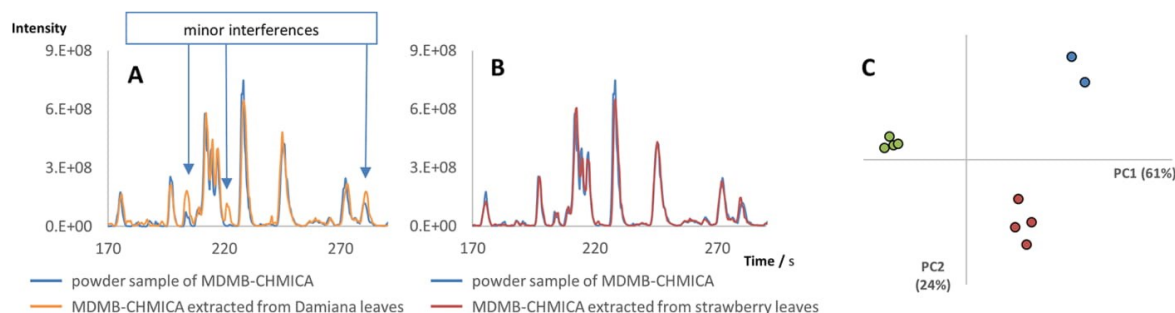


**Figure 5.** (A, B) Excerpts of the most discriminating areas of the base peak chromatograms (BPC) for impurity profiles of **1** after extraction from damiana (orange, A) and strawberry (red, B) leaves compared to the corresponding powder sample (blue, A and B). (C) Scores plot of the individual combined impurity fractions of 10 seized herbal blend samples containing MDMB-CHMICA of three different herbal blend brands (marked by different colors).

than profiling of the pure substances due to the presence of matrix components from the herbal material or residues of other synthetic cannabinoids. However, this form of consumption is the most common for synthetic cannabinoids, evidenced by the large amounts seized by customs and police every year<sup>28</sup> and a major potential field of application for the developed profiling concept. By transferring the sample workflow from powder samples to the more complex herbal matrixes, seizures and test purchases from various Internet shops could be connected through their impurity profiles, disclosing cooperation between herbal blend producers and individual shops, or the affiliation of different shops to one producer, providing important information for police investigations. Hence, our profiling should be able to cope with this difficult matrix and identify impurity profiles of synthetic cannabinoids, in our case with focus on **1**, even though sprayed on herbal material.

For that purpose, two herbal blends with **1** were prepared with the most common herbal matrixes, chopped leaves of damiana and strawberry plants (10% w:w **1**:leaves), to compare the impurity profiles after extraction from the plant to that of the correspondingly used original powder sample (Figure 5). The chromatographic impurity profile (in this case the BPC) of **1** from the strawberry leaves extract (B) is highly similar to that of the pure power sample, showing no interferences or ion suppression effects of potentially coextracted matrix components from the herbal material. For damiana (A), minor interference from additional signals can be observed in several areas of the BPC; however, when integrating single  $m/z$  values in the extracted ion chromatograms (via bucketing), the peak areas of the impurities related to **1** are highly similar for both samples over the complete chromatographic range.

As application to seized samples, ten herbal blend samples sold in online shops in early 2016 were available containing **1** ( $2 \times 4$  and  $1 \times 2$  products of the same brand). Because all herbal blends were from the same seizure, at least the samples from the same brand are expected to originate from the same manufacturer and thus carry the same batch of **1** and its impurities. In this substudy, to exclude all potentially extracted plant components from the evaluation via PCA, only the  $m/z$  values of impurities found in the powder samples from the Luxembourg seizure were considered. Figure 5(C) shows the scores plot of the impurity profiles with color labels, depending on the brand name of the herbal blend. Three clusters are

formed, each consisting of all samples with the same brand. According to the impurity profiles, the **1** used in each of the brands seems to originate from a distinct reaction batch, despite the fact that they are from the same seizure. However, all packages from the same brand carry indistinguishable impurity profiles, verifying the feasibility of the developed sample preparation setup to profile **1** in herbal blends.

## CONCLUSION

We showed that the combination of flash-LC, LC-MS, and multivariate data analysis proves to be a promising tool to isolate synthesis impurities from the main component in NPS samples with an extraction efficiency of more than 99%, reproducibly maintaining the profile of the original sample and enabling profiling of highly pure substances such as synthetic cannabinoids. With only limited effort, flash-LC gradient programs for three structurally diverse synthetic cannabinoids were implemented and executed. This enables a rapid adaption of the presented profiling workflow to new synthetic cannabinoids appearing on the fast-paced NPS market without prolonged validation of the sample preparation method. With this high adaptability and efficiency, even applications outside of the NPS phenomenon might be found, for example targeting pharmaceutical drug imitations or highly pure illicit drugs such as crystalline methamphetamine.

By multivariate analysis of their impurity signatures, 40 **1** kg samples of MDMB-CHMICA from a large seizure could be assigned into clusters, the largest representing a batch of approximately 10 kg pure synthetic cannabinoid. Three of the 40 samples were identified as outliers, which were most probably manufactured by a different synthesis pathway.

In the process of extracting pooled impurity fractions via F-LC, the main component is cleaned up and isolated as well and, thus, made available for other purposes, for example to generate reference standards or allow measurements via isotope ratio mass spectrometry for a comprehensive profiling setup. The data generated by this orthogonal analytical technique can be implemented into the data evaluation, combining information about the impurities (synthesis procedures) and the isotopic composition (sample origin). For 5F-PB-22, results are already published,<sup>30</sup> and for MDMB-CHMICA, a larger sample collective of pure and cleaned-up material from "Spice-Products" has already been measured and the results of this study will be published elsewhere. Another perk of the flexible F-LC is the possibility to fractionize the



chromatographic run as needed, for example to cut out highly abundant impurities for their identification via NMR, as demonstrated for **4** (methyl 2-(2-(1-(cyclohexylmethyl)-1H-indole-3-carboxamido)-3,3-dimethylbutanamido)-3,3-dimethylbutanoate).

Lastly, with the presented workflow it is possible to assess the impurity profile of MDMB-CHMICA extracted from herbal blends while excluding herbal matrix components. This is, however, limited to preparations with only one synthetic cannabinoid to avoid overlapping of peaks in the F-LC as well as the UHPLC-MS.

## ■ ASSOCIATED CONTENT

### 5 Supporting Information

The Supporting Information is available free of charge on the ACS Publications website at DOI: 10.1021/acs.analchem.8b02679.

Details about the extraction of main components via flash chromatography and analytical data for the identification of **4** (PDF)

## ■ AUTHOR INFORMATION

### Corresponding Author

\*E-mail: sascha.muenster-mueller@uni-rostock.de.

### ORCID

Sascha Münster-Müller: 0000-0003-3949-2818

Ralf Zimmermann: 0000-0002-6280-3218

### Notes

The authors declare no competing financial interest.

## ■ ACKNOWLEDGMENTS

All presented data, if not cited otherwise, were generated within the project “SPICE-profiling”, funded within the EU’s ISEC 2013 programme (Directorate General JUST/2013/ISEC/DRUGS/AG/ISEC/4000006421). Our thanks are due to Serge Schneider from the Laboratoire National de Santé in Luxembourg, who kindly provided us with aliquots from the large seizure of MDMB-CHMICA by Luxembourg customs. Additionally, we want to thank Vincent Guillou from the Federal Criminal Police, Forensic Science Institute in Germany, for the NMR measurements and the corresponding spectra interpretation.

## ■ REFERENCES

- (1) Sinnema, A.; Verweij, A. M. *Bull. Narc.* **1981**, 33, 37–54.
- (2) Lambrechts, M.; Rasmussen, K. E. *Bull. Narc.* **1984**, 36, 47–57.
- (3) Esseiva, P.; Anglada, F.; Dujourdy, L.; Taroni, F.; Margot, P.; Pasquier, E. D.; Dawson, M.; Roux, C.; Doble, P. *Talanta* **2005**, 67, 360–367.
- (4) Sobol, S. P.; Sperling, A. R. *In Forensic Sci.* **1975**, 13, 170–182.
- (5) Stromberg, L.; Lundberg, L.; Neumann, H.; Bobon, B.; Huizer, H.; van der Stelt, N. W. *Forensic Sci. Int.* **2000**, 114, 67–88.
- (6) Janzen, K. E.; Fernando, A. R.; Walter, L. *Forensic Sci. Int.* **1994**, 69, 23–29.
- (7) Janzen, K. E.; Walter, L.; Fernando, A. R. *J. Forensic Sci.* **1992**, 37, 436–445.
- (8) Moore, J. M.; Casale, J. F. *Forensic Sci. Rev.* **1998**, 10, 13–46.
- (9) Cheng, W. C.; Poon, N. L.; Chan, M. F. *J. Forensic Sci.* **2003**, 48, 1249–1259.
- (10) Gimeno, P.; Besacier, F.; Chaudron-Thozet, H.; Girard, J.; Lamotte, A. *Forensic Sci. Int.* **2002**, 127, 1–44.
- (11) Palhol, F.; Boyer, S.; Naulet, N.; Chabrilat, M. *Anal. Bioanal. Chem.* **2002**, 374, 274–281.
- (12) Kunalan, V.; Nic Daéid, N.; Kerr, W. J.; Buchanan, H. A. S.; McPherson, A. R. *Anal. Chem.* **2009**, 81, 7342–7348.
- (13) Aalberg, L.; Andersson, K.; Bertler, C.; Boren, H.; Cole, M. D.; Dahlen, J.; Finnon, Y.; Huizer, H.; Jalava, K.; Kaa, E.; Lock, E.; Lopes, A.; Poortman-van der Meer, A.; Sippola, E. *Forensic Sci. Int.* **2005**, 149, 219–229.
- (14) Ballany, J.; Caddy, B.; Cole, M.; Finnon, Y.; Aalberg, L.; Janhunen, K.; Sippola, E.; Andersson, K.; Bertler, C.; Dahlen, J.; Kopp, I.; Dujourdy, L.; Lock, E.; Margot, P.; Huizer, H.; Poortman, A.; Kaa, E.; Lopes, A. *Sci. Justice* **2001**, 41, 193–196.
- (15) Pikkarainen, A. L. *Forensic Sci. Int.* **1996**, 82, 141–152.
- (16) Chiarotti, M.; Marsili, R.; Moreda-Pineiro, A. J. *Chromatogr. B: Anal. Technol. Biomed. Life Sci.* **2002**, 772, 249–256.
- (17) Zacca, J. J.; Grobériio, T. S.; Maldaner, A. O.; Vieira, M. L.; Braga, J. W. B. *Anal. Chem.* **2013**, 85, 2457–2464.
- (18) Zhang, J. X.; Zhang, D. M.; Han, X. G. *Forensic Sci. Int.* **2008**, 182, 13–19.
- (19) ICH. Impurities in new drug products Q3b (R2), International Council for Harmonisation of Technical Requirements for Pharmaceuticals for Human Use, 2006.
- (20) Sacre, P. Y.; Deconinck, E.; Daszykowski, M.; Courselle, P.; Vancauwenberghe, R.; Chiap, P.; Crommen, J.; De Beer, J. O. *Anal. Chim. Acta* **2011**, 701, 224–231.
- (21) Deconinck, E.; Sacre, P. Y.; Courselle, P.; De Beer, J. O. *Talanta* **2012**, 100, 123–133.
- (22) Custers, D.; Krakowska, B.; De Beer, J. O.; Courselle, P.; Daszykowski, M.; Apers, S.; Deconinck, E. *Anal. Bioanal. Chem.* **2016**, 408, 1643–1656.
- (23) Dumarey, M.; van Nederkassel, A. M.; Stanimirova, I.; Daszykowski, M.; Bensaid, F.; Lees, M.; Martin, G. J.; Desmurs, J. R.; Smeys-Verbeke, J.; Vander Heyden, Y. *Anal. Chim. Acta* **2009**, 655, 43–51.
- (24) Schneider, A.; Wessjohann, L. A. *J. Pharm. Biomed. Anal.* **2010**, 53, 767–772.
- (25) Carrier, D.; Eckers, C.; Arnoult, T.; Thurston, T.; Major, H. *Rapid Commun. Mass Spectrom.* **2007**, 21, 3946–3948.
- (26) Auwärter, V.; Dresen, S.; Weinmann, W.; Müller, M.; Pütz, M.; Ferreirós, N. *J. Mass Spectrom.* **2009**, 44, 832–837.
- (27) Piggee, C. *Anal. Chem.* **2009**, 81, 3205–3207.
- (28) EMCDDA. Synthetic cannabinoids in Europe (Perspectives on drugs), EMCDDA, 2017.
- (29) Collins, M.; Doddridge, A.; Salouros, H. *Drug Test. Anal.* **2016**, 8, 903–909.
- (30) Münster-Müller, S.; Scheid, N.; Holdermann, T.; Schneiders, S.; Pütz, M. *Drug Test. Anal.* **2018**, in press. DOI: 10.1002/dta.2407
- (31) Schäffer, M.; Gröger, T.; Pütz, M.; Zimmermann, R. *Forensic Toxicol.* **2013**, 31, 251–262.
- (32) Still, W. C.; Kahn, M.; Mitra, A. J. *Org. Chem.* **1978**, 43, 2923–2925.
- (33) Roge, A. B.; Firke, S. N.; Kawade, R. M.; Sarje, S. K.; Vadvalkar, S. M. *Int. J. Pharm. Sci. Res.* **2011**, 2, 1930–1937.
- (34) Kamboj, S.; et al. *Curr. Pharm. Anal.* **2014**, 10, 145–160.
- (35) Patsavas, M. C.; Byrne, R. H.; Liu, X. *Mar. Chem.* **2013**, 150, 19–24.
- (36) Ullsten, S.; Danielsson, R.; Bäckström, D.; Sjöberg, P.; Bergquist, J. *J. Chromatogr. A* **2006**, 1117, 87–93.
- (37) Chan, E. C. Y.; Yap, S.-L.; Lau, A.-J.; Leow, P.-C.; Toh, D.-F.; Koh, H.-L. *Rapid Commun. Mass Spectrom.* **2007**, 21, 519–528.
- (38) Weljie, A. M.; Newton, J.; Mercier, P.; Carlson, E.; Slupsky, C. M. *Anal. Chem.* **2006**, 78, 4430–4442.
- (39) Pütz, M.; Schneiders, S.; Auwärter, V.; Münster-Müller, S.; Scheid, N. *Toxichem Krimtech* **2015**, 82, 273–283.
- (40) Angerer, V.; Franz, F.; Schwarze, B.; Moosmann, B.; Auwärter, V. *J. Anal. Toxicol.* **2016**, 40, 240–242.
- (41) Backberg, M.; Tworek, L.; Beck, O.; Helander, A. *J. Med. Toxicol.* **2017**, 13, 52–60.
- (42) Westin, A. A.; Frost, J.; Brede, W. R.; Gundersen, P. O.; Einvik, S.; Aarset, H.; Slordal, L. *J. Anal. Toxicol.* **2016**, 40, 86–87.
- (43) Adamowicz, P. *Forensic Sci. Int.* **2016**, 261, e5–10.

(44) EMCDDA, Report on the risk assessment of MDMA-CHMICA in the framework of the Council Decision on new psychoactive substances, EMCDDA 2017

(45) Uchiyama, N.; Matsuda, S.; Wakana, D.; Kikura-Hanajiri, R.; Goda, Y. *Forensic Toxicol.* **2013**, *31*, 93–100.

(46) Weber, C.; Pusch, S.; Schollmeyer, D.; Münster-Müller, S.; Pütz, M.; Opatz, T. *Beilstein J. Org. Chem.* **2016**, *12*, 2808–2815.



## 6.2 Publication 2

*Chemical profiling of the synthetic cannabinoid MDMB-CHMICA: identification, assessment and stability study of synthesis-related impurities in seized and synthesized samples*

Sascha Münster-Müller, Steven Hansen, Till Opatz, Ralf Zimmermann, Michael Pütz

Drug Testing and Analysis

2019

11(8): 1192-1206

Received: 7 March 2019 | Revised: 17 May 2019 | Accepted: 17 May 2019

DOI: 10.1002/dta.2652

## RESEARCH ARTICLE

WILEY

# Chemical profiling of the synthetic cannabinoid MDMB-CHMICA: Identification, assessment, and stability study of synthesis-related impurities in seized and synthesized samples

Sascha Münster-Müller<sup>1,2</sup>  | Steven Hansen<sup>3</sup> | Till Opatz<sup>3</sup>  | Ralf Zimmermann<sup>2,4</sup>  | Michael Pütz<sup>1</sup>

<sup>1</sup> Federal Criminal Police Office, Forensic Science Institute, Wiesbaden, Germany

<sup>2</sup> Joint Mass Spectrometry Centre, Institute of Chemistry, Chair of Analytical Chemistry, University of Rostock, Rostock, Germany

<sup>3</sup> Johannes Gutenberg University Mainz, Institute of Organic Chemistry, Mainz, Germany

<sup>4</sup> Joint Mass Spectrometry Centre, Cooperation Group "Comprehensive Molecular Analytics", Helmholtz Zentrum Muenchen, Neuherberg, Germany

## Correspondence

Sascha Münster-Müller, Bundeskriminalamt (Federal Criminal Police Office), Forensic Science Institute, Appelallee 45, 65203, Wiesbaden, Germany.  
Email: sascha.muenster-mueller@uni-rostock.de

## Funding information

Directorate-General for Justice, Grant/Award Number: JUST/2013/ISEC/DRUGS/AG/ISEC/400006421

## Abstract

In this work, the most discriminating synthesis-related impurities found in samples from seizures and controlled synthesis of the synthetic cannabinoid MDMB-CHMICA (methyl (S)-2-(1-(cyclohexylmethyl)-1H-indole-3-carboxamido)-3,3-dimethylbutanoate) were characterized. Based on 61 available powder samples of MDMB-CHMICA, 15 key-impurities were assessed, isolated in larger quantities via flash chromatography and structurally elucidated and characterized via high resolution mass spectrometry and nuclear magnetic resonance spectroscopy. Apart from verifying the relation of the impurities to the major component, the interpretation of their chemical structures with distinct structural elements provided first insights into the manufacturing process and the precursor compounds used. Following liquid chromatography mass spectrometry analysis of the 15 key-impurities, the 61 seized samples of MDMB-CHMICA were evaluated and classified via multivariate data analysis based on the corresponding relative peak areas. In a second part of this work, stability tests and multiple controlled syntheses of MDMB-CHMICA were carried out to better understand variations in impurity signatures and to assess the significance of variations in the impurity patterns of seized samples. The last coupling step of the amino acid with 1-(cyclohexylmethyl)-1H-indole-3-carboxylic acid was performed using the coupling agents oxalyl chloride, thionyl chloride, and HATU. Furthermore, the impact of reaction time and temperature on the impurity profile were investigated. Overall, eight new impurities were found in the controlled syntheses and two degradation products of MDMB-CHMICA were found in the course of the stability tests. Replicates of a synthesis conducted on the same day showed similar impurity signatures; on different days they showed discriminable signatures. The use of different coupling reagents or conditions gave clearly distinguishable impurity signatures.

## KEYWORDS

controlled synthesis, impurity profiling, LC-MS, MDMB-CHMICA, new psychoactive substances (NPS)

We confirm that this manuscript has not been published elsewhere and is not under review by another journal. All authors have approved the manuscript and agree with submission to Drug Testing and Analysis. Furthermore, no competing financial interest or safety considerations are declared by the authors.

## 1 | INTRODUCTION

Seized samples of illicit drugs produced under clandestine lab conditions generally are complex mixtures of the main active ingredient and a variety of by-products, for example natural products from leaf extractions in the case of cocaine,<sup>1-3</sup> or synthesis impurities of synthetic drugs like amphetamine.<sup>4-7</sup> It could be expected that samples originating from the same general process exhibit the same by-product profile. However, their overall presence and concentration may show large variations due to changes in the nature of the starting material, processing pathway, and manufacturing parameters, as well as distribution and storage conditions. The chromatographic separation and quantitative analysis of these by-products (impurity profiling) is a method often used by forensic scientists contributing to several investigative purposes: establish links between two or more seized samples; classify material from different seizures into larger groups revealing potential distribution networks; identify the geographical origin of a sample; and monitor the manufacturing procedures of clandestine laboratories.<sup>8</sup>

In the first step of common impurity-profiling workflows, the seized material is dissolved and impurities are separated from the main component by acid–base liquid–liquid extraction (LLE), followed by analysis of the enriched impurity extract via liquid or gas chromatography coupled to mass spectrometry (LC–MS or GC–MS).<sup>9-12</sup> The integrated peak signals of a list of pre-defined key-impurities are then matched via chemometric models to databases of previously seized samples.<sup>2,3,13,14</sup> The decision whether two samples are somehow linked (eg, come from the same synthesis, the same laboratory, or the same synthesis route) or are not related to each other, requires a thoroughly assessed scientific basis, especially with respect to the legal defensibility of the profiling results. It is essential for the development of a valid and statistically robust profiling method to provide experimental studies demonstrating the relevance and eligibility of chosen key impurities, their relation to the main component, at which point differences between sample profiles are significant, and which magnitudes of influence can be responsible for these differences. Various publications are available detailing structural elucidation of impurities by MS-fragmentation experiments, high resolution MS (HRMS) or nuclear magnetic resonance (NMR) spectroscopy<sup>5,15-18</sup>; by controlled syntheses to assess route specific impurities and the overall reproducibility of the chemical profile<sup>6,17,19-21</sup>; by stability tests to identify impacts on the profile of a drug sample as a result of different storing conditions, for example exposure to heat, sunlight, or moisture, which could lead to a decomposition of the main component or related impurities.<sup>22</sup>

Several international impurity-profiling programs for classical drugs have already been validated<sup>13,23,24</sup> or are in constant development to cope with changes in illicit drug manufacturing and distribution. For synthetic cannabinoids, stimulants (derived from phenethylamine) and opioids, all part of the new psychoactive substances (NPS) phenomenon, few chemical profiling approaches are published.<sup>25-27</sup> Nevertheless, the number of newly detected NPS rose every year up to 2018, with 899 individual substances reported to the Early Warning Advisory (EWA) of the United Nations Office on Drugs and Crime (UNODC).<sup>28</sup> This phenomenon grew to a major concern of legislative

and prosecution agencies all over the world. In Germany, the most popular NPS group comprises the synthetic cannabinoids, either sold as research chemicals (RCs) in pure form such as powders and more prevalent, applied onto a herbal matrix, called herbal blends or “spice-products.”<sup>29,30</sup> Little is known about the production and distribution of these substances and the designer drug products made from them, which is why a new profiling concept for this sub-class was developed in a previous paper to link seizures and to gain more insight in the manufacturing process like batch and synthesis pathway discrimination.<sup>31</sup> Due to several differences between synthetic cannabinoids and classical drugs, like their much higher chemical purity and the non-applicability of acid–base LLE for the isolation of active constituents, it was necessary to adapt the established profiling routines to a new workflow consisting of flash-chromatography, LC–MS, and multivariate data evaluation.<sup>31</sup> Continuous database-supported monitoring and evaluation would not be reasonable for synthetic cannabinoids, as individual active substances typically do not stay on the market for more than one to two years.<sup>32</sup> For the same reason, the establishment of a broad scientific basis for the chemical profiling of every newly emerging synthetic cannabinoid would not be worth the effort. However, an in-depth analysis with a focus on one highly prevalent cannabinoid could provide comprehensive insights into its clandestine synthesis and, thus, contribute to a better understanding of the variations in the impurity composition of seized material and their significance for NPS-targeted forensic profiling applications in general. The methodological approach presented here will serve as model for the interpretation of impurities found by forensic institutes when analyzing seized synthetic cannabinoids with indole, indazole, and carbazole core structures, as similar synthesis procedures with related reaction by-products are expected for newly arising specimens of these three sub-classes. In the presented work, the most discriminating key impurities found in seized and bought (Internet test purchases) samples of the synthetic cannabinoid methyl (2S)-2-[[1-(cyclohexylmethyl)indole-3-carbonyl]amino]-3,3-dimethylbutanoate (**1**) (MDMB-CHMICA, Figure 1) were identified and structurally elucidated, MDMB-CHMICA being the most prevalent cannabinoid in 2016 in Germany<sup>30,33</sup> (and thus continued the previously published work on this compound<sup>31</sup>). Due to the high purity of the available samples of **1** (> 98%), it was necessary to isolate the synthesis impurities from the main component via flash-chromatography (FC). Tentative identification via fragmentation experiments and corresponding sum formula generation via HRMS was carried out and, if applicable, the most abundant impurities were isolated in larger quantities for structural elucidation via NMR spectroscopy (Figure 1).

After the assessment of suitable target components in the first part of this work, controlled syntheses of **1** were carried out to better understand variations in impurity signatures and to assess the significance of variations in the impurity patterns of seized samples. The focus was put on what is presumably the last reaction step for most of the “modern” synthetic cannabinoids, the coupling of the amino acid moiety to the aminoalkylindole core, from a single batch of the precursor material 1-(cyclohexylmethyl)-1H-indole-3-carboxylic acid. Only hypothetical considerations are possible on how the clandestine

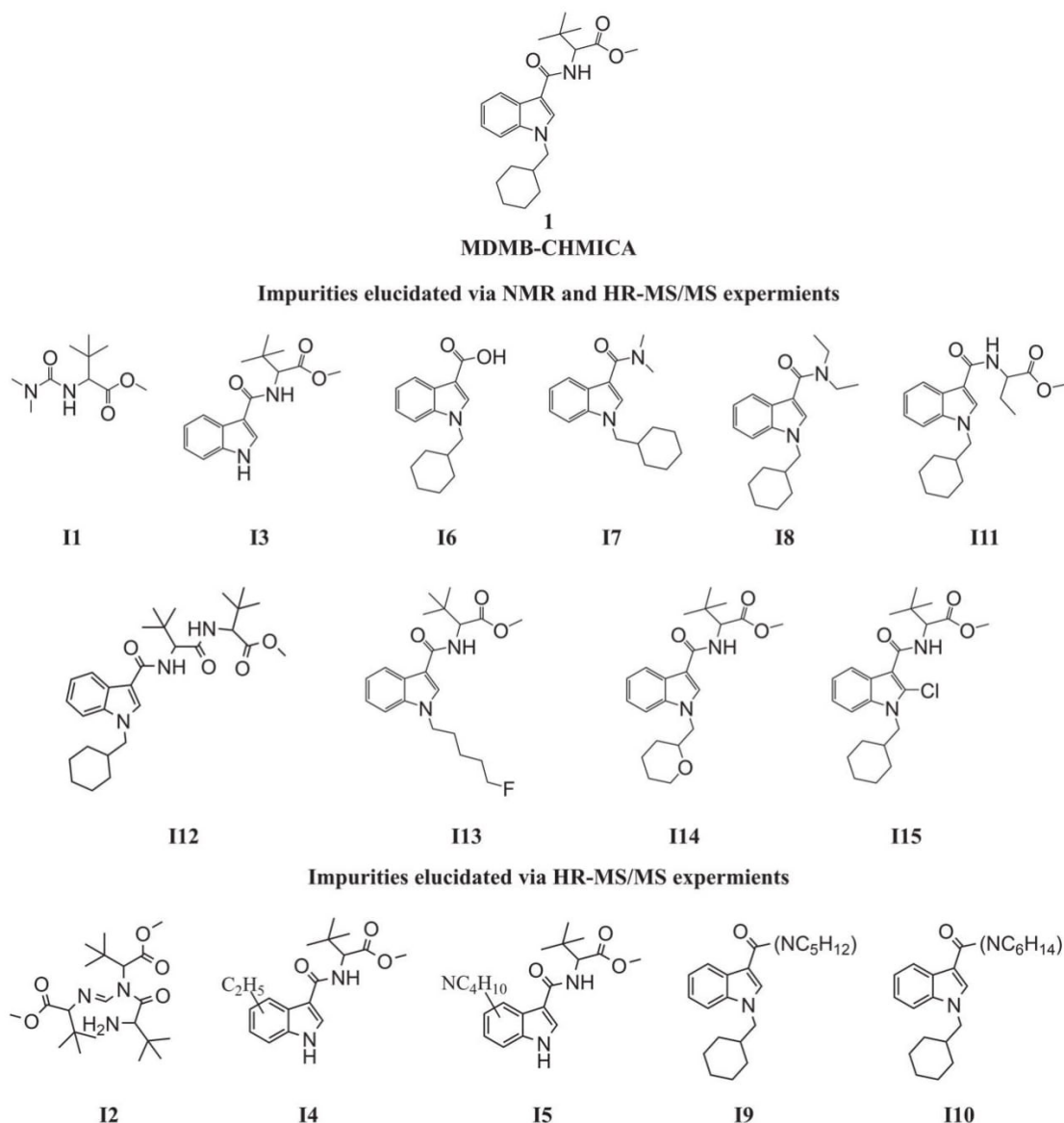


**FIGURE 1** Structural formulas for MDMB-CHMICA and fifteen assessed key-impurities with high discriminating potential to distinguish between individual synthesis batches in seized samples. Five impurities were only elucidated via HR-MS/MS experiments, the remaining ten were characterized by both NMR and HR-MS experiments

manufacturers conduct their synthesis. Most probably, previously published procedures are tested, evaluated, and modified to enable up-scaling from laboratory to pilot-plant scale and to improve the economic aspects of the synthesis. The scientific groundwork for the majority of the modern substances was laid by research groups beginning in the late 1980s, who developed new substances that act on the human endocannabinoid system, for the pharmaceutical industry.<sup>34–37</sup> Most of the synthetic cannabinoids found on the market were directly described in these patents or papers, or at least were inspired by them with respect to the general synthesis procedures (eg, exchange of indazole core with indole for **1** or carbazole core for MDMB-CHMCZA<sup>38</sup>), except for a few rare cases like 5F-PB-22.<sup>39</sup> Since no

information on the actual synthesis routes employed by the manufacturers is available, the initial synthesis conditions were based on the patented version for the indazole analog of **1** from Buchler et al<sup>34</sup> and the parameters were adjusted, for example other coupling reagents, according to identified impurities found in the original seized samples. Three different synthesis variations were performed, using the coupling reagents [dimethylamino (triazolo[4,5-b]pyridine-3-yloxy)methylidene]-dimethylazanium hexafluorophosphate (HATU) as stated in the patent by Buchler et al<sup>34</sup> and additionally the chlorinating agents oxalyl chloride and thionyl chloride according to a highly abundant impurity (chlorinated derivative of MDMB-CHMICA), frequently observed in seized samples of MDMB-CHMICA. In two other



synthesis procedures, the reaction time and temperature were varied for the coupling with oxalyl chloride. Only one factor was varied at a time, disregarding interaction between single parameters. However, compared to the manufacturers providing bulk material for the European market, the syntheses in this study were performed on a small scale. It was not intended to exactly reproduce the synthesis of the original manufacturer but to work as closely as possible to their assumed synthesis of choice.

## 2 | METHODS

### 2.1 | Impurity profiling

The complete impurity profiling workflow including sample preparation via FC, UHPLC-MS, and the subsequent data processing and multivariate data analysis was already reported in a previous paper<sup>31</sup> and will be stated in brief.

#### 2.1.1 | Chemicals and samples

Deionized water was tapped by a Milli-Q Synthesis A10 device (Millipore, Schwalbach, Germany); hypergrade acetonitrile (MeCN) for LC-MS was purchased from Merck (Darmstadt, Germany); and formic acid (~98%), ammonium formate (> 99%), *n*-hexane (> 99.99%), and ethyl acetate (≥ 99.0%) were purchased from Fluka (Buchs, Switzerland).

Overall, 61 samples of pure **1** were available from a 40 kg seizure by Luxembourg customs in December 2014 (labeled as Lux), customs seizures in Finland (labeled as FL), and from test purchases in Internet shops by the University Medical Center Freiburg (labeled as FR).

#### 2.1.2 | Instruments

Separation of synthesis-related impurities from the main component was achieved by normal phase preparative FC with a Sepacore system X50 from Büchi Labortechnik (Flawil, Switzerland) consisting of two pump modules (max. 50 bar pressure), a UV-VIS spectrometer (set to 285 nm), an automated fraction collector, and a control unit. Prepacked 4 g silica gel HP column from Büchi (particle size 15–40 µm) were used and run with mixtures of *n*-hexane and ethyl acetate as the mobile phase.

UHPLC measurements were conducted on a ternary system Ultimate 3000 by Dionex (Thermo Scientific, Waltham, MA, USA), consisting of a pump module, an autosampler, and a column compartment. Separation was achieved on a Kinetex C18 (2.6 µm, 100 Å, 100 x 2 mm inner diameter) column from Phenomenex (Aschaffenburg, Germany) at 40°C. Each analysis was carried out with a binary mobile phase consisting of eluent A (98.9% water, 1% acetonitrile, 0.1% formic acid, 2mM ammonium formate) and eluent B (1% water, 98.9% acetonitrile, 0.1% formic acid, 2mM ammonium formate). For MS, a Bruker amaZon Speed ion trap MS (Billerica, MA, USA) was operated in ultra-scan mode from 70 to 600 *m/z* with 32 500 *m/z*/s. The dry gas flow rate was set to 10 L/min at a temperature of 320°C.

For high resolution measurements, an LTQ Orbitrap hybrid MS with a "Max Ion Source" ESI or APCI ionization source, an LTQ XL ion trap, and an Orbitrap (Thermo Scientific, Waltham, MA, USA) were used. Separation was done by an Accela-HPLC device with autosampler, HPLC pump, and photodiode array detector (Thermo Scientific, Waltham, MA, USA). For separation, a gradient was applied of Eluent A (94.9:5:0.1 water: acetonitrile: formic acid) and Eluent B (94.9:5:0.1 acetonitrile: water: formic acid). The ESI operated in positive mode with 3.75 kV and the mass range of the mass spectrometer was set to 130–2000 *m/z* with a data-dependent scan threshold for MS<sup>2</sup> of 10<sup>6</sup> counts. The instrument was calibrated by measuring crystal violet and comparing the measured *m/z* values to the theoretical. If deviations >5 ppm occurred, the instrument was recalibrated.

NMR spectra were recorded on a Bruker Avance-II 400 (400 MHz for <sup>1</sup>H NMR and 100.6 MHz for <sup>13</sup>C NMR, including 2D NMR) or on a Bruker-Biospin Avance 500 (500 MHz for <sup>1</sup>H NMR) using 5 mm probes and standard pulse sequences. 600 MHz NMR spectra were recorded on a Bruker Avance III spectrometer (Rheinstetten, Germany) equipped with a 5 mm TCI cryoprobe. Standard gradient-enhanced pulse sequences were used for all experiments. Chemical shifts are reported as parts per million (ppm) downfield from tetramethyl silane and are references to the respective solvent signal: CDCl<sub>3</sub> (<sup>1</sup>H: δ = 7.26 ppm; <sup>13</sup>C: δ = 77.16 ppm); DMSO-*d*<sub>6</sub> (<sup>1</sup>H: δ = 2.50 ppm; <sup>13</sup>C: δ = 39.52 ppm); Acetone-*d*<sub>6</sub> (<sup>1</sup>H: δ = 2.05 ppm; <sup>13</sup>C: δ = 206.68 ppm, 29.92 ppm).

#### 2.1.3 | Data-processing

The LC-MS data was processed via a rectangular bucketing algorithm (ProfileAnalysis, Bruker, Billerica, MA, USA), integrating the signals of all *m/z* values from 150 to 600 individually in intervals of 0.5 minutes from minute 1 to 9.5 of chromatographic runtime, forming so-called buckets. Most of these buckets consisted of measurement noise with no relevant information. Therefore, the next step was to work out those buckets carrying actual signals of eluting peaks, further described as substance or impurity, as each of these buckets should carry the complete integral of a present substance. Accordingly, the complete bucket table was processed via PCA and those substances with high-intensity values and inter-sample variation were picked as "key impurities" carrying the majority of discrimination potential. For the available complex of 61 samples of pure **1**, 15 impurities (**I1-I15**) were assessed fulfilling these requirements. The corresponding PCA for assessment of impurities and hierarchical cluster analysis (HCA, using Ward's method) for sample clustering was computed with the software Unscrambler X (Camo, Oslo, Norway).

## 2.2 | Synthesis of MDMB-CHMICA

### 2.2.1 | Chemicals and materials

All air- and moisture-sensitive reactions were carried out in oven-dried glassware under an inert atmosphere of nitrogen using standard Schlenk techniques. Removal of solvents was performed using a rotary

evaporator (40°C bath temperature) and a membrane pump. The used solvents were dried and purified by standard procedures. For this purpose, triethylamine (TEA) and dichloromethane (DCM) were distilled from CaH<sub>2</sub>. Dimethylformamide (DMF) was purchased in pre-dried quality from Acros Organics (Geel, Belgium) and stored over molecular sieves (4 Å). All other chemicals were purchased from commercial suppliers and used without further purification unless mentioned otherwise. For analytical TLC, silica-coated aluminum plates (E. Merck, silica 60 F<sub>254</sub>) and aluminum oxide plates (Marcherey-Nagel, N/UV<sub>245</sub>, ALOX) were used. Details on all instruments used for characterization of the synthesis intermediates or target compounds can be taken from the Supporting Information.

## 2.2.2 | Synthesis details

### L-tert-leucine methyl ester hydrochloride

The title compound was synthesized according to a modified procedure from Imaramovsky et al.<sup>40</sup>

In an oven-dried Schlenk-flask, L-tert-leucine (500 mg, 3.81 mmol, 1.0 eq) was dissolved in dry methanol (15 mL) and cooled to 0°C. Subsequently, freshly distilled thionyl chloride (907 mg, 7.62 mmol, 2.0 eq.) was added dropwise at a constant temperature of 5°C. The clear, yellowish reaction mixture was allowed to reach room temperature by removing the cold bath and stirring vigorously for 40 hours. The solvent was removed under reduced pressure and the remaining residue was dissolved again in a mixture of dichloromethane and methanol (10:1). To remove residual L-tert-leucine, the solution was filtered over aluminum oxide (Particle size: 50–200 mm, Acros Organics, Geel, Belgium). The filtrate was acidified with ethereal HCl and evaporated to dryness. L-tert-Leucine methyl ester hydrochloride was obtained as a colorless crystalline solid. The corresponding analytical characterization can be taken from the Supporting Information.

### 1-(Cyclohexylmethyl)-1H-indole-3-carboxylic acid

The title compound was synthesized according to an optimized method as part of a classified Master's dissertation by Steven Hansen. The material was thoroughly purified by FC. For a general procedure of the synthesis of 1-(cyclohexylmethyl)-1H-indole-3-carboxylic acid, refer to Banister et al.<sup>41</sup> The corresponding analytical characterization data of the product from the stated synthesis can be taken from the Supporting Information.

### Methyl (2S)-2-[[1-(cyclohexylmethyl)indole-3-carbonyl]amino]-3,3-dimethylbutanoate (1) (MDMB-CHMICA)

The title compound was synthesized according to a modified procedure from Buchler et al.<sup>34</sup> The coupling conditions for each synthesis are summarized in Table 1.

#### Coupling via HATU:

A solution of 1-(cyclohexylmethyl)-1H-indole-3-carboxylic acid (100 mg, 0.389 mmol, 1.0 eq.) and triethylamine (134.5 µL, 0.970 mmol, 2.5 eq.) in DMF (5 mL) was supplemented with HATU (163 mg, 0.43 mmol, 1.1 eq.) and stirred for 15 minutes at room temperature. To the yellow reaction mixture, L-tert-leucine methyl ester hydrochloride (106 mg, 0.584 mmol, 1.5 eq.) was added and the mixture was stirred for another 2 hours at room temperature.

The reaction mixture was diluted with ethyl acetate (30 mL), washed with HCl (1 mol/L, 2 x 10 mL) and brine (2 x 20 mL), dried (Na<sub>2</sub>SO<sub>4</sub>), and evaporated to dryness, giving a crude yellowish solid (122 mg, 82%).

#### Coupling via oxalyl chloride and thionyl chloride:

A solution of 1-(cyclohexylmethyl)-1H-indole-3-carboxylic acid (50 mg, 0.194 mmol, 1.0 eq.) in DCM (4 mL) was supplemented with oxalyl chloride (20.3 mL, 0.233 mmol, 1.2 eq.) and cooled to 0°C. Subsequently, DMF was added dropwise (14.63 mL, 0.190 mmol, 0.98 eq.) and stirred for 2 hours. L-tert-Leucine methyl ester (52.86 mg, 0.291 mmol, 1.5 eq.) and triethylamine (67.23 µL, 0.485 mmol, 2.5 eq.) was added and the mixture was stirred for another 2 hours at room temperature.

The reaction was stopped by addition of water (5 mL) and conc. NaOH until a pH of 10 was reached. The phases were separated and the organic phase was washed twice with DCM, 0.5 M NaOH, and brine (5 mL each). After evaporation to dryness, **1** was obtained as a crude colorless solid (73 mg, 98%, residues of DMF or TEA might be present).

The complete procedure was repeated with a reaction temperature of 0°C after the amino acid was added and repeated again, where aliquots of the reaction mixture were taken 1, 2, 3, and 23 hours after the amino acid was added.

For the coupling with thionyl chloride, the same reaction conditions were used, except for an addition of thionyl chloride (16.89 µL, 0.233 mmol, 1.2 eq) instead of oxalyl chloride.

**TABLE 1** List of the controlled synthesis variations with corresponding parameters for the last reaction step (coupling of the amino acid) for MDMB-CHMICA. Each synthesis was run in triplicate in parallel

Name	Coupling Agent	Solvent	Base	Catalyst	Temp.	Time	Replicates
Oxal (1)	Oxalyl chloride	DCM	TEA	DMF	25°C	2 h	3
Oxal (2)	Oxalyl chloride	DCM	TEA	DMF	25°C	1 h, 2 h, 3 h, 23 h	3
Oxal (3)	Oxalyl chloride	DCM	TEA	DMF	0 °C	2 h	3
Thio (4)	Thionyl chloride	DCM	TEA	DMF	25 °C	2 h	3
HATU (5)	HATU	DMF	TEA	-	25 °C	2 h	3



The corresponding analytical characterization can be taken from the Supporting Information.

### 3 | RESULTS AND DISCUSSION

#### 3.1 | Discrimination of seized samples of MDMB-CHMICA based on their impurity signatures

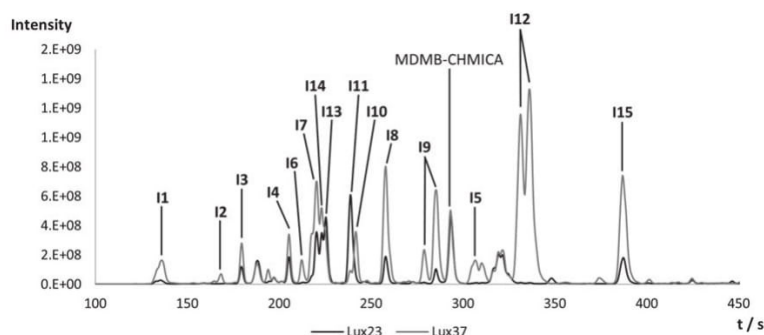
In Münster-Müller et al.,<sup>31</sup> links between 40 samples of a large seizure of **1** from Luxembourg customs were worked out via PCA, based on the 57 most abundant impurities found in the corresponding chromatographic impurity signatures. The work mainly focused on the newly developed workflow of impurity separation and enrichment via FC, determination of relative peak areas for a selection of synthesis-related impurities via UHPLC-MS and pattern evaluation via multivariate data analysis, proving the general applicability of the impurity profiling concept for synthetic cannabinoids. In the presented work, the scientific basis for this profiling concept for the synthetic cannabinoid **1** was generated and validated by increasing the analyzed sample set by 21 additional samples with no previously known relationship from customs seizures in Finland and Internet test purchases by the University Medical Center Freiburg. It is possible that samples from different sources might be synthesized by another manufacturer or route, or under completely different conditions, reflected by the composition and concentration of impurities. No reference material of multiple reaction batches under controlled conditions from the original manufacturer were available which could provide a scientific basis to classify samples of unknown sources into individual batches. Thus, the relative distance set for the batch discrimination of the 40 packaging units of the Luxembourg seizure was employed as "calibration distance." Furthermore, the impurities used for batch discrimination in Münster-Müller et al were reevaluated.<sup>31</sup> The majority of the 57 impurities detected in the previous study proved to be present in comparatively small concentrations or with no inter-sample variations, having minor impact on the statistical model. Therefore, the list of targeted "key impurities" for **1** was reduced to those 15 (I1 to I15) with the highest abundance and inter-sample variation, carrying the majority of sample discrimination potential. Although not being a part of the data evaluation, a list of the excluded impurities with expected affiliation to **1** can be taken from the Supporting Information. Figure 2

exemplarily shows two overlaid base peak chromatograms (BPCs) of the impurity signatures for two unrelated samples of **1** with highlighted impurity peaks I1 to I15, displaying their large fluctuation in abundance and overall relative intensity.

The 15 newly selected key impurities were employed to compare the available seized samples from different sources to reveal potential links. For the samples from the Luxembourg seizure (Lux01 to 40), consisting of 40 individual 1 kg packages, a single source/manufacturer was expected and a production batch discrimination was already carried out in a previous publication.<sup>31</sup> This again provided a foundation on which the impurity signatures of samples with no previously known relation could be evaluated when submitted to one chemometric model, in this case 18 samples seized by Finnish customs (FL01 to 18) and three test purchases in online shops by the University Medical Center Freiburg (FR01 to 03). The table in Figure 3 depicts the impurity signatures for all 61 available powder samples of **1**. A greyscale (individual for each impurity) indicates the relative intensities (integrated peak areas of the total ion chromatogram), where white represents a complete absence of signal and black the highest signal value for this impurity. In the last line of the table, the average intensity ratios between the impurities are compared and normalized to the least abundant to convey their absolute abundances. A hierarchical cluster analysis (HCA) using Ward's method was carried out to group them according to their relative distance in impurity signatures. The resulting dendrogram is attached next to the table for better visual interpretation of the data. No prior normalization was carried out, resulting in the impurities with higher intensity values to be the most influential (eg, I15) for the cluster formation.

Apart from the three outliers (as already reported<sup>31</sup>) Lux14, Lux21, and Lux37, the samples from the Luxembourg seizure form individual clusters of five to ten samples, presumably representing individual synthesis batches. Two of the test purchase samples, FR01 and FR02, also fall into one of these clusters in addition to the fact that both the large seizure and these two test purchase samples were acquired in the same time-frame (end of 2014/beginning of 2015). Taking into account the relative distance threshold used for batch discrimination of the Lux samples, the similarities in impurity composition for FR01 and FR02 to the Lux samples should not be a coincidence. Possibly, aliquots of the corresponding synthesis batch were sold to the European market before the shipment of the 40 kg order and recovered by chance in the form of online test purchase samples. This

**FIGURE 2** Overlaid UHPLC-MS base peak chromatograms (BPCs) of impurity signature for two MDMB-CHMICA samples. The impurity peaks carrying the most discrimination potential to distinguish between samples are numbered from I1-I15



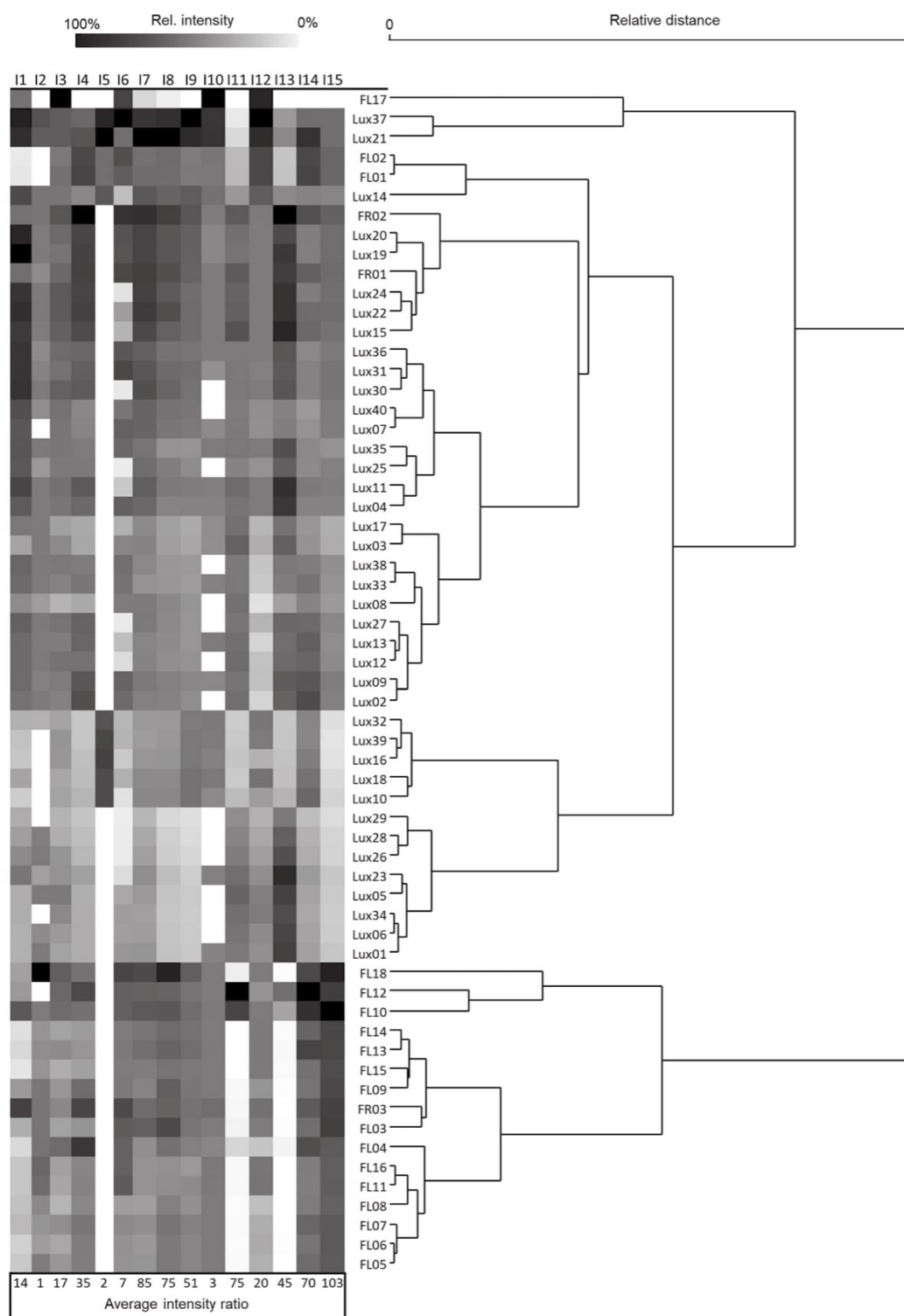


**FIGURE 3** Table (left) with impurity signatures for 61 powder samples of MDMB-CHMICA, with a greyscale individual for each impurity that indicates the relative integrated peak areas measured in each sample, where white represents a complete absence of signal and black the highest signal value for this impurity. The relative intensity ratio between the impurities is indicated in the last row to convey their absolute abundances. The dendrogram (HCA, Ward's method, right) shows the calculated relative distance between the samples on the basis of their impurity signatures



hypothesis is validated, as the two test purchase samples fall into the same cluster.

The additional test purchase sample (FR03) from October 2015, seems to be related to FL03, FL09, and FL13–15, which were seized in September–October 2015. Another two clusters consisting of two (FL01–02, seized February 2015, one day apart) and seven (FL04–08, FL11, FL16, seized at the end of 2015) samples can be observed, indicating a common source, possibly even the same synthesis batch. The four remaining samples (FL10, FL12, FL17, and FL18) could not be assigned to clusters and stood individually.

### 3.2 | Impurities found in seized samples of MDMA-CHMICA

Ten of the 15 key impurities could be isolated via FC in larger quantities and structural elucidation via HR-MS/MS and NMR was carried out for them. For the remaining five, only HR-MS/MS experiments were performed. All HR-MS and NMR spectra used for structure elucidation are shown in the Supporting Information. The corresponding structural formulas of **I1** to **I15** are depicted in Figure 1.

Compound **I1** appears to be a reaction product of *tert*-leucine methyl ester (TLME) and DMF after its oxidative conversion to *N,N*-dimethylcarbamoyl chloride (DMCC) by a chlorinating agent (oxalyl chloride, thionyl chloride or phosphorus oxychloride).<sup>42</sup> DMF is a common solvent for organic reactions and can be used to catalyze peptide couplings through acyl chloride intermediates<sup>43</sup> and was likely used in the synthesis of the original manufacturer. The fragmentation pattern and exact mass suggest that the structure of compound **I2** consists of at least two *tert*-leucine methyl ester amino acids. With the given MS data, no consistent structure for this impurity could be proposed.

Furthermore, a series of *N*-alkylated amides were identified with carbon chains in different lengths and branching, in the majority of cases with more than one constitutional isomer in varying intensity ratios. Ions with *m/z* 285 (two isomers), 313 (three isomers), 327 (two isomers), and 341 (three isomers) could be observed, representing the cyclohexylmethyl-substituted indole core with NC<sub>2</sub>H<sub>6</sub>, NC<sub>4</sub>H<sub>10</sub>, NC<sub>5</sub>H<sub>12</sub>, and NC<sub>6</sub>H<sub>14</sub> residues bound to the carbonyl linker group, respectively. For *m/z* 285, two closely eluting isomers with an chromatographic peak area ratio of approximately 1:5 were observed of which the more intense could be isolated and identified as 1-(cyclohexylmethyl)-*N,N*-dimethyl-1*H*-indole-3-carboxamide (**I7**). Since only one other isomer for NC<sub>2</sub>H<sub>6</sub> is possible, the second, less-intense species of *m/z* 285 is believed to be 1-(cyclohexylmethyl)-*N*-ethyl-1*H*-indole-3-carboxamide. For *m/z* 313, already seven isomers are possible, three of which were observed, two of them, however, only in trace amounts. The most abundant isomer was isolated and identified as 1-(cyclohexylmethyl)-*N,N*-diethyl-1*H*-indole-3-carboxamide (**I8**). For the remaining two isomers, no structures for the aliphatic portion are proposed, since the amide bond is cleaved in  $\alpha$ -position in the first fragmentation step of MS/MS experiments, giving no additional information about the branching of the carbon chain. None of the isomers of *m/z* 327 (**I9**) and 341 (**I10**) could be

isolated in sufficient amounts and purity for NMR measurements; therefore no further structural information was obtained other than the molecular formulas and fragmentation patterns. Small but significant quantities of TEA were found in the seized samples from Luxembourg customs,<sup>43</sup> indicating its use as a base in the peptide coupling step. It is possible that the TEA used was contaminated with primary and secondary amines of varying branching and chain length resulting in the observed congeners of **1** with aliphatic residues attached to amide bond.

Two nearly co-eluting signals with identical fragmentation patterns of *m/z* 498 were found in the LC-MS chromatogram of some of the seized samples. With FC, it was not possible to isolate both substances individually but only a mixture. Subsequent NMR measurements revealed two highly similar overlapping set of signals for what are most probably two diastereomers of methyl 2-(2-(1-(cyclohexylmethyl)-1*H*-indole-3-carboxamido)-3,3-dimethylbutanamido)-3,3-dimethylbutanoate (**I12**) as reported by Münster-Müller et al.<sup>31</sup> The exact configuration of both isomers is difficult to assess analytically and its formation can have several reasons. In the amino acid reactant, a small concentration of dimers might already have been present, which can undergo an internal rearrangement and epimerization via an 2,5-diketopiperazine (DKP).<sup>44,45</sup> Since the terminal amino acid in **I12** is present as the methyl ester, the epimerization over a DKP must take place before or during the esterification of *tert*-leucine to *tert*-leucine methyl ester due to loss of the C-terminal ester moiety in the DKP formation. Another possibility is that the amino acid reactant (*tert*-leucine methyl ester) still contains free *tert*-leucine, which is coupled to the 1-(cyclohexylmethyl)-1*H*-indole-3-carboxylic acid residue, providing another carboxylic acid for a second peptide coupling, possibly through a mixed anhydride intermediate. Activated *N*-acyl amino acids are known to epimerize via formation of oxazolonium intermediates<sup>46</sup> followed by coupling of the second amino acid, resulting in an diastereomeric dimer. In any case, the abundance ratio of these two diastereomers was different in all of the seized samples and some of the controlled syntheses. Furthermore, in the syntheses in this study, another constitutional isomer with *m/z* 498 was found in the trace area of the chromatogram, which had the same molecular formula but a different fragmentation pattern in comparison to the diastereomeric pair. This impurity was not structurally elucidated and is not further considered in this work due to the very small signal intensity. The factors influencing the ratio of the diastereomers or the formation of the third isomer as well as its structure are still unknown, albeit their presence and ratio seem to be highly discriminating in a batch-to-batch comparison. Unfortunately, the applied bucketing algorithm for automated integration of the LC-MS spectra is not able to distinguish these signals from each other due to the almost identical retention time, summing up the total recorded signal for *m/z* 498 independent of the number of individual peaks in this close elution range. Therefore, with respect to the profiling, when two samples look similar in their overall impurity signatures generated by this bucketing (numeric values), especially the bucket for *m/z* 498, an inspection of the LC-MS data (chromatogram and precut ion spectrum of all signals for *m/z* 498) might provide additional

discriminating information before a final conclusion about the relationship of the samples in question is drawn.

Compound **I13** was identified as 5F-MDMB-PICA which itself is a synthetic cannabinoid which was first detected on the European market in 2016.<sup>47</sup> The main difference to **1** is the substitution of the N-linked cyclohexylmethyl group with a 5-fluoropentyl chain, which is a common aliphatic residue for various synthetic cannabinoids already on the market (eg, 5F-PB-22, Cumyl-5F-PINACA). Speculating about the origin of this impurity, two scenarios are considered. The producers of **1** could have previously synthesized a cannabinoid with a 5F-pentyl chain and residues of 5-fluoropentyl halide remained in the reaction vessels and unintentionally reacted with precursor material of **1**. Alternatively, the manufacturers or a large customer could have contaminated (by accident or on purpose) a large batch of **1** with residues of previously stored MDMB-5F-PICA. In any case, this impurity does not provide information on the synthesis conditions but might be an important marker for its source and is most likely specific for a particular synthesis site or wholesaler. **I13** was present in almost all available powder samples of **1**, leading to the assumption that there is only one large producer and distributor of **1**, responsible for the shipment of the large Luxembourg seizure and distribution of partial quantities of their "contaminated" **1** to vendors around Europe.

One of the most abundant impurities found in the majority of available seized samples of **1** was methyl 2-(2-chloro-1-(cyclohexylmethyl)-1H-indole-3-carboxamido)-3,3-dimethylbutanoate (**I15**). In the patented synthesis, no potential chlorine source is used for the indazole analog of **1**, apart from simple washing steps with brine or precipitation of intermediates via diluted HCl. Therefore, either the indole used for coupling already contains the chlorine impurity or a reactive chlorinating agent is used for the coupling to the amino acid through the acid chloride. A possible explanation could be an electrophilic reaction attacking the free 2-position of the indole or a radical reaction in which the more stable benzylic radical is formed through attack onto the 2-position which is known for its preference to react with electrophilic radicals. Alternatively, an oxindole impurity in the parent indole-3-carboxylic acid is converted to the 2-chloroindole derivative under dehydrating conditions, which itself would be a redox-neutral process.<sup>48</sup>

Another very insightful contaminant found exclusively in seized **1**, and not in samples prepared under controlled conditions, was **I11**, in which the *tert*-leucine moiety is replaced by 2-aminobutyric acid. It is hard to imagine how a formal double demethylation in the  $\beta$ -position of an amino acid could take place in a non-destructive fashion, so the most probable source of this impurity is *tert*-leucine itself. A link between *tert*-leucine and 2-aminobutyric acid is the industrial production of these non-proteinogenic amino acids which involves similar multienzyme processes.<sup>49,50</sup> Once the general technology has been established at a given site, the producer can extend its portfolio from one amino acid to the other relatively easily and at least one example of dual production within an otherwise very limited product portfolio is known. Overall, the presence and concentration of this impurity provide information about the purity of the amino acid precursor.

**I14** was characterized as methyl 3,3-dimethyl-2-(1-((tetrahydro-2H-pyran-2-yl)methyl)-1H-indole-3-carboxamido)butanoate. As for **I12**, the NMR data suggest the presence of two diastereomers with (*R*) and (*S*) tetrahydropyran-2-yl-methyl residues. No valid explanation regarding the formation could be found for this impurity, except for an impure batch of the CHM precursor material or the contamination with a yet unknown experimental cannabinoid. Although other cannabinoid compounds with a structurally related tetrahydropyran-4-yl-methyl residue were already reported (Cumyl-THPINACA<sup>37</sup> or Adamantyl-THPINACA<sup>51</sup>), it is unlikely that their synthesis or distribution stand in any relation to **I14** in form of batch mingling or contaminated synthesis equipment. However, like **I13**, this compound seems to be characteristic for a distinct manufacturer or distributor due to its specific structural element.

Interestingly, several of the structural elements of the impurities (eg, chlorinated, dimer or N-N-dimethyl specimens) were also found in seized samples of other cannabinoids with indole, indazole, and carbazole core structures (unpublished in-house data). As the synthesis of cannabinoids with these core structures can be regarded as a modular system, exchanging single structural elements, it seems that the general synthesis procedures such as precursor material or coupling reagents remain constant producing similar types of impurities.

### 3.3 | Controlled syntheses on the amino acid coupling step and impact of varied reaction parameters on the impurity profile

The present profiling routines for classical drugs are based on target impurities, which have been selected according to criteria like discrimination potential or chemical stability.<sup>4</sup> From studies based on controlled syntheses, the appearance and discrimination potential of route-specific by-products as well as the overall reproducibility of the chemical profile can be assessed.<sup>20,52</sup> To better understand differences in seized samples of **1**, the target was to reproduce different scenarios with controlled syntheses that are possible when comparing the impurity signatures of two samples of unknown source. The focus was put on what is expected to be the last reaction step in the synthesis of **1**, the coupling of the amino acid to the alkyl-indole. Larger quantities of 1-(cyclohexylmethyl)-1H-indole-3-carboxylic acid were synthesized and cleaned thoroughly. Thus, carry-over from preceding operations should be prevented and all by-products are a result of the ultimate coupling step to the final product. All seized samples of **1** were present in crystalline form and of high purity. It is assumed that the manufacturers purify their final reaction mixture, removing the majority of organic solvents and reactants. Hence, all of the syntheses were worked up with standard extraction protocols (washing with water and brine) until a colorless, crude material was obtained. By-products were then separated via FC and analyzed by UHPLC-MS and HPLC-HR-MS as was done for the seized material.

By interpreting the impurities found in the seized samples, the following conclusions on how to adapt the controlled syntheses starting from the patented version for the indazole analogue from Buchler et al



were drawn: Diisopropylethylamine (Hünig's base) was replaced by TEA, since small quantities of TEA were found in the seized samples.<sup>43</sup> DMF is used either as catalyst or solvent, indicated by the presence of **I1** and the high abundance of the dimethyl isomer of **I7**. And finally, oxalyl chloride was chosen as a coupling agent for two reasons. The highly abundant chlorinated **I15** might be a result of a coupling reaction via an acyl chloride utilizing a chlorinating agent. In addition, considering the economic aspects of the synthesis, coupling via oxalyl chloride on a large scale is much cheaper than using HATU or equivalent.<sup>53</sup>

Different clandestine synthesis scenarios are considered (the expected relations of the corresponding impurity signatures are highlighted in brackets). The samples originate from

- the same batch. It is expected that these samples show highly similar or even indistinguishable impurity profiles ("strong link"). However, if two aliquots of this batch are stored differently, high temperatures, moisture or exposure to daylight might lead to decomposition. Therefore, the impurity profile of one batch was analyzed directly after synthesis and again after one-month storage either in the freezer or exposure to direct sunlight and room air.
- different batches, which were prepared under identical conditions ("link"). For this purpose, three batches were prepared and worked up in parallel.
- Different batch syntheses conducted on different days with otherwise identical conditions ("link").
- different batches prepared with slightly altered reaction parameters, in this study the temperature and time, respectively ("undecided"). One synthesis was carried out with a reaction temperature of 0°C instead of 25°C after the amino acid was added. In a second run, aliquots of the reaction mixture were taken and worked up 1, 2, 3, and 23 hours after the amino acid was added.
- Different batches with different coupling agents ("no-link"). Two more syntheses with thionyl chloride and HATU (as stated in Buchler et al.<sup>34</sup>) as coupling agents were conducted.

All batches were compared on the basis of the previously assessed target impurities in seized samples of **1** (**I1–I15**). Not surprisingly, several impurities found in the seized samples were completely absent in the controlled syntheses, for example those with no CHM-substituent attached to the indole (**I3**, **I4**, **I5**) or different substituents (**I13**, **I14**) at this position. All of these products were expected to originate from carry-over of different products from the preceding coupling reaction of CHM to the indole (either incomplete or wrong substituent). Furthermore, any form of chlorinated impurity of **1** was absent in all controlled syntheses. Either the original manufacturers used another coupling agent, such as phosphorus tri- or pentachloride, which was not included in the controlled synthesis experiments, or the reaction mixture was contaminated with catalysts or highly potent reactants leading to oxidation of the indole core, or an already chlorinated indole was a carry-over from preceding reaction steps. However, in the controlled syntheses, several additional reaction by-products were found, never observed in the seized samples (**I16–I25**). Since some of these by-products were

characteristic of a specific coupling reagent and therefore could be used for batch discrimination, they were implemented in the comparison of the controlled synthesis products and a tentative structural elucidation via MS<sup>n</sup> and HR-MS experiments was carried out. They might be important synthesis pathway markers when investigating the impurity profiles of newly arising synthetic cannabinoids in the future.

Table 1 provides an overview of the conditions for the synthesis variations in this study. All five synthesis variations were carried out in triplicate on the same day. The impact of the different reaction conditions on the target analytes are shown in four bar plots in Figure 4. Each bar in the plots (B)–(D) represents the averaged value of a by-product for the triplicate synthesis with error bars (max and min value).

### 3.3.1 | Stability test and comparative analysis of the impurity profile from a single batch of MDMB-CHMICA with oxalyl chloride as coupling reagent

A single finished and worked-up reaction batch of Oxal (**1**) was split into three aliquots for a stability test. The first aliquot was directly submitted to F-LC and the present impurities were assessed by LC-MS to generate a snapshot of the original impurity composition. Another aliquot was stored in a freezer at –20°C and the last aliquot was stored under sunlight exposure at 25°C. After a month of exposure, the impurity profiles of both stored samples were reassessed and compared to the profile of the aliquot recorded directly after the synthesis.

No deviation in the impurity composition was observed for the sample stored in the freezer, demonstrating the stability of the main component and the by-products under these conditions. The aliquot exposed to sunlight and air became yellowish after a few days. After one month, LC-MS assessment of the impurity profile showed the presence of two new ions with *m/z* 389 (**I24**; +4 u in comparison to **1**) and 417 (**I25**; +32 u in comparison to **1**). Unfortunately, these substances could not be obtained in sufficient quantities for NMR analysis. The sum formula generated by HR-MS for **I25** was similar to **1** with two additional oxygen atoms most probably attached to or implemented into the indole core. Tryptophan, an amino acid with an indole residue, is known to form *N*-formylkynurenine with elemental oxygen under basic conditions and irradiation with light.<sup>54,55</sup> This might also be the case for the indole core of **1** and would match the recorded fragmentation pattern of **I25**. Additionally, *N*-formylkynurenine is known to form kynurenine via hydrolysis and loss of formic acid,<sup>56</sup> explaining the presence of **I24**, which most probably is the hydrolysis product of **I25**.

After a thorough evaluation of the LC-MS chromatogram of the sample stored in sunlight, no degradation products of any key impurity could be identified and all signal intensities remained constant. Not surprisingly, **1** as the main component, seems to be most affected by this oxidation. In any case, the characterization of degradation products of the main component might be important for the analytics of indole-based synthetic cannabinoids, as these oxidized products might be found as by-products in any seized or purchased samples.

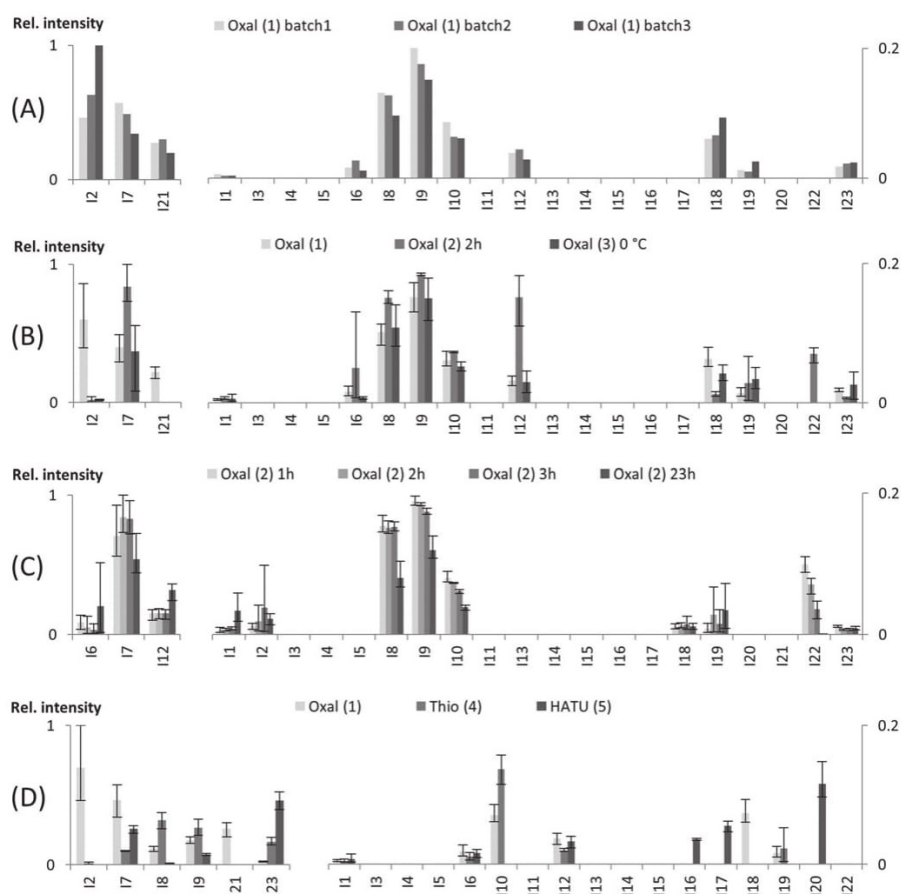


**FIGURE 4** Bar plots of the by-product signatures of controlled synthesis of MDMB-CHMICA. (A) Three batches of Oxal (1) run in parallel with identical conditions. (B) Oxal (1), Oxal (2) 2h with identical conditions conducted on different days. Additionally, Oxal (3) conducted on a different day with reduced reaction temperature to 0 °C. (C) Four aliquots of Oxal (2) taken from the reaction mixture after the reaction was started (1h, 2h, 3h, 23h). (D) Couplings via the reagents oxalyl chloride (Oxal (1)), thionyl chloride (Thio (4)) and HATU (HATU (5))

### 3.3.2 | Intra-day reproducibility with oxalyl chloride as coupling agent

As stated before, all five synthesis variations stated in Table 1 were carried out in triplicate (in parallel, on the same day). The impurity compositions of the three replicates for Oxal (1) are shown in Figure 4A as typical example and for illustration purposes. For the remaining four synthesis variations, fluctuations in the impurity composition between the replicates is indicated by error bars for each impurity individually (all bars in Figure 4B–D).

In general, the replicates of all five synthesis variations exhibited the same set of by-products, albeit with variations in peak areas. In particular, the polar substances eluting with short retention times in reverse chromatography like **I2**, **I6**, and **I7**, showed large fluctuation of abundances. Variations in the washing steps of the reaction mixture with water and brine could result in more or less efficient extraction of these by-products, even though they were carried out as evenly as possible to keep the degree of extraction of water-soluble components equal for all replicates. The aim of the profiling method

described in the first part of this study was to discriminate individual synthesis batches of **1** based on the impurity signatures, including **I2**, **I6**, and **I7**. If the washing step indeed has an influence on their abundance, these impurities could lose their batch-discriminating potential when multiple aliquots of a single reaction batch are cleaned up differently. However, this scenario was considered unlikely for a large-scale production of **1**, which is why it was decided to still include these three compounds as target analytes in the profiling model.

### 3.3.3 | Impact of the temperature on the impurity profile and inter-day reproducibility with oxalyl chloride as coupling agent

To compare the inter-day reproducibility and influence of the reaction temperature, Figure 4B shows the by-product signatures for Oxal (1), the 2 hour aliquot from Oxal (2) and Oxal (3) with a reduced reaction temperature of 0 °C. Apart from the polar components already discussed, comparison of the by-product profiles of Oxal (1) and Oxal (2), at 2 hours, revealed several other major differences. **I21** was only



present in Oxal (1), whereas **I22** was only found in Oxal (2) 2 hours, and **I12** exhibited a five-fold more intense signal. Regarding the differences between the inter-day related variances of Oxal (1) and Oxal (2) 2 hours, it was difficult to assess variations in the profile as a result of the temperature reduction to 0°C for Oxal (3). Compared to Oxal (1), an absence of **I2** and **I21** was observed. In any case, both the execution of the synthesis on different days, as well as the reduction of the reaction temperature led to distinguishable by-product signatures.

### 3.3.4 | Impact of the reaction time with oxalyl chloride as coupling agent

Oxal (2) was run in triplicate, from which aliquots were taken and worked up after 1, 2, 3, and 23 hours after the amino acid was added. The by-product signatures of these aliquots are shown in Figure 4C. Some major abundance fluctuations were again observed between the three replicates for the polar components (**I7** in all time aliquots, **I6** after 23 hours, **I2** after 3 hours, and **I19** after 2 and 23 hours), making it difficult to draw conclusions about their reaction time dependencies. However, for the abundances of the impurities with aliphatic amine residues of varying length and branching (**I8**, **I9**, **I10**, and **I22**), a negative correlation with increased reaction time was observed. Possibly the sterically unhindered smaller amines react with the activated carboxylic acid faster than the free amino acid. However, after a longer reaction time, more main component was formed. It has to be kept in mind that the dilution factor of the impurity fraction depends on the amount of corresponding isolated main component after FC. Because of this increased dilution the signal intensity of the already formed components seem to diminish in relation to the samples taken earlier from the reaction mixture. For **I1** and **I12**, an increased abundance was recorded after 23 hours. Obviously, long reaction times favor the formation of amino acid cross reactions, either with the catalyst (DMF) or by formation of dimers. Although a major concentration decrease in the starting material **I6** is expected over long reaction times, in one of the replicates for 23 hours this impurity showed a high abundance, possibly due to insufficient washing of the final reaction mixture.

### 3.3.5 | Impact of the coupling reagents oxalyl-chloride, thionyl chloride, and HATU

Figure 4D shows the by-product signatures produced by the three different amino acid coupling reagents oxalyl chloride [Oxal (1)] thionyl chloride (Thio (4)) and HATU (HATU (5)). The profiles generated by these three coupling reagents are easily distinguishable; only **I1**, **I6**, and **I12** showed similar but comparatively low abundances. Two route specific markers **I21** and **I18** were identified for oxalyl chloride. **I2**, with the highest overall abundance, can also be counted among the oxalyl chloride specific markers, although a small signal was also observed in the synthesis with thionyl chloride. **I16**, **I17**, and **I20** were specific for a coupling with HATU, via an activated carboxylic acid intermediate and two new by-products with residues of NCH<sub>3</sub> and NC<sub>3</sub>H<sub>7</sub> attached to the amide bond, filling the gaps in the homologous series of aliphatically substituted impurities already identified in the

seized samples (**I7**, **I8**, **I9**, and **I10**). Thionyl chloride did not produce any specific markers; however, it gave the highest abundances for three by-products of the homologous series **I8**, **I9**, and **I10**. Figure 5 shows an Euler diagram, summarizing which impurities were found in seized samples and samples from the controlled syntheses using different coupling reagents. **I24** and **I25** are excluded from this diagram, as they are the result of forced degradation within the stability studies and are not occurring as the result of the synthesis pathway

The authors are aware of the fact that the syntheses were not a perfect reproduction of the original synthesis and this may be reflected in the final impurity profiles. However, considering Oxal (1) or Thio (4) for example, only those seven impurities are absent which are expected to be a result of preceding reaction steps or impure reactants and precursors (considering **I1**–**I15**). For the controlled synthesis using HATU, four additional impurities, three of which were specific for HATU, and no signals for **I2** and **I10** were observed compared to the seized samples, thus, being the least likely coupling reagent used by the clandestine manufacturer. The coupling with oxalyl chloride also yielded five additional impurities; however, **I21** and **I22**, both oxalyl chloride specific, seem to be formed with a high degree of variation as evidenced by the inter-day reproducibility shown in Figure 4B. For thionyl chloride, only two additional impurities were observed in the controlled synthesis and the remaining set of impurities was relatively similar to those of the seized samples. However, for thionyl chloride, only three syntheses were carried out on the same day, providing no information about inter-day reproducibility or change in synthesis conditions. To reproduce the complete profile, all reaction steps would have to be carried out in different sequences with different reagents and conditions. Since it is assumed that syntheses of synthetic cannabinoids consist of at least three steps and no information about the precursor materials is available (in particular which indole core structure is used), extensive synthesis screening would be extremely time-consuming. However, with the given set of information, the authors assume that the coupling step using thionyl chloride

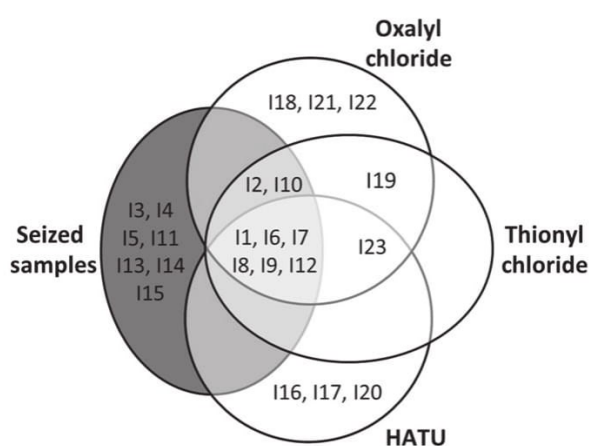


**FIGURE 5** Euler diagram of the key impurities **I1** to **I15**, assessed in seized samples of MDMB-CHMICA, and **I16** to **I23**, found in controlled syntheses of the amino acid coupling using the three different coupling reagents HATU, thionyl chloride and oxalyl chloride

seems to be the most likely synthesis procedure of choice for the manufacturing of the seized samples of **1**, although the most abundant impurity **I15** with a chlorine attached to the 2-position of the indole is still absent.

Each of the batches that were synthesized in the survey was discriminable by their by-product signatures. Although the triplicate syntheses carried out in parallel showed the same overall pattern, some signal fluctuations for several impurities could be observed, especially for the polar components. To fully assess the actual impact of the washing steps on the presence of these by-products, further controlled syntheses need to be carried out with a structured series of varying work-up procedures. However, the batch discriminability of the conducted controlled syntheses validates the batch discrimination assignment carried out for the seized samples as described in the first part of this work and in a previously published work.<sup>31</sup> It was even possible to unambiguously discriminate those syntheses via impurity signatures, which were conducted in parallel.

## 4 | CONCLUSION

In this study, 15 key impurities in seized samples of MDMB-CHMICA were assessed and structurally elucidated, of which 14 were described for the first time. By interpreting the chemical structures of the impurities, a deeper insight into the manufacturing process of synthetic cannabinoids was obtained. Sixty-one samples of pure MDMB-CHMICA from customs seizures and Internet test purchases were grouped by multivariate data analysis of their impurity patterns. This provides a powerful tool for impurity profiling of synthetic cannabinoids to acquire basic information about the distribution and market structures by analyzing and grouping powder samples from different sources. To further strengthen the discrimination power of the impurity profiling concept, the impurity patterns could be combined in a unified chemometric model with isotope ratio mass spectrometry (IRMS) data as orthogonal analytical information providing additional information about the origin of precursor material. It appears that the impurity profiles of samples seized or bought in similar time-frames tend to match. Possibly, the manufacturers of **1** produce individual batches depending on the demand of their recipients and ship them to Europe consecutively.

As a second part of this study, the reaction by-products in a set of controlled syntheses of a synthetic cannabinoid were investigated to better understand variations in impurity signatures and to assess the significance of variations in the impurity patterns of seized samples in order to establish links between them. Eight new by-products were identified in the products of the controlled syntheses and two additional decomposition compounds formed in the subsequent stability tests. All of the eight new by-products were not present in any of the 61 investigated seized samples and showed high abundances or discriminating potential for a specific synthesis pathway. The coupling via thionyl chloride was the most likely synthesis route used by the clandestine manufacturer, as only two additional impurities were formed in the controlled synthesis. However, still a few of the key-impurities found in the seized material could not be reproduced by

the different controlled synthesis approaches, like the chlorinated derivative of **1**, suggesting that the clandestinely applied synthesis procedure has not yet been identified in minute detail. The aspects of single-batch discriminability, inter- and intra-day reproducibility, the influence of the reaction temperature and time and, lastly, the influence of the coupling agent were investigated. Regarding the inter-day reproducibility, statistically relevant differences in impurity patterns were found, which, however, is a positive aspect for the applicability of batch-to-batch comparison as performed in the first part of this study. The degree of variations in the impurity profile correlated with the magnitude of variation in synthesis reaction parameters which, thus, provides a reliable evidence base for the assignment of sample relations based on impurity signatures of the synthetic cannabinoid MDMB-CHMICA targeted in this study.


## ACKNOWLEDGEMENTS

All presented data, if not cited otherwise, were generated within the project "SPICE-profiling," funded within the EU's ISEC 2013 program (Directorate-General for Justice JUST/2013/ISEC/DRUGS/AG/ISEC/4000006421). Again, our thanks are due to Serge Schneider from the Laboratoire National de Santé in Luxembourg, who kindly provided us with aliquots from the large seizure of MDMB-CHMICA by the Luxembourg Customs, Ilmary Szilvay for providing aliquots seized by the Finnish Customs, and Volker Auwärter and Verena Angerer from the University Medical Centre Freiburg for supplying samples from Internet test purchases. Furthermore, we want to thank Dieter Kirsch, Steven Luhn, and Vincent Guillou from the Federal Criminal Police, Forensic Science Institute in Germany for their help with HR-MS and NMR measurements.

## ORCID

Sascha Münster-Müller  <https://orcid.org/0000-0003-3949-2818>

Till Opatz  <https://orcid.org/0000-0002-3266-4050>

Ralf Zimmermann  <https://orcid.org/0000-0002-6280-3218>

## REFERENCES

1. Ehleringer JR, Casale JF, Lott MJ, Ford VL. Tracing the geographical origin of cocaine. *Nature*. 2000;408(6810):311-312.
2. Janzen KE, Fernando AR, Walter L. A database for comparison analysis of illicit cocaine samples. *Forensic Sci Int*. 1994;69(1):23-29.
3. Janzen KE, Walter L, Fernando AR. Comparison analysis of illicit cocaine samples. *J Forensic Sci*. 1992;37(2):436-445.
4. Ballany J, Caddy B, Cole M, et al. Development of a harmonised pan-European method for the profiling of amphetamines. *Sci Justice*. 2001;41(3):193-196.
5. Hauser F, Rößler T, Hulshof J, Weigel D, Zimmermann R, Pütz M. Identification of specific markers for amphetamine synthesised from the pre-precursor APAAN following the Leuckart route and retrospective search for APAAN markers in profiling databases from Germany and the Netherlands. *Drug Test Anal*. 2018;10(4):671-680.
6. Pikkarainen AL. Systematic approach to the profiling analysis of illicit amphetamine. *Forensic Sci Int*. 1996;82(2):141-152.
7. Sinnema A, Verweij AM. Impurities in illicit amphetamine: review. *Bull Narc*. 1981;33(3):37-54.



8. UNODC. *Drug Characterization/Impurity profiling*. Vienna: UNODC; 2001 Available at <https://www.unodc.org/pdf/publications/st-nar-32-rev1.pdf>. Accessed 26. March 2019.
9. Chiarotti M, Marsili R, Moreda-Pineiro A. Gas chromatographic-mass spectrometric analysis of residual solvent trapped into illicit cocaine exhibits using head-space solid-phase microextraction. *J Chromatogr B Analyt Technol Biomed Life Sci*. 2002;772(2):249-256.
10. Zacca JJ, Grobério TS, Maldaner AO, Vieira ML, Braga JWB. Correlation of cocaine hydrochloride samples seized in Brazil based on determination of residual solvents: an innovative chemometric method for determination of linkage thresholds. *Anal Chem*. 2013;85(4):2457-2464.
11. Zhang JX, Zhang DM, Han XG. Identification of impurities and statistical classification of methamphetamine hydrochloride drugs seized in the China. *Forensic Sci Int*. 2008;182(1-3):13-19.
12. Palhol F, Boyer S, Naulet N, Chabrilat M. Impurity profiling of seized MDMA tablets by capillary gas chromatography. *Anal Bioanal Chem*. 2002;374(2):274-281.
13. Stromberg L, Lundberg L, Neumann H, Bobon B, Huizer H, van der Stelt NW. Heroin impurity profiling. A Harmonization Study for Retrospective Comparisons. *Forensic Sci Int*. 2000;114(2):67-88.
14. Perkal M, Ng YL, Pearson JR. Impurity profiling of methylamphetamine in Australia and the development of a national drugs database. *Forensic Sci Int*. 1994;69(1):77-87.
15. Power JD, Kavanagh P, McLaughlin G, et al. Forensic analysis of P2P derived amphetamine synthesis impurities: identification and characterization of indene by-products. *Drug Test Anal*. 2017;9(3):446-452.
16. Kunalan V, Nic Daéid N, Kerr WJ, Buchanan HAS, McPherson AR. Characterization of route specific impurities found in methamphetamine synthesized by the Leuckart and reductive amination methods. *Anal Chem*. 2009;81(17):7342-7348.
17. Doughty D, Painter B, Pigou P, Johnston MR. The synthesis and investigation of impurities found in clandestine laboratories: Baeyer-Villiger route part II; synthesis of Phenyl-2-propanone (P2P) analogues from substituted benzaldehydes. *Forensic Chem*. 2018;9:1-11.
18. Toske SG, Cooper SD, Morello DR, Hays PA, Casale JF, Casale E. Neutral heroin impurities from tetrahydrobenzylisoquinoline alkaloids. *J Forensic Sci*. 2006;51(2):308-320.
19. Stojanovska N, Fu S, Tahtouh M, Kelly T, Beavis A, Kirkbride KP. A review of impurity profiling and synthetic route of manufacture of methylamphetamine, 3,4-methylenedioxymethylamphetamine, amphetamine, dimethylamphetamine and p-methoxyamphetamine. *Forensic Sci Int*. 2013;224(1):8-26.
20. Aalberg L, Andersson K, Bertler C, et al. Development of a harmonized method for the profiling of amphetamines. I Synthesis of Standards and Compilation of Analytical Data. *Forensic Sci Int*. 2005;149(2-3):219-229.
21. Toske SG, McConnell JB, Brown JL, et al. Isolation and characterization of a newly identified impurity in methamphetamine synthesized via reductive amination of 1-phenyl-2-propanone (P2P) made from phenylacetic acid/lead (II) acetate. *Drug Test Anal*. 2015;9(3):453-461.
22. Aalberg L, Andersson K, Bertler C, et al. Development of a harmonised method for the profiling of amphetamines: II Stability of Impurities in Organic Solvents. *Forensic Sci Int*. 2005;149(2):231-241.
23. Dujourdy L, Dufey V, Besacier F, et al. Drug intelligence based on organic impurities in illicit MA samples. *Forensic Sci Int*. 2008;177(2-3):153-161.
24. UNODC. *Impurity profiling of heroin and cocaine*. Vienna: UNODC; 2005 Available at [https://www.unodc.org/pdf/publications/report\\_st-nar-35.pdf](https://www.unodc.org/pdf/publications/report_st-nar-35.pdf). Accessed 26. March 2019.
25. Collins M, Doddridge A, Salouros H. Cathinones: isotopic profiling as an aid to linking seizures. *Drug Test Anal*. 2016;8(9):903-909.
26. Münster-Müller S, Scheid N, Holdermann T, Schneiders S, Pütz M. Profiling of new psychoactive substances by using stable isotope ratio mass spectrometry: study of the synthetic cannabinoid 5F-PB-22. *Drug Test Anal*. 2018;in press;10(8):1323-1327.
27. Schäffer M, Gröger T, Pütz M, Zimmermann R. Assessment of the presence of damiana in herbal blends of forensic interest based on comprehensive two-dimensional gas chromatography. *Forensic Toxicol*. 2013;31(2):251-262.
28. UNODC. *Current NPS Threats*. Vienna: UNODC; 2019 Available at [https://www.unodc.org/pdf/opioids-crisis/Current\\_NPS\\_Threats\\_Volume\\_I.pdf](https://www.unodc.org/pdf/opioids-crisis/Current_NPS_Threats_Volume_I.pdf). Accessed 26. March 2019.
29. Auwärter V, Dresen S, Weinmann W, Müller M, Pütz M, Ferreirós N. 'Spice' and other herbal blends: harmless incense or cannabinoid designer drugs? *J Mass Spectrom*. 2009;44(5):832-837.
30. Langer N, Lindigkeit R, Schiebel H-M, Papke U, Ernst L, Beuerle T. Identification and quantification of synthetic cannabinoids in "spice-like" herbal mixtures: update of the German situation for the spring of 2016. *Forensic Sci Int*. 2016;269:31-41.
31. Münster-Müller S, Zimmermann R, Pütz M. A novel impurity-profiling workflow with the combination of flash-chromatography, UHPLC-MS, and multivariate data analysis for highly pure drugs: a study on the synthetic cannabinoid MDMB-CHMICA. *Anal Chem*. 2018;90(17):10559-10567.
32. EMCDDA. *Synthetic cannabinoids in Europe (Perspectives on drugs)*. Lisbon: EMCDDA; 2017 Available at [http://www.emcdda.europa.eu/system/files/publications/2753/POD\\_Synthetic%20cannabinoids\\_0.pdf](http://www.emcdda.europa.eu/system/files/publications/2753/POD_Synthetic%20cannabinoids_0.pdf). Accessed 26. March 2019.
33. EMCDDA. *Report on the risk assessment of MDMB-CHMICA in the framework of the Council Decision on new psychoactive substances*. Lisbon: EMCDDA; 2017 Available at [http://www.emcdda.europa.eu/system/files/publications/4093/TDAK16002ENN\\_PDFWEB.pdf](http://www.emcdda.europa.eu/system/files/publications/4093/TDAK16002ENN_PDFWEB.pdf). Accessed 26. March 2019.
34. Buchler P. Indazole derivatives. WO2009106980; 2009.
35. Huffman JW, Dai D, Martin BR, Compton DR. Design, synthesis and pharmacology of cannabimimetic indoles. *Bioorg Med Chem Lett*. 1994;4(4):563-566.
36. Makriyannis A, Hongfeng D. Cannabimimetic indole derivatives. US6900236 B1; 2005.
37. Bowden M, Williamson J. Cannabinoid Compounds. WO2014167530, 2014.
38. Weber C, Pusch S, Schollmeyer D, Münster-Müller S, Pütz M, Opatz T. Characterization of the synthetic cannabinoid MDMB-CHMCZCA. *Beilstein J Org Chem*. 2016;12:2808-2815.
39. Uchiyama N, Matsuda S, Kawamura M, Kikura-Hanajiri R, Goda Y. Two new-type cannabimimetic quinolinyl carboxylates, QUPIC and QUCHIC, two new cannabimimetic carboxamide derivatives, ADB-FUBINACA and ADBICA, and five synthetic cannabinoids detected with a thiophene derivative  $\alpha$ -PVT and an opioid receptor agonist AH-7921 identified in illegal products. *Forensic Toxicol*. 2013;31(2):223-240.
40. Imramovsky A, Jorda R, Pauk K, et al. Substituted 2-hydroxy-N-(arylalkyl)benzamides induce apoptosis in cancer cell lines. *Eur J Med Chem*. 2013;68:253-259.
41. Banister SD, Longworth M, Kevin R, et al. Pharmacology of valinate and tert-leucinate synthetic cannabinoids 5F-AMBICA, 5F-AMB, 5F-ADB, AMB-FUBINACA, MDMB-FUBINACA, MDMB-CHMICA, and their analogues. *ACS Chem Neurosci*. 2016;7(9):1241-1254.
42. Stare M, Laniewski K, Westermarck A, Sjögren M, Tian W. Investigation on the formation and hydrolysis of N,N-dimethylcarbamoyl chloride

- (DMCC) in vilsmeier reactions using GC/MS as the analytical detection method. *Org Process Res Dev.* 2009;13(5):857-862.
43. Andernach L, Pusch S, Weber C, et al. Absolute configuration of the synthetic cannabinoid MDMB-CHMICA with its chemical characteristics in illegal products. *Forensic Toxicol.* 2016;34(2):344-352.
  44. Gaines SM, Bada JL. Aspartame decomposition and epimerization in the diketopiperazine and dipeptide products as a function of pH and temperature. *J Org Chem.* 1988;53(12):2757-2764.
  45. Nitecki DE, Halpern B, Westley JW. Simple route to sterically pure diketopiperazines. *J Org Chem.* 1968;33(2):864-866.
  46. Davies JS, Mohammed AK. Assessment of racemisation in N-alkylated amino-acid derivatives during peptide coupling in a model dipeptide system. *J Chem Soc, Perkin Trans.* 1981;1(0):2982-2990.
  47. Risseuw MDP, Blanckaert P, Coopman V, Van Quekelberghe S, Van Calenbergh S, Cordonnier J. Identification of a new tert-leucinate class synthetic cannabinoid in powder and "spice-like" herbal incenses: methyl 2-[[1-(5-fluoropentyl)indole-3-carbonyl]amino]-3,3-dimethylbutanoate (5F-MDMB-PICA). *Forensic Sci Int.* 2017;273:45-52.
  48. Powers JC. Chloroindoles. *J Org Chem.* 1966;31(8):2627-2631.
  49. Tao R, Jiang Y, Zhu F, Yang S. A one-pot system for production of L-2-aminobutyric acid from L-threonine by L-threonine deaminase and a NADH-regeneration system based on L-leucine dehydrogenase and formate dehydrogenase. *Biotechnol Lett.* 2014;36(4):835-841.
  50. Menzel A, Werner H, Altenbuchner J, Gröger H. From enzymes to "designer bugs" in reductive amination: a new process for the synthesis of L-tert-leucine using a whole cell-catalyst. *Eng Life Sci.* 2004;4(6):573-576.
  51. Asada A, Doi T, Tagami T, Takeda A, Sawabe Y. Isomeric discrimination of synthetic cannabinoids by GC-El-MS: 1-adamantyl and 2-adamantyl isomers of N-adamantyl carboxamides. *Drug Test Anal.* 2017;9(3):378-388.
  52. Schwemer T, Rössler T, Ahrens B, et al. Characterization of a heroin manufacturing process based on acidic extracts by combining complementary information from two-dimensional gas chromatography and high resolution mass spectrometry. *Forensic Chem.* 2017;4:9-18.
  53. Dunetz JR, Magano J, Weisenburger GA. Large-scale applications of amide coupling reagents for the synthesis of pharmaceuticals. *Org Process Res Dev.* 2016;20(2):140-177.
  54. Nakagawa M, Watanabe H, Kodato S, et al. A valid model for the mechanism of oxidation of tryptophan to formylkynurenine—25 years later. *Proc Natl Acad Sci U S A.* 1977;74(11):4730-4733.
  55. Saito I, Matsuura T, Nakagawa M, Hino T. Peroxidic intermediates in photosensitized oxygenation of tryptophan derivatives. *Acc Chem Res.* 1977;10(9):346-352.
  56. Dreaden TM, Chen J, Rexroth S, Barry BA. N-formylkynurenine as a marker of high light stress in photosynthesis. *J Biol Chem.* 2011;286(25):22632-22641.

## SUPPORTING INFORMATION

Additional supporting information may be found online in the Supporting Information section at the end of the article.

**How to cite this article:** Münster-Müller S, Hansen S, Opatz T, Zimmermann R, Pütz M. Chemical profiling of the synthetic cannabinoid MDMB-CHMICA: Identification, assessment, and stability study of synthesis-related impurities in seized and synthesized samples. *Drug Test Anal.* 2019;11:1192-1206. <https://doi.org/10.1002/dta.2652>



## 6.3 Publication 3

*Profiling of synthesis-related impurities of the synthetic cannabinoid Cumyl-5F-PINACA in seized samples of e-liquids via multivariate analysis of UHPLC-MS<sup>n</sup> data*

Sascha Münster-Müller, Isabelle Matzenbach, Thomas Knepper,  
Ralf Zimmermann, Michael Pütz

Drug Testing and Analysis  
2019  
In press, DOI: 10.1002/dta.2673

Received: 7 March 2019 | Revised: 29 June 2019 | Accepted: 1 July 2019

DOI: 10.1002/dta.2673

## SHORT COMMUNICATION

WILEY

# Profiling of synthesis-related impurities of the synthetic cannabinoid Cumyl-5F-PINACA in seized samples of e-liquids via multivariate analysis of UHPLC-MS<sup>n</sup> data

Sascha Münster-Müller<sup>1,3†</sup> | Isabelle Matzenbach<sup>2†</sup> | Thomas Knepper<sup>2</sup> |  
Ralf Zimmermann<sup>3,4</sup> | Michael Pütz<sup>1</sup>

<sup>1</sup>Bundeskriminalamt (Federal Criminal Police Office), Forensic Science Institute, Wiesbaden, Germany

<sup>2</sup>Hochschule Fresenius, University of Applied Sciences, Idstein, Germany

<sup>3</sup>Joint Mass Spectrometry Centre, Institute of Chemistry, Chair of Analytical Chemistry, University of Rostock, Rostock, Germany

<sup>4</sup>Joint Mass Spectrometry Centre, Cooperation Group "Comprehensive Molecular Analytics", Helmholtz Zentrum München, Neuherberg, Germany

## Correspondence

Sascha Münster-Müller, Bundeskriminalamt (Federal Criminal Police Office), Forensic Science Institute, Appelallee 45, 65203, Wiesbaden, Germany  
Email: sascha.muenster-mueller@uni-rostock.de

## Funding information

Directorate-General for Justice, Grant/Award Number: JUST/2013/ISEC/DRUGS/AG/ISEC/400006421; Federal Criminal Institute; University Medical Clinic Freiburg; National Forensic Laboratory of Slovenia; EU's ISEC 2013 programme

## Abstract

Vaping of synthetic cannabinoids via e-cigarettes is growing in popularity. In the present study, we tentatively identified 12 by-products found in a pure sample of the synthetic cannabinoid Cumyl-5F-PINACA (1-(5-fluoropentyl)-N-(2-phenylpropan-2-yl)-1H-indazole-3-carboxamide), a prevalent new psychoactive substance (NPS) in e-liquids, via high-resolution mass spectrometry fragmentation experiments (HRMS/MS). Furthermore, we developed a procedure to reproducibly extract this synthetic cannabinoid and related by-products from an e-liquid matrix via chloroform and water. The extracts were submitted to flash chromatography (F-LC) to isolate the by-products from the main component. The chromatographic impurity signature was subsequently assessed by ultra-high-performance liquid chromatography coupled to mass spectrometry (UHPLC-MS) and evaluated by automated integration. The complete sample preparation sequence (F-LC + UHPLC-MS) was validated by comparing the semi-quantitative signal integrals of the chromatographic impurity signatures of five self-made e-liquids with varying concentrations of Cumyl-5F-PINACA [0.1, 0.2, 0.5, 0.7 and 1.0% (w/w)], giving an average relative standard deviation of 6.2% for triplicate measurements of preparations of the same concentration and 10.5% between the measurements of the five preparations with different concentrations. Lastly, the chromatographic signatures of 14 e-liquid samples containing Cumyl-5F-PINACA from police seizures and Internet test purchases were evaluated via hierarchical cluster analysis for potential links. For the e-liquid samples originating from test purchases, it was found that the date of purchase, the identity of the online shop, and the brand name are the critical factors for clustering of samples.

## KEYWORDS

cumyl-5F-PINACA, e-liquids, impurity profiling, LC-MS, synthetic cannabinoids

## 1 | INTRODUCTION

Drug profiling can be defined as the quantitative assessment of the physical and chemical properties of a drug sample subsequent to an

extraction procedure. It can be used to link seizures, identify trafficking and synthesis routes, or provide information on precursor materials and their origin.<sup>1</sup> The manufacturing route of a drug is considered to have a major influence on the chemical profile of

<sup>†</sup>Isabelle Matzenbach and Sascha Münster-Müller contributed equally.

samples, producing a distinct set of by-products or impurities depending on the used educts, coupling reagents, catalysts or overall reaction conditions.<sup>2-4</sup> Several methodologies of the analysis of organic impurities or by-products were developed for classic drugs like cocaine, heroin, and amphetamine.<sup>5,6</sup> They mostly consisted of a straightforward liquid-liquid extraction (LLE) or solid-phase extraction (SPE) procedure to remove the main active substance and to enrich related by-products, followed by analysis via gas chromatography (GC) or liquid chromatography (LC) coupled to different types of detectors.<sup>7-9</sup> The chromatographic signatures were then quantitatively evaluated via database-assisted chemometric models. In 2018, a new impurity profiling workflow aimed at highly pure drug substances, for example pure new psychoactive substances (NPS) or methamphetamine, was developed by Münster-Müller et al.<sup>10</sup> with preparative flash-chromatography (F-LC) as a central element. By selective fractionation of the chromatographic run, more than 99% of the main component could be removed from a sample while accumulating present by-products at the same time. This opened up new possibilities to profile even pure substances (> 98% purity) for which the common extraction and enrichment methods (LLE, SPE) fail. The new workflow was successfully tested on different pure synthetic cannabinoids, a class of designer drug within the NPS phenomenon. Synthetic cannabinoids are of great concern as they represent the largest group in terms of the overall number reported until the end of 2017 (251 synthetic cannabinoids among a total of 803 NPS of all classes).<sup>11</sup> The most popular form of consumption of these substances are so-called spice products,<sup>12</sup> in which the pure synthetic cannabinoids are applied to the surface of an inactive herbal matrix. The new workflow with F-LC was also successfully adapted to these spice products,<sup>10</sup> by including a straightforward preceding extraction step to isolate the synthetic compounds from the surface of the herbal matrix. It was proven that even though a synthetic cannabinoid was applied to and extracted from an herbal matrix, the original by-product profile could be maintained. A more thorough study of the impurity profile of the synthetic cannabinoid MDMB-CHMICA was recently published,<sup>13</sup> including batch discrimination of a larger collective of pure samples, the characterization of single impurities via nuclear magnetic resonance (NMR) and controlled synthesis using different coupling reagents and reaction conditions.

Our aim in the study presented here was to extend and validate the range of applications of the workflow to substances, in this case synthetic cannabinoids, dissolved in an e-liquid matrix. Different from the comprehensive study on MDMB-CHMICA, this work focuses on the more complex e-liquid matrices and the analytical challenges of reproducibly assessing the impurity profile of synthetic cannabinoids dissolved therein, in particular the prevalent compound Cumyl-5F-PINACA<sup>14</sup> (1-(5-fluoropentyl)-N-(2-phenylpropan-2-yl)-1H-indazole-3-carboxamide, **1**, Figure 1). Cumyl-5F-PINACA, also referred to as SGT-25,<sup>15</sup> belongs to the substance class of indazole carboxamides and is a liquid at room temperature, making it a prime candidate for mixing with a liquid matrix. With the increasing popularity of the e-cigarette, more and more NPS distributors are expanding their product portfolios by e-liquids containing dissolved

synthetic cannabinoids for several reasons. The products can be consumed in public places without raising suspicions by ominous odors and, although controversial discussion is still ongoing, vaping e-liquids is considered healthier in comparison to smoking products with an herbal matrix.<sup>16-18</sup> E-liquids generally consist of a polar mixture of propylene glycol (PG), vegetable glycerin (VG), and ethanol; aroma compounds; and an active substance (eg, nicotine or an NPS). Some reports are available concerning the analysis of e-liquids containing different types of classic cannabinoids and synthetic cannabinoids.<sup>19-22</sup> In comparison to the preparation of herbal formulations of synthetic cannabinoids such as spice products, the isolation of the active component and related impurities from the polar matrix of e-liquids is more challenging. The samples could not be dissolved in eluent and directly injected into the F-LC for separation, as the polar matrix disrupts the chromatography. A more onerous sample preparation had to be developed in order to be able to perform the previously developed impurity profiling workflow.<sup>10</sup>

As first step, it was necessary to assess and characterize key impurities and their overall abundance in a pure sample of **1** via HRMS and fragmentations experiments (MS<sup>n</sup>) to provide a basis on which the sample preparation procedure and seized samples could be evaluated on. As only less than 100 mg of pure **1** was available for method development and all performed analytical studies, it was not possible to additionally isolate selected impurities in a larger quantity for unequivocal structural identification via NMR. However, the HRMS data, including systematic fragmentations experiments, were sufficient to identify characteristic structural elements already identified in impurities of MDMB-CHMICA with an acceptable grade of certainty. Indole- and indazole-based synthetic cannabinoids are expected to be synthesized by a modular design, following similar synthesis instructions. Thus, by comparing the tentatively identified impurities of **1** to the NMR-characterized impurities of MDMB-CHMICA, parallels between applied synthesis pathways might be found. As distinct from the procedure applied to spice products (herbal blends), an additional preceding rapid LLE procedure using a mixture of chloroform and water was developed and validated to remove the majority of the polar e-liquid matrix compounds to minimize impairment of the subsequent isolation of synthesis-related impurities by F-LC. To demonstrate the suitability of the profiling procedure, a small set of e-liquid samples from police seizures and Internet test purchases containing **1** were evaluated for potential links using the complete workflow.

## 2 | MATERIALS AND METHODS

The complete profiling workflow via F-LC, UHPLC-MS and the subsequent data processing method was already reported in our previous publication<sup>10</sup> and will not be stated again in full. The main aim of the work presented here was to adapt the previously published profiling workflow<sup>10</sup> to the e-liquid matrix which has not yet been tested so far.

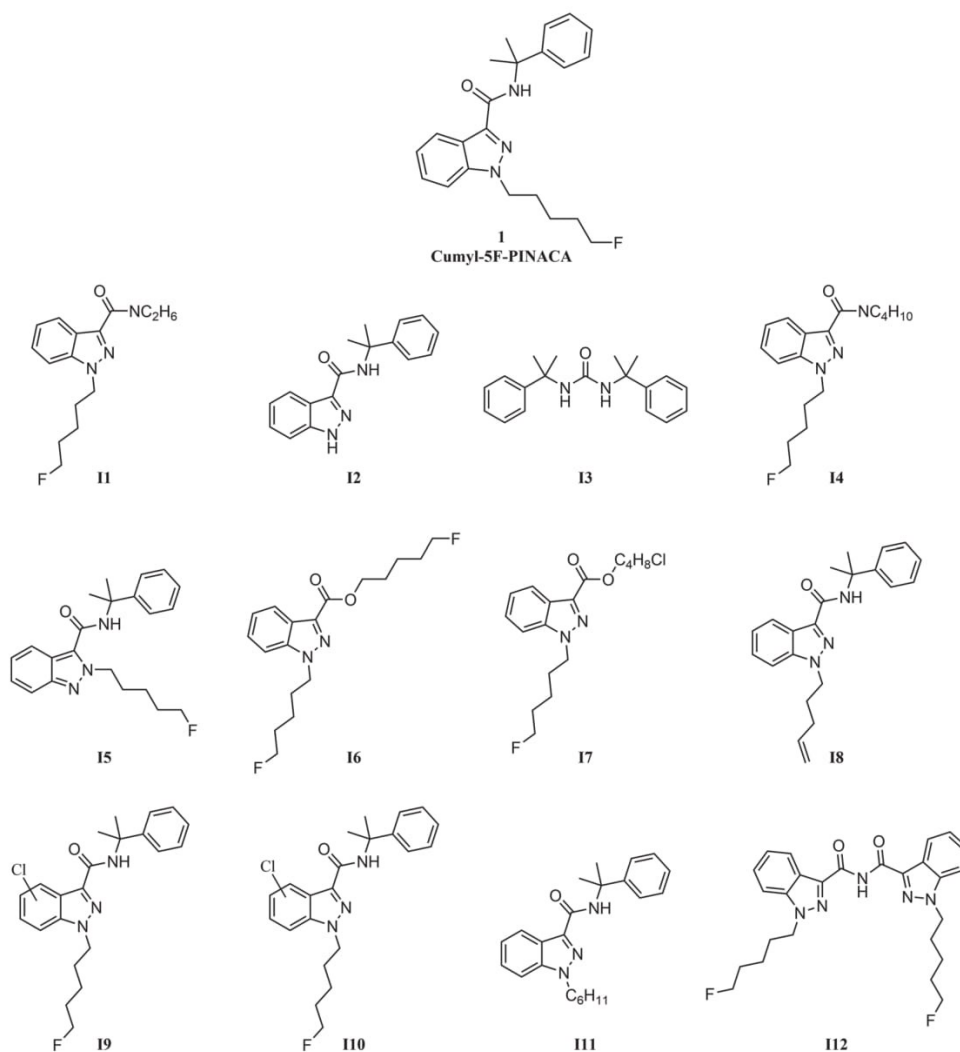


**FIGURE 1** Structural formula of Cumyl-5F-PINACA<sup>1</sup> and 12 related synthesis impurities. Tentative structural characterization of the impurities was carried out via HRMS<sup>3</sup> experiments.

## 2.1 | Chemicals and reagents

Ethanol, chloroform, and acetonitrile were purchased from Merck (Darmstadt, Germany), acetone was obtained by VWR Chemicals (Darmstadt, Germany), n-hexane and ammonium formate were bought from Sigma Aldrich (Steinheim, Germany), ethyl acetate and formic acid were purchased from Fluka (Steinheim, Germany), and propylene glycol and glycerine were obtained from ReiTrade (Vaihingen, Germany). Deionized water was prepared using a Milli-Q Synthesis A10 apparatus (Millipore, Schwalbach, Germany).

## 2.2 | E-liquid samples

One pure sample of 1 (LJP) and four e-liquids (LJ01-LJ04) containing 1 as main active ingredient were available from a clandestine laboratory seized in Ljubljana, Slovenia in August 2015. Furthermore, ten e-liquids from Internet test purchases (FR01-FR10) containing 1

were available from the University Medical Center in Freiburg/Germany.

To validate the extraction procedure and the overall sample preparation reproducibility, self-made e-liquids consisting of PG, VG, and ethanol (40:40:20) (v/v) and containing 0.1, 0.2, 0.5, 0.7 and 1.0% (w/w) of pure 1 (Ljubljana seizure), respectively, were employed.

## 2.3 | Micro extraction

Before the cannabinoid compounds in the e-liquid samples could be separated into by-products and a main component by means of F-LC, it was first necessary to perform a liquid-liquid micro extraction in order to remove the polar matrix components PG and VG as they disturb the normal phase chromatography. For that purpose, 200 µL of e-liquid, 4 mL of chloroform and 5 mL of deionized water were pipetted into a 15 mL glass vial and vortexed for 20 seconds. The



chloroform phase was transferred to a 4 mL glass vial and dried under a steady stream of nitrogen. The resin-like residue was then dissolved in 1.5 mL ethyl acetate/hexane (1:2, v:v) for injection into the F-LC.

## 2.4 | Instruments

Separation of impurities from the main component was achieved with a Sepacore F-LC system X50 from Büchi Labortechnik (Flawil, Switzerland) consisting of two pump modules (max. 50 bar pressure), a UV-VIS spectrometer (set to 284 nm), an automated fraction collector and a control unit. A prepacked 4 g silica gel HP column from Büchi (particle size 15–40  $\mu\text{m}$ ) was used and run with a gradient system of *n*-hexane and ethyl acetate. The complete 1.5 mL of dissolved sample after the micro extraction were loaded for each run. Separation was achieved with a flow rate of 20 mL/min starting with 40 seconds of 0% eluent B, followed by an increase to 15% B over 65 seconds, holding these 15% B for 25 seconds, followed by an increase to 30% B over 20 seconds. After holding for 50 seconds, eluent B was further increased to 100% over 20s and held there for another 160 seconds, giving an overall runtime of 380 seconds. **1** was collected from second 225 to 255, evaporated to dryness and weighed. The remaining fractions were combined, evaporated to dryness and again dissolved in 1 mL acetonitrile.

The combined impurity fractions were diluted according to the corresponding weight of the isolated main component as normalization step and measured on an UltiMate 3000 UHPLC system (Thermo Scientific, Waltham, MA, USA) coupled to an amaZon speed ion trap mass spectrometer (Bruker, Billerica, MA, USA) with electrospray ionization (ESI) source. The used eluents contained 98.9% water, 1.0% acetonitrile and 0.1% formic acid (eluent A) and 1.0% water, 98.9% acetonitrile and 0.1% formic acid (eluent B), respectively. The total run time was 12 minutes at a flow rate of 0.5 mL/min and the injection volume was 5  $\mu\text{L}$ . The ESI was run in positive mode with a voltage of 4.5 kV, the mass range was set to  $m/z$  70–600 with a scan speed of 32500  $m/z/s$  in Ultra-Scan mode. The dry gas flow rate was set to 10 L/min at a temperature of 320°C. Fragmentation mode was Auto MS<sup>3</sup> using collision induced dissociation.

High-resolution data were obtained by an Accela HPLC system and an LTQ Orbitrap-MS (Thermo Scientific, Bremen, Germany). The eluents contained 94.9% water, 5.0% acetonitrile and 0.1% formic acid (eluent A) and 5.0% water, 94.9% acetonitrile and 0.1% formic acid (eluent B), respectively. The injection volume was 1  $\mu\text{L}$ . The ESI was operated in positive mode with 3.75 kV and the mass range of the MS was set to 130–2000  $m/z$  with a data dependent scan threshold for MS<sup>2</sup> of 10<sup>6</sup> counts.

## 2.5 | Data processing

The LC-MS data were processed via a rectangular bucketing algorithm (ProfileAnalysis, Bruker, Billerica, MA, USA), integrating the signals of all  $m/z$  values from 150 to 500 individually in intervals of 0.5 minutes from minute 2 to 9.5 of chromatographic runtime, forming so called

buckets. Those buckets containing the required information about the assessed key-impurities were picked out and used for further interpretation. A more thorough description of the bucketing process can be taken from our previous work.<sup>10</sup>

Hierarchical cluster analysis (HCA) via Ward's method was computed with the software Unscrambler X (Camo, Oslo, Norway).

## 3 | RESULTS AND DISCUSSION

### 3.1 | Assessment and characterization of by-products found in a pure sample of Cumyl-5F-PINACA

UHPLC-MS measurements of the pure cannabinoid majorly showed an intense signal for **1** with only few detectable by-product signals in the base line region of the chromatogram, insufficient for a reliable semi-quantitative profiling setup (Figure 2A). Thus, the pure sample of **1** was submitted to F-LC and the combined impurity fractions of the chromatographic run were analyzed again via UHPLC-MS, this time injected with a smaller dilution factor, as most of the main component was depleted from the sample. Figure 2B shows the corresponding base peak chromatogram (BPC) of the combined impurity fractions

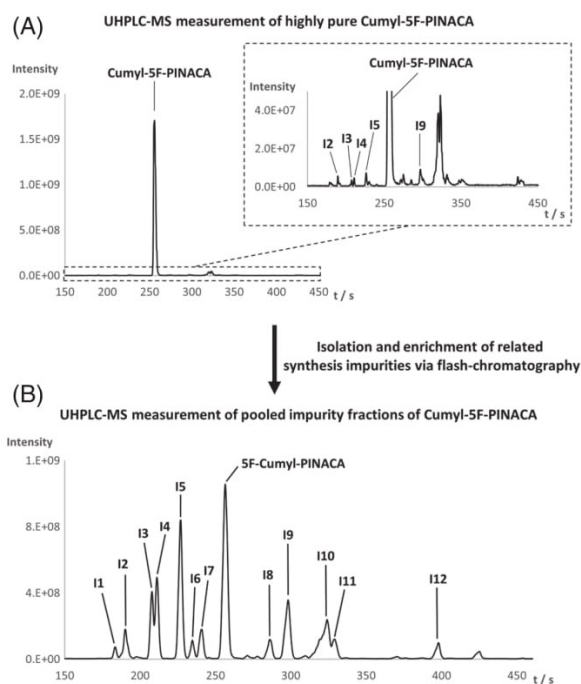


**FIGURE 2** Excerpts of two UHPLC-MS BPCs of a seized sample of Cumyl-5F-PINACA. A, Without prior sample treatment. For related synthesis impurities, few signals can be observed in the low intensity range with small signal to noise ratios. B, The same sample after isolation and enrichment of synthesis impurities via F-LC. Being able to inject the sample with a lower dilution factor, previously absent and superimposed signals of impurities are now more intense. Related impurity peaks are numbered from I1- I12.

after F-LC with the most abundant by-products of **1** highlighted from **I1** to **I12**. As stated before, the sample amount of pure **1** available for this was not sufficient for extensive isolation of single impurities for structural elucidation via NMR. Tentative structure elucidation of by-products was done on the basis of HRMS<sup>3</sup>-fragmentation experiments to verify the chemical relationship of detected chromatographic signals to the main component. The interpretation of corresponding product-ion spectra was based on the fragmentation pattern of **1**, since a certain structural similarity of by-products to the main product was expected. Neutral losses or product-ions with known exact masses were assigned to partial structural elements of **1** (in most cases the 5F-pentyl chain and the cumene residue).

With the described set of impurities, only hypothetical considerations regarding the synthesis pathway and reaction conditions can be made. Even though synthesis procedures for a variety of synthetic cannabinoid compounds like **1** can be found in the original patent from Bowden et al.,<sup>15</sup> the actual manufacturers have probably implemented their own synthesis procedures with higher economic efficiency or better suitability for upscaling. The patented synthesis conditions are summarized in the Supporting Information in Figure S14.<sup>15</sup> However, the synthesis procedures for synthetic cannabinoids with indole and indazole core structures are considered to be based on a modular design, only exchanging the building blocks for the side-chain and the linked residue. Similarities between characteristic structural elements of impurities for different synthetic cannabinoids might result from related synthesis procedures. Recently, we published an extensive study on impurity profiling for the synthetic cannabinoid MDMB-CHMICA including NMR and HRMS characterization of 15 impurities, including detailed discussion about their origin, based on series of controlled syntheses under varying conditions. In the work presented here, we used this scientific basis for the interpretation of accordances between characteristic structural elements found in impurities of **1** and those identified in MDMB-CHMICA, with respect to conclusions about the synthesis pathway.

The corresponding analytical data and the proposed structures are summarized in Figure 1, a corresponding table including analytical data and related HRMS spectra including fragmentation experiments up to MS<sup>3</sup> can be found in the Supporting Information. As only one sample of pure **1** was available, these by-products were selected as target impurities for the comparison of e-liquid samples without further knowledge, if they exhibit significant discriminating potential within a bigger set of pure samples.

The available literature suggests that both the formation of the amide bond or the *N*-alkylation can be performed as a last reaction step in the synthesis of synthetic cannabinoids,<sup>23</sup> in the case of **1** the coupling of *N*-alkyl-3-indazole-carboxylic acid and cumylamine or the coupling of 1-bromo-5-fluoropentane (or the like) to *N*-(2-phenylpropan-2-yl)-1*H*-indazole-3-carboxamide.<sup>15</sup> However, we consider the amide bond formation as the last step, evidenced by the majority of impurities having the alkyl chain already attached to the indazole core (except for **I2** and **I3**) and the presence of **I6** in particular. With an additional 5-fluoropentyl chain coupled via an ester, it is likely that free 1*H*-indazole-3-carboxylic acid was present

during the *N*-alkylation with 1-bromo-5-fluoropentane (or the like). The formation of **I7** with an ester bound C<sub>6</sub>H<sub>6</sub>Cl residue cannot be explained, as both, the attached chlorine and the reduced chain length of four carbon atoms, do not fit any allegedly used educt. **I8** is expected to be the product of **1** after HF elimination, with either a double bond within the alkyl chain or formation of a ring. **I11** consist of a C<sub>6</sub>H<sub>11</sub> aliphatic residue (as a ring or with a double bond) attached to the indazole core, possibly formed by *N*-alkylation with impure 1-bromo-5-fluoropentane (or the like). **I5** showed the same exact mass but a slightly different fragmentation pattern and retention time compared to **1**. We expect this impurity to be a result of an annular tautomerization of the indazole core<sup>24</sup> with the 5F-pentyl chain attached to the 2-*H* position or the initial coupling of the 5-fluoropentyl to the 2-position of the 2*H*-indazole tautomer. In any case it is likely that for other indazole based synthetic cannabinoids also impurities in form of 2-alkyl-2*H*-indazole analogues can be observed. **I12** is expected to be a coupling product of two 1-(5-fluoropentyl)-1*H*-indazole structures via an amide linker and **I3** appears to be a urea derivative with two *N*-linked cumyl residues, both possibly formed in the active reaction mixture.

For the remaining impurities **I1**, **I2**, **I4**, **I9**, and **I10** several accordances in relation to the impurities of MDMB-CHMICA could be found,<sup>13</sup> for example **I1** and **I4** with C<sub>2</sub>H<sub>6</sub> and C<sub>4</sub>H<sub>10</sub> aliphatic residues on the carboxamide linker group, identified as dimethyl and diethyl amides in the case of MDMB-CHMICA. Both of these impurities were also found in the controlled synthesis batches of MDMB-CHMICA using different types of coupling reagents and triethyl amine as base for amide bond formation. Possibly, they result from a side reaction of the activated carboxylic acid with primary or secondary amine contaminations of triethylamine. **I2** most probably is a carry-over product from a preceding reaction step with a failed *N*-alkylation of the pentyl chain in 1-*H* position of the indazole core. A structurally similar impurity was identified in seized samples of MDMB-CHMICA, a MDMB-ICA without the cyclohexyl methyl attached to the indole core. Lastly, two chlorinated derivatives of **1** were found with the chlorine attached to different positions of the indazole core. Without NMR confirmation, the exact position cannot be assessed. In the case of MDMB-CHMICA, a 2-Cl derivative was identified to be the most abundant impurity for the majority of seized samples. As source for the chlorine, an amide coupling reaction via acyl halide formation is proposed, using common reactants like oxalyl chloride or thionyl chloride for activation of the carboxylic acid instead of [dimethylamino (triazolo[4,5-*b*]pyridine-3-yl)oxy)methylidene]-dimethylazanium hexafluorophosphate (HATU) or *N,N'*-dicyclohexylcarbodiimide (DCC). Alternatively, but less probable, already chlorinated indazole derivatives could have been used from the beginning of the synthesis.

Regarding the batches of MDMB-CHMICA produced in the controlled synthesis series, it is apparent that the highest accordance in impurity composition compared to **1** can be observed for the coupling step via thionyl chloride and oxalyl chloride, the use of which was also strongly indicated by the high concentration of the 2Cl-MDMB-CHMICA impurity. Thus, it was expected that the activation of the carboxylic acid via acyl halide is the most probable



synthesis procedure for MDMB-CHMICA. For **1** several impurity analogues to MDMB-CHMICA were found like **I1**, **I4** and especially **I9** and **I10**, suggesting again the pathway via acyl halide for amide bond coupling. However, based on our experimental data it is not possible to explain the presence of several other impurities of **1** without further knowledge of the reaction behavior of the indazole core or the cumyl amine. A series of controlled syntheses would have to be carried out for a better understanding of the formation of the described reaction by-products, which, however, was not the scope of this work.

### 3.2 | Validation of the sample preparation process of micro extraction, F-LC, and UHPLC-MS

Before any real-life samples can be submitted to the profiling with the here presented combination of an extraction, F-LC and UHPLC-MS, the complete sample preparation procedure needs to be validated to ascertain that it does not have any impact on the by-product profile of **1**. We prepared e-liquids with varying concentrations of **1** [0.1, 0.2, 0.5, 0.7 and 1.0% of **1** in e-liquid matrix (w/w)] where the by-product composition is known from previous experiments with no e-liquid matrix. By comparing the by-product profile of pure **1** to the profiles obtained after the sample preparation procedure, any loss of signals or additional signals can easily be determined. The previously assessed impurity composition (relation of impurity peaks to each other) serves as an internal standard to investigate potential changes in the profile throughout the extraction and enrichment process.

All self-made e-liquid samples were worked up via the micro-extraction procedure, giving an average extraction yield of 72% for **1**. We found that in the organic phase (chloroform) a small, but constant portion of matrix is still present, which however had no measurable impact on the further workup with F-LC.

Each of the differently concentrated e-liquid samples were extracted and submitted to F-LC in triplicate. The corresponding by-product fractions were measured via UHPLC-MS and the signals of all previously assessed key-impurities were integrated. The overall profile of the pure sample of **1** was very similar to the profiles of the e-liquid extracts, although several additional matrix signals could be observed in the latter, which, however, were easily discriminable and non-interfering. For the triplicates, an average relative standard deviation (RSD) of all key-impurity signals was found to be 6.2%. Comparing the five differently concentrated e-liquids, an overall RSD of 10.5% was calculated. These low values and the recovery of all expected impurities in the e-liquid samples indicate, that the sample preparation process has no major influence on the by-product composition and concentration.

Of course, in this validation study we only used PG and VE as matrix components. It is, however, commonly observed that commercially available e-liquids contain a range of flavors which might appear as additional signals in the measurements of the isolated impurity fractions. That is why we chose to select only the previously

assessed key impurities as target analytes to be assessed when comparing seized and on-line purchased e-liquids containing **1**. All other observed chromatographic peaks are excluded from the profiling procedure and will, therefore, have no impact on the actual impurity-profiling of the main component.

### 3.3 | Application of profiling workflow to seized and bought e-liquid samples containing Cumyl-5F-PINACA

The previously selected target-impurities were used to compare seized samples of e-liquids containing **1**. Ideally, the chromatographic profiles of samples with **1** from the same production batch should show identical by-product patterns. Contrarily, samples from different batches are supposed to show variations in their by-product profile, caused by the choice of synthesis route, precursor chemicals and purification steps. In this small case study, we included the pure sample and four e-liquids available from a seized clandestine laboratory in Ljubljana, Slovenia. The aim was to investigate, if at least one of these e-liquids was produced with the available seized pure material, proven by the by-product signatures. Furthermore, ten e-liquid samples from Internet test purchases were available from the University Medical Center in Freiburg. The samples were bought from different vendors and at different points of time.

All 15 samples were processed according to the described sample preparation procedure and the pooled impurity fraction for each sample was measured via UHPLC-MS. The LC-MS data were automatically integrated and the intensity values of the targeted by-products (**I1** to **I15**) subsequently analyzed via HCA. A matrix of the available samples of **1** and the corresponding key-impurities was generated for better visualization of the data (table in Figure 3). A greyscale, individual for each impurity, indicates the relative intensities (white: complete absence of signal, black: the highest signal value). The last line of the table describes the average intensity ratios between the impurities, normalized to the least abundant. An HCA using Ward's

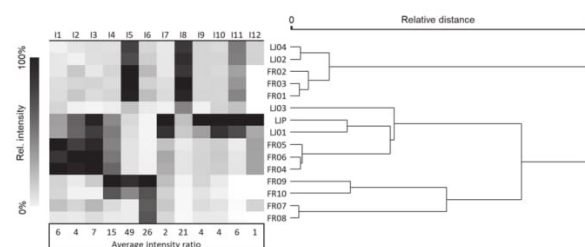


**FIGURE 3** Table shows the relative intensities for the assessed key impurities **I1** to **I12** in seized and online test purchased e-liquid samples of Cumyl-5F-PINACA (labeled FR and LJ). For each impurity, the relative intensities are shown in individual greyscales (white: complete absence of signal for this impurity, black: highest signal value for this impurity). The last line of the table states the average intensity ratio for each impurity normalized for **I1** to **I12**. Grouping of samples based on the overall semiquantitative impurity signatures was done via HCA. The resulting dendrogram is attached next to the table for a better visual interpretation of the data.

**TABLE 1** List of seized (labeled LJ) and online test purchased (labeled FR) e-liquids samples containing Cumyl-5F-PINACA used for this study to group samples according to their chromatographic impurity signatures, including the date of purchase/seizure, source, brand and flavor type of each e-liquid (if available)

Sample	Date	Source	Brand	Flavor
LJP LJ01-LJ04	Aug 2015	Seizure	n.a.	n.a.
FR01				Bubblegum
FR02	Sep 2014	Online-shop 1	Brand 1	Blueberry
FR03				Vanilla
FR04				Bubblegum
FR05	Apr 2015	Online-shop 1	Brand 1	Blueberry
FR06				Vanilla
FR07	Jul 2015	Online-shop 2	Brand 2	Blueberry
FR08	Oct 2015			Bubblegum
FR09	Oct 2015	Online-shop 3	Brand 3	Blueberry
FR10	Mar 2016	Online-shop 1	Brand 1	Blackberry menthol

method (dendrogram in Figure 3) was carried out to group the 15 e-liquid samples according to their relative distance in impurity signatures. Additional information about the samples can be taken from Table 1.

Surprisingly, the pure sample of the seized laboratory in Ljubljana (LJP) showed no accordance to any of the four e-liquid samples from the same seizure with respect to the by-product signature. Especially the high relative abundance of **I9** to **I12** separated LJP from the remaining sample pool. Only LJ01 tends to be similar to LJP, but not to such an extent that a strong link between the two samples can be established. LJ03 was majorly different from the remaining sample set. LJ02 and LJ04 seem to be produced with aliquots of a single batch material of **1**, as they show very similar by-product patterns. Since these e-liquids had no label on them, it was impossible to evaluate the given data with any more background information like brand name. Three samples from an online test-purchase from Freiburg (FR01-FR03, bought in September 2014, same brand, same online shop, different flavors) clustered and were found to be relatively similar to LJ02 and LJ04, although the seizure and test purchase were approximately one year apart and no other connection between the samples can be drawn. All five samples showed an increased relative abundance of **I5** and **I8** and a low relative abundance for all other impurities. To exclude a false positive cluster assignment in this HCA model, the relative distance between the first two clusters seemed to be sufficient to discriminate between samples consisting different batches of **1**.

Two other cluster formations could be observed for FR07-FR08 (bought in July and October 2015, same brand, same online shop, different flavors) and FR04-FR06 (bought in April 2015, same brand, same online shop, different flavors). The latter three samples were a repetition purchase of FR01-FR03, but bought approximately half a year later. They showed majorly different relative abundances of **I1**

to **I4**, although all samples had the same brand and originated from the same online shop.

The given data suggest that the flavor is insignificant and the date of purchase, the identity of the online shop, and the brand are critical factors for cluster formation. Based on this small case study, the modus operandi of the manufacturers can be hypothetically described as follows: One large batch of e-liquid matrix is prepared and pure material of **1** is dissolved. This large batch is then split into smaller aliquots and mixed with various flavors. These aliquots are filled into small bottles with equal brand names but different flavor types and sold. This process is repeated whenever an e-liquid runs out of stock as observed for the repetitive purchase of FR01-FR03 and FR4-FR06, most certainly produced with different batches of **1**.

## 4 | CONCLUSION

In this study, we developed and successfully applied a profiling procedure based on the isolation of related by-products from a pure sample of the synthetic cannabinoid Cumyl-5F-PINACA via F-LC. To 12 of these by-products, a tentative structure could be assigned to by MS/MS experiments. By implementing a straightforward LLE procedure via chloroform and water in combination with F-LC and UHPLC-MS, the profiles of the targeted by-products of Cumyl-5F-PINACA could be also reproducibly assessed in an e-liquid matrix. This enabled the comparative analysis of a set of seized and purchased e-liquid samples containing Cumyl-5F-PINACA for potential links. It was found that the date of purchase, the identity of the online shop, and the brand name were the critical factors for differences in the by-product profiles of samples. Decomposition and pyrolysis products formed of active substances in e-liquids when consumed in e-cigarettes and other vaping devices are highly relevant and a topic for future research activities.

## ACKNOWLEDGEMENTS

All presented data, if not cited otherwise, were generated within the project SPICE-profiling, funded within the EU's ISEC 2013 programme (Directorate-General for Justice JUST/2013/ISEC/DRUGS/AG/ISEC/4000006421). Our thanks are due to Dr Sonja Klemenc from the National Forensic Laboratory of Slovenia for providing the samples seized in Ljubljana and to Verena Angerer and Volker Auwärter from the University Medical Clinic Freiburg for providing us with the e-liquids from Internet test purchases. Additionally, we want to thank Dieter Kirsch from the Federal Criminal Institute for carrying out the HRMS measurements.

## ORCID

Sascha Münster-Müller  <https://orcid.org/0000-0003-3949-2818>

Ralf Zimmermann  <https://orcid.org/0000-0002-6280-3218>

## REFERENCES

1. UNODC. *Drug characterization/Impurity profiling*. Vienna: UNODC; 2001 Available from: <https://www.unodc.org/pdf/publications/st-nar-32-rev1.pdf>. Accessed 26. March 2019.



2. Doughty D, Painter B, Pigou P, Johnston MR. The synthesis and investigation of impurities found in clandestine laboratories: Baeyer-Villiger route part II; synthesis of phenyl-2-propanone (P2P) analogues from substituted benzaldehydes. *Forensic Chem.* 2018;9:1-11.
3. Hauser F, Rößler T, Hulshof J, Weigel D, Zimmermann R, Pütz M. Identification of specific markers for amphetamine synthesised from the pre-precursor APAAN following the Leuckart route and retrospective search for APAAN markers in profiling databases from Germany and the Netherlands. *Drug Test Anal.* 2018;10(4):671-680.
4. Kunalan V, Nic Daéid N, Kerr WJ, Buchanan HAS, McPherson AR. Characterization of route specific impurities found in methamphetamine synthesized by the Leuckart route and reductive amination methods. *Anal Chem.* 2009;81(17):7342-7348.
5. Ballany J, Caddy B, Cole M, et al. Development of a harmonised pan-European method for the profiling of amphetamines. *Sci Justice.* 2001;41(3):193-196.
6. UNODC. *Impurity profiling of heroin and cocaine.* Vienna: UNODC; 2005 Available from: [https://www.unodc.org/pdf/publications/report\\_st-nar-35.pdf](https://www.unodc.org/pdf/publications/report_st-nar-35.pdf). Accessed 26. March 2019.
7. Chiarotti M, Marsili R, Moreda-Pineiro A. Gas chromatographic-mass spectrometric analysis of residual solvent trapped into illicit cocaine exhibits using head-space solid-phase microextraction. *J Chromatogr B Analyt Technol Biomed Life Sci.* 2002;772(2):249-256.
8. Zacca JJ, Grobério TS, Maldaner AO, Vieira ML, Braga JWB. Correlation of cocaine hydrochloride samples seized in Brazil based on determination of residual solvents: an innovative chemometric method for determination of linkage thresholds. *Anal Chem.* 2013;85(4):2457-2464.
9. Zhang JX, Zhang DM, Han XG. Identification of impurities and statistical classification of methamphetamine hydrochloride drugs seized in the China. *Forensic Sci Int.* 2008;182(1-3):13-19.
10. Münster-Müller S, Zimmermann R, Pütz M. A novel impurity-profiling workflow with the combination of flash-chromatography, UHPLC-MS, and multivariate data analysis for highly pure drugs: a study on the synthetic cannabinoid MDMB-CHMICA. *Anal Chem.* 2018;90(17):10559-10567.
11. UNODC. *UNODC World drug report 2018.* Vienna: UNODC; 2018 Available from: [https://www.unodc.org/wdr2018/prelaunch/WDR18\\_Booklet\\_3\\_DRUG\\_MARKETS.pdf](https://www.unodc.org/wdr2018/prelaunch/WDR18_Booklet_3_DRUG_MARKETS.pdf). Accessed March 2019.
12. Auwärter V, Dresen S, Weinmann W, Müller M, Pütz M, Ferreirós N. 'Spice' and other herbal blends: harmless incense or cannabinoid designer drugs? *J Mass Spectrom.* 2009;44(5):832-837.
13. Münster-Müller S, Hansen S, Opatz T, Zimmermann R, Pütz M. Chemical profiling of the synthetic cannabinoid MDMB-CHMICA: identification, assessment, and stability study of synthesis-related impurities in seized and synthesized samples. *Drug Test Anal.* 2019;1-15. in press. <https://doi.org/10.1002/dta.2652>
14. Angerer V, Franz F, Moosmann B, Bisel P, Auwärter V. 5F-Cumyl-PINACA in 'e-liquids' for electronic cigarettes: comprehensive characterization of a new type of synthetic cannabinoid in a trendy product including investigations on the in vitro and in vivo phase I metabolism of 5F-Cumyl-PINACA and its non-fluorinated analog Cumyl-PINACA. *Forensic Toxicol.* 2019;37(1):186-196.
15. Bowden M, Williamson J. Cannabinoid compounds. WO2014167530, 2014.
16. Goniewicz ML, Knysak J, Gawron M, et al. Levels of selected carcinogens and toxicants in vapour from electronic cigarettes. *Tob Control.* 2014;23(2):133-139.
17. Rowell TR, Tarran R. Will chronic e-cigarette use cause lung disease? *Am J Physiol Lung Cell Mol Physiol.* 2015;309(12):L1398-L1409.
18. Schripp T, Markewitz D, Uhde E, Salthammer T. Does e-cigarette consumption cause passive vaping? *Indoor Air.* 2013;23(1):25-31.
19. Giroud C, de Cesare M, Berthet A, Varlet V, Concha-Lozano N, Favrat B. E-cigarettes: a review of new trends in cannabis use. *Int J Environ Res Public Health.* 2015;12(8):9988-10008.
20. Peace MR, Butler KE, Wolf CE, Poklis JL, Poklis A. Evaluation of two commercially available cannabidiol formulations for use in electronic cigarettes. *Front Pharmacol.* 2016;7:279.
21. Peace MR, Krakowiak RI, Wolf CE, Poklis A, Poklis JL. Identification of MDMB-FUBINACA in commercially available e-liquid formulations sold for use in electronic cigarettes. *Forensic Sci Int.* 2017;271:92-97.
22. Varlet V, Concha-Lozano N, Berthet A, et al. Drug vaping applied to cannabis: is "Cannavaping" a therapeutic alternative to marijuana? *Sci Rep.* 2016;6(1):25599.
23. Buchler P. Indazole derivatives. WO2009106980, 2009.
24. Catalan J, del Valle JC, Claramunt RM, et al. Acidity and basicity of indazole and its N-methyl derivatives in the ground and in the excited state. *J Phys Chem.* 1994;98(41):10606-10612.

## SUPPORTING INFORMATION

Additional supporting information may be found online in the Supporting Information section at the end of the article.

**How to cite this article:** Münster-Müller S, Matzenbach I, Knepper T, Zimmermann R, Pütz M. Profiling of synthesis-related impurities of the synthetic cannabinoid Cumyl-5F-PINACA in seized samples of e-liquids via multivariate analysis of UHPLC-MS<sup>n</sup> data. *Drug Test Anal.* 2019;1-8. <https://doi.org/10.1002/dta.2673>

## 6.4 Publication 4

*Profiling of new psychoactive substances (NPS) by using stable isotope ratio mass spectrometry (IRMS): study on the synthetic cannabinoid 5F-PB-22*

Sascha Münster-Müller, Nicole Scheid, Thomas Holdermann,  
Sabine Schneiders, Michael Pütz

Drug Testing and Analysis  
2018,  
10(8): 1323-1327

Received: 15 January 2018 | Revised: 8 May 2018 | Accepted: 9 May 2018

DOI: 10.1002/dta.2407

## SHORT COMMUNICATION

WILEY

# Profiling of new psychoactive substances by using stable isotope ratio mass spectrometry: Study of the synthetic cannabinoid 5F-PB-22

S. Münster-Müller  | N. Scheid | T. Holdermann | S. Schneiders | M. Pütz

Bundeskriminalamt (Federal Criminal Police Office), Forensic Science Institute, Wiesbaden, Germany

**Correspondence**

Sascha Münster-Müller, Bundeskriminalamt (Federal Criminal Police Office), Forensic Science Institute, Äppelallee 45, 65203 Wiesbaden, Germany.  
Email: sascha.muenster-mueller@uni-rostock.de

**Funding information**

Directorate-General for Justice, Grant/Award Number: JUST/2013/ISEC/DRUGS/AG/ISEC/4000006421

**Abstract**

In this paper, the results of a pilot study on the profiling of the synthetic cannabinoid receptor agonist 5F-PB-22 (5F-QUPIC, pentylfluoro-1*H*-indole-3-carboxylic acid-8-quinolinyl ester) via isotope ratio mass spectrometry are presented. It focuses on  $\delta^{13}\text{C}$ ,  $\delta^{15}\text{N}$  and  $\delta^2\text{H}$  isotope ratios, which are determined using elemental analyser (EA) and high temperature elemental analyser (TC/EA) coupled to an isotope ratio mass spectrometer (IRMS). By means of a sample of pure material of 5F-PB-22, it is shown that the extraction of 5F-PB-22 from herbal material, a rapid clean-up procedure, or preparative column chromatography had no influence on the isotope ratios. Furthermore, 5F-PB-22 was extracted from 14 different herbal blend samples ("Spice products" from police seizures) and analysed via IRMS, yielding 3 clusters containing 7, 5, and 2 samples, distinguishable through their isotopic composition, respectively. It is assumed that herbal blends in each cluster have been manufactured from individual batches of 5F-PB-22.

**KEYWORDS**

5F-PB-22, drug profiling, EA-IRMS, new psychoactive substances (NPS), stable isotope ratio analysis

**1 | INTRODUCTION**

Since 2008, synthetic cannabinoids, a subclass of the new psychoactive substance (NPS) phenomenon, have been sold in the form of herbal smoking blends, also known as "Spice products", via Internet shops.<sup>1</sup> One or more synthetic cannabinoids are sprayed on to inherently inactive plant material such as *Damiana* (dried leaves of *Turnera diffusa* Willd. Ex Schults. var *aphrodisica*) and packed into professionally designed sachets with the intention of specifically attracting young consumers presenting an allegedly "legal" alternative to cannabis products. The number of newly detected substances in these products has increased every year up to a total number of 169 synthetic cannabinoids as reported by the European Monitoring Centre for Drugs and Drug Addiction (EMCDDA) via the European early warning system (EWS) at the end of 2016.<sup>2</sup>

Knowledge of the production and the supply chain of synthetic cannabinoids or other NPS is still very limited and quite different from

classic synthetic drugs (amphetamine-type-stimulants) which are typically clandestinely produced in European countries. Most of the NPS are presumably produced by specialised chemical companies in Asia, typically in China. To extend the knowledge base of the origin and distribution patterns of these substances, isotope ratio mass spectrometry (IRMS), the measurement of stable isotope ratios for elements like carbon, nitrogen, or hydrogen, is a promising tool. It has already been demonstrated for various drug-profiling applications targeting the cultivation area of drugs manufactured from natural resources like cocaine<sup>3</sup> or heroin<sup>4</sup> and origins of precursor compounds of synthetic drugs like amphetamine<sup>5</sup> or methamphetamine.<sup>6</sup> In the case of NPS, only IRMS profiling of stimulant cathinone derivatives has been reported as of yet.<sup>7</sup> In this paper, we present the first pilot study on the profiling of synthetic cannabinoids in herbal mixtures via IRMS, focusing on the synthetic cannabinoid 5F-PB-22<sup>8</sup> (5F-QUPIC, 1-pentylfluoro-1*H*-indole-3-carboxylic acid-8-quinolinyl ester; Figure 1), which was one of the most prevalent synthetic cannabinoids

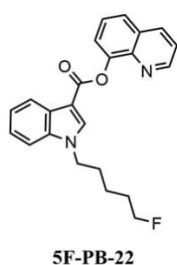


**FIGURE 1** Structural formula of 5F-PB-22

in Germany between 2013 and 2015. Our primary goal in this study was to ascertain whether it is possible to extract synthetic cannabinoids from the herbal matrices without impairment of the isotope ratios and if stable isotope data of 5F-PB-22 can be used for the batch-to-batch comparison of different varieties of Spice products containing 5F-PB-22 as the sole active substance.

The majority of samples available for this study consisted of herbal mixtures (Spice products), necessitating an upstream extraction procedure before any measurements with IRMS could be performed. However, even after extraction of the synthetic cannabinoid, contaminants from the herbal matrix were still present in the purified sample, possibly leading to deviations in measured isotopic data for the pure cannabinoid. Therefore, we investigated 2 clean-up procedures for the herbal extracts of 5F-PB-22 concerning their potential influence on the isotope composition of the analyte of interest. Furthermore, 5F-PB-22 extracts from herbal blend samples from different police seizures were investigated for accordance of their isotopic data to reveal potential correlations of sample origin.

## 2 | Materials and methods

### 2.1 | Samples of 5F-PB-22

Two pure samples of 5F-PB-22 **P1** and **P2** from police seizures as well as 14 herbal blends (HBs) of varying brands containing 5F-PB-22 were available for this study. Eleven of these herbal blends originated from 1 large police seizure (**HB1.1–HB1.11**) in a German internet shop; the remaining 3 were from unrelated smaller police seizures (**HB2.1–HB2.3**). The product brands of all of the named herbal blends presumably originate from 1 large European designer drug manufacturer.

A self-made herbal blend was prepared by dissolving 100 mg of the pure **P1** ( $97.08 \pm 0.34\%$  purity as assessed by quantitative nuclear magnetic resonance (NMR)<sup>9</sup>) in 3 mL acetone and impregnating 1 g of damiana herb with the solution to give an approximately 10% (w:w) herbal blend after drying; this is a common concentration of active ingredient in products available on the market.<sup>10</sup>

### 2.2 | Rapid extraction

To extract 5F-PB-22 from the seized and self-made herbal material, the complete contents of each package were poured onto a clean, plain surface. The material was then evenly divided until an aliquot of ca. 200 mg was obtained, which was subsequently collected in a 4-mL vial and rinsed with 2 mL of acetonitrile. The contact time

between solvent and herbal material was minimised to reduce undesired extraction of plant-related matrix components. The solvent was evaporated to dryness under a steady stream of nitrogen. The dried residue was overlaid with 1 mL of methanol and gently pivoted until a spherical precipitation was visible. After 30 seconds of pivoting, the methanol was removed and evaporated to dryness, yielding 5F-PB-22 in the form of greenish-white crystals (if necessary, crystallisation can be facilitated by addition of small volumes of diethyl ether).

### 2.3 | Preparative column chromatography

Herbal extracts were cleaned up using preparative column-chromatography (PCC). A glass column with a length of 600 mm, a diameter of 30 mm, and a PTFE stopcock (Lenz, Wertheim, Germany) was used for preparative column chromatography, packed with Silica gel 60 (not less than 0.063 mm) and fine granular quartz from Merck (Darmstadt, Germany). Separation was done with a mobile phase of *n*-hexane: ethylacetate 1:1 (v:v). Fractions were collected in intervals of 12 mL. Fractions containing 5F-PB-22 were pooled and evaporated to dryness.

### 2.4 | Elemental analyser – isotope ratio mass spectrometry

Half a milligram of 5F-PB-22 was weighed into 3.3 mm × 5 mm tin capsules (IVA Analysentechnik e.K., Meerbusch, Germany). These were flash combusted on an Elemental Analyser Flash EA 1112 (ThermoFisher, Bremen, Germany) coupled online to an IRMS (Model delta V plus, ThermoFisher, Bremen, Germany) via a ConFlo interface (Model ConFlo IV, ThermoFisher, Bremen, Germany). Catalytic oxidation and reduction beds were held at 1020°C and 650°C, respectively.

Dual measurement of  $\delta^{15}\text{N}$  and  $\delta^{13}\text{C}$  in the same analysis was performed. Pulses of working standard gas (purity at least 4.5 for  $\text{CO}_2$  and 5.0 for  $\text{N}_2$ , Linde, München, Germany) were introduced via the ConFlo interface before and after the sample gases.

The isotope ratios are expressed relative to the international standards (Vienna Pee Dee Belemnite (V-PDB) and AIR, respectively) using the delta definition equation. Here, an example for stable carbon isotope measurements is given:<sup>11</sup>

$$\delta^{13}\text{C}_{\text{unknown}} = \left( \frac{R(^{13}\text{C}/^{12}\text{C})_{\text{unknown}} - R(^{13}\text{C}/^{12}\text{C})_{\text{standard}}}{R(^{13}\text{C}/^{12}\text{C})_{\text{standard}}} \right) \quad (1)$$

For scale calibration (2-point end-member normalisation) of the raw data, in-house standards, Peptone (Sigma-Aldrich, Steinheim, Germany,  $\delta^{13}\text{C}_{\text{V-PDB}}$ : -13.79 ‰;  $\delta^{15}\text{N}_{\text{AIR}}$ : 6.18 ‰) and Acetaminophen (>99% purity, Sigma-Aldrich, Steinheim, Germany,  $\delta^{13}\text{C}_{\text{V-PDB}}$ : -28.7 ‰;  $\delta^{15}\text{N}_{\text{AIR}}$ : -3.39 ‰), were used daily. These in-house standards and the working gases were calibrated against international referencing material as IAEA-CH6 ( $\delta^{13}\text{C}_{\text{V-PDB}}$ : -10.45 ‰) and IAEA-CH7 ( $\delta^{13}\text{C}_{\text{V-PDB}}$ : -32.15 ‰) for  $\text{CO}_2$  and USGS-40 ( $\delta^{15}\text{N}_{\text{AIR}}$ : -4.52 ‰) and USGS-43 ( $\delta^{15}\text{N}_{\text{AIR}}$ : 8.44 ‰) for  $\text{N}_2$ .

Acetanilide p.a. (Merck, Darmstadt, Germany,  $\delta^{13}\text{C}_{\text{V-PDB}}$ : -34.21 ‰;  $\delta^{15}\text{N}_{\text{AIR}}$ : 1.80 ‰) was analysed as in-house standard to routinely check accuracy and long-time reproducibility of the system. Expanded



measurement uncertainty ( $k = 2$ ) was determined to be 0.27 ‰ for  $\delta^{13}\text{C}$  and 0.45 ‰ for  $\delta^{15}\text{N}$  respectively.

The 3D-graphic was generated using The Unscrambler X (Camo, Oslo, Norway).

## 2.5 | High temperature/elemental analyser–isotope ratio mass spectrometry

For determination of the isotope ratios of hydrogen ( $\delta^2\text{H}$ ), a high temperature elemental analyser (TC/EA, ThermoFisher Scientific, Bremen) was coupled to the IRMS. Approximately 0.25 mg of 5F-PB-22 was weighed into 3.3 mm × 5 mm silver capsules (Ag 99.99%, IVA Analysentechnik e.K., Meerbusch, Germany). To create a standardised method to analyse samples, including exchangeable hydrogen, all samples (standards and unknown samples) were dried over Sicapent® (Merck, Darmstadt) for a week. After that, the samples were transported via autosampler (under He atmosphere) into the reaction tube (pyrolysis reactor), where the reaction products hydrogen ( $\text{H}_2$ ), carbon monoxide (CO), carbon (C) and nitrogen ( $\text{N}_2$ ) were generated at a temperature of 1440°C. The gases were separated using a packed column (molecular sieve 5 Å) and subsequently introduced via open split interface to the MS.

For scale calibration (2-point end-member normalisation) of the raw data, in-house standards, IAEA-CH-7 (IAEA, Wien, Austria,  $\delta^2\text{H}_{\text{V-SMOW}}$ : -100.3‰) and Cumarin Sigma (Sigma-Aldrich, Steinheim, Germany,  $\delta^2\text{H}_{\text{V-SMOW}}$ : -2.32‰), were used daily. Pulses of working standard gas (purity at least 5.6 for  $\text{H}_2$ , Linde, München, Germany) were introduced via the ConFlo interface before and after the sample gas. A sample of 3,4-methylenedioxymethamphetamine hydrochloride (MDMA) (lab internal standard,  $\delta^2\text{H}_{\text{V-SMOW}}$ : -80.26‰) was analysed daily as in-house standard to routinely check accuracy and long-time reproducibility of the system. The MDMA internal standard was generated of a large seizure of high purity material some years ago. MDMA was selected as main lab standard due to the high number of MDMA case samples processed in routine work. The standard is measured in every sequence (EA- and TC/EA-IRMS). Expanded measurement uncertainty ( $k = 2$ ) for  $\delta^2\text{H}$  was determined to be 5.1 ‰.

## 3 | RESULTS AND DISCUSSION

### 3.1 | Influence of the extraction procedures on the isotope ratios

To test whether the extraction procedure had any impact on the isotope ratios because of atom substitution (especially of hydrogen atoms), **P1** and **P2** were measured in original form, after a rapid-step extraction (RE) procedure and PCC, respectively. Additionally, **P1** was extracted from 3 self-made herbal blends and cleaned via PCC to investigate whether the extraction from the herbal matrix had an influence on the isotopic composition. Table 1 shows the resulting values for  $\delta^{13}\text{C}$ ,  $\delta^{15}\text{N}$ , and  $\delta^2\text{H}$  with the corresponding standard deviations (STD) for the replicates. Following the in-house standard operation procedure (SOP), samples measured in one sequence show significant differences with deviations greater than  $2\sigma$  (calculated for all measurements of **P1** in Table 1:  $\delta^{13}\text{C}$  0.05 ‰,  $\delta^{15}\text{N}$  0.08 ‰,  $\delta^2\text{H}$  1.32 ‰).

No significant changes in the isotope ratio for  $\delta^{13}\text{C}$  were detected for **P1**. Slightly increased values for  $\delta^{15}\text{N}$  and  $\delta^2\text{H}$  were detected after the column chromatography (**P1 after PCC** and **P1 on HB after PCC**). A plausible explanation might be the separation of nitrogen-containing contaminants from the main component via column chromatography. Residues of triethylamine were found in **P1** (Supporting Information), which potentially influenced the  $\delta^{15}\text{N}$  and  $\delta^2\text{H}$  values. Since methanol should dissolve triethylamine and its salts, the isotopic values for the rapid extraction (**P1 after RE**) were similar to those of **P1**.

Additionally, **P2**, another seizure of pure 5F-PB-22, was extracted and cleaned via PCC (Table 1). For these preparations, the isotopic compositions of all 3 elements are indistinguishable.

Based on this data, a significant isotopic fractionation for 5F-PB-22 by the extraction and purification methods presented here can be ruled out.

**TABLE 1** Isotope ratios  $\delta^{13}\text{C}$ ,  $\delta^{15}\text{N}$  and  $\delta^2\text{H}$  of **P1** and **P2** with standard deviation of triplicate measurements of the original material, and additionally for **P1** after a rapid-extraction procedure (RE), preparative column chromatography (PCC) and the extraction from self-made herbal blends followed by a clean-up via PCC. Both clean-up procedures conducted for the pure material and the extraction from herbal blends followed by PCC were carried out in 3-fold repetition

5F-PB-22 (P)	$\delta^{13}\text{C}_{\text{V-PDB}}[\text{‰}]$ average $\pm$ STD	$\delta^{15}\text{N}_{\text{AIR}}[\text{‰}]$ average $\pm$ STD	$\delta^2\text{H}_{\text{V-SMOW}}[\text{‰}]$ average $\pm$ STD
P1	-25.57 $\pm$ 0.04	8.89 $\pm$ 0.08	-142.32 $\pm$ 0.51
P1 after RE (1)	-25.55 $\pm$ 0.03	8.95 $\pm$ 0.07	-139.85 $\pm$ 0.54
P1 after RE (2)	-25.54 $\pm$ 0.05	9.05 $\pm$ 0.01	-140.34 $\pm$ 0.68
P1 after RE (3)	-25.52 $\pm$ 0.01	9.02 $\pm$ 0.02	-140.06 $\pm$ 1.08
P1 after PCC (1)	-25.50 $\pm$ 0.03	9.42 $\pm$ 0.03	-137.68 $\pm$ 0.40
P1 after PCC (2)	-25.49 $\pm$ 0.02	9.32 $\pm$ 0.06	-138.21 $\pm$ 0.49
P1 after PCC (3)	-25.48 $\pm$ 0.02	9.39 $\pm$ 0.02	-138.69 $\pm$ 0.78
P1 on HB after PCC (1)	-25.58 $\pm$ 0.03	9.35 $\pm$ 0.05	-139.33 $\pm$ 0.76
P1 on HB after PCC (2)	-25.59 $\pm$ 0.01	9.32 $\pm$ 0.05	-140.10 $\pm$ 0.74
P1 on HB after PCC (3)	-25.58 $\pm$ 0.01	9.14 $\pm$ 0.02	-140.31 $\pm$ 0.61
P2	-24.77 $\pm$ 0.06	9.95 $\pm$ 0.02	-137.71 $\pm$ 0.49
P2 after RE	-24.89 $\pm$ 0.01	9.94 $\pm$ 0.05	-138.22 $\pm$ 1.44
P2 after PCC	-24.87 $\pm$ 0.05	9.97 $\pm$ 0.19	-138.82 $\pm$ 0.66

### 3.2 | Isotope ratios of 5F-PB-22 from police seizures

Samples of Spice products produced from the same batch of 5F-PB-22 are expected to have similar isotope ratio values. To demonstrate this for a small sample collective, we measured 15 purified extracts of herbal blend samples of different varieties of Spice products and investigated the results for potential relationships via cluster formation. For some of the herbal blends, a common origin of the contained 5F-PB-22 active substance was considered probable, as they were seized at the same time in the same place with the product brands all originating from a big European manufacturer.

All available HB samples containing 5F-PB-22 and the pure samples were measured tri-fold and the resulting mean values for  $\delta^{13}\text{C}$ ,  $\delta^{15}\text{N}$  and  $\delta^2\text{H}$  are shown in a 3D-plot (Figure 2). The isotope ratios for all HB are listed in Table 2 with STD. The isotopic composition of 5F-PB-22 extracted from HB should not be influenced by contaminants (as for the pure sample P1) due to preceding clean up via PCC.

All preparations of P2 exhibited high values for  $\delta^2\text{H}$ ,  $\delta^{13}\text{C}$  and  $\delta^{15}\text{N}$  (Table 1), separating it from any of the other samples. More difficult to distinguish are the 11 simultaneously seized samples HB1.1–HB1.11 (Table 2) and all preparations of P1 (Table 1), which can be assigned to 3 individual clusters of 6 and 5 samples for the herbal blend and another with all preparations of P1. Regarding the herbal blends, the 5F-PB-22 in each of the 2 clusters might come from the same production batch, which is not surprising as, based on the information on the product labels, all 11 products originate from the same European manufacturer. Apparently, the herbal blend manufacturer had at least 2 batches of 5F-PB-22 available to prepare their Spice products. One of the initially unrelated herbal blends from HB2 is also located close to 1 of these clusters. Although this sample

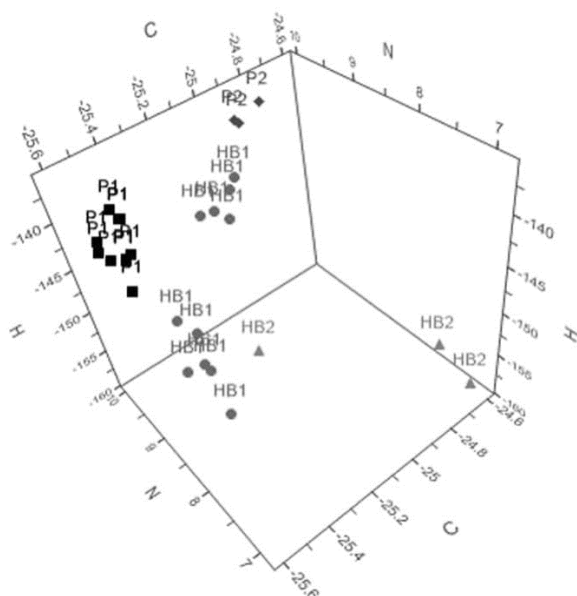


**FIGURE 2** 3D plot of the mean values of triplicate measurements for  $\delta^{13}\text{C}$ ,  $\delta^{15}\text{N}$ , and  $\delta^2\text{H}$  of 5F-PB-22. HB1 (circles) are the 11 herbal blend samples from 1 seizure; HB2 (triangles) are the 3 herbal blends from unrelated seizures; P1 (squares) and P2 (rhombuses) are all preparations from the extraction and purification study of pure material [Colour figure can be viewed at [wileyonlinelibrary.com](http://wileyonlinelibrary.com)]

**TABLE 2** Isotope ratios of herbal extracts of 5F-PB-22 for  $\delta^{13}\text{C}$ ,  $\delta^{15}\text{N}$  and  $\delta^2\text{H}$ , after preparative column chromatography

5F-PB-22 from herbal blend samples (HB)		$\delta^{13}\text{C}_{\text{V-PDB}}[\text{‰}]$ average $\pm$ STD	$\delta^{15}\text{N}_{\text{AIR}}[\text{‰}]$ average $\pm$ STD	$\delta^2\text{H}_{\text{V-SMOW}}[\text{‰}]$ average $\pm$ STD
HB 1	HB 1.1	-25,31 $\pm$ 0,02	8,15 $\pm$ 0,05	-152,39 $\pm$ 0,78
	HB 1.2	-25,15 $\pm$ 0,00	8,71 $\pm$ 0,15	-136,46 $\pm$ 1,21
	HB 1.3	-25,19 $\pm$ 0,04	8,64 $\pm$ 0,05	-136,94 $\pm$ 0,88
	HB 1.4	-25,21 $\pm$ 0,02	8,66 $\pm$ 0,10	-139,42 $\pm$ 2,73
	HB 1.5	-25,26 $\pm$ 0,00	8,64 $\pm$ 0,01	-137,93 $\pm$ 0,49
	HB 1.6	-25,31 $\pm$ 0,01	8,64 $\pm$ 0,11	-137,65 $\pm$ 0,73
	HB 1.7	-25,45 $\pm$ 0,04	8,36 $\pm$ 0,04	-150,31 $\pm$ 0,56
	HB 1.8	-25,46 $\pm$ 0,05	8,41 $\pm$ 0,04	-149,60 $\pm$ 0,28
	HB 1.9	-25,47 $\pm$ 0,04	8,29 $\pm$ 0,12	-145,28 $\pm$ 0,38
	HB 1.10	-25,51 $\pm$ 0,04	8,40 $\pm$ 0,12	-143,80 $\pm$ 0,65
	HB 1.11	-25,53 $\pm$ 0,01	8,39 $\pm$ 0,02	-149,11 $\pm$ 0,98
HB 2	HB 2.1	-25,34 $\pm$ 0,05	7,84 $\pm$ 0,07	-146,94 $\pm$ 0,28
	HB 2.2	-24,62 $\pm$ 0,03	6,96 $\pm$ 0,02	-159,01 $\pm$ 1,14
	HB 2.3	-24,61 $\pm$ 0,02	7,51 $\pm$ 0,06	-157,46 $\pm$ 0,30

originated from an unrelated police seizure, it had the same brand name and sachet design as one of the products from this cluster. Therefore, based on the obtained isotopic data a possible link could be established between 2 products from different sources, verified by brand and sachet design. The 2 remaining herbal blends showed indistinguishable values for  $\delta^2\text{H}$  and  $\delta^{13}\text{C}$ , with a slight deviation for  $\delta^{15}\text{N}$ , and are separated from the remaining collective. These 2 samples might also have been manufactured from one batch of 5F-PB-22, although no relation between the seizures is known.

## 4 | CONCLUSION

The determination of stable isotope ratio data ( $\delta^{13}\text{C}$ ,  $\delta^{15}\text{N}$  and  $\delta^2\text{H}$ ) is a helpful concept to elucidate links between different 5F-PB-22 batches in Spice products, or to assign seizures of pure material to herbal blend samples. Although the pilot study presented here was based on a comparatively small collective of 15 samples, the potential of synthetic cannabinoid profiling via isotope ratio data was still illustrated. In addition, it was successfully demonstrated that 2 different procedures for the extraction of 5F-PB-22 from herbal products had no significant influence on the stable isotope ratio data. This fact is very important for further IRMS applications of NPS profiling and should be verified for every new compound.

## ACKNOWLEDGEMENTS

The authors thank their co-workers for their support in this project. All presented data, if not cited otherwise, were generated within the SPICE-profiling project, funded within the EU's ISEC 2013 programme (Directorate-General for Justice, JUST/2013/ISEC/DRUGS/AG/ISEC/4000006421).

## ORCID

S. Münster-Müller  <http://orcid.org/0000-0003-3949-2818>

## REFERENCES

1. Auwärter V, Dresen S, Weinmann W, Müller M, Putz M, Ferreiros N. 'Spice' and other herbal blends: harmless incense or cannabinoid designer drugs? *J Mass Spectrom.* 2009;44:832-837. <https://doi.org/10.1002/jms.1558>



2. EMCDDA. *Synthetic Cannabinoids in Europe (Perspectives on Drugs)*. Lisbon: EMCDDA; 2017.
3. Ehleringer JR, Casale JF, Lott MJ, Ford VL. Tracing the geographical origin of cocaine. *Nature*. 2000;408:311-312. <https://doi.org/10.1038/35042680>
4. Dautraix S, Guilluy R, Chaudron-Thozet H, Brazier JL, Lamotte A. <sup>13</sup>C Isotopic analysis of an acetaminophen and diacetylmorphine mixture. *J Chromatog A*. 1996;756:203-210. [https://doi.org/10.1016/S0021-9673\(96\)00640-1](https://doi.org/10.1016/S0021-9673(96)00640-1)
5. Carter JF, Titterton EL, Grant H, Sleeman R. Isotopic changes during the synthesis of amphetamines. *Chem Commun*. 2002;21:2590-2591. <https://doi.org/10.1039/B207775B>
6. Kurashima N, Makino Y, Sekita S, Urano Y, Nagano T. Determination of origin of ephedrine used as precursor for illicit methamphetamine by carbon and nitrogen stable isotope ratio analysis. *Anal Chem*. 2004;76:4233-4236. <https://doi.org/10.1021/ac035417c>
7. Collins M, Doddridge A, Salouros H. Cathinones: Isotopic profiling as an aid to linking seizures. *Drug Test Anal*. 2016;8:903-909. <https://doi.org/10.1002/dta.1886>
8. Uchiyama N, Matsuda S, Kawamura M, Kikura-Hanajiri R, Goda Y. Two new-type cannabimimetic quinolinyl carboxylates, QUPIC and QUCHIC, two new cannabimimetic carboxamide derivatives, ADB-FUBINACA and ADBICA, and five synthetic cannabinoids detected with a thiophene derivative  $\alpha$ -PVT and an opioid receptor agonist AH-7921 identified in illegal products. *Forensic Toxicol*. 2013;31:223-240. <https://doi.org/10.1007/s11419-013-0182-9>
9. Schoenberger T. Determination of standard sample purity using the high-precision <sup>1</sup>H-NMR process. *Anal Bioanal Chem*. 2012;403:247-254. <https://doi.org/10.1007/s00216-012-5777-1>
10. Langer N, Lindigkeit R, Schiebel H-M, Papke U, Ernst L, Beuerle T. Identification and quantification of synthetic cannabinoids in "spice-like" herbal mixtures: Update of the German situation for the spring of 2016. *Forensic Sci Int*. 2016;269:31-41. <https://doi.org/10.1016/j.forsciint.2016.10.023>
11. Brand WA. New reporting guidelines for stable isotopes – an announcement to isotope users. *Isotopes Environ Health Stud*. 2011;47:535-536. <https://doi.org/10.1080/10256016.2011.645702>

#### SUPPORTING INFORMATION

Additional supporting information may be found online in the Supporting Information section at the end of the article.

**How to cite this article:** Münster-Müller S, Scheid N, Holdermann T, Schneiders S, Pütz M. Profiling of new psychoactive substances by using stable isotope ratio mass spectrometry: Study of the synthetic cannabinoid 5F-PB-22. *Drug Test Anal*. 2018;1–5. <https://doi.org/10.1002/dta.2407>

## 7. Appendix

### 7.1 List of Abbreviations

Abbreviations for synthetic cannabinoids will not be listed in this work. A good reference for names and structures of classical and modern synthetic cannabinoids is the chemical supplier Cayman Chemicals (<https://www.caymanchem.com/>).

ATS	amphetamine-type stimulants
NPS	new psychoactive substances
UNODC	United Nations Office on Drugs and Crime
THC	$\Delta^9$ -tetrahydrocannabinol
CB1/CB2	cannabinoid receptor 1/2
MDMA	3,4-methylenedioxymethamphetamine
RC	research chemical
EL	E-liquids
SP	Spice-Product
EWS	Early Warning System
EMCDDA	European Monitoring Centre for Drugs and Drug Addiction
AMG	Medicinal Products Act (Arzneimittelgesetz)
BtMG	Narcotic Drugs Act (Betäubungsmittelgesetz)
BtMÄndV	Betäubungsmittelrechts-Änderungsverordnung
NpSG	New Psychoactive Substance Law (Neue-psychoaktive-Stoffe-Gesetz)
CP	Charles Pfizer
HU	Hebrew University
WIN	Sterling-Winthrop
JWH	John William Huffman
AM	Alexander Makriyannis
IC <sub>50</sub>	specific inhibitory concentration
PG	propylene glycol
VG	vegetable glycerin
HS	headspace
GC	gas chromatography
(U)HPLC	(ultra) high pressure liquid chromatography
MS	mass spectrometry
CE	capillary electrophoresis
UV	ultraviolet
IR	infrared spectroscopy
ICP	inductive coupled plasma
AES	atomic emission spectroscopy
SNIF	site-specific isotope fractionation
NMR	nuclear magnetic resonance spectroscopy
IRMS	isotope ratio mass spectrometry

LLE	liquid-liquid extraction
SPE	solid phase extraction
HR-MS	high resolution MS
BJA	Federal Criminal Police Office
FR	University Medical Center Freiburg
INPS	Institut National de Police Scientifique
F-LC	flash chromatography
ESI	electro-spray ionization
MDA	multivariate data analysis
TLME	tert-leucine methyl ester
RLP	Land Office of Criminal Investigation of Rhineland Palatine
RP	reverse phase
m/z	mass to charge ratio
ISD	in-source decay
RT	retention time
BPC	base peak chromatogram
TIC	total ion chromatogram
PCA	principle component analysis
PC	principle component
HCA	hierarchical cluster analysis
FWHM	full width at half-maximum
TOF	time of flight
FT-ICR	Fourier transform ion cyclotron resonance spectroscopy
COSY	<sup>1</sup> H- <sup>1</sup> H correlation spectroscopy
HSQC	heteronuclear single quantum coherence
NOESY	nuclear overhauser enhancement and exchange spectroscopy
DCC	N,N-dicyclohexylcarbodiimide
EDC	1-ethyl-3-(3-dimethylaminopropyl) carbodiimide hydrochloride
HOBt	hydroxybenzotriazole
HATU	O-(7-azabenzotriazol-1-yl)-1,1,3,3-tetramethyluronium hexafluorophosphate
EI	electron impact
IAEA	International Atomic Energy Agency in Vienna
V-PDB	Vienna Pee Dee Belemnite
V-SMOW	Vienna Standard Mean Ocean Water

## 7.2 List of Figures

Figure 1: Leading causes of death attributable to drug use, 2016 <sup>1</sup> . Data taken from the World Drug Report 2018 <sup>2</sup> .....	1
Figure 2 Structural formulas of selected opioids, cannabinoids and stimulants.....	2
Figure 3: NPS reported to the EWS for the first time 2005-2017: per year (left) and per category (right). The graphic is taken from the EMCDDA <sup>29</sup> .....	5
Figure 4: Example for the systematic naming of synthetic cannabinoids according to its structure.....	9
Figure 5: Structural formulas of THC and a selection of classical and modern synthetic cannabinoids. Colouring of the individual molecule structure was done according to the same code as Figure 4 (Linked residue - TailCoreLinker) to highlight the structural similarities between the different types of cannabinoids.....	10
Figure 6: Synthetic cannabinoids can be obtained in three different formulations: as pure “research chemical” in powder form (left), as "Spice-Product", laced on a herbal matrix (middle), or as e-liquid, dissolved in a matrix of propylene-glycol and glycerine (right) .....	11
Figure 7: Scheme of the distribution channels of synthetic cannabinoids, starting from the production in China, over the shipment of pure material via air or ship to European distributors, which either sell the pure material as research-chemical, dissolved in an E-liquid matrix or sprayed onto a herbal matrix via online shops. These products can then be ordered in online-shops and are send to the individual customers by mail.....	16
Figure 8: Seizure of 40 kg pure MDMB-CHMICA by Luxembourg customs in December 2014 going from Shanghai to Madrid. ....	21
Figure 9: Sepacore® X50 Flash-Chromatography system by Büchi, consisting of two pumps, a UV-VIS spectrometer, an automated fraction collector and a control unit. The pictures belong to and is used with the allowance of Büchi. ....	22
Figure 10: Schematic of rectangular bucketing via Profile Analysis with subsequent data treatment for assessment of discriminating key-impurities. The 3D-graphic was modelled using MZmine 2.38 <sup>130</sup> ..	26
Figure 11: Examples for the different types of information that can be extracted from a PCA Scores (left) and Loadings plot (right). ....	27
Figure 12: Exemplary dendrogram of an HCA .....	28
Figure 13: Last step of the amino acid coupling in the synthesis of MDMB-CHMICA using five different reaction conditions .....	30
Figure 14: Excerpts of overlaid UHPLC-MS base peak chromatograms. red: native sample of MDMB-CHMICA, blue: isolated impurities of the corresponding red labeled sample injected with a lower dilution factor. ....	32
Figure 15: Sketched summary of the final workflow for impurity profiling of synthetic cannabinoids with the assignment of individual parts to their respective publications. Green is the general workflow, blue the method development with structural identification of single impurities and controlled synthesis, orange the adaption of the workflow to samples in e-liquid matrices, red the adaption to samples on herbal matrices including the comprehensive profiling of the main active ingredient via IMRS and purple the controlled synthesis and binding studies of specific synthetic cannabinoids. In general, the respective publications were mixtures of the individual parts of the workflow.....	33
Figure 16: Structural formulas of the fifteen assessed key-impurities for MDMB-CHMICA. (top) elucidated via NMR and HR-MS/MS experiments. (bottom) elucidated only by HR-MS/MS experiments. ....	35
Figure 17: Excerpts of the most discriminating areas of the base peak chromatograms (BPC) for impurity profiles of MDMB-CHMICA after extraction from damiana (orange, A) and strawberry (red, B) leaves compared to the corresponding powder sample (blue, A and B). ....	37

Figure 18:  $\delta^{13}\text{C}$  and  $\delta^{15}\text{N}$  values for all “Spice-Products” of MDMB-CHMICA, either measured via EA- or GC-IRMS. Colouring of samples is corresponding to the date of purchase or seizure of the “Spice-Products” in intervals of 5 month (● September 2014 to February 2014; ● March 2015 to July 2015; ● August 2015 to December 2015)..... 39

Figure 19:  $\delta^{13}\text{C}$  and  $\delta^{15}\text{N}$  values for all samples of MDMB-CHMICA (green), Cumyl-PeGaClone (red) and 5F-PB-22 (orange). Each synthetic cannabinoid clustered individually. .... 39

Chemical structures were drawn with ChemDraw Professional 17.1 (PerkinElmer) and illustrations were prepared via the MS Office package.

### 7.3 List of Tables

Table 1 Analgesic potency of a selection of opioids, referenced to morphine = 1..... 3

Table 2 Affinity of the three most prevalent ATS to synaptic receptors and transporter proteins. Dopamine (DA), nor-adrenaline (NE), and serotonin (5-HT)..... 4

Table 3: List of  $K_i$  values for CB1 and CB2 receptors of a selection of cannabinoids ..... 8

Table 4: Listing and additional information for the synthetic cannabinoid seizures and online-test purchases used in this work..... 20

### 7.4 Oral/poster presentations and conferences

Conference presentation, 7th European Academy of Forensic Science Conference (EAFS 2015), 06.-11.09.2015, Prague/CZ, ca. 1100 participants

Poster presentation "First approaches for the impurity profiling of cannabimimetic designer drugs by UHPLC-MSn and GC-MS"

Conference presentation, 54th Annual TIAFT meeting (The International Association of Forensic Toxicologists), 28.08.-01.09.2016, Brisbane/AU, ca. 1000 participants

Poster presentation "Identification and chemometric assessment of key impurities in seized samples of the synthetic cannabinoid MDMB-CHMICA"

Workshop presentation, Annual GTFCh workshop (German Society of Toxicological and Forensic Chemistry), 13.-14.10.2016, Freiburg/DE, ca. 150 participants

Oral workshop "Profiling bei Neuen Psychoaktiven Stoffen"

Conference presentation, 27. Doktorandenseminar des AK Separation Science, 09.01-10.01.2017, Hohenroda, ca. 120 participants:

Oral presentation “Identification and chemometric assessment of key impurities in seized samples of the synthetic cannabinoid MDMB-CHMICA“

Conference presentation, Bruker Anwendertreffen, 20.03.2017, Kassel, ca. 70 participants:

Oral presentation “Identification and chemometric assessment of key impurities in seized samples of the synthetic cannabinoid MDMB-CHMICA“

Conference presentation, XX. GTFCh Symposium, 27. - 29.04.2017, Mosbach, ca. 450 participants:

Oral presentation “Identification and chemometric assessment of key impurities in seized samples of the synthetic cannabinoid MDMB-CHMICA“

Conference presentation, Thermo Scientific Forensics Workshop 10. – 11.06.2017, ca. 150 participants:

Oral presentation “Entwicklung und Anwendung eines Impurity-Profiling Verfahrens für synthetische Cannabinoide am Beispiel von MDMB-CHMICA“



## 7.5 Scientific curriculum vitae

**SASCHA MÜNSTER-MÜLLER**

Analytischer Chemiker

## STUDIUM

Heute	<b>Dr. rer. nat.</b>
-	Universität Rostock, Rostock
Nov 2014	<ul style="list-style-type: none"> <li>• Am Lehrstuhl für analytische Chemie</li> </ul>
Juli 2014	<b>Master of Bio- and Pharmaceutical Analysis</b>
-	Hochschule Fresenius, Idstein
Okt 2013	<ul style="list-style-type: none"> <li>• Gesamtnote: 1,3</li> </ul>
Sep 2013	<b>International Bachelor of Applied Chemistry</b>
-	Hochschule Fresenius, Idstein
Okt 2009	<ul style="list-style-type: none"> <li>• Gesamtnote: 1,9</li> </ul>

## ZUSÄTZLICHE INFORMATIONEN

**Präsentationen und Konferenzen**

19. und 20. Symposium der GTFCh  
(2015 und 2017)

*400 Teilnehmer, Poster + Vortrag*

7th European Academy of Forensic  
Science Conference (EAFS 2015),

*1100 Teilnehmer, Poster*

54th Annual TIAFT meeting (The  
International Association of Forensic  
Toxicologists)

*1100 Teilnehmer, Poster*

Jährlicher GTFCh Workshop 2017

*150 Teilnehmer, Vorträge*

27. PhD Seminar des AK Separation  
Science (GDCH)

*100 Teilnehmer, Vortrag*

Bruker Anwendertreffen 2017

*150 Teilnehmer, Vortrag*

Thermo Scientific Forensics  
Workshop 2017

*150 Teilnehmer, Vortrag*

**Eigene Publikationen:**

- Muenster-Mueller S, Scheid N, Holdermann T, Schneiders S, Puetz M "Profiling of new psychoactive substances (NPS) by using stable isotope ratio mass spectrometry (IRMS): study on the synthetic cannabinoid 5F-PB-22" *Drug Test. Anal.* 2018, 10(8): 1323-1327
- Muenster-Mueller S, Zimmermann R, Puetz M "A novel impurity-profiling workflow with the combination of flash-chromatography, UHPLC-MS, and multivariate data analysis for highly pure drugs: A study on the synthetic cannabinoid MDMB-CHMICA" *Anal. Chem.* 2018, 90(17): 10559-10567
- Muenster-Mueller S, Hansen S, Opatz T, Zimmermann R, Puetz M „Chemical profiling of the synthetic cannabinoid MDMB-CHMICA: identification, assessment and stability study of synthesis-related impurities in seized and synthesized samples“, *Drug Test. Anal.* 2019, 11(8): 1192-1206
- Matzenbach I, Muenster-Mueller S, Knepper T, Puetz M „Profiling of synthesis-related impurities of the synthetic cannabinoid Cumyl-5F-PINACA in seized samples of e-liquids via multivariate analysis of UHPLC-MSn data“, *Drug Test. Anal.* 2019, in press
- Muenster-Mueller S, Scheid N, Puetz M „Combination of stable isotope ratio data and chromatographic impurity signatures as a comprehensive concept for the profiling of highly prevalent synthetic cannabinoids and their precursors“ accepted, *Analytica Chimica Acta*

**Beitrag zu anderen Publikationen:**

- Andernach L, Pusch S, Weber C, Schollmeyer D, Muenster-Mueller S, Puetz M, Opatz T „Absolute configuration of the synthetic cannabinoid MDMB-CHMICA with its chemical characteristics in illegal products“ *Forensic Toxicol* 2016, 34:344-352
- Weber C, Pusch S, Schollmeyer D, Muenster-Mueller S, Puetz M, Opatz T "Characterization of the synthetic cannabinoid MDMB-CHMCZCA" *Beilstein J. Org. Chem.* 2016, 12: 2808-2815
- Puetz M, Auwaerter V, Muenster-Mueller S, Schneiders S „The EU-project „SPICE-profiling“ (2015-2017) - objectives and results of a pre-study“, *Toxichem Krimtech (Special Issue)* 2015, 82:273-283

## 7.6 Scientific publications (submitted)

**Publication 5:** Münster-Müller et al., *Analytica Chimica Acta*  
2019, Submitted

Pages 94 - 118

### 7.5.1 Publication 5

*Combination of stable isotope ratio data and chromatographic impurity signatures as a comprehensive concept for the profiling of highly prevalent synthetic cannabinoids and their precursors*

Sascha Münster-Müller, Nicole Scheid, Michael Pütz

Submitted to Analytica Chimica Acta

# Combination of stable isotope ratio data and chromatographic impurity signatures as a comprehensive concept for the profiling of highly prevalent synthetic cannabinoids and their precursors

**\*Sascha Münster-Müller<sup>a,b</sup>, Nicole Scheid<sup>a</sup>, Ralf Zimmermann<sup>b,c</sup>, Michael Pütz<sup>a</sup>**

<sup>a</sup>Federal Criminal Police Office, Forensic Science Institute, Äppelallee 45, 65203 Wiesbaden, Germany

<sup>b</sup>Joint Mass Spectrometry Centre, Institute of Chemistry, Chair of Analytical Chemistry, University of Rostock, 18057 Rostock, Germany

<sup>c</sup>Joint Mass Spectrometry Centre, Cooperation Group “Comprehensive Molecular Analytics”, Helmholtz Zentrum Muenchen, 85764 Neuherberg, Germany

\*Corresponding Author: Sascha Münster-Müller, University of Rostock, Dr.-Lorenz-Weg 2, 18059 Rostock, Germany, Sascha.muenster-mueller@uni-rostock.de, Phone: (+49) 177 3882571

*Keywords:* new psychoactive substances; MDMB-CHMICA; Cumyl-PeGaClone; isotope ratio mass spectrometry; impurity profiling

## Abstract

In this study, we utilized elemental analyser (EA) and gas-chromatography (GC) isotope ratio mass spectrometry (IMRS) and ultra-high-performance liquid chromatography coupled to mass spectrometry (UHPLC-MS) in a comprehensive profiling approach assessing the chromatographic impurity signatures and  $\delta^{13}\text{C}$  and  $\delta^{15}\text{N}$  isotope ratios of synthetic cannabinoids from police seizures and internet test purchases. Main target of this study was the highly prevalent synthetic cannabinoid MDMB-CHMICA (methyl (2S)-2-([1-(cyclohexylmethyl)-1H-indol-3-yl]formamido)-3,3-dimethylbutanoate). Overall, 61 powder and 118 herbal blend (also called “Spice-Products”) samples were analysed using both analytical techniques and evaluated in a joint model to link samples from a common source. As a key finding, three agglomerates of Spice-product samples with similar dates of purchase were identified in the IRMS data, possibly representing larger shipments of MDMB-CHMICA, each produced with the same precursor material, successively delivered to the European market. The three agglomerates were refined into multiple sub-clusters based on the impurity profiling data, each representing an individual synthesis batch. One of the agglomerates identified in the IRMS data was found to consist two groups of four sub-clusters, respectively, with majorly different impurity profiles, demonstrating the necessity for both analytical techniques to extract the maximum amount of information from a limited sample pool. Additionally, 31 samples containing the recently surfaced synthetic cannabinoid Cumyl-PeGaClone (5-pentyl-2-(2-phenylpropan-2-yl)-2,5-dihydro-1H-pyrido[4,3-b]indol-1-one) were analysed for their  $\delta^{13}\text{C}$  and  $\delta^{15}\text{N}$  isotope ratios to put the isotopic data recorded for MDMB-CHMICA in a more global perspective. Three building blocks of precursor chemicals (indole, tert-leucine, cumylamine) potentially used for the synthesis of the two named synthetic cannabinoids were

acquired from different global vendors and measured for their  $\delta^{13}\text{C}$  and  $\delta^{15}\text{N}$  isotope ratios to better understand variations in the isotopic composition of the synthetic cannabinoids and to trace their origin.

## 1. Introduction

Classic drugs like Cannabis, cocaine, heroin or amphetamine type stimulants (ATS) make up the largest amount of seized drugs of abuse worldwide [1]. Forensic profiling is a well-established method for law enforcement agencies to obtain basic information on the manufacturing and trafficking of these drugs. The two most frequently used analytical techniques are profiling of synthesis-related chemical impurities (impurity profiling) and stable isotope ratio analysis (SIRA), each providing orthogonal information on the history of a sample. Chemical profiling mainly targets the arising natural and synthetic by-products and impurities as a result of the synthesis pathway and chosen precursor material [2-6]. The analysis of the composition of stable isotopes for elements like carbon, nitrogen or hydrogen via isotope ratio mass spectrometry (IRMS) can provide information on the origin of precursor compounds of synthetic drugs like amphetamine [7, 8] or methamphetamine [9, 10] and was used to geographically narrow down the cultivation area of plant-based drugs like cocaine [11, 12] or heroin [13]. Buchanan et al. [14] published one of the few available literature sources where both techniques were used individually and as combination to discriminate between in-house produced samples of 3,4-methylenedioxymethamphetamine (MDMA), synthesized using two batches of piperonyl methyl ketone (PMK) and three different synthetic routes (Al/Hg,  $\text{NaBH}_4$  and  $\text{Pt/H}_2$ ). Via impurity-profiling it was possible to discriminate between the three synthesis routes due to differences in the chemical impurity composition. According to the authors, the IRMS data did not allow for unambiguous discrimination between neither the synthesis pathway, nor the starting material due to isotopic fractionation. However, a combination of impurity profiling and stable isotope analysis data allowed for the discrimination between both, the origin of the precursor material and the applied synthesis route, using pattern recognition techniques such as principle component analysis (PCA). In the work presented here, we investigated, to which extent the combination of these two analytical techniques can support the strategical evaluation, in particular the discrimination of batches and synthesis pathways, of new psychoactive substances (NPS). Since 2006, the appearance of new classes of NPS on the illicit drug market significantly increased in number of individually reported substances (overall 803 NPS in the period of 2009-2017) as well as in seized volume (22 tons in 2016), growing to a major drug-related issue of the twenty-first century [1]. Most of these substances, including synthetic cathinones, opioids or cannabinoids, were originally developed in legitimate pharmaceutical research and are now misused as recreational drugs [15-17]. The exact modus operandi of manufacturing, sourcing of precursor chemicals and trafficking of NPS are yet a topic of ongoing research and are expected to be majorly different to other synthetic drugs such as ATS, which are typically produced in clandestine laboratories in Europe. The majority of NPS are presumably produced by chemical companies in Asia, typically China, with professional instrumentation and trained chemists, reflected by the high purity of NPS on the market [18]. The pure drug substances are then shipped by air or sea to Europe where they are employed as active ingredients of designer drug products sold openly in internet-shops as so-



called “legal-highs” or “research chemicals”. In Germany, synthetic cannabinoids are the most prevalent NPS subclass and are mostly sold as herbal smoking blends, known as “Spice-Products” (SP) [19, 20]. The pure cannabinoids are sprayed onto an inactive dried plant matrix such as Damiana (*Turnera diffusa* Willd. Ex Schults. var *aphrodisica*) or strawberry leaf and packed into plastic sachets with professionally designed logos and recurrent branding. From the perspective of forensic investigation, tracing back the source of seized material of synthetic cannabinoids (either in pure form or laced onto herbal material) by analysis of the impurity composition or isotopic profile is very difficult, as usually no authentic reference materials from the original manufacturing sites are available. The history of each sample can be regarded as “black-box” which only enables the generation of links between individual seizures, but not reveals the original source. However, pure material from a single synthesis batch of synthetic cannabinoids carries a specific impurity profile and isotopic composition, which is maintained even though sprayed onto a herbal matrix [21, 22]. Multiple batches synthesized from the same precursor material also should exhibit a similar isotopic composition, when using the same synthesis pathway [23, 24]. Thus, by IRMS analysis it can be possible to link seized samples that were synthesized in different batches, but come from a single manufacturing site using the same precursor material for all syntheses. By analysis of the impurity composition, it can be possible to additionally discriminate between the individual synthesis batches even though the same precursor material was used. In this study, we aimed at interpreting both techniques individually for their discrimination potential and finally combine the information of both datasets to link Spice products from internet test purchases and obtain general information about underlying distribution channels and market structures. By implementing metadata into the data evaluation, for example the date of purchase of a specific SP, a time dependant correlation might be revealed.

IRMS profiling of three cathinone derivatives [25] and of the synthetic cannabinoid 5F-PB-22 [21] **3** (5F-QUPIC, 1-pentylfluoro-1*H*-indole-3-carboxylic acid-8-quinolinyl ester, Figure 1) were published, using the stable isotope ratios of  $\delta^2\text{H}$ ,  $\delta^{13}\text{C}$  and  $\delta^{15}\text{N}$  to link seizures. Differences in isotopic composition for the presented sample pool of both the cathinone derivatives and the synthetic cannabinoid are expected to be a result of a different synthesis procedure or in the case of multiple consecutive batches with the same synthesis route, the use of multiple lots of a specific precursor material with altering isotopic composition. Recently, we demonstrated based on an impurity profiling study on the synthetic cannabinoids MDMB-CHMICA **1** (Methyl (2*S*)-2-([1-(cyclohexylmethyl)-1*H*-indol-3-yl]formamido)-3,3-dimethylbutanoate, Figure 1), that NPS manufacturers produce multiple synthesis batches to supply the demand on the drug market [22]. A large police seizure by Luxembourg customs in December 2014 of forty 1 kg bags of pure **1** stacked into two barrels was analysed for chromatographic impurity compositions. By comparative multivariate data analysis it was found, that the complete seizure comprised of at least six synthesis batches in sizes of 5 to 10 kg. Whether the manufacturers used the same precursor material for these syntheses is yet unknown, which is why we analysed samples of the named 40 bags of MDMB-CHMICA additionally via IRMS in the study presented here to obtain orthogonal information to the impurity data. The results from both techniques will provide a deeper insight into the manufacturing process for this specific sample pool and help to better interpret the correlation of isotopic and impurity composition of other seized samples. Although the Luxembourg

seizure alone comprised for around 40 million single doses, still numerous RC and SP containing **1** could be found on the European market from 2014 to 2016, proving that other shipments of this synthetic cannabinoid have reached its destination in Europe. Considering the scenario of successive synthesis of large batches of **1**, over the period of two years it is likely that the manufacturer of **1** was forced to restock their depleted precursor material, which again might carry a different isotopic composition. This replacement cycle in the precursor material should be detectable in the isotopic data of the corresponding material of **1** found in street samples. Therefore, seized and online test-purchased pure samples and SPs containing **1** from the end of 2014 to the end of 2015 were analyzed for their impurity composition and  $\delta^{13}\text{C}$  and  $\delta^{15}\text{N}$  isotope ratio data to identify potential links of samples from a common source. Although a large number of online-shops sell a variety of different SPs products with varying brands and logos, the synthetic cannabinoid material used to produce these SPs might come from a common source.

Cumyl-PeGaClone **2** (5-pentyl-2-(2-phenylpropan-2-yl)-2,5-dihydro-1H-pyrido[4,3-b]indol-1-one [26], Figure 1) was one of the highly prevalent synthetic cannabinoids in 2017 after the German NPS law was put into force, specifically launched to circumvent the generic submission of indole and indazole core structures of synthetic cannabinoids. Multiple SPs and one RC of **2** were available at that time, which is why we measured these samples via IRMS to assess their overall diversity in isotopic composition and put the isotopic data recorded for **1** in a more global perspective.

Additionally, we measured the  $\delta^{13}\text{C}$  and  $\delta^{15}\text{N}$  isotope ratios of precursor material potentially used in the synthesis of **1** (indole, tert-leucine and tert-leucine methyl ester) and **2** (cumylamine), acquired from different global vendors. Our aim was to assess the diversity of isotopic data in this precursor material, to better understand the variations in the final products and, thus, to validate the data interpretation and generated links. Only material in crystalline form was measured. Other potential precursors, such as cyclohexyl methyl bromide or pentyl bromide are liquids and were not included in this study.

This work combines the different analytical methodologies we developed in a series of previous publications targeting the impurity profiling and stable isotope analysis of synthetic cannabinoids. The experimental procedures will not be stated in their full length and can be taken from the corresponding literature [21, 22, 27].

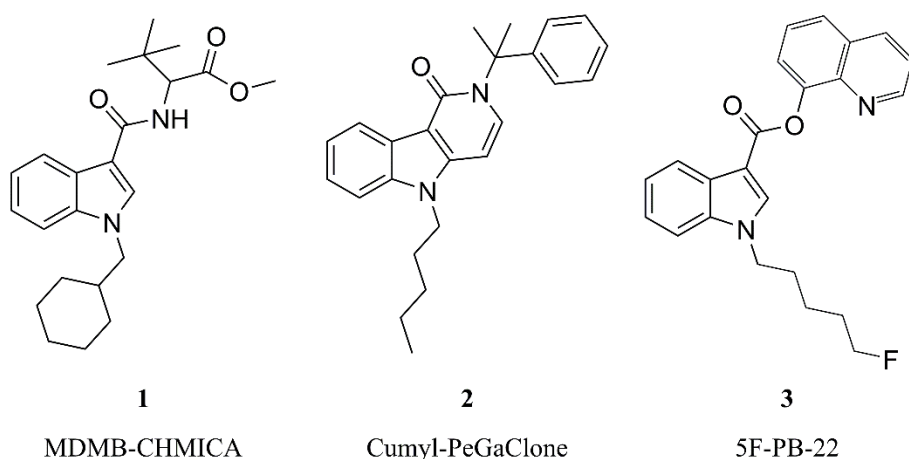


Figure 1: Structural formulas of MDMB-CHMICA and Cumyl-PeGaClone

## 2. Materials and methods

### 2.1 Synthetic cannabinoids

#### 2.1.1 MDMB-CHMICA

Overall 61 pure samples of **1** were available, of which 40 were from one large seizure by Luxembourg customs in December 2014 (MDMB-01 to MDMB-40), 17 from seizures by the Finish customs (MDMB-41 to MDMB-57), 3 from online test-purchases by the University Medical Center in Freiburg (MDMB-58 to MDMB-60) and 1 from a seizure in Slovenia (MDMB-61).

Furthermore, 118 SP samples containing **1** as sole cannabinoid were available. 74 samples were from online test purchases by the University Medical Center in Freiburg between November 2014 and December 2015 (SP\_MDMB-001 to SP\_MDMB-74) and 44 from seizures by the Land Office of Criminal Investigation of Rhineland Palatine between September 2014 and June 2015 (SP\_MDMB-75 to SP\_MDMB-118).

#### 2.1.2 Cumyl-PeGaClone

One pure sample of **2** from a police seizure by the Federal Criminal Institute (Peg-01) and 30 SPs from internet test-purchases containing **2** as sole cannabinoid by the University Medical Center in Freiburg between December 2016 and July 2017 (SP\_Peg-01 to SP\_Peg-30) were available.

### 2.2 Precursor chemicals

Indole was purchased from eight different global vendors: Sigma Aldrich (US), TCI (Japan), ABCR (Germany), Merck (Germany), Acros Chemicals (Belgium), Alfa Aesar (United Kingdom), BePharm (China) and MP Biomedicals (France). Tert-leucin was purchased once as (L) from and in triplicate as (D) form (same lot) from Alfa Aesar (United Kingdom). Tert-leucine methyl ester was purchased from two different Asian vendors BePharma (China) and TCI (Japan). Cumylamine was purchased from four different global vendors: ABCR (Germany), Acella (China), Enamine (Ukraine) and TCI (Japan) in liquid form and subsequently crystallized as cumylamine hydrochloride for measurements on EA-IRMS.

### 2.3 Extraction procedure

For both the seized and bought SPs, the material was poured onto a clean, plane surface and evenly divided into aliquot of ca. 500 mg. If less than 500 mg were available, the complete sample was extracted. The herbal material was rinsed twice with MeCN, once with 5 mL and again with 2 mL. The two extracts were combined and evaporated to dryness and dissolved again in 1.5 mL ethyl acetate/hexane (1:2, v:v) for injection into the flash-chromatography (F-LC).

Self-made SPs were prepared for **1** (MDMB-07,  $97.5 \pm 2$  % purity [28]) and **2** (Peg-01  $98.4 \pm 2$  % purity [28]) by dissolving 300 mg of pure substance in 10 mL Acetone and impregnating 3 g of damiana herb. After drying for 24 hours, each of these SPs were prepared according to the sample preparation procedure of seized SP. Each self-made SP was extracted and cleaned

up in triplicate. The corresponding isotopic data can be taken from the supplementary material. A maximum difference of 0.15 ‰ for  $\delta^{13}\text{C}$  and 0.20 ‰ for  $\delta^{15}\text{N}$  between all measurements for **1**, and 0.12 ‰ for  $\delta^{13}\text{C}$  and 0.13 ‰ for  $\delta^{15}\text{N}$  between all measurements for **2** was calculated. Hence, neither the extraction from herbal material, nor the subsequent clean up via F-LC had influence on the isotopic composition of any synthetic cannabinoid.

#### *2.4 Isolation of the main component and assessment of impurity signatures*

In comparison to our previous IRMS measurements of synthetic cannabinoids [21], the manual preparative column chromatography was replaced with automated preparative F-LC as sample preparation tool as reported in a previous study [22]. By precise fractionation of the F-LC (Sepacore X50, Büchi Labortechnik), the main component fraction can be selectively cut out of the chromatographic run and is available for analysis via IRMS. The remaining fractions containing related synthesis impurities are pooled again for analysis of the chromatographic impurity signatures via UHPLC-MS (Dionex 3000, Thermo Scientific; AmaZon Speed, Bruker). Further data treatment was done by an automated bucketing algorithm (Profile Analysis, Bruker) that integrates the LC-MS run in distinct pairs of  $m/z$  and retention time. A set of previously assessed fifteen key impurities are then semi-quantitatively compared on multivariate basis (Unscrambler X, Camo) to discriminate between individual synthesis pathways or production batches.

The F-LC gradient program used for **1** to separate related synthesis impurities from the main component and **2** for main component clean-up can be taken from the supplementary material. The purity (absence of by-products or matrix components from herbal material) of the main components were validated via UHPLC-MS and GC-MS prior to IRMS measurements.

#### *2.5 Isotope ratio mass spectrometry*

Stable isotope ratios were recorded on an EA-IRMS and GC-IRMS. Generally, EA-IRMS is the preferred technique as it is faster, easier to handle and less prone for malfunction compared to GC-IRMS. However, in some cases, the quantity of purified main component did not exceed 6-8 mg, which was the minimum sample amount for weighting enough solid material into the tin cups (in triplicate) for EA. These specific samples were dissolved as whole in acetonitrile and diluted adequately for subsequent analysis via GC-IRMS.

##### *2.5.1 Elemental Analyser - Isotope Ratio Mass Spectrometry (EA-IRMS)*

EA-IRMS analysis of pure and extracted material of synthetic cannabinoids was performed in triplicate for  $\delta^{15}\text{N}$  and  $\delta^{13}\text{C}$ , expressed as average  $\pm$  SD, as reported in our previous study [21].

##### *2.5.2 Gas Chromatography - Isotope Ratio Mass Spectrometry (GC-IRMS)*

For GC-IRMS, the Isotope ratio mass spectrometer Delta V plus with gas chromatograph TRACE 1310 (including autosampler TriPLUS RSH), ISQ LT (Single Quadrupole Mass Spectrometer) and Interface Conflo IV (all Thermo Fisher Scientific, Bremen, Germany) was used.

All injections were conducted splitless into a hot injector (250°C) with constant flow (constant flow 1.5 mL/min). The analytical column was a Zebron ZB-5MSi (30 m x 0.32 mm ID x 0.50µm film thickness; phenomenex, Made in USA). The Combustion reactor for  $\delta^{13}\text{C}$ - and  $\delta^{15}\text{N}$ - measurements was a NiO tube/CuO-NiO reactor (Thermo Fisher Scientific, P/N 1255321). This reactor consists of a ceramic tube filled with a Ni-tube and NiO/CuO and Platinum wires. As it contains both an oxidation and a reduction unit in contrast to the EA, an additional reduction reactor was not necessary for nitrogen measurements ( $\text{NO}_x$  reduction to  $\text{N}_2$ ). The operating temperature of the reactor was set to 1000°C. The reactor was initially oxidized for 6h at 600°C, 4h at 900°C, and 2h at 1000°C (as recommended by Thermo Fisher Scientific). Repeated oxidation was routinely performed at the beginning of each sequence [for  $\delta^{13}\text{C}$  30 min oxidation (60 min Backflush mode) and for  $\delta^{15}\text{N}$  1 to 5 min oxidation (30 min Backflush mode)].

As validation and quality control (QC) standards, MDMB-07 (previously isotopically characterized by EA-IRMS for comparative purposes), Methyl-N-methylanthranilat (M-MA) (for  $\delta^{15}\text{N}$ ) and Dodecane (for  $\delta^{13}\text{C}$ ) were analyzed. The injection volume is 10 µL for each run. The isotope ratios of carbon and nitrogen were measured in separate runs. Each sample was analysed at least four times and averaged. Cannabinoid samples were dissolved in 1 mL acetonitrile with concentration ranges of 80-100 µg mL<sup>-1</sup> for  $\delta^{13}\text{C}$  and 600-700 µg mL<sup>-1</sup> for  $\delta^{15}\text{N}$ . The GC temperature programs for the samples and QC standards are shown in Table 1.

Table 1 GC temperature program for synthetic cannabinoids (in Acetonitrile), M-MA (in MTBE) and Dodecane (in hexane)

	Synthetic cannabinoid			M-MA			Dodecane		
	Rate (°C min <sup>-1</sup> )	T (°C)	Hold (min)	Rate (°C min <sup>-1</sup> )	T (°C)	Hold (min)	Rate (°C min <sup>-1</sup> )	T (°C)	Hold (min)
Initial		70	2		40	2		80	2
1	15	270	0	15	280	0	15	250	1
2	5	320	8	50	40	4	70	40	3

**To validate that both IRMS instruments are able to measure isotopic compositions with equal results apart from the regularly checked QC standards**, thirteen randomly chosen herbal blend samples containing **1** were extracted, cleaned up and measured with both techniques. The corresponding isotopic data can be taken from the supplementary material. EA-IRMS shows a good precision for both elements with a maximum STD of 0.06 ‰ for  $\delta^{13}\text{C}$  and 0.11 ‰ for  $\delta^{15}\text{N}$ . The GC-IMRS measurements showed increased maximum STDs of 0.24 ‰ for  $\delta^{13}\text{C}$  and 0.40 ‰ for  $\delta^{15}\text{N}$ . The maximum  $\Delta$  between the averaged values for GC-IRMS and EA-IRMS measurements were 0.18 ‰ for  $\delta^{13}\text{C}$  and 0.34‰ for  $\delta^{15}\text{N}$ . Despite the increased measurement uncertainty of the GC-IMRS, on average the results obtained with both instruments are comparable and in acceptable limits for the purposes of this work.



### 3. Results and discussion

#### 3.1 Isotope ratios of precursor material of MDMB-CHMICA and Cumyl-PeGaClone

Since the identification of JWH-018 in SPs in 2008, the general structure of newly appearing synthetic cannabinoids has followed a recognizable pattern. They can be synthesized by a modular system consisting of a core structure, aliphatic residue, linker and linked residue, following similar synthesis procedures as published in various patents and publications by the pharmaceutical industry [16, 29]. Although most of the published syntheses start from the native core molecule like indole or indazole, it is yet unknown which exact precursor material the NPS manufacturers use. However, it is generally considered, that a minimum of two synthesis steps are taken: the coupling of the aliphatic residue to the N-atom of the core structure and the coupling of the linked residue to the linker (and thus the core), necessitating at least three individual precursor substances. Figure X shows the structural elements of **1** and **2** which are expected to be used in the course of their respective synthesis. In the case of **1**, these precursors should be indole or an indole derivative (indole-3-carboxylic acid, carboxylate or carbaldehyde), (bromomethyl)cyclohexane and tert-leucine methyl ester (TLME). In the case of **2**, a 2-methyl-indole or a derivative (2-methyl-indole-3-carboxylic acid, carboxylate or carbaldehyde), 1-bromopentyl and cumylamine.

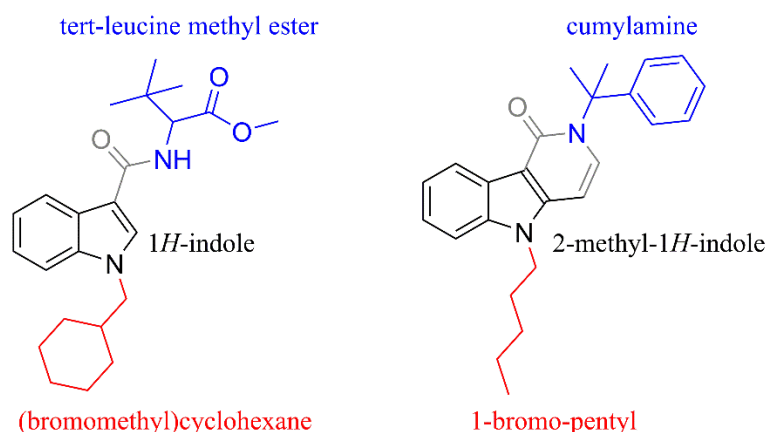


Figure 2: Potential precursor substances for MDMB-CHMICA (left) and Cumyl-PeGaClone (right)

Counting the number of carbon atoms in each precursor for **1**, their influence on the overall  $\delta^{13}\text{C}$  value is nearly equal (Indole:  $\text{C}_8$ ; Cyclohexyl methyl:  $\text{C}_7$ ; TLME:  $\text{C}_7$ ). For  $\delta^{15}\text{N}$ , only the indole and TLME, each with one nitrogen, have an impact on the corresponding isotope ratios. The synthesis of **2** is slightly more complex in comparison to synthetic cannabinoids with indole or indazole core structures. The gamma-carboline-1-one structure is expected to be synthesized by ring formation of a 2-methyl-indole derivative, following general synthesis instructions from Clark et al. [30] (Figure 3). Bristol-Meyer Squibb Co. patented the synthesis of a broad spectrum of gamma-carboline-1-one based cannabinoid receptor agonists similar to **2** [31]. This pathway is considered to be likely used by the NPS manufacturers as it is convenient to adapt the synthesis procedures of indole or indazole based core structures (such as Cuymil-5F-PICA) to 2-methyl-indoles with limited effort. Thus, in the stated synthesis, cumylamine (2-phenyl-2-propanamine) should be one of the precursors, contributing one of the two nitrogen and nine of the twenty-five carbon (36%) present in the molecule.

Jasper et al. analysed a set of active pharmaceutical ingredients (API) from different manufacturers and lots for their stable isotope ratios of  $\delta D$ ,  $\delta^{13}C$ ,  $\delta^{15}N$  and  $\delta^{18}O$  and found that each manufacture synthesized material with a specific isotopic composition, independent from the lot number [32]. It is generally agreed, that it is virtually impossible to artificially synthesize compounds with a target isotopic composition, considering the difficulty to even predetermine the ratio of a single isotope. Wokovitch et al. analysed the isotope ratios of the API Naproxen® and found a maximum inter-batch variation of 2.52 ‰ for  $\delta^{13}C$  for five different batches from a manufacturer in India [33]. It is not stated whether these differences are the result of an isotopically different precursor material or a poorly conducted or even different synthesis pathway. However, it was still possible to clearly discriminate all five batches from material of five other manufactures for Naproxen. With a global range of  $> 140$  ‰  $\delta^{13}C$  [34], 2.52 ‰ only make up for approximately 2 % of the naturally occurring range. Thus, we expect that two samples of synthetic cannabinoids with similar isotopic compositions to be produced by a single manufacturer, and material with indistinguishable isotopic compositions to be produced by a single manufacturer in a single batch or by the same combination of precursor material with distinct isotopic composition in multiple batches. A scenario, where two individual manufactures produce isotopically equal synthetic cannabinoids from precursor material of different sources is considered unlikely.

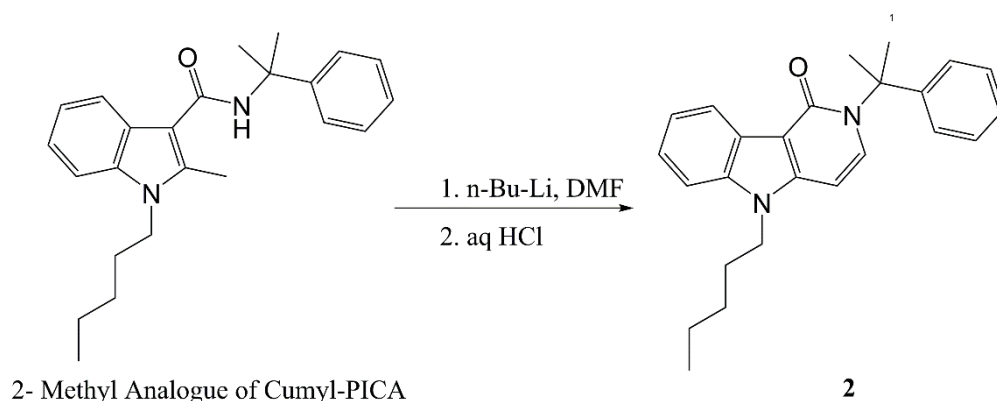


Figure 3: Sketched synthesis of Cumyl-PeGaClone from a 2-methyl-indole derivative of Cumyl-PICA following the synthesis instructions from Clark et al. [30]

Indole was purchased from eight different global vendors. Tert-leucine was obtained in (L) and (D), both from AlfaAeser. (D)-tert-leucine was purchased three-fold, whereas the lot number on all three containers were equal, thus they came from a single synthesis or biotransformation batch. TLME was purchased from two different Asian vendors and cumylamine from four different global vendors. Table 2 shows the  $\delta^{13}C$  and  $\delta^{15}N$  measured via EA-IRMS for all available precursor substances. Whether the manufactures obtain their precursors from other wholesalers or produce them on their own is unknown.

The measured values of  $\delta^{13}C$  for all precursors of **1** ranged from -32.91 to -21.04 ‰ ( $\Delta$  11.87 ‰), which is the typical range of petro- or plant-based chemicals[35-37].  $\delta^{15}N$  ranged from 2.00 to 9.66 ‰ ( $\Delta$  7.66 ‰) for the indoles, and from -2.34 to 0.74 ‰ ( $\Delta$  3.08 ‰) for the tert-leucines.

Indole can be synthesized by several pathways in industrial scale. Thus, the origin of the nitrogen cannot be assessed. Tert-leucine can be produced on industrial scale by reductive amination of ammonium trimethyl pyruvate by a semi-synthetic route involving leucine dehydrogenase as reducing enzyme, NADH as cofactor and format dehydrogenase for cofactor regeneration[38]. Ammoniac or ammonium is the source of nitrogen in this bio catalytic reaction, which itself is most probably manufactured by the Haber-Bosch process from atmospheric nitrogen, explaining the  $\delta^{15}\text{N}$  values close to zero (atmospheric  $\text{N}_2$  is defined as standard with 0.0 ‰ for  $\delta^{15}\text{N}$ ). All three samples of (D)-tert-Leucine from the same lot exhibit indistinguishable isotopic composition, indicating batch homogeneity.

The measured values of cumylamine ranged from -26.43 to -40.77 ‰ ( $\Delta$  14.34 ‰) for  $\delta^{13}\text{C}$  and -19.05 to 8.34 ‰ ( $\Delta$  27.39 ‰) for  $\delta^{15}\text{N}$ , which is, compared to the other precursor substances, a significantly broader range. The low values for both elements are unexpected, however, agree with the measured values for **2** as listed in Table A-2 and shown in Figure 5.

Table 2:  $\delta^{13}\text{C}$  and  $\delta^{15}\text{N}$  values including standard deviation of triplicate measurements on EA-IRMS for potential precursor substances of MDMB-CHMICA and Cumyl-PeGaClone, purchased from different global vendors.

	Vendor	$\delta^{13}\text{C}_{\text{V-PDB}}[\text{‰}]$	$\delta^{15}\text{N}_{\text{AIR}}[\text{‰}]$
		average $\pm$ STD	average $\pm$ STD
Indole	Sigma Aldrich	-21.04 $\pm$ 0.05	6.83 $\pm$ 0.04
	TCI	-26.80 $\pm$ 0.02	3.09 $\pm$ 0.13
	ABCR	-30.85 $\pm$ 0.04	2.08 $\pm$ 0.03
	Merck	-21.81 $\pm$ 0.02	8.78 $\pm$ 0.05
	Acros Chem.	-21.56 $\pm$ 0.03	9.15 $\pm$ 0.05
	AlfaAeser	-30.82 $\pm$ 0.04	2.00 $\pm$ 0.06
	BePharm	-22.25 $\pm$ 0.02	8.36 $\pm$ 0.03
	MP Biomed.	-28.99 $\pm$ 0.02	9.66 $\pm$ 0.05
(D)-tert-Leucine	AlfaAeser (same lot)	-29.81 $\pm$ 0.02	0.37 $\pm$ 0.03
		-29.84 $\pm$ 0.03	0.35 $\pm$ 0.02
		-29.84 $\pm$ 0.03	0.34 $\pm$ 0.05
(L)-tert-Leucine	AlfaAeser	-24.32 $\pm$ 0.02	-2.34 $\pm$ 0.02
(L)-TLME	TCI	-32.91 $\pm$ 0.02	0.74 $\pm$ 0.02
	BePharm	-24.02 $\pm$ 0.10	-1.57 $\pm$ 0.05
Cumyl-amine	ABCR	-26.43 $\pm$ 0.02	-13.11 $\pm$ 0.03
	Acella	-40.77 $\pm$ 0.02	-19.05 $\pm$ 0.07
	Enamine	-32.23 $\pm$ 0.01	8.34 $\pm$ 0.02
	TCI	-26.74 $\pm$ 0.02	-9.20 $\pm$ 0.04

### 3.2 Isotopic composition of 40 kg pure MDMB-CHMICA from a large seizure by Luxembourg customs

In a previously published profiling study, forty kilograms of **1** from a police seizure in Luxembourg in December 2014 (MDMB-01 to 40) were assigned into individual synthesis batches of 5-10 kg due to their organic impurity signatures [22]. For three of those forty kilograms, the impurity signatures were majorly different to the remaining sample complex, presumably the result of a differently conducted synthesis. After EA-IRMS analysis of the corresponding  $\delta^{13}\text{C}$  and  $\delta^{15}\text{N}$  values, the same three samples (MDMB-14, MDMB-21 and MDMB-37, batch 1 marked black in Figure 4) were outliers to the cluster of the remaining

thirty-seven samples (batches 2 to 6 in Figure 4) ranging from -27.87 to -27.51 ‰ ( $\Delta$  0.36 ‰) for  $\delta^{13}\text{C}$  and 3.25 to 3.79 ‰ ( $\Delta$  0.54 ‰) for  $\delta^{15}\text{N}$ . A similar linear “dilution” pattern of MDMB-21 and MDMB-14 could be observed in the impurity profiling, with MDMB-37 showing the most dissimilar impurity composition to the remaining sample pool. The two “intermediate” samples MDMB-21 and MDMB-14 seem to be blends in varying composition of MDMB-37 with at least one of the thirty-seven other samples. Hypothetically, MDMB-37 was mixed with batch 4 (violet), indicated by the increased values for  $\delta^{13}\text{C}$  and  $\delta^{15}\text{N}$  of one of the violet samples in comparison to the remaining samples from batch 4. Mixing of batches, either with the same or a different isotopic composition might occur, e.g. when the finished products from multiple synthesis batches are stored in larger containers for interim storage, leading to a blurring of both the corresponding isotopic and impurity composition. Considering the isotope ratios of the measured precursor substances for **1** (Table 2), it is unlikely that material from alternative providence was used to synthesize the batches 2-6 (Figure 4), as already the exchange of the indole core would significantly influence the isotopic composition, either by the nitrogen or carbon or both values, and would let the corresponding samples stick out of the collective.

This seizure is of special interest as it represents a unique collection of samples with previously known connection. In this case, both the impurity profiling and the stable isotope analysis show their individual strengths to draw conclusions about the sample history. IRMS allows to conclude that thirty-seven of the samples were synthesized using the same combination precursor material and three samples seem to be different, either by their origin of precursor or by a different synthesis. However, no further information can be extracted at that point. Via impurity profiling, the same three samples were identified as outliers with distinct impurity signatures as the result of a different synthesis and the remaining thirty-seven samples could be divided into individual synthesis batches by minor but still significant variations in their impurity signatures. Structural identification of specific impurities can provide valuable information about the applied synthesis pathway[27]. However, no information about the provenance of the precursor material is obtained and thus no conclusions about a common origin of the different batches can be drawn, although the relatively similar impurity compositions of the thirty-seven samples are highly indicative. Combining the information obtained from both techniques in a larger forensic context, also considering the information about the shipment as such (e.g. packaging), provides unique insights into the manufacturing of this sample collective. As shown in Figure 4, IRMS data provides an overview of the precursor relationship, impurity profiling reveals the fine structure of the underlying synthesis batches. It validates our previous assumption that only one manufacturer synthesized and shipped the forty kg material of **1** seized by Luxembourg customs. The whole material was packed equally into 1 kg packages without any visual difference (apart from the colour of the powder). The clustering thirty-seven samples were synthesized in multiple batches, repeating a specific synthesis procedure, using the same combination of precursor material (Indole, TLME and cyclohexyl methyl). One batch was synthesized by another synthesis procedure and mixed with other batches, which again indicates a common location of storage and/or packaging and thus validates the idea of a common source for this material.

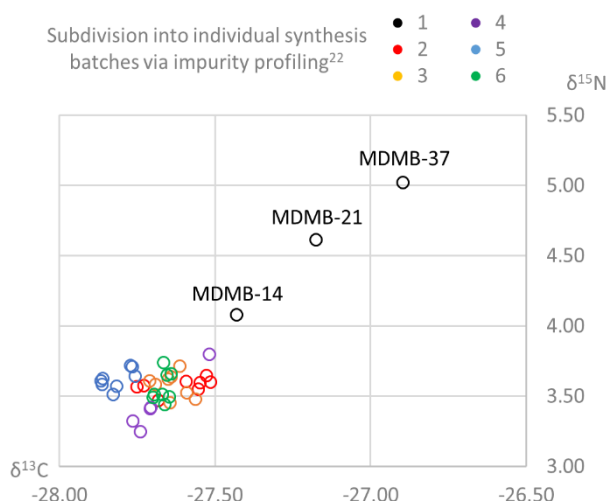


Figure 4: Measured  $\delta^{13}\text{C}$  and  $\delta^{15}\text{N}$  values for the 40 kg seizure (40 individual samples) of MDMB-CHMICA conducted by Luxembourg customs in December 2014. Each samples was coloured according to the batch discrimination by the impurity profiling conducted in a previous study [22].

### 3.3 Isotopic data for the complete sample pool of MDMB-CHMICA and Cumyl-PeGaClone

No IRMS measurements were published for synthetic cannabinoids so far, apart from our early work on 5F-PB-22[21]. Thus, we collected a large sample pool of seized and online test-purchased pure samples and SPs of **1** (61 pure, 120 SP) and **2** (1 pure, 30 SP), two highly prevalent synthetic cannabinoids in Germany from 2014 to 2017, and assessed their isotope ratios for  $\delta^{13}\text{C}$  and  $\delta^{15}\text{N}$  via EA-IRMS and GC-IRMS with the intention to identify potential links between samples that share a common history or origin. Secondly, we wanted to generate an overview of the overall isotopic range for these two synthetic cannabinoids and investigate if there is a large scattering or tight clustering of samples from different sources and dates of receipt. In a previous chapter, we have proven that neither the extraction from the herbal matrix, nor the clean-up via F-LC had an influence on the  $\delta^{13}\text{C}$  and  $\delta^{15}\text{N}$  values of the synthetic cannabinoids.

Figure 5 shows the measured  $\delta^{13}\text{C}$  and  $\delta^{15}\text{N}$  values of all available samples of **1** and **2** and the previously assed values for 5F-PB-22 [21]. A clustering of the individual synthetic cannabinoids can be observed. The values for all samples of **1** ranged from -27.87 to -25.94 ‰ ( $\Delta$  1.93 ‰) for  $\delta^{13}\text{C}$  and 2.39 to 6.35 ‰ ( $\Delta$  3.97 ‰) for  $\delta^{15}\text{N}$ . All samples of **2** (December 2016 to July 2017) showed values ranging from -33.83 to -35.26 ‰ ( $\Delta$  1.43 ‰) for  $\delta^{13}\text{C}$  and -10.34 to -12.70 ‰ ( $\Delta$  2.36 ‰) for  $\delta^{15}\text{N}$ , clearly separating them from the other two synthetic cannabinoids.

Comparing the samples on the outer borders of the respective clusters of **1** and **2**, their overall delta is higher than the measurement uncertainty, indicating multiple reaction batches with precursor material with different isotopic composition or, as already known for **1**, different synthesis. However, despite these significant intra-cluster variations, the individual clustering of the synthetic cannabinoids cannot be considered as pure coincidence. We expect that each of these cannabinoids were synthesized by one manufacturer, in the case of **1** the same that is responsible for the 40kg seizure by Luxembourg customs, who repeatedly uses bulk material of precursor substances from a specific provenance. Slight variations in isotopic composition



are most probably the result of a different synthesis procedure leading to isotopic fractionation or the manufacturer supplementing his precursor stock. The latter is considered as very likely scenario. We already have proven that the 40 kg seizure by Luxembourg customs consisted of multiple reaction batches, indicating a successive production of this cannabinoid. As this delivery was taken from the European market, the manufacturers had to substitute the lost material. The high prevalence of **1** through 2015 is evidence for other deliveries reaching the European market, either as large shipments or small packages. The here presented values of precursor substances from different global vendors, especially those of carbon (e.g. the indoles with an overall  $\Delta$  of 11.87 ‰ for  $\delta^{13}\text{C}$ ), and the comparatively tight clustering of the individual synthetic cannabinoids are a clear indication that the precursor material for each cannabinoid is coming from a single producer, who synthesizes large batches with only minor isotopic varieties.

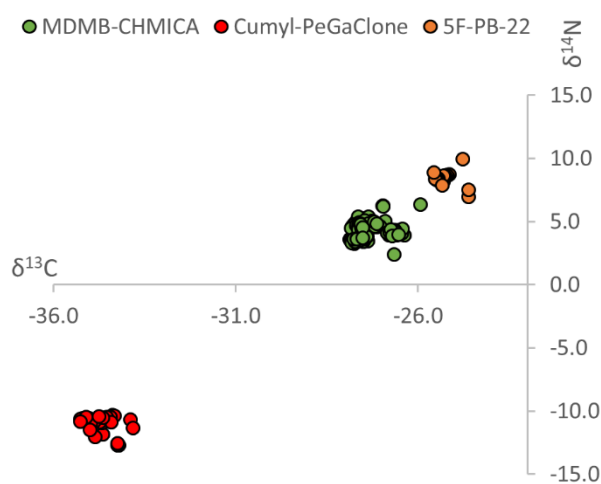


Figure 5:  $\delta^{13}\text{C}$  and  $\delta^{15}\text{N}$  values for all samples of MDMB-CHMICA (green), Cumyl-PeGaClone (red) and 5F-PB-22 [21] (orange). All samples of synthetic cannabinoids of the same type clustered individually.

The isotopic composition for all samples of **1** fit the isotopic range of the corresponding precursor substances if no excessive isotopic fractionation occurs while synthesizing. The unusually low levels of  $\delta^{15}\text{N}$  for both **2** and three of the four cumylamines validate our assumed synthesis procedure involving this precursor, especially considering the low values of -40.77 ‰ for  $\delta^{13}\text{C}$  and -19.05 for  $\delta^{15}\text{N}$  of the cumylamine from Acella.

### 3.4 Impurity profiling and isotope ratios and of “Spice-Products” of MDMB-CHMICA

Via IRMS analysis of police seizures and online test-purchases of SPs, in our case with focus on **1**, links between samples with synthetic cannabinoids of a common source can be generated. These links do not necessary describe co-operations between specific internet-shops or single SP brands, but provide a bigger-picture of the relationships between all available SP samples of **1**.

All samples of **1** extracted from SP ranged from -27.83 to -26.37 ‰ ( $\Delta$  1.46 ‰) for  $\delta^{13}\text{C}$  and 3.29 to 5.39 ‰ ( $\Delta$  2.10 ‰) for  $\delta^{15}\text{N}$  (Table A.3, Figure 6). Three agglomerations of samples

can be observed. The agglomerate nomenclature in the following discussion is dependent on which of the following Figures (Figure 6 or Figure 7) is referred to, as the combined information of both Figures might be discussed (A-C: The agglomerates as such, A<sub>1</sub>-C<sub>1</sub>: Figure 6 showing the IRMS data including the time correlation, A<sub>2</sub>-C<sub>2</sub>: Figure 7 showing the same IRMS data, this time including sub-clustering according to the impurity profiling). For all nomenclatures, the same set of samples are described.

The branding and origin of samples in each of these agglomerates are highly diverse, e.g. some of the SP were police seizures in mail items and search of persons and other were test-purchases in online shops. Thus, the complete distribution channel between online-shop and customer is displayed by our sample collective. Interpretation of isotopic data was aided by implementing the dates of online test-purchase or date of seizure. All SPs were labelled in intervals of five months, starting from September 2014 until December 2015. It should be kept in mind that this timely classification is dependent on the acquisition date of samples and is not a description of the actual date of synthesis. The online-market is regulated by demand and some products sell faster than others do, thus SP with “old” material of **1** might be sold month after the initial production of the SP or the corresponding synthesis. Agglomerate B<sub>1</sub> in Figure 6 shows an isotopic composition within the range of the already identified clusters of the large seizure by Luxembourg customs with approximately 3.6 ‰ for  $\delta^{15}\text{N}$ . Aliquots of pure material of **1** with this distinct isotopic composition, most probably from the same respective manufacturer, might be shipped in larger quantities to Europe either before or after the seizure in Luxembourg was made. The majority of SPs in this isotopic range were bought or seized in the late 2014 and early 2015 (the Luxembourg seizure was December 2014). Agglomerate C<sub>1</sub> primarily consists of samples seized or bought between March and July 2015, whereas agglomerate A<sub>1</sub> mainly comprises samples from the period from August to December 2015. As mentioned before, this timely classification is not exact, however, a tendency of agglomeration of samples from similar periods can be observed. Possibly, each agglomerate represents one or multiple synthesis batches similar to the seizure in Luxembourg, which were delivered by a single manufacturer to the European market in intervals in the course of the years 2014 and 2015. This conclusion has several implications on larger scale: Keeping in mind that each agglomerate consists of samples from different internet-shops and seizures, including a large variability of product brands, single larger shipments would need to be distributed amongst the European SP producers, who then use this specific delivery/batch of **1** for their SP in a given period. The pre-packaging in 1 kg bags of the 40 kg from Luxembourg is an indication for the intention of reselling or distributing single bags of pure material to multiple SP producers. That again implies that the majority of SP producers have some kind of co-operation or internal distribution network, at least for ordering and distributing new pure material from the original manufacturer. Hypothetically, placing the delivery order of material in each agglomerate into a rough timeline according to the date of purchase or seizure for their respective samples, B<sub>1</sub> would be the first delivery that reached Europe, C<sub>1</sub> the second, and A<sub>1</sub> the most recent. However, with this classification and no further data, it is difficult to explain the presence of samples from the period September 2014 to February 2015 in agglomerate A<sub>1</sub>.

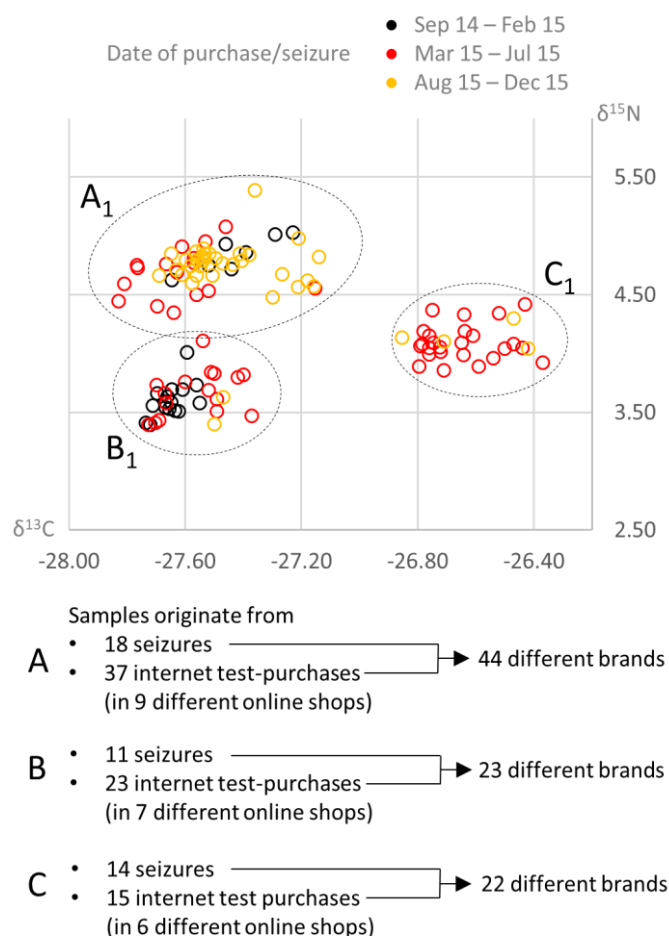


Figure 6: (Top)  $\delta^{13}\text{C}$  and  $\delta^{15}\text{N}$  values for all “Spice-Products” of MDMA-CHMICA, either measured via EA- or GC-IRMS. Colouring of samples is corresponding to the date of purchase or seizure of the “Spice-Products” in intervals of 5 month (● September 2014 to February 2014; ● March 2015 to July 2015; ● August 2015 to December 2015). (Bottom) Summarizing overview of the origin for samples located in each corresponding agglomerates A, B and C.

Therefore, as for the seizure of 40 kg pure **1**, an impurity profiling was carried out for all samples shown here in order to determine the fine structure of the dataset, with special interest in agglomerate A. Considering the hypothesis that each agglomerate represents a large shipment like the Luxembourg seizure, this shipment should include multiple synthesis batches. Our target was the identification of the individual batches in the agglomerates of isotopically indistinguishable samples. No reference material of multiple reaction batches under controlled conditions from the original manufacturer were available which could provide a scientific basis to classify samples of unknown source into individual batches. Thus, we used the relative distance set for the batch discrimination of the Luxembourg seizure as “calibration” for the here presented pool of SPs. The chromatographic impurity signatures of the previously assessed 15 key-impurities for both the Luxembourg seizure (excluding the three outliers MDMA-14, MDMA-21 and MDMA-37, as they would disrupt the chemometric model) and the individual SPs were analysed via PCA and HCA. In this model, the relative distance at which the thirty-seven samples from the Luxembourg seizure were classified into their individual synthesis batches was also set as relative distance for the classification of SPs into individual batches. This way, fourteen sub-clusters were identified for the 118 SPs, which again were implemented into the IRMS data to reveal the fine structure of the three individual agglomerates, as shown in the three zooms of agglomerate A, B and C in Figure 7. The impurity-profiling sub-cluster

are numbered consecutively from 1 to 14 and coloured differently for each zoom, respectively. The samples located in one of the agglomerates in the IRMS data (A, B or C) always clustered in the impurity profiling with other samples from the same agglomerates and never with a sample from one of the other two agglomerates. That again validates the IRMS measurement accuracy to some extent, although a few deviations between impurity and isotopic data can be found, for example the two intermediate samples between agglomerate A and B that are rated to B<sub>2</sub> according to the impurity data or the single sample with 5.4 ‰ for  $\delta^{15}\text{N}$  in agglomerate A<sub>2</sub> that is rated to samples with  $\delta^{15}\text{N}$  values of approximately 4.6 ‰. Logically speaking, the impurity profiling cannot suggest a batch relationship of two samples that are clearly distinguishable via IRMS as both samples should come from different reaction batches. As already described for the Luxembourg seizure before, a mixing of batches is always a possibility to consider, in addition to the measurement uncertainty, which leads to a blurring of both the isotope values and impurity signatures.

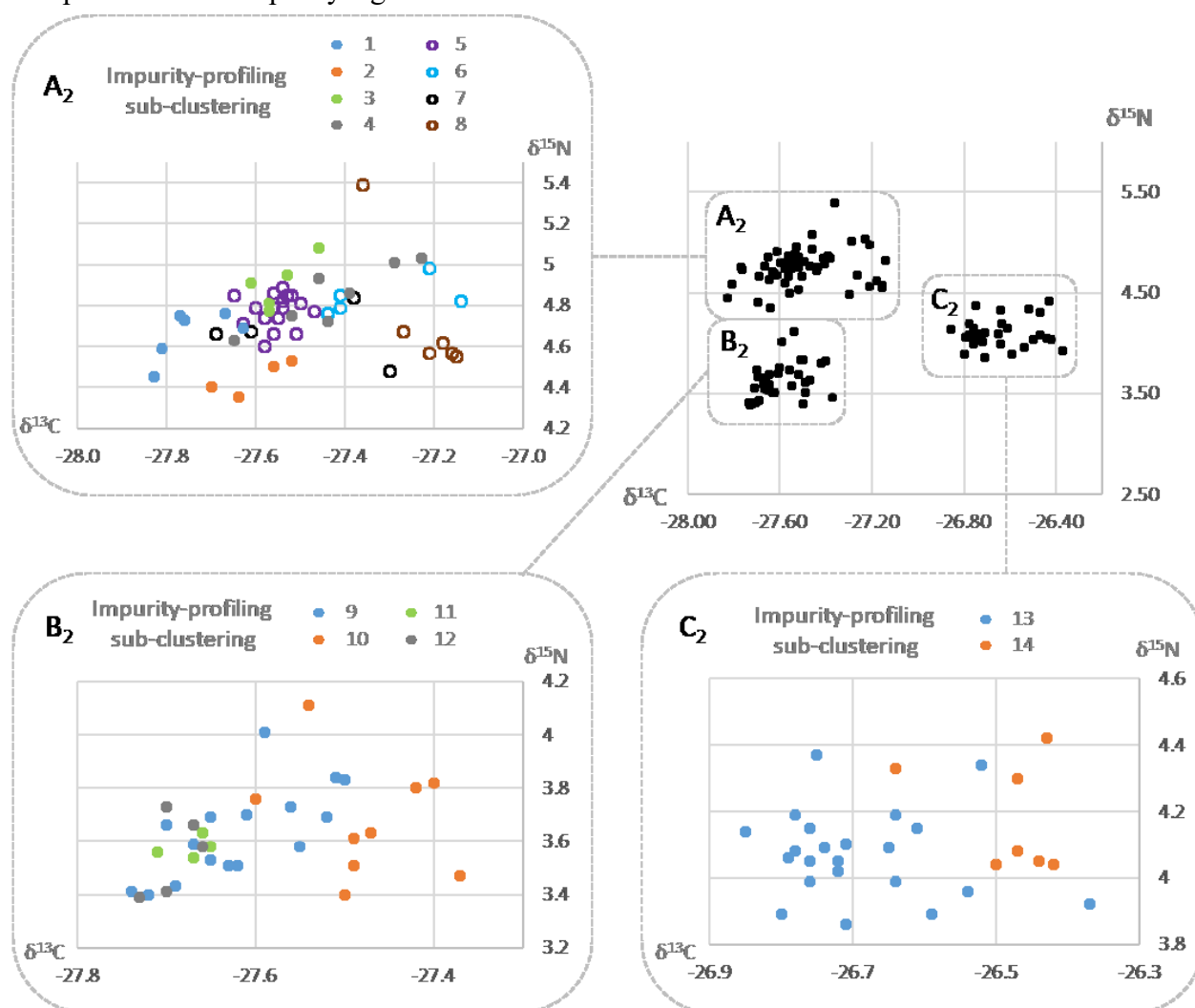


Figure 7: Zoom of the sample agglomerations A<sub>2</sub>, B<sub>2</sub>, and C<sub>2</sub> in the IRMS data with implemented sub-clusters according to the organic impurity-profiling. The fourteen assessed sub-clusters were numbered from 1 to 14 and coloured differently in each zoom for better visualisation. Agglomerate A<sub>2</sub> consist of eight sub-clusters, possibly representing individual synthesis batches, whereas the impurity signatures of sub-cluster 1-4 were majorly different from sub-cluster 5-8 (refer to Figure 8 for more information). In agglomerate B<sub>2</sub>, four sub-cluster were assigned, each possibly representing an individual synthesis batch. In agglomerate C<sub>2</sub>, two potential synthesis batches were found.

Agglomerate B<sub>2</sub> as such is subdivided into four sub-clusters of four, five, nine and sixteen SP samples. Agglomerate C<sub>2</sub> is divided into two sub-clusters of seven and twenty-two SP samples. The sub-clustering of samples in both B<sub>2</sub> and C<sub>2</sub> was due to minor differences in their overall impurity signatures, indicating individual synthesis batches with the same precursor material (evidenced by IRMS analysis) and the same synthesis procedure (evidenced by impurity profiling), similar to the thirty-seven samples from the Luxembourg seizure.

In agglomerate A<sub>1</sub>, eight sub-clusters were identified ranging between four and eighteen samples. However, compared to the agglomerates B<sub>2</sub> and C<sub>2</sub>, a major difference in impurity composition was observed. Figure 8 shows a PCA of the chromatographic impurity signatures for all samples located in agglomerate A, clearly dividing the sample set in (at least) two sections with high and low scores on PC1, respectively. The corresponding Loadings plot showed, that majorly the two impurities **I11** (methyl 2-(1-(cyclohexylmethyl)-1H-indole-3-carboxamido)butanoate) and **I4** (tentatively identified as methyl 2-(1H-indole-3-carboxamido)-3,3-dimethylbutanoate with C<sub>2</sub>H<sub>5</sub> attached to the indole)[27] were responsible for this division. On the right part of Figure 8, the average relative intensity of **I11** and **I4** for the respective samples of both sub-cluster groups are shown, to visualize the corresponding difference in abundance.

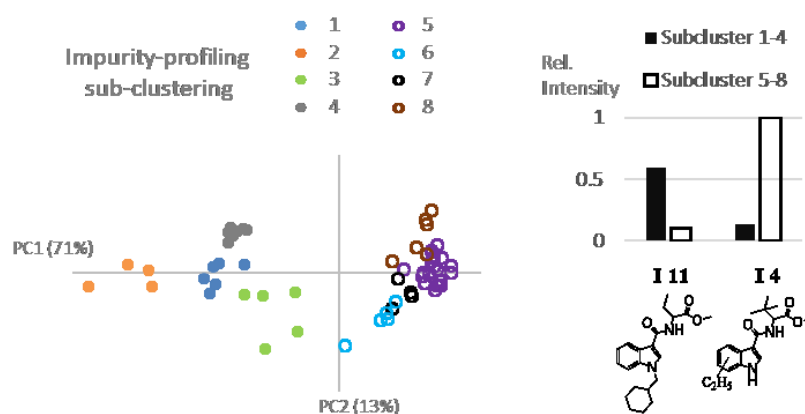


Figure 8: On the left a PCA of the chromatographic impurity signatures for the samples located in the IRMS agglomerate A (referring to Figure 6 and 7). The sample collective is subdivided into eight individual sub-cluster, each possibly representing an individual synthesis batch. However, between sub-cluster 1 to 4 and 5 to 8 a major difference in abundance of the two impurities **I11** and **I4** (as numbered and characterized in a previous study[27]) was found. On the right, the relative intensity of **I11** and **I4** for the respective samples of both sub-cluster groups are shown. Possibly, the samples assigned to sub-cluster 1 to 4 were synthesized by a different instrumentation, chemist or synthesis pathway than sub-cluster 5 to 8, although the IRMS data (referring again to Figure 6 and 7) suggests a relationship between both sub-cluster groups.

We concluded, that the sub-cluster 1 to 4 and 5 to 8 belong to two separate synthesis series, although the IRMS data suggests a relationship between both sub-cluster groups. This conclusion is further validated by including the dates of purchase for the samples in each sub-cluster. All samples in agglomerate A<sub>1</sub> from the early period of September 2014 to February 2015 (marked black in Figure 6) are included by sub-cluster 4. Furthermore, sub-cluster 1, 2 and 3 primarily consist of SP bought or seized in the period between March and July 2015 (marked red in Figure 6), and sub-cluster 5 to 8 consist of the majority of SPs from the period between August and December 2015. This implies that the previous placement of the agglomerates, presumably representing individual larger shipments of **1**, on the timeline was not 100% accurate. With the additional information from the impurity profiling, agglomerate

A is expected to consist of two larger shipments of multiple successive synthesis batches, one reaching the European market in 2014, explaining the seized and bought SP from this period falling into agglomerate A, and another shipment in 2015, which was used to produce the majority of SP from the end of 2015.

#### **4. Conclusion**

IRMS analysis of a larger sample collective of the two synthetic cannabinoids MDMB-CHMICA and Cumyl-PeGaClone consisting of both Spice-product extracts and pure material suggested that for each of these cannabinoids only one manufacturer is responsible. This hypothesis is validated by the diverse isotope ratios of precursor substances, making it virtually impossible for two different manufacturers to synthesize material within the specific isotopic range as it was found for these two cannabinoids.

From the larger strategic perspective, the time dependant resolution of the data provided the most valuable implication for the supply and distribution of the synthetic cannabinoid MDMB-CHMICA. Larger batches of pure material seem to be delivered consecutively to the European market in intervals of multiple months. These deliveries are then distributed amongst the European Spice-Products producers, indicated by the variety of different sources for the samples (multiple internet-shops, street seizures) and individual products brands that are assigned into the respective agglomerates. On the basis of the synthesis batch discrimination carried out for the seizure of 40 kg pure MDMB-CHMICA by Luxembourg customs, the MDMB-CHMICA in Spice-product samples was assigned to corresponding synthesis batches. After implementation of this fine structure, two larger groups of sub-clusters were identified in one of the agglomerates observed in IRMS, which otherwise would be indistinguishable.

Combining IRMS and impurity profiling as analytical tools, generating orthogonal information, provides unique insights into the structure of a sample pool of unknown origin. Both techniques target a different part of the sample history, IRMS the origin of the precursor material and impurity profiling the corresponding synthesis pathway in which these precursors were used. By implementing the batch discrimination of the impurity profiling into the isotope ratio agglomerates or clusters, the fine-structure of the observed sample pool is visualized.

#### **5. Acknowledgements**

All presented data, if not cited otherwise, were generated within the project “SPICE-profiling”, funded within the EU’s ISEC 2013 programme (Directorate-General JUST/2013/ISEC/DRUGS/AG/ISEC/4000006421). Our thanks are due to Serge Schneider, Ilmari Szilvay and Dr. Sonja Klemenc who kindly provided us with aliquots from seizures of MDMB-CHMICA. Furthermore, we want to thank Dr. Verena Angerer and Prof. Volker Auwärter from the University Medical Clinic Freiburg for providing us with pure and “Spice-Product” samples from internet test-purchases and Siegfried Zörnlein and Sonja Metternich for providing us with seizures of “Spice-Products” from Rhineland-Palatine.

#### **6. References**

[1] UNODC, UNODC World drug report 2018, (2018).



- [2] V. Kunalan, N. Nic Daéid, W.J. Kerr, H.A.S. Buchanan, A.R. McPherson, Characterization of Route Specific Impurities Found in Methamphetamine Synthesized by the Leuckart and Reductive Amination Methods, *Analytical Chemistry*, 81 (2009) 7342-7348.
- [3] J. Ballany, B. Caddy, M. Cole, Y. Finnon, L. Aalberg, K. Janhunen, E. Sippola, K. Andersson, C. Bertler, J. Dahlen, I. Kopp, L. Dujourdy, E. Lock, P. Margot, H. Huizer, A. Poortman, E. Kaa, A. Lopes, Development of a harmonised pan-European method for the profiling of amphetamines, *Sci. Justice*, 41 (2001) 193-196.
- [4] L. Stromberg, L. Lundberg, H. Neumann, B. Bobon, H. Huizer, N.W. van der Stelt, Heroin impurity profiling. A harmonization study for retrospective comparisons, *Forensic Sci. Int.*, 114 (2000) 67-88.
- [5] A.L. Pikkarainen, Systematic approach to the profiling analysis of illicit amphetamine, *Forensic Sci. Int.*, 82 (1996) 141-152.
- [6] J.J. Zacca, T.S. Grobério, A.O. Maldaner, M.L. Vieira, J.W.B. Braga, Correlation of Cocaine Hydrochloride Samples Seized in Brazil Based on Determination of Residual Solvents: An Innovative Chemometric Method for Determination of Linkage Thresholds, *Analytical Chemistry*, 85 (2013) 2457-2464.
- [7] J.F. Carter, E.L. Titterton, H. Grant, R. Sleeman, Isotopic changes during the synthesis of amphetamines, *Chemical Communications*, (2002) 2590-2591.
- [8] S. Schneiders, T. Holdermann, R. Dahlenburg, Comparative analysis of 1-phenyl-2-propanone (P2P), an amphetamine-type stimulant precursor, using stable isotope ratio mass spectrometry, *Science and Justice*, 49 (2009) 94-101.
- [9] N. Kurashima, Y. Makino, S. Sekita, Y. Urano, T. Nagano, Determination of Origin of Ephedrine Used as Precursor for Illicit Methamphetamine by Carbon and Nitrogen Stable Isotope Ratio Analysis, *Analytical Chemistry*, 76 (2004) 4233-4236.
- [10] H. Salouros, G.J. Sutton, J. Howes, D.B. Hibbert, M. Collins, Measurement of Stable Isotope Ratios in Methamphetamine: A Link to Its Precursor Source, *Analytical Chemistry*, 85 (2013) 9400-9408.
- [11] J.R. Ehleringer, J.F. Casale, M.J. Lott, V.L. Ford, Tracing the geographical origin of cocaine, *Nature*, 408 (2000) 311.
- [12] J.R. Mallette, J.F. Casale, J. Jordan, D.R. Morello, P.M. Beyer, Geographically Sourcing Cocaine's Origin – Delineation of the Nineteen Major Coca Growing Regions in South America, *Sci. Rep.*, 6 (2016) 23520.
- [13] S. Dautraix, R. Guilluy, H. Chaudron-Thozet, J.L. Brazier, A. Lamotte,  $^{13}\text{C}$  Isotopic analysis of an acetaminophen and diacetylmorphine mixture, *J. Chromatogr. A*, 756 (1996) 203-210.
- [14] H.A.S. Buchanan, W.J. Kerr, W. Meier-Augenstein, N.N. Daéid, Organic impurities, stable isotopes, or both: A comparison of instrumental and pattern recognition techniques for the profiling of 3,4-methylenedioxymethamphetamine, *Analytical Methods*, 3 (2011) 2279-2288.
- [15] S.D. Brandt, L.A. King, M. Evans-Brown, The new drug phenomenon, *Drug. Test. Anal.*, 6 (2014) 587-597.
- [16] J.W. Huffman, D. Dai, B.R. Martin, D.R. Compton, Design, Synthesis and Pharmacology of Cannabimimetic Indoles, *Bioorganic & Medicinal Chemistry Letters*, 4 (1994) 563-566.
- [17] R. Mechoulam, J.J. Feigenbaum, N. Lander, M. Segal, T.U.C. Järbe, A.J. Hiltunen, P. Consroe, Enantiomeric cannabinoids: stereospecificity of psychotropic activity, *Experientia*, 44 (1988) 762-764.
- [18] T.M. Brunt, A.M. Atkinson, T. Nefau, M. Martinez, E. Lahaie, A. Malzcewski, M. Pazitny, V. Belackova, S.D. Brandt, Online test purchased new psychoactive substances in 5 different European countries: A snapshot study of chemical composition and price, *Int. J. Drug Policy*, 44 (2017) 105-114.
- [19] V. Auwarter, S. Dresen, W. Weinmann, M. Muller, M. Putz, N. Ferreiros, 'Spice' and other herbal blends: harmless incense or cannabinoid designer drugs?, *J. Mass Spectrom.*, 44 (2009) 832-837.
- [20] EMCDDA, Synthetic cannabinoids in Europe (Perspectives on drugs), Perspectives on Drugs (PODs), EMCDDA, Lisbon, 2017.
- [21] S. Münster-Müller, N. Scheid, T. Holdermann, S. Schneiders, M. Pütz, Profiling of new psychoactive substances by using stable isotope ratio mass spectrometry: Study of the synthetic cannabinoid 5F-PB-22, *Drug. Test. Anal.*, 10 (2018) 1323-1327.

- [22] S. Münster-Müller, R. Zimmermann, M. Pütz, A Novel Impurity-Profiling Workflow with the Combination of Flash-Chromatography, UHPLC-MS, and Multivariate Data Analysis for Highly Pure Drugs: A Study on the Synthetic Cannabinoid MDMB-CHMICA, *Anal. Chem.*, 90 (2018) 10559-10567.
- [23] H.A.S. Buchanan, N.N. Daéid, W. Meier-Augenstein, H.F. Kemp, W.J. Kerr, M. Middleditch, Emerging Use of Isotope Ratio Mass Spectrometry as a Tool for Discrimination of 3,4-Methylenedioxymethamphetamine by Synthetic Route, *Anal. Chem.*, 80 (2008) 3350-3356.
- [24] N. NicDaeid, W. Meier-Augenstein, H.F. Kemp, O.B. Sutcliffe, Using isotopic fractionation to link precursor to product in the synthesis of (+/-)-mephedrone: a new tool for combating "legal high" drugs, *Anal. Chem.*, 84 (2012) 8691-8696.
- [25] M. Collins, A. Doddridge, H. Salouros, Cathinones: Isotopic profiling as an aid to linking seizures, *Drug Testing and Analysis*, 8 (2016) 903-909.
- [26] V. Angerer, L. Mogler, J.-P. Steitz, P. Bisel, C. Hess, C.T. Schoeder, C.E. Müller, L.M. Huppertz, F. Westphal, J. Schäper, V. Auwärter, Structural characterization and pharmacological evaluation of the new synthetic cannabinoid CUMYL-PEGACLONE, *Drug. Test. Anal.*, 10 (2018) 597-603.
- [27] S. Münster-Müller, S. Hansen, T. Opatz, R. Zimmermann, M. Pütz, Chemical profiling of the synthetic cannabinoid MDMB-CHMICA: Identification, assessment, and stability study of synthesis-related impurities in seized and synthesized samples, *Drug Test. Anal.*, 11 (2019) 1192-1206.
- [28] T. Schoenberger, Determination of standard sample purity using the high-precision <sup>1</sup>H-NMR process, *Anal. Bioanal. Chem.*, 403 (2012) 247-254.
- [29] P. Buchler, Indazole derivatives, WO2009106980, US, 2009
- [30] R.D. Clark, A.B. Miller, J. Berger, D.B. Repke, K.K. Weinhardt, B.A. Kowalczyk, R.M. Eglen, D.W. Bonhaus, C.H. Lee, 2-(Quinuclidin-3-yl)pyrido[4,3-b]indol-1-ones and isoquinolin-1-ones. Potent conformationally restricted 5-HT<sub>3</sub> receptor antagonists, *J. Med. Chem.*, 36 (1993) 2645-2657.
- [31] S.T. Wroblewski, P. Chen, J. Hynes, S. Lin, D.J. Norris, C.R. Pandit, S. Spergel, H. Wu, J.S. Tokarski, X. Chen, K.M. Gillooly, P.A. Kiener, K.W. McIntyre, V. Patil-koota, D.J. Shuster, L.A. Turk, G. Yang, K. Leftheris, Rational Design and Synthesis of an Orally Active Indolopyridone as a Novel Conformationally Constrained Cannabinoid Ligand Possessing Antiinflammatory Properties, *J. Med. Chem.*, 46 (2003) 2110-2116.
- [32] J.P. Jasper, B.J. Westenberger, J.A. Spencer, L.F. Buhse, M. Nasr, Stable isotopic characterization of active pharmaceutical ingredients, *J. Pharm. Biomed. Anal.*, 35 (2004) 21-30.
- [33] A.M. Wokovich, J.A. Spencer, B.J. Westenberger, L.F. Buhse, J.P. Jasper, Stable isotopic composition of the active pharmaceutical ingredient (API) naproxen, *J. Pharm. Biomed. Anal.*, 38 (2005) 781-784.
- [34] T.B. Coplen, J. Hopple, J. Boehike, H. Peiser, S. Rieder, Compilation of minimum and maximum isotope ratios of selected elements in naturally occurring terrestrial materials and reagents, US Geology Survey, (2002).
- [35] J.A. Calder, P.L. Parker, Stable carbon isotope ratios as indexes of petrochemical pollution of aquatic systems, *Environ. Sci. Technol.*, 2 (1968) 535-539.
- [36] Z. Sofer, Stable carbon isotope compositions of crude oils: application to source depositional environments and petroleum alteration, *AAPG bulletin*, 68 (1984) 31-49.
- [37] T.B. Coplen, J. Hopple, J. Boehike, H. Peiser, S. Rieder, Compilation of minimum and maximum isotope ratios of selected elements in naturally occurring terrestrial materials and reagents, (2002).
- [38] H. Slusarczyk, S. Felber, M.R. Kula, M. Pohl, Stabilization of NAD-dependent formate dehydrogenase from *Candida boidinii* by site-directed mutagenesis of cysteine residues, *Eur. J. Biochem.*, 267 (2000) 1280-1289.

## 7.6 Scientific publications (submitted)

Table A.1  $\delta^{13}\text{C}$  and  $\delta^{15}\text{N}$  values including standard deviation of triplicate measurements for all pure samples of MDMB-CHMICA

	$\delta^{13}\text{C}_{\text{V-PDB}}[\text{‰}]$	$\delta^{15}\text{N}_{\text{AIR}}[\text{‰}]$		$\delta^{13}\text{C}_{\text{V-PDB}}[\text{‰}]$	$\delta^{15}\text{N}_{\text{AIR}}[\text{‰}]$
	average $\pm$ STD	average $\pm$ STD		average $\pm$ STD	average $\pm$ STD
MDMB-01	-27.76 $\pm$ 0.01	3.64 $\pm$ 0.08	MDMB-32	-27.76 $\pm$ 0.03	3.32 $\pm$ 0.08
MDMB-02	-27.51 $\pm$ 0.01	3.60 $\pm$ 0.10	MDMB-33	-27.55 $\pm$ 0.03	3.55 $\pm$ 0.07
MDMB-03	-27.75 $\pm$ 0.05	3.56 $\pm$ 0.14	MDMB-34	-27.82 $\pm$ 0.02	3.57 $\pm$ 0.04
MDMB-04	-27.61 $\pm$ 0.02	3.71 $\pm$ 0.03	MDMB-35	-27.69 $\pm$ 0.05	3.58 $\pm$ 0.13
MDMB-05	-27.77 $\pm$ 0.02	3.71 $\pm$ 0.08	MDMB-36	-27.67 $\pm$ 0.01	3.51 $\pm$ 0.00
MDMB-06	-27.77 $\pm$ 0.03	3.71 $\pm$ 0.08	MDMB-37	-26.90 $\pm$ 0.02	5.02 $\pm$ 0.09
MDMB-07	-27.64 $\pm$ 0.01	3.45 $\pm$ 0.05	MDMB-38	-27.56 $\pm$ 0.03	3.48 $\pm$ 0.10
MDMB-08	-27.68 $\pm$ 0.02	3.47 $\pm$ 0.09	MDMB-39	-27.74 $\pm$ 0.03	3.25 $\pm$ 0.04
MDMB-09	-27.53 $\pm$ 0.03	3.64 $\pm$ 0.09	MDMB-40	-27.66 $\pm$ 0.03	3.44 $\pm$ 0.09
MDMB-10	-27.71 $\pm$ 0.03	3.41 $\pm$ 0.04	MDMB-41	-26.65 $\pm$ 0.12	2.39 $\pm$ 0.30
MDMB-11	-27.64 $\pm$ 0.04	3.64 $\pm$ 0.10	MDMB-42	-27.69 $\pm$ 0.03	5.02 $\pm$ 0.06
MDMB-12	-27.59 $\pm$ 0.01	3.60 $\pm$ 0.03	MDMB-43	-27.45 $\pm$ 0.01	5.23 $\pm$ 0.08
MDMB-13	-27.55 $\pm$ 0.01	3.59 $\pm$ 0.02	MDMB-44	-27.56 $\pm$ 0.04	4.72 $\pm$ 0.07
MDMB-14	-27.43 $\pm$ 0.21	4.08 $\pm$ 0.27	MDMB-45	-27.56 $\pm$ 0.04	4.72 $\pm$ 0.04
MDMB-15	-27.65 $\pm$ 0.01	3.62 $\pm$ 0.10	MDMB-46	-27.53 $\pm$ 0.03	4.82 $\pm$ 0.07
MDMB-16	-27.71 $\pm$ 0.03	3.42 $\pm$ 0.07	MDMB-47	-27.55 $\pm$ 0.02	4.72 $\pm$ 0.16
MDMB-17	-27.73 $\pm$ 0.01	3.57 $\pm$ 0.04	MDMB-48	-27.57 $\pm$ 0.04	4.82 $\pm$ 0.21
MDMB-18	-27.52 $\pm$ 0.19	3.79 $\pm$ 0.29	MDMB-49	-27.66 $\pm$ 0.01	3.57 $\pm$ 0.10
MDMB-19	-27.67 $\pm$ 0.01	3.74 $\pm$ 0.15	MDMB-50	-27.61 $\pm$ 0.02	3.59 $\pm$ 0.02
MDMB-20	-27.65 $\pm$ 0.07	3.65 $\pm$ 0.05	MDMB-51	-26.95 $\pm$ 0.04	6.22 $\pm$ 0.04
MDMB-21	-27.18 $\pm$ 0.07	4.61 $\pm$ 0.22	MDMB-52	-26.98 $\pm$ 0.01	6.25 $\pm$ 0.05
MDMB-22	-27.64 $\pm$ 0.00	3.66 $\pm$ 0.05	MDMB-53	-26.95 $\pm$ 0.02	6.20 $\pm$ 0.06
MDMB-23	-27.83 $\pm$ 0.04	3.51 $\pm$ 0.08	MDMB-54	-27.48 $\pm$ 0.01	4.90 $\pm$ 0.05
MDMB-24	-27.70 $\pm$ 0.03	3.51 $\pm$ 0.03	MDMB-55	-27.47 $\pm$ 0.01	5.01 $\pm$ 0.09
MDMB-25	-27.71 $\pm$ 0.04	3.61 $\pm$ 0.05	MDMB-56	-27.65 $\pm$ 0.02	5.36 $\pm$ 0.00
MDMB-26	-27.87 $\pm$ 0.04	3.61 $\pm$ 0.02	MDMB-57	-25.94 $\pm$ 0.01	6.35 $\pm$ 0.01
MDMB-27	-27.59 $\pm$ 0.00	3.52 $\pm$ 0.06	MDMB-58	-27.71 $\pm$ 0.01	3.63 $\pm$ 0.18
MDMB-28	-27.86 $\pm$ 0.01	3.58 $\pm$ 0.07	MDMB-59	-27.67 $\pm$ 0.04	3.66 $\pm$ 0.04
MDMB-29	-27.86 $\pm$ 0.02	3.62 $\pm$ 0.06	MDMB-60	-27.46 $\pm$ 0.03	4.88 $\pm$ 0.08
MDMB-30	-27.70 $\pm$ 0.01	3.49 $\pm$ 0.02	MDMB-61	-27.04 $\pm$ 0.01	4.62 $\pm$ 0.04
MDMB-31	-27.65 $\pm$ 0.03	3.49 $\pm$ 0.05			

Table A.2  $\delta^{13}\text{C}$  and  $\delta^{15}\text{N}$  values including standard deviation of triplicate measurements for one pure sample and all "Spice-Products" of Cumyl-PeGaClone

	$\delta^{13}\text{C}_{\text{V-PDB}}[\text{‰}]$	$\delta^{15}\text{N}_{\text{AIR}}[\text{‰}]$		$\delta^{13}\text{C}_{\text{V-PDB}}[\text{‰}]$	$\delta^{15}\text{N}_{\text{AIR}}[\text{‰}]$
	average $\pm$ STD	average $\pm$ STD		average $\pm$ STD	average $\pm$ STD
Peg-01	-34.65 $\pm$ 0.09	-11.83 $\pm$ 0.05	SP_Peg-16	-34.73 $\pm$ 0.19	-10.80 $\pm$ 0.12
SP_Peg-01	-34.21 $\pm$ 0.01	-12.69 $\pm$ 0.07	SP_Peg-17	-34.74 $\pm$ 0.03	-10.91 $\pm$ 0.01
SP_Peg-02	-34.23 $\pm$ 0.27	-12.70 $\pm$ 0.22	SP_Peg-18	-34.98 $\pm$ 0.21	-10.87 $\pm$ 0.11
SP_Peg-03	-34.69 $\pm$ 0.16	-10.54 $\pm$ 0.12	SP_Peg-19	-34.64 $\pm$ 0.01	-10.56 $\pm$ 0.02
SP_Peg-04	-34.43 $\pm$ 0.28	-10.77 $\pm$ 0.10	SP_Peg-20	-34.25 $\pm$ 0.03	-12.58 $\pm$ 0.04
SP_Peg-05	-34.39 $\pm$ 0.15	-10.34 $\pm$ 0.02	SP_Peg-21	-34.89 $\pm$ 0.08	-10.91 $\pm$ 0.06
SP_Peg-06	-33.88 $\pm$ 0.01	-10.68 $\pm$ 0.01	SP_Peg-22	-35.21 $\pm$ 0.02	-10.59 $\pm$ 0.02
SP_Peg-07	-34.49 $\pm$ 0.13	-10.51 $\pm$ 0.13	SP_Peg-23	-35.01 $\pm$ 0.10	-10.58 $\pm$ 0.03

## 7.6 Scientific publications (submitted)

SP_Peg-08	-34.77 ± 0.29	-10.85 ± 0.08	SP_Peg-24	-34.98 ± 0.16	-10.98 ± 0.02
SP_Peg-09	-34.67 ± 0.22	-10.97 ± 0.08	SP_Peg-25	-34.75 ± 0.12	-10.46 ± 0.01
SP_Peg-10	-34.57 ± 0.09	-10.62 ± 0.08	SP_Peg-26	-34.86 ± 0.03	-12.04 ± 0.11
SP_Peg-11	-34.34 ± 0.23	-10.38 ± 0.02	SP_Peg-27	-35.26 ± 0.02	-10.63 ± 0.02
SP_Peg-12	-34.43 ± 0.14	-10.46 ± 0.02	SP_Peg-28	-35.11 ± 0.13	-10.51 ± 0.16
SP_Peg-13	-34.54 ± 0.08	-10.49 ± 0.06	SP_Peg-29	-35.00 ± 0.03	-11.47 ± 0.07
SP_Peg-14	-34.41 ± 0.13	-10.87 ± 0.03	SP_Peg-30	-35.26 ± 0.02	-10.83 ± 0.05
SP_Peg-15	-33.83 ± 0.14	-11.36 ± 0.11			

*Table A.3  $\delta^{13}\text{C}$  and  $\delta^{15}\text{N}$  values including standard deviation of triplicate measurements for all “Spice-Products” of MDMB-CHMICA*

	$\delta^{13}\text{C}_{\text{V-PDB}}[\text{‰}]$	$\delta^{15}\text{N}_{\text{AIR}}[\text{‰}]$		$\delta^{13}\text{C}_{\text{V-PDB}}[\text{‰}]$	$\delta^{15}\text{N}_{\text{AIR}}[\text{‰}]$
	average ± STD	average ± STD		average ± STD	average ± STD
SP_MDMB-01	-27.67 ± 0.02	3.54 ± 0.05	SP_MDMB-60	-27.54 ± 0.01	4.89 ± 0.02
SP_MDMB-02	-27.62 ± 0.04	3.51 ± 0.06	SP_MDMB-61	-27.54 ± 0.02	4.82 ± 0.02
SP_MDMB-03	-27.65 ± 0.04	3.58 ± 0.09	SP_MDMB-62	-27.54 ± 0.06	4.79 ± 0.05
SP_MDMB-04	-27.65 ± 0.04	3.53 ± 0.04	SP_MDMB-63	-27.61 ± 0.04	4.67 ± 0.07
SP_MDMB-05	-27.63 ± 0.03	3.51 ± 0.06	SP_MDMB-64	-27.63 ± 0.03	4.71 ± 0.00
SP_MDMB-06	-27.65 ± 0.02	3.69 ± 0.07	SP_MDMB-65	-27.65 ± 0.02	4.85 ± 0.02
SP_MDMB-07	-27.70 ± 0.04	3.66 ± 0.12	SP_MDMB-66	-27.30 ± 0.07	4.48 ± 0.29
SP_MDMB-08	-27.72 ± 0.02	3.40 ± 0.10	SP_MDMB-67	-26.71 ± 0.02	4.10 ± 0.07
SP_MDMB-09	-27.71 ± 0.02	3.56 ± 0.04	SP_MDMB-68	-27.56 ± 0.04	4.86 ± 0.07
SP_MDMB-10	-27.59 ± 0.05	4.01 ± 0.01	SP_MDMB-69	-27.51 ± 0.04	4.66 ± 0.08
SP_MDMB-11	-27.66 ± 0.01	3.63 ± 0.04	SP_MDMB-70	-27.58 ± 0.01	4.74 ± 0.07
SP_MDMB-12	-27.74 ± 0.03	3.41 ± 0.10	SP_MDMB-71	-27.69 ± 0.03	4.66 ± 0.03
SP_MDMB-13	-27.61 ± 0.03	3.70 ± 0.13	SP_MDMB-72	-26.42 ± 0.02	4.04 ± 0.14
SP_MDMB-14	-27.69 ± 0.01	3.43 ± 0.06	SP_MDMB-73	-27.47 ± 0.02	3.63 ± 0.15
SP_MDMB-15	-27.77 ± 0.02	4.75 ± 0.08	SP_MDMB-74	-26.47 ± 0.08	4.30 ± 0.31
SP_MDMB-16	-27.81 ± 0.03	4.59 ± 0.09	SP_MDMB-75	-27.52 ± 0.10	4.75 ± 0.30
SP_MDMB-17	-27.76 ± 0.05	4.73 ± 0.10	SP_MDMB-76	-27.39 ± 0.07	4.86 ± 0.27
SP_MDMB-18	-27.37 ± 0.07	3.47 ± 0.19	SP_MDMB-77	-27.29 ± 0.04	5.01 ± 0.17
SP_MDMB-19	-27.49 ± 0.05	3.61 ± 0.05	SP_MDMB-78	-27.65 ± 0.02	4.63 ± 0.06
SP_MDMB-20	-27.49 ± 0.13	3.51 ± 0.16	SP_MDMB-79	-27.23 ± 0.08	5.03 ± 0.21
SP_MDMB-21	-27.70 ± 0.02	3.73 ± 0.11	SP_MDMB-80	-27.44 ± 0.14	4.72 ± 0.15
SP_MDMB-22	-27.66 ± 0.04	3.58 ± 0.13	SP_MDMB-81	-27.46 ± 0.08	4.93 ± 0.10
SP_MDMB-23	-27.70 ± 0.04	3.41 ± 0.12	SP_MDMB-82	-26.47 ± 0.11	4.08 ± 0.39
SP_MDMB-24	-27.70 ± 0.02	4.40 ± 0.09	SP_MDMB-83	-26.50 ± 0.10	4.04 ± 0.24
SP_MDMB-25	-27.73 ± 0.02	3.39 ± 0.10	SP_MDMB-84	-26.37 ± 0.09	3.92 ± 0.25
SP_MDMB-26	-27.83 ± 0.06	4.45 ± 0.07	SP_MDMB-85	-27.64 ± 0.06	4.35 ± 0.09
SP_MDMB-27	-26.72 ± 0.01	4.02 ± 0.01	SP_MDMB-86	-27.67 ± 0.10	3.66 ± 0.13
SP_MDMB-28	-27.63 ± 0.04	4.69 ± 0.01	SP_MDMB-87	-27.56 ± 0.08	4.50 ± 0.14
SP_MDMB-29	-26.64 ± 0.06	3.99 ± 0.03	SP_MDMB-88	-26.78 ± 0.05	4.19 ± 0.14
SP_MDMB-30	-26.79 ± 0.07	4.06 ± 0.06	SP_MDMB-89	-27.60 ± 0.02	3.76 ± 0.05
SP_MDMB-31	-26.78 ± 0.04	4.08 ± 0.05	SP_MDMB-90	-27.54 ± 0.06	4.11 ± 0.40
SP_MDMB-32	-26.74 ± 0.03	4.09 ± 0.13	SP_MDMB-91	-27.50 ± 0.08	3.83 ± 0.27
SP_MDMB-33	-26.76 ± 0.07	4.15 ± 0.12	SP_MDMB-92	-26.52 ± 0.11	4.34 ± 0.19
SP_MDMB-34	-26.76 ± 0.05	3.99 ± 0.01	SP_MDMB-93	-27.51 ± 0.17	3.84 ± 0.11

## 7.6 Scientific publications (submitted)

SP_MDMB-35	-26.76 ± 0.02	4.05 ± 0.15	SP_MDMB-94	-27.53 ± 0.10	4.95 ± 0.10
SP_MDMB-36	-27.67 ± 0.02	4.76 ± 0.09	SP_MDMB-95	-27.55 ± 0.07	3.58 ± 0.22
SP_MDMB-37	-26.80 ± 0.02	3.89 ± 0.06	SP_MDMB-96	-27.61 ± 0.07	4.91 ± 0.20
SP_MDMB-38	-26.64 ± 0.03	4.19 ± 0.09	SP_MDMB-97	-27.46 ± 0.08	5.08 ± 0.18
SP_MDMB-39	-26.72 ± 0.02	4.05 ± 0.02	SP_MDMB-98	-27.57 ± 0.10	4.81 ± 0.14
SP_MDMB-40	-27.15 ± 0.04	4.55 ± 0.07	SP_MDMB-99	-26.44 ± 0.21	4.05 ± 0.24
SP_MDMB-41	-27.54 ± 0.01	4.82 ± 0.02	SP_MDMB-100	-27.40 ± 0.16	3.82 ± 0.32
SP_MDMB-42	-27.27 ± 0.01	4.67 ± 0.06	SP_MDMB-101	-26.43 ± 0.22	4.42 ± 0.27
SP_MDMB-43	-26.85 ± 0.04	4.14 ± 0.07	SP_MDMB-102	-26.64 ± 0.22	4.33 ± 0.04
SP_MDMB-44	-27.44 ± 0.05	4.76 ± 0.05	SP_MDMB-103	-27.42 ± 0.05	3.80 ± 0.35
SP_MDMB-45	-27.41 ± 0.01	4.79 ± 0.07	SP_MDMB-104	-26.59 ± 0.11	3.89 ± 0.21
SP_MDMB-46	-27.50 ± 0.31	3.40 ± 0.11	SP_MDMB-105	-27.38 ± 0.11	4.84 ± 0.14
SP_MDMB-47	-27.21 ± 0.02	4.57 ± 0.03	SP_MDMB-106	-27.18 ± 0.09	4.62 ± 0.20
SP_MDMB-48	-27.16 ± 0.02	4.57 ± 0.07	SP_MDMB-107	-26.65 ± 0.15	4.09 ± 0.10
SP_MDMB-49	-27.56 ± 0.03	4.79 ± 0.12	SP_MDMB-108	-26.61 ± 0.06	4.15 ± 0.15
SP_MDMB-50	-27.56 ± 0.03	4.66 ± 0.05	SP_MDMB-109	-26.75 ± 0.04	4.37 ± 0.23
SP_MDMB-51	-27.60 ± 0.03	4.79 ± 0.03	SP_MDMB-110	-26.71 ± 0.18	3.86 ± 0.04
SP_MDMB-52	-27.58 ± 0.01	4.60 ± 0.10	SP_MDMB-111	-27.56 ± 0.08	3.73 ± 0.23
SP_MDMB-53	-27.41 ± 0.01	4.85 ± 0.04	SP_MDMB-112	-27.67 ± 0.06	3.59 ± 0.05
SP_MDMB-54	-27.53 ± 0.01	4.85 ± 0.02	SP_MDMB-113	-27.57 ± 0.09	4.77 ± 0.13
SP_MDMB-55	-27.55 ± 0.03	4.74 ± 0.03	SP_MDMB-114	-26.54 ± 0.08	3.96 ± 0.16
SP_MDMB-56	-27.36 ± 0.07	5.39 ± 0.06	SP_MDMB-115	-27.52 ± 0.09	4.53 ± 0.39
SP_MDMB-57	-27.52 ± 0.03	4.85 ± 0.03	SP_MDMB-116	-27.52 ± 0.07	3.69 ± 0.14
SP_MDMB-58	-27.47 ± 0.02	4.77 ± 0.11	SP_MDMB-117	-27.21 ± 0.07	4.98 ± 0.09
SP_MDMB-59	-27.50 ± 0.01	4.81 ± 0.10	SP_MDMB-118	-27.14 ± 0.10	4.82 ± 0.19